


August 2020

# The Impact of Myeloid-Mediated Co-Stimulation and Immunosuppression on the Anti-Tumor Efficacy of Adoptive T cell Therapy

Pasquale Patrick Innamarato  
*University of South Florida*

Follow this and additional works at: <https://digitalcommons.usf.edu/etd>

 Part of the [Cell Biology Commons](#), [Immunology and Infectious Disease Commons](#), and the [Oncology Commons](#)

---

## Scholar Commons Citation

Innamarato, Pasquale Patrick, "The Impact of Myeloid-Mediated Co-Stimulation and Immunosuppression on the Anti-Tumor Efficacy of Adoptive T cell Therapy" (2020). *Graduate Theses and Dissertations*.  
<https://digitalcommons.usf.edu/etd/9026>

This Dissertation is brought to you for free and open access by the Graduate School at Digital Commons @ University of South Florida. It has been accepted for inclusion in Graduate Theses and Dissertations by an authorized administrator of Digital Commons @ University of South Florida. For more information, please contact [scholarcommons@usf.edu](mailto:scholarcommons@usf.edu).

The Impact of Myeloid-Mediated Co-Stimulation and Immunosuppression on the Anti-Tumor  
Efficacy of Adoptive T cell Therapy

by

Pasquale Patrick Innamarato

A dissertation submitted in partial fulfillment  
of requirements for the degree of  
Doctor of Philosophy  
Department of Cell Biology, Microbiology, and Molecular Biology  
College of Arts and Sciences  
University of South Florida

Major Professor: Shari Pilon-Thomas, PhD  
Daniel Abate-Daga, PhD  
Amer Beg, PhD  
Paulo Rodriguez, PhD  
Ken Wright, PhD  
Suzanne Ostrand-Rosenberg, PhD

Date of Approval:  
August 26, 2020

Keywords: 41BB, MDSCs, T cells, hematopoiesis, tumor infiltrating lymphocytes

Copyright© 2020, Pasquale Patrick Innamarato

## **DEDICATION**

I dedicate this work to the memory of my mother, Therese Innamarato. It was my mother's passing from her long battle with breast cancer during my time in college that motivated me to pursue a career in cancer research. My mother worked as a Registered Nurse and Nurse Manager at the Fox Chase Cancer Center in Philadelphia all the while receiving chemotherapy, radiation, and other treatment for her metastatic cancer. Her devotion to taking care of family and caring for cancer patients, even though she was among those afflicted by the disease, was so inspirational. I miss her every day and I hope that my work can go towards helping future cancer patients and preventing the untimely loss of dear loved ones. My mother's strength during her decade long battle with cancer is something that I will always remember, and I cherish all of the moments we had together. Thank you mom for all of the love, lessons, and courage that you gave me.

## ACKNOWLEDGEMENTS

Firstly, I want to acknowledge my mentor, Dr. Shari Pilon-Thomas. It was truly an honor and a privilege to have had the opportunity to complete my graduate studies in her laboratory. I truly appreciate the nature of our relationship. Her style of mentoring nurtured my scientific curiosity which enabled the expansion of my skill set and my ability to think critically. I thoroughly enjoyed the ability to take on science in a discovery-based manner. Her patience, interpersonal skills, intelligence, creativity, and work-ethic are all factors that I hope to harness if I am lucky enough to run my own laboratory one day. Shari has been an excellent role model and I am ecstatic to be able to have her as a mentor, a colleague, and a friend throughout my professional career.

The group of people that I have worked with in the labs of Dr. Pilon-Thomas, Dr. John Mullinax, and Dr. James Mulé have truly been special. Both current and previous members of these groups have been such a pleasure to work with. I would not have been able to get to this point of my professional career without having a wonderful group of people to surround me. I deeply appreciate the support and the contributions from everyone that helped progress my projects. The relationships that we built together is something that I will always cherish.

I also want to extend my gratitude to Dr. Amod Sarnaik. I am grateful for the resources and guidance that Dr. Sarnaik has been able to provide to myself and the rest of the Pilon-Thomas Laboratory. The ability to conduct translational research has been an exciting experience and I am grateful to have had this opportunity to make an impact that can benefit the lives of cancer patients. I express my thanks to Dr. Sarnaik, Dr. Mullinax, and Dr. Pilon-Thomas for

having such a wonderful relationship that enables trainees like myself to pursue exciting aspects of translational research.

I express my gratitude for the guidance and feedback provided by my committee, Dr. Daniel Abate-Daga, Dr. Amer Beg, Dr. Paulo Rodriguez, and Dr. Ken Wright. Thank you all for your valuable guidance, technical assistance, and inclusion in research projects throughout my graduate studies. To my Dissertation Defense Chair, Dr. Suzanne Ostrand-Rosenberg, thank you sincerely for taking the time to be a part of this special event in my life. Your research has continuously inspired my own research and I am honored to have received guidance and feedback from you.

To the wonderful core facilities at the Moffitt Cancer Center, the resources provided by the Flow Cytometry Core, Molecular Genomics Core, Bioinformatics and Biostatistics Cores, and the Vivarium staff allowed my research to blossom. The leadership and staff provided invaluable assets and guidance during my graduate studies. I express my thanks to Jodi Kroeger, John Robinson, Neel Chaudhary, Sean Yoder, Tania Mesa, Andrew Smith, Chaomei Zhang, Ling Cen, and the entire group of veterinary and husbandry staff in the vivarium.

To the Cancer Biology PhD program, thank you for your astounding efforts in providing a wonderful graduate program. Thank you for giving me the opportunity to earn a PhD in this great program. I especially want to thank Dr. Ken Wright, Cathy Gaffney, Janet Opel, Sarah Riordan, and Danielle Dorsett for their support in the past 6 years.

Lastly, I want to thank my family. To my girlfriend, Ashley, thank you for being a constant source of support, love, inspiration, and encouragement. Without you, I would not have succeeded in my pursuit of a career in cancer research and the success is something that we equally share. To my father Pat Innamarato III, thank you for your immense support, advice,

guidance, and love are critical aspects that have helped me achieve this dream. To the parents of Ashley: Tony and Mary, you have welcomed me into your family and your love and support is something that I deeply cherish. Thank you for helping me through this journey. To my sister and her fiancé, Christen Innamarato and Bryan Stammerjohann, I am thrilled that our families are merging. Christen, thank you for your friendship, the love and the encouragement during my graduate studies. I am grateful to begin the next stage of my life along with a wonderful family and group of friends.

## TABLE OF CONTENTS

List of Tables .....	iv
List of Figures .....	v
Abstract .....	ix
Chapter One: Introduction .....	1
Adoptive T cell therapy for the treatment of human malignancies .....	1
Preparative lymphodepletion is essential to elicit durable therapeutic responses to ACT.....	5
Strategies to enhance the efficacy of ACT .....	11
Chapter Two: Intratumoral activation of 41BB co-stimulatory signals enhances CD8 T cell expansion and modulates tumor infiltrating myeloid cells .....	20
Introduction.....	20
The blockade of inhibitory signals enhances anti-tumor T cell functions.....	20
Triggering co-stimulation through 41BB revives tumor-cytotoxic T cells.....	21
An overview 41BB-41BBL activity on myeloid cells.....	23
Results.....	24
Intratumoral 41BB activation leads to tumor regression in multiple models.....	24
Intratumoral treatment with a 41BB agonist increases CD8 T cell infiltration .....	26
Intratumoral 41BB activation remodels the tumor immune microenvironment.....	26
Intratumoral $\alpha$ 41BB alters the immune stimulatory capacity of myeloid cells .....	27
41BB agonistic antibodies promote ex vivo human TIL expansion.....	30
Stimulation of the 41BB-41BBL axis alters myeloid cell phenotype and function .....	33
The stimulation of TIL is potentiated by 41BBL on APCs .....	37
Discussion.....	39
Methods.....	46
Human TIL specimens and tumor digest preparation.....	47
Isolation and culture of human myeloid cells from peripheral blood mononuclear cells .....	47
Human TIL co-culture assays .....	47

Detection of cytokines from primary melanomas.....	48
Flow cytometry .....	48
Mouse models .....	50
Murine cell lines and in vivo treatment .....	50
Tumor-myeloid cell co-culture with OT-I T cells .....	51
Isolation of murine TILs .....	52
Statistical analysis.....	52
Study Approval .....	52
Chapter Three: Reactive myelopoiesis triggered by lymphodepleting chemotherapy limits the efficacy of adoptive T cell therapy .....	54
Introduction.....	54
Cancer co-opts myeloid cells to promote immunosuppression and tumor progression.....	54
Myeloid-derived suppressor cells are orchestrators of tumor-mediated immunosuppression .....	55
Reactive myelopoiesis – an immunological process that promotes MDSC accumulation .....	57
The role of reactive myelopoiesis in Adoptive T cell Therapy .....	60
Results.....	61
The accumulation of myeloid cells reduces the therapeutic efficacy of ACT with tumor infiltrating lymphocytes .....	62
Myeloid derived suppressor cells rapidly expand after treatment with lymphodepleting chemotherapy in mice.....	69
MDSCs differentiate from mobilized hematopoietic progenitor cells in mice and humans.....	70
The abrogation of CCR2 in recipient mice does not enhance the efficacy of ACT .....	76
IL-6 promotes MDSC activity after lymphodepletion treatment.....	82
Lymphodepleting chemotherapy induces the production of IL-6 in bone marrow .....	83
IL-6 regulates the survival and resistance to Fas-induced apoptosis in lymphodepletion-induced MDSCs.....	88
IL-6 signaling during progenitor differentiation to MDSCs is essential for the regulation of Fas expression and resistance to apoptosis.....	91
Discussion .....	100
Methods.....	107
Study Design.....	107
Patient Samples.....	107
Myeloid cell isolation for functional assays .....	108
Generation of human melanoma cell line and tumor conditioned medium.....	109
MDSC differentiation .....	109
Mouse models and treatment .....	110
Murine Cell Lines .....	111
In vitro T cell culture, lymphodepletion, adoptive transfer, and in vivo treatment .....	111



Flow Cytometry .....	112
IL-6 detection and in vitro stimulation of IL-6 signaling .....	113
MDSC apoptosis .....	114
TCR-beta sequencing and analysis .....	115
RNA-Sequencing .....	115
Statistical analysis .....	116
Study Approval .....	117
Chapter Four: Conclusions and Future Perspectives .....	118
References .....	123
Appendix A: Funding .....	136
Appendix B: Institutional Animal Care and Use Committee Approval .....	137
Appendix C: Copyright Use and Permission Form .....	141

## LIST OF TABLES

Table 1. Summary of clinical trials exploring various pre-conditioning regimens for ACT.....	12
Table 2. List of references for Figure 3 .....	20

## LIST OF FIGURES

Figure 1. A schema of ACT with TILs. ....	4
Figure 2. The increased availability of IL-7 and IL-15 induced by lymphodepletion promotes the efficacy of ACT.....	8
Figure 3. Strategies to Enhance ACT. ....	18
Figure 4. Intratumoral treatment with agonistic 41BB antibodies promotes tumor regression in multiple mouse tumor models. ....	25
Figure 5. Intratumoral treatment with agonistic 41BB antibodies increases CD8 T cell infiltration.....	28
Figure 6. Remodeling of the immune microenvironment after intratumoral administration of anti-41BB antibodies. ....	29
Figure 7. Intratumoral anti-41BB treatment alters myeloid immunostimulatory capacity.....	31
Figure 8. Tumor-associated myeloid cells alter PD-1 expression on T cells.....	32
Figure 9. 41BB agonism enhances the growth of TILs from primary human melanomas.....	34
Figure 10. Activation of 41BB and 41BBL alter myeloid cell phenotype and function .....	36
Figure 11. Cytokine production in TIL-APC co-cultures. ....	40
Figure 12. Sustained 41BB agonism enhances CXCL10 expression in mouse tumors.....	41
Figure 13. 41BBL is necessary to induce TIL proliferation in co-cultures with APCs.....	41
Figure 14. Potential mechanisms of 41BB agonism in the context of APC-mediated stimulation.....	45

Figure 15. MDSCs are dynamic immunosuppressive cells that promote tumor progression. ....	56
Figure 16. Reactive myelopoiesis is a driver of tumor-induced immunosuppression. ....	59
Figure 17. The effect of lymphodepleting chemotherapy in melanoma patients receiving ACT with TILs. ....	62
Figure 18. Gating strategy for identification of myeloid cell subsets in patients. ....	62
Figure 19. Myeloid cell frequency was determined by flow cytometry prior to and after treatment with lymphodepleting chemotherapy and TIL infusion in melanoma patients. ....	63
Figure 20. MDSCs suppress autologous TILs ....	63
Figure 21. PMN-MDSCs are abundant after lymphodepletion and TIL infusion. ....	64
Figure 22. MDSC suppressive capacity before and after TIL infusion. ....	64
Figure 23. Expansion of MDSCs in NSCLC patients receiving ACT with TIL. ....	65
Figure 24. The accumulation of MDSCs after lymphodepletion and TIL infusion is associated with patient outcomes. ....	67
Figure 25. The ratio of myeloid cells to CD8 <sup>+</sup> T cells is associated with poor patient survival. ....	68
Figure 26. Survival associations with the number of infused TILs and Pre-treatment myeloid cell frequency. ....	68
Figure 27. The <i>in vivo</i> persistence of TILs is diminished by an abundance of myeloid cells. ....	68
Figure 28. Tracking TIL clonotypes and identification of endogenous T cells. ....	69
Figure 29. The reduction of TIL persistence in relation to myeloid cell frequency is associated with poor survival in melanoma patients. ....	69
Figure 30. Lymphodepleting chemotherapy induces the expansion of MDSCs in mice. ....	71
Figure 31. Lymphodepletion-generated MDSCs are suppressive. ....	72

Figure 32. Gating strategy to identify mouse HSPCs .....	73
Figure 33. Lymphodepleting chemotherapy mobilizes HSPCs.....	73
Figure 34. Mobilized HSPCs differentiate into MDSCs in lymphodepleted hosts .....	74
Figure 35. HSPCs increase in melanoma patients after treatment with lymphodepleting chemotherapy and TIL infusion.....	76
Figure 36. Phenotype of CD34 <sup>+</sup> cells in melanoma patients that received ACT with TIL. ....	77
Figure 37. Frequency of CD34 <sup>+</sup> in a melanoma patient. Week 1 Post-Treatment CD34 <sup>+</sup> cells were used to generate MDSCs as in Figure 37-38.....	77
Figure 38. Differentiation of immunosuppressive myeloid cells from lymphodepletion mobilized CD34 <sup>+</sup> cells. ....	78
Figure 39. MDSCs generated from mobilized CD34 <sup>+</sup> cells suppress TIL effector function. ....	78
Figure 40. MDSC reconstitution in CCR2 <sup>KO</sup> mice. ....	80
Figure 41. Assessment of early T cell infiltration after ACT and depletion of MDSCs .....	81
Figure 42. ACT in CCR2 <sup>KO</sup> mice does not enhance anti-tumor efficacy. ....	81
Figure 43. RNA sequencing on MDSCs isolated from untreated and lymphodepleted tumor-bearing mice. ....	84
Figure 44. Upstream cytokines regulators of MDSCs from lymphodepleted mice.....	85
Figure 45. IL-6 promotes the suppressive capacity of post-LD MDSCs.....	85
Figure 46. The induction of IL-6R signaling fails to rescue MDSC suppressive capacity. ....	85
Figure 47. The efficacy of ACT is enhanced in IL-6 <sup>KO</sup> recipients. ....	86
Figure 48. IL-6R blockade enhances the efficacy of ACT. ....	86
Figure 49. Co-transfer of MDSCs with T cells.....	87

Figure 50. IL-6R expression in MDSCs and myeloid progenitors .....	89
Figure 51. IL-6 production is induced in the bone marrow by lymphodepleting chemotherapy. ....	90
Figure 52. RNA sequencing of WT and IL-6 <sup>KO</sup> MDSCs from non-treated and lymphodepleted mice. ....	92
Figure 53. IL-6 reduces Fas expression in MDSCs that expand post-lymphodepletion. ....	93
Figure 54. In vivo JAK/STAT3 inhibition reduces PMN-MDSC survival. ....	94
Figure 55. Exogenous IL-6 does not alter MDSC suppressive capacity. ....	95
Figure 56. IL-6 does not promote MDSC suppression of TILs .....	95
Figure 57. IL-6 differentiation signals reduces Fas expression and increases MDSC survival.....	97
Figure 58. IL-6 differentiation signals promote resistance to Fas-induced cell death.....	98
Figure 59. Graphical Abstract.....	99

## ABSTRACT

Adoptive T cell therapy (ACT) in combination with lymphodepleting chemotherapy is an effective strategy to induce the eradication of tumors, providing long-term regression in cancer patients. However, only a minority of patients that receive ACT with tumor infiltrating lymphocytes (TILs) exhibit durable benefit. Thus, there is an urgent need to define strategies that potentiate anti-tumor activity conducted by adoptively transferred T cells. In these studies, we aimed to identify novel strategies to enhance the therapeutic efficacy of ACT. Accordingly, we describe the disparate roles of myeloid cells in the context of ACT characterized by the augmentation of TIL proliferation in the presence of 41BB-mediated co-stimulation and the dampening of anti-tumor immunity orchestrated by myeloid derived suppressor cells (MDSCs).

The efficient expansion of T cells is a critical aspect of ACT, which is aided by culturing tumors and TILs in IL-2 and 41BB agonistic antibodies. However, the impact of 41BB-mediated co-stimulation conducted by constituent myeloid cells within tumors on the expansion of TILs is unclear. Here, we describe that the intratumoral administration of 41BB agonistic antibodies led to increases in CD8 T cell infiltration followed by tumor regression in murine models. We found that granulocytes and monocytes rapidly replaced macrophages and dendritic cells in tumors following administration of anti-41BB antibodies. Overall, myeloid cells from anti-41BB treated tumors had an improved capacity to stimulate T cells in comparison to myeloid cells from control treated tumors. In human co-culture systems, we demonstrated that the agonism of the 41BB-41BBL axis enhanced co-stimulatory signals and effector functions among antigen

presenting cells and autologous TILs. Thus, myeloid-mediated co-stimulation is a critical factor in potentiating the proliferation of TILs and their anti-tumor activity.

Despite that lymphodepleting regimens condition the host for optimal engraftment and expansion of adoptively transferred T cells, lymphodepletion concomitantly promotes immunosuppression during the course of endogenous immune recovery. Here, we have identified that lymphodepleting chemotherapy initiates the mobilization of hematopoietic progenitor cells that differentiate to immunosuppressive myeloid cells, leading to a dramatic increase of peripheral MDSCs. In melanoma and lung cancer patients, MDSCs rapidly expanded in the periphery within one week after completion of a lymphodepleting regimen and infusion of autologous tumor infiltrating lymphocytes (TIL). This expansion was associated with disease progression, poor survival, and reduced TIL persistence in melanoma patients. We demonstrated that the IL-6 driven differentiation of mobilized hematopoietic progenitor cells promoted the survival and immunosuppressive capacity of post-lymphodepletion MDSCs. Furthermore, the genetic abrogation or therapeutic inhibition of IL-6 in mouse models enhanced host survival and reduced tumor growth in mice that received ACT. Thus, the expansion of MDSCs in response to lymphodepleting chemotherapy may contribute to ACT failure and targeting myeloid-mediated immunosuppression may support anti-tumor immune responses.

Collectively, we demonstrate that exploiting the immunostimulatory capacity of myeloid cells and the curtailment of myeloid-mediated immunosuppression are strategies that can augment the expansion and anti-tumor activity of TILs. The novel mechanistic insights of these studies highlight the importance of modulating myeloid cells to promote the therapeutic efficacy of ACT.



## CHAPTER ONE

### INTRODUCTION

#### **Adoptive T cell therapy for the treatment of human malignancies**

For nearly 30 years, the infusion of T cells possessing the capability of recognizing and eliminating tumor cells has been explored in patients with cancer. Early studies demonstrated that the administration of IL-2 could expand T cells *in vivo*, leading to durable regressions in patients with metastatic melanoma (1). This groundbreaking discovery was some of the first evidence that therapies targeting the immune system, but not tumor cells, could lead to the eradication of cancer in human subjects. Subsequent studies demonstrated that the *ex vivo* expansion of tumor infiltrating lymphocytes (TIL) followed by the infusion of these cells to patients with metastatic melanoma led to complete regression of disease (2). In recent years, adoptive T cell therapy (ACT) with TIL has led to complete regressions and possibly curative responses in patients with metastatic melanoma, breast cancer, human papilloma virus associated cancers, and colorectal cancer (3-6). To generate a clinical infusion product, first a tumor is surgically excised from a patient, fragmented, and then cultured in high concentrations of IL-2 (7) (Figure 1). TILs will proliferate and egress from tumor fragments whereby their expansion is maintained for a few weeks in culture. Upon successful expansion, TILs are tested for tumor-specific reactivity against the patient's autologous tumor cells and/or human leukocyte antigen (HLA)-matched tumor cell lines that may share antigen specificity. The tumor-reactive TILs are determined via IFN-gamma production or upregulation of activation markers, including 41BB, and undergo a rapid expansion protocol (REP), which entails the culture of TILs with irradiated

allogeneic feeder cells with the addition of IL-2 and agonistic CD3 antibodies, routinely yielding  $>5 \times 10^{10}$  cells (3, 8).

While the infusion of autologous TILs has demonstrated that ACT is an effective treatment for patients with cancer, the genetic modification of T cells with the purpose of directing tumor-specificity has also been implemented in the clinic. Chimeric antigen receptor (CAR) T cells have shown great promise in treating and potentially curing patients with hematological malignancies. In contrast to ACT with TIL that utilizes the patient's endogenous tumor-specific T cells, CAR T cells involve the engineering of patients' peripheral T cells with a synthetic receptor that binds to a singular tumor antigen. The CAR is typically a construct of a single-chain variable fragment (scFv) of an antibody with known specificity, and components of the T cell receptor (TCR) synapse, CD3 $\zeta$  and co-stimulatory domains, such as CD28 or 41BB (9). The CAR is forcefully expressed within T cells via transduction with a virus that encodes the scFv of an antibody and the components of the TCR synapse.

CD19-directed CAR T cells have provided complete regressions in 90% of treated children, young adults, and older individuals with acute lymphoblastic leukemia (ALL) (10). The remarkable success of CAR T cell treatment in patients with hematological malignancies has catalyzed investigators to engineer T cells directed against antigens that are expressed in solid tumors (11). Exciting results have shown that tumor regression can occur after infusion of CAR T cells directed against antigens expressed in multiple cancers, including glioblastoma, pancreatic cancer, and neuroblastoma (12-15). However, the high complete response rates exhibited in patients treated with CD19-directed CAR T cells has not been observed in patients infused with CAR T cells directed against solid tumor antigens. Low response rates in patients with solid tumors treated with CAR T cells has been attributed to multiple resistance

mechanisms, including target antigen loss (16), ineffective T cell trafficking (17), and immunosuppression in the tumor microenvironment (18, 19). These findings have spurred investigators to further modify CAR T cells and apply other therapeutics in combination with ACT to potentiate enhanced anti-tumor efficacy (discussed later in this chapter).

In addition to ACT with TILs or CAR T cells, the engineering of T cells to express a TCR that recognizes a single tumor antigen has proven to be efficacious in patients. In contrast to CAR T cells, transgenic-TCR T cells utilize endogenous TCRs that have specificity against tumor antigens and depend on antigen presentation through MHC (major histocompatibility complex). The cloned TCR is inserted into T cells, which forces their antigen specificity toward a particular tumor-antigen (20). A recent trial in patients with acute myeloid leukemia (AML) demonstrated that the infusion of T cells engineered to express TCRs specific for the Wilms Tumor 1 (WT1) antigen prevented disease relapse in 100% of patients after a hematopoietic stem cell transplant (HSCT) (21). However, much like the experience with CAR T cell therapy, the marked success of ACT with transgenic-TCR T cells is highly dependent on the disease, treatment strategy, and target-antigen specificity. Many transgenic-TCR T cells are designed to target shared or “self” antigens aberrantly expressed by tumor cells such as the New York Esophageal Squamous Cell Carcinoma-1 (NY-ESO-1) antigen (22). Clinical trials that evaluated the efficacy of NY-ESO-1 specific transgenic-TCR T cells in patients with melanoma and synovial cell sarcoma demonstrated a partial response rate of 35% and 55% respectively, with 4 of 20 melanoma patients and 1 of 18 sarcoma patients experiencing complete responses (23). In myeloma patients, ACT with NY-ESO-1 specific T cells in combination with autologous HSCT resulted in responses in 11 of 25 patients and a median progression-free survival of 13.5 months (24). While NY-ESO-1 is one of many target antigens, many other antigens expressed by tumor

cells have been explored for the development of transgenic-TCR T cells for multiple hematological and solid tumor malignancies (20).

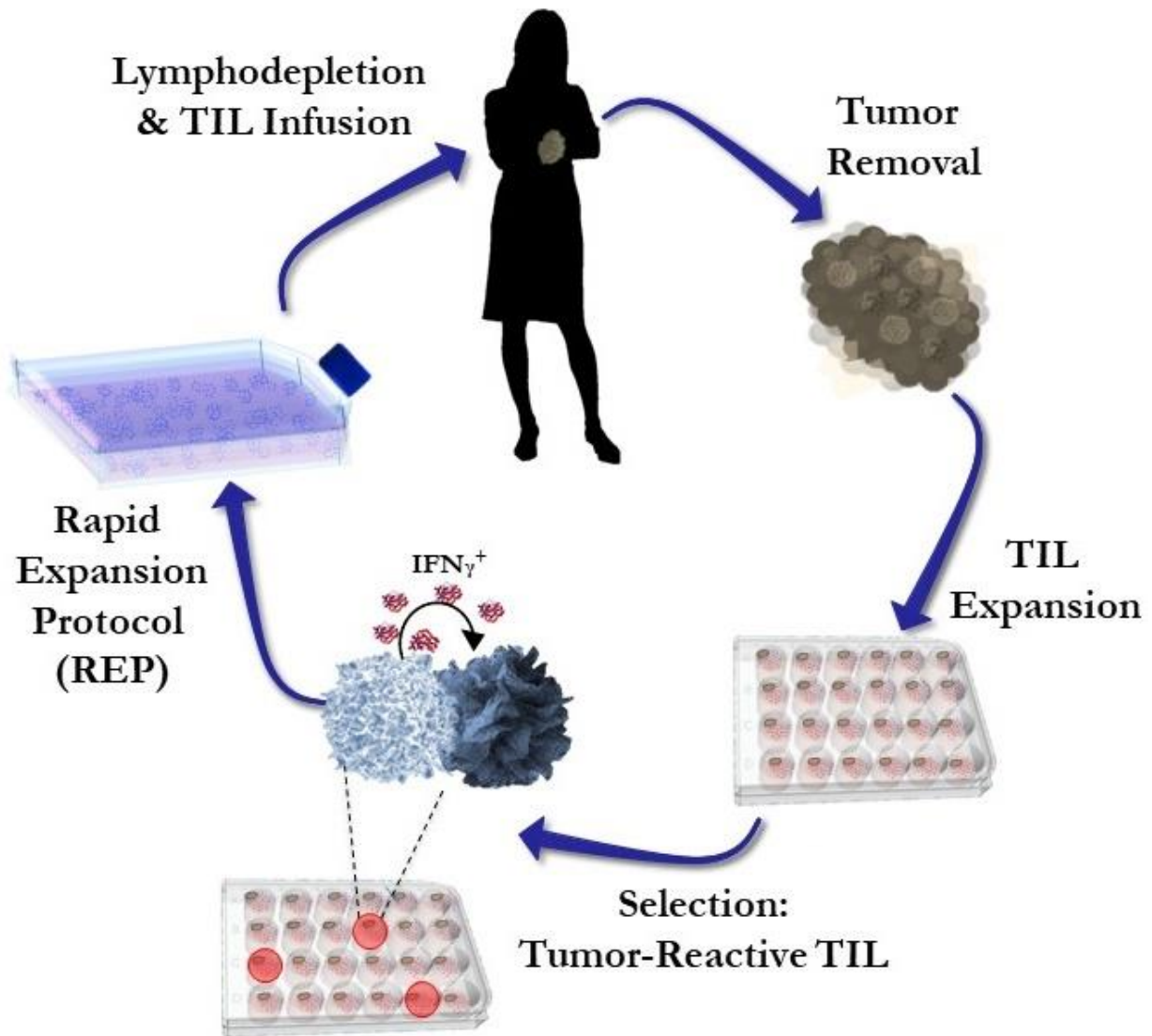


**Figure 1. A schema of ACT with TILs.**

A tumor is surgically resected from a patient and fragmented. Tumor fragments are grown in media containing IL-2 to promote TIL expansion. Expanded TILs are then tested for tumor-reactivity by culturing the TILs with autologous tumor cells and assessing the production of effector molecules, such as IFN- $\gamma$ . The selected tumor-reactive TILs are then expanded under a REP to a magnitude typically  $>5 \times 10^{10}$  cells. Prior to re-infusion, patients are lymphodepleted with non-myeloablative doses of cyclophosphamide and fludarabine. Image generated by: MacLean Hall and Luz Nagle, Dr. Shari Pilon-Thomas Laboratory.

## **Preparative lymphodepletion is essential to elicit durable therapeutic responses to ACT**

The infusion of melanoma-specific T cells can effectively kill tumor cells in patients, which can cause the cytotoxicity of non-malignant melanocytes as an “on-target/off-tumor” side effect since antigen epitopes for melanoma cells and melanocytes are shared (25). Despite that the killing of tumor cells can be elicited after the infusion of tumor-specific T cells in patients, clinical response rates were not consistently observed until ACT was combined with lymphodepleting chemotherapy and/or total body radiation TBI (2, 26). Lymphodepleting regimens typically consist of non-myeloablative (NMA) doses of cyclophosphamide and fludarabine and/or TBI (27). The rationale to combine ACT with lymphodepleting regimens was drawn from the experience of creating optimal conditions in a host to facilitate engraftment after HSCT. In HSCT regimens, complete myeloablation is induced via chemotherapy to simultaneously eliminate malignant immune cells, provide a niche for the engraftment of donor cells, and prevent tissue rejection after allogeneic transplantation (28). For ACT however, the goal of pre-conditioning regimens is to eliminate lymphocytes that compete for cytokines necessary for the proliferation and function of adoptively transferred T cells *in vivo* (discussed later in this chapter). Notably, most cancers are relatively sensitive to chemotherapy or radiotherapy. However, melanomas are largely resistant to chemotherapeutic agents and radiation therapy, particularly in comparison to immune-based therapies (29, 30). Hence, a lymphodepleting regimen for ACT purposes in melanoma patients does not provide therapeutic benefit. Rather, lymphodepleting doses of cyclophosphamide and fludarabine mainly facilitate the optimal engraftment of adoptively transferred TILs. In contrast, chemotherapy agents like cyclophosphamide and fludarabine in other malignancies, such as acute lymphoid leukemia (ALL), are therapeutically efficacious as a standard of care treatment (31, 32). Thus,

lymphodepleting regimens have a direct anti-tumor benefit against leukemic cells and the combination with CAR-T cell infusion can further clear target cells. Many chemotherapeutic compounds also have lymphodepleting effects. The combination of a lymphodepleting temozolomide regimen and ACT with Epidermal Growth Factor variant III (EGFRvIII)-directed CAR T cells in glioblastoma multiforme (GBM) mouse models demonstrated increased persistence of infused T cells and enhanced regression of tumors in the combination therapy compared to ACT with CAR T cells alone (33). In addition, this work provided support for a clinical trial in patients with Grade IV Glioma (NCT02664363). Thus, it is an attractive strategy to augment the success of ACT in human malignancies by exploring the utilization of chemotherapy agents that simultaneously lymphodeplete patients to provide a supportive niche for infused T cells and induce the cytotoxicity of tumor cells.

Preclinical mouse models have demonstrated that the infusion of gp100-specific pmel T cells in B16 tumor-bearing mice could significantly induce tumor regression, but only when ACT was combined with non-myeloablative TBI (Figure 2) (34). Moreover, the efficacy of ACT in combination with TBI was attributed to increased serum levels of IL-7 and IL-15 indicating that infused T cells take advantage of the availability of homeostatic cytokines to mount effective anti-tumor responses. In contrast to these results, IL-7 is not elevated in tumor-bearing BALB/C mice after lymphodepleting cyclophosphamide treatment (35). However, several studies in C57BL/6 mice have demonstrated the importance of IL-7 in a post-lymphodepletion setting, suggesting that the increase of homeostatic cytokines after lymphodepleting regimens could be model specific (34, 36-39). Importantly, several clinical trials investigating the combination of lymphodepletion regimens with ACT demonstrated increases of IL-7 and/or IL-15 post-lymphodepletion and T cell infusion confirming the previous findings in murine models (26, 40-

44). Elevated serum and plasma levels of IL-7 and IL-15 in response to a lymphodepleting regimen were first demonstrated by Dudley et. al. in melanoma patients receiving ACT with TIL (26). Recent studies demonstrated similar findings in synovial sarcoma patients treated with NY-ESO-1-directed transgenic T cells, whereby increases of IL-7 and IL-15 were only observed in patients pre-conditioned with both cyclophosphamide and fludarabine compared to cyclophosphamide alone (43). Additionally, Ramachandran et. al. demonstrated that lymphodepleting regimens containing higher doses of fludarabine are necessary for enhanced *in vivo* T cell persistence and improved clinical response rates exhibited in this trial, suggesting that IL-7 and IL-15 are necessary for T cell support after infusion (43). Moreover, lymphoma remissions and the magnitude of anti-CD19 CAR T cell expansion have been associated with high serum abundance of IL-7, IL-15, and CCL-2 (40, 44). Therefore, the increased availability of cytokines such as IL-7 and IL-15 are critical for efficacious responses in patients undergoing ACT in combination with lymphodepleting regimens.

The abundance of homeostatic cytokines and enhanced tumor regression rates has been associated with increased intensity lymphodepleting regimens when in combination with ACT (26, 43). Initial studies in mice indicated that an increased degree of lymphodepletion (i.e. myeloablation) with ACT in combination HSCT could enhance tumor regression (34, 45). B16 tumor-bearing mice that received myeloablative or non-myeloablative TBI with HSCT in combination with ACT had an increased persistence of pmel T cells and an enhanced rate of tumor rejection compared to mice that did not receive HSCT (45). This suggested that not only could a higher intensity of lymphodepletion promote the efficacy of ACT, but that hematopoietic stem cells also work in conjunction with adoptively transferred T cells to eliminate tumors. Subsequent clinical studies by Rosenberg et. al. initially validated these findings reporting that

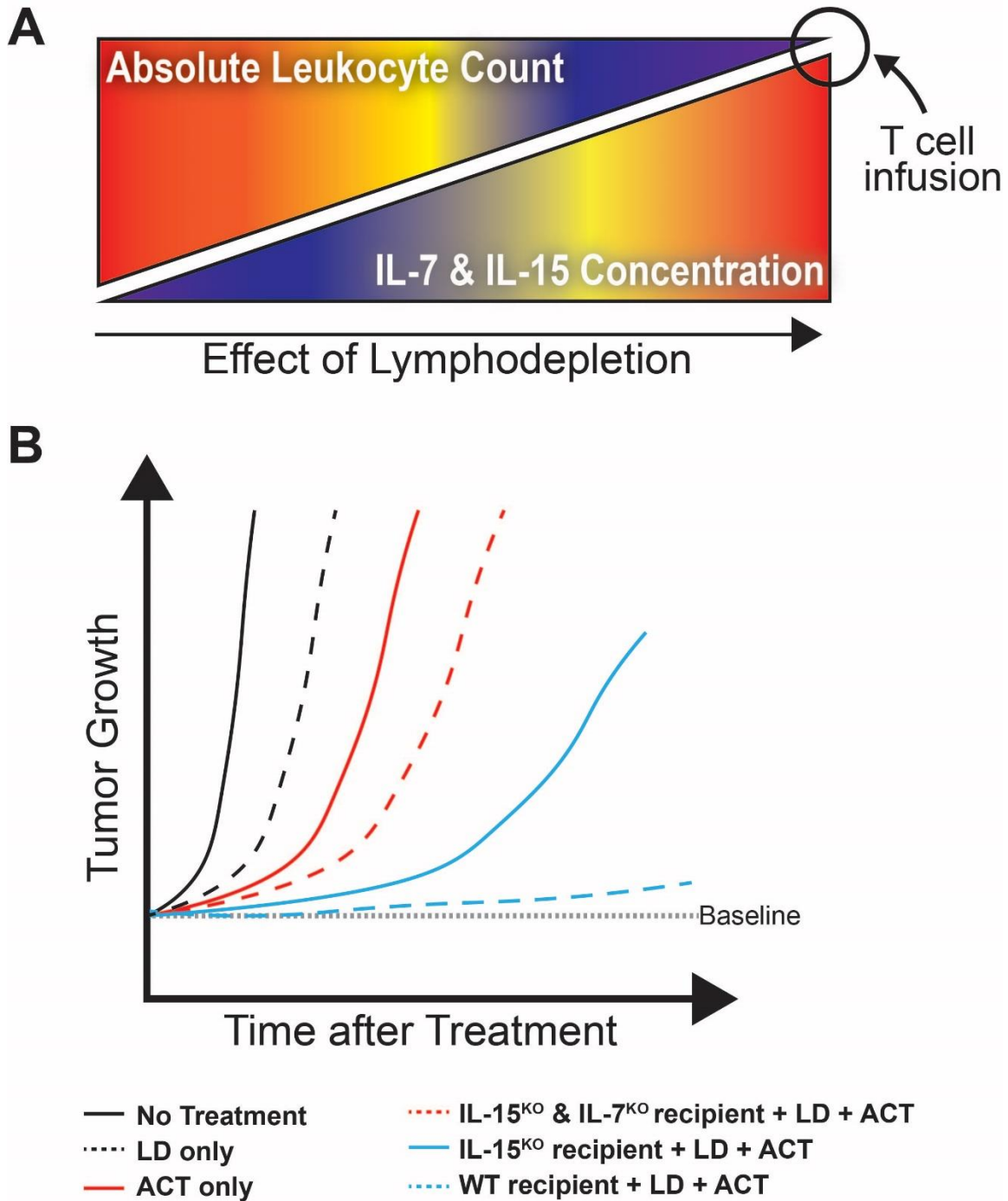


**Figure 2. The increased availability of IL-7 and IL-15 induced by lymphodepletion promotes the efficacy of ACT.** (A) The absolute leukocyte count (ALC) and the concentrations of IL-7 and IL-15 are inversely related. At the nadir of the ALC, T cells are adoptively transferred to take advantage of an increased pool of IL-7 and IL-15. (B) The induction of IL-7/IL-15 by lymphodepletion regimens are necessary to induce potent anti-tumor responses after adoptive T cell transfer. Each line is a representation of tumor growth over time in mice. Graph is adapted from (34). LD=lymphodepletion.



response rates were higher in melanoma patients that received ACT in combination with myeloablative therapy and HSCT compared to patients that received ACT with NMA chemotherapy alone (Overall response rate: 72% and 48% respectively) (26). These findings indicated that an increased intensity of lymphodepletion could promote anti-tumor immunity elicited by ACT with TILs in human melanoma patients. However, the same group later conducted a randomized clinical trial and reported contradictory findings in that response rates were not significantly different between patients that received ACT with TILs in combination with myeloablative chemotherapy and HSCT in comparison to patients that received ACT plus NMA chemotherapy without HSCT (27). The authors concluded that the contradiction of earlier findings could be attributed to patient selection and emphasized the importance of randomization for clinical trials. Overall, lymphodepletion is necessary to combine with ACT to achieve clinical efficacy, but the increased intensity of lymphodepleting regimens and subsequent HSCT may not have a clinical benefit to melanoma patients.

The rationale for increased intensity lymphodepleting regimens for ACT is not unfounded. Many clinical trials have investigated various lymphodepleting regimens in combination with ACT for the treatment of solid tumors and hematologic malignancies (Table 1). Compared to lymphodepleting regimens with cyclophosphamide alone, the administration of both cyclophosphamide and fludarabine has demonstrated the following: 1. Increased the abundance of serum IL-7 and IL-15 (43, 46), 2. Higher complete/partial clinical response rates in synovial sarcoma patients receiving NY-ESO-1-directed transgenic T cells (43), 3. Longer progression-free survival in lymphoma patients receiving anti-CD19 CAR T cells (46). Hence, the addition of fludarabine may be required to enhance the efficacy of ACT and future studies need to address what degree of lymphodepletion is necessary to achieve the best clinical

responses. Conversely, the benefit of myeloablative regimens in addition to HSCT and ACT regimens may be beneficial for specific indications. The survival rates of patients with acute lymphoblastic leukemia (ALL) treated with CD19-directed CAR T cells were significantly higher when these patients received lymphodepletion and consolidation HSCT compared to patients that received consolidation HSCT and CAR T cells without lymphodepletion (47, 48). Notably, patients that had a complete response to the CAR T cell therapy underwent consolidation HSCT because that is the standard of care treatment for pediatric ALL patients that are negative for minimal residual disease to minimize the probability of disease recurrence (48). Likewise, the infusion of WT1-specific T cells preceded by allogeneic HSCT in acute myeloid leukemia (AML) patients demonstrated a 100% relapse-free survival rate with a median duration of 44 months post-infusion of T cells (21). Hence, the combination of ACT with complete myeloablation and HSCT may provide a therapeutic benefit to cancer patients, but the efficacy is likely dependent on the disease, patient cohort, and treatment strategy.

Ample evidence has been provided in support of combining lymphodepleting regimens with ACT. However, increased dosing of chemotherapy and myeloablation is consistent with regimen-associated toxicity, including exacerbated neutropenia, infection, anemia, thrombotic microangiopathy, thrombocytopenia, pancreatitis, neurotoxicity, cardiotoxicity, and death (5, 8, 26, 27, 46, 49). Additionally, the exposure to cyclophosphamide has been associated with an increased risk of developing bladder cancer, non-melanoma skin cancer, and myeloid leukemia (50, 51). Moreover, the prior treatment of chemotherapy is associated with an increased risk of developing myelodysplastic syndrome (MDS) and AML as determined among a cohort of >700,000 patients with solid tumors consisting of 22 different malignancies (52). Despite that lymphodepleting regimens augment the efficacy of ACT, the usage of cytotoxic agents in

patients with solid tumors for this purpose is not without significant risks. Hence, regimen-associated toxicities and risks should be strongly considered when investigating pre-conditioning regimens prior to ACT. Ultimately, the elimination of lymphodepleting regimens prior to ACT would be ideal to reduce treatment-associated morbidities and potentiate patient-treatment eligibility. Some clinical trials have observed tumor shrinkage and complete regressions after ACT without any pre-conditioning lymphodepletion (53-55). However, a universal solution that circumvents the utilization of cytotoxic lymphodepleting regimens to promote the activity of ACT, particularly in patients with solid tumors has yet to be implemented successfully in the clinic.

### **Strategies to enhance the efficacy of ACT**

In contrast to TILs, genetic modifications are inherent to the production of CAR-T cells and TCR-transgenic T cells. Several groups have utilized innovative approaches to further modify T cells to enhance their *in vivo* persistence, resistance to exhaustion, and increase cytotoxic capabilities, which has been extensively reviewed in recent literature (60, 61). A list of strategies to enhance the efficacy of ACT focused on the **enrichment**, the **expansion**, the **modification**, and **host-conditioning** aspects are summarized here (see Figure 3; Table 2).

The identification of target antigens and the **enrichment** of tumor-specific T cell clones is a critical aspect of promoting a robust anti-tumor response via ACT. However, recent findings have highlighted the scarcity of tumor-reactive T cells within tumors. Tumors are commonly infiltrated with T cells, known as bystander T cells that hold specificity for non-overlapping antigens, such as viral epitopes (including Epstein-Barr virus, human cytomegalovirus, and human influenza) (62). Within the past three years, several studies have identified the presence

**Table 1. Summary of clinical trials exploring various pre-conditioning regimens for ACT**

Disease	ACT Strategy	Lymphodepleting Regimen	Additional Therapy	Key Findings	Reference
Melanoma	TIL	Cy/Flu	None	<ul style="list-style-type: none"> <li>Enhanced survival with TBI combined with HSCT</li> </ul>	(26)
		Cy/Flu + 200cGy TBI	HSCT		
		Cy/Flu + 1200cGy TBI	HSCT		
Melanoma	TIL	Cy/Flu	None	<ul style="list-style-type: none"> <li>No survival difference observed with Cy/Flu+TBI+HSCT in randomized trial</li> </ul>	(27)
		Cy/Flu + 1200cGy TBI	HSCT		
Neuroblastoma	GD2-directed EBV-CTLs or ATCs	None	None	<ul style="list-style-type: none"> <li>Similar persistence of both EBV-CTLs and ATCs</li> <li>Higher peak expansion of CAR EBV-CTLs</li> <li>CRs and NED observed</li> </ul>	(54)
Neuroblastoma	GD2-directed ATCs	None	Anti-PD-1 (pembrolizumab)	<ul style="list-style-type: none"> <li>Elevated IL-15 and CAR-T persistence in cohorts receiving Cy/Flu</li> </ul>	(41)
		Cy/Flu			
Pancreatic Cancer	Mesothelin CAR-T	None	None	<ul style="list-style-type: none"> <li>Cy enhanced CAR-T expansion <i>in vivo</i></li> </ul>	(56)
		Cy			
Multiple Myeloma	NY-ESO-1 TCR-transgenic T cells	Prior HSCT	Lenalidomide	<ul style="list-style-type: none"> <li>Long-term persistence of T cells</li> <li>CRs and NED observed</li> </ul>	(57)
Synovial Sarcoma	NY-ESO-1 TCR-transgenic T cells	Cy <sup>high/low</sup> /Flu	None	<ul style="list-style-type: none"> <li>Elevated IL-7 &amp; IL-15 and T cell engraftment with Cy/Flu vs. Cy alone</li> </ul>	(43)
		Cy			
NHL	CD19 CAR-T	Cy <sup>low</sup> /Flu	None	<ul style="list-style-type: none"> <li>Elevated IL-7 and CCL-2</li> <li>Cy<sup>high</sup>/Flu associated with increased CAR-T expansion &amp; better clinical responses</li> </ul>	(40)
		Cy <sup>high</sup> /Flu			
NHL	CD19 CAR-T	Cy/Flu	HSCT 2° CAR-T	<ul style="list-style-type: none"> <li>Enhanced CAR-T expansion &amp; clinical responses with Flu</li> </ul>	(58)
		Cy/Etoposide			
		Cy			
DLBCL	CD19 CAR-T	None	None	<ul style="list-style-type: none"> <li>Poor ORR without LD</li> <li>ORR similar between Cy/Flu and bendamustine</li> </ul>	(59)
		Cy/Flu			
		Bendamustine			
EBV <sup>+</sup> HL/NHL	EBV-CTLs	None	2° EBV-CTLs	<ul style="list-style-type: none"> <li>Long-term persistence of T cells</li> <li>CRs and NED observed</li> </ul>	(55)
EBV <sup>+</sup> HL	DN-TGFβRII EBV-CTLs	None	Various	<ul style="list-style-type: none"> <li>Long-term persistence of T cells</li> <li>CRs and NED observed</li> </ul>	(53)
EBV <sup>+</sup> nasopharyngeal carcinoma	EBV CTLs	Anti-CD45 mAbs	None	<ul style="list-style-type: none"> <li>1 CR</li> <li>Long-term persistence of T cells</li> </ul>	(42)
B cell malignancies	Donor CD19 CAR-VSTs	Prior HSCT	1°-3° CAR-T	<ul style="list-style-type: none"> <li>Long-term persistence of T cells</li> <li>CRs and NED observed</li> </ul>	(55)

Abbreviations: TIL (tumor infiltrating lymphocytes); Cy/Flu (cyclophosphamide/fludarabine); cGy (centigray); TBI (total body irradiation); HSCT (hematopoietic stem cell transplant); GD2 (disialoganglioside); EBV-CTLs (Epstein-Barr virus cytotoxic T lymphocytes); ATCs (activated T cells); CR (complete response); NED (no evidence of disease); NHL (non-Hodgkin's lymphoma); HL (Hodgkin's lymphoma); 1°, 2°, 3° (primary, secondary, or tertiary T cell infusions); DLBCL (Diffuse Large B cell Lymphoma).

of both tumor-specific and bystander TILs in multiple cancer types (63-66). Transcriptomic and phenotypic analysis revealed that tumor-specific TILs have inherent exhaustion characteristics and phenotypes resembling tissue-resident memory T cells as defined by the expression of CD69, CD103, and CD39 in combination with exhaustion markers such as PD-1 and TIM-3 (62, 64-66). These findings have provided direction into identifying tumor-specific T cells that may be exploited to generate clinical infusion products.

Recently, the identification of both tumor neoantigens and cognate antigen-specific TILs in patients has provided exciting new routes of treatment for cancer patients on a highly personalized level and eliminates the possibility of outgrowing bystander TILs. Tran et. al. identified T cells specific for the oncogenic mutant protein, KRAS<sup>G12D</sup>, in a patient with colorectal cancer (3). Their approach to identify KRAS<sup>G12D</sup>-specific TILs leveraged whole exome sequencing and RNA sequencing to identify nonsynonymous mutations within the patient's tumor for the purpose of synthesizing peptides derived from mutant proteins (67). These peptides are then presented through autologous antigen presenting cells (APCs), which are co-cultured with the patient's TILs. Through this approach, the APCs stimulate TILs that are specific for the library of synthesized peptides that can then be expanded for the purpose of ACT. The infusion of  $>1 \times 10^{11}$  KRAS<sup>G12D</sup>-specific TILs to the colorectal cancer patient led to complete regression of lung metastases, demonstrating that targeting a singular neoantigen with ACT can provide robust therapeutic responses in cancer patients. Recently, the same group reported that a heavily pretreated metastatic breast cancer patient exhibited a complete response after ACT with TILs specific for 4 mutant proteins - SLC3A2, KIAA0368, CADPS2 and CTSB (4). Notably, this patient's complete response was associated with the detection and persistence of the infused TIL 17 months after cell transfer. This finding indicated that immunotherapy and

ACT could be effective in cancer patients even if the disease generally immunologically inert, as in the case of breast cancer (68). With this approach, Rosenberg et. al. have identified TILs specific for multiple neoantigens across several cancer types, some of which are commonly mutated in a variety of diseases, including mutant p53, the most commonly mutated gene in cancer (67, 69, 70). While targeting p53 with this approach is limited by the HLA restriction elements specific to each individual patient, there is potential for the synthesis of TCRs specific for common oncogenic and mutated tumor-suppressor proteins like KRAS and p53 that would act as an “off the shelf” ACT strategy. This highly personalized mode of therapy provides a powerful means to promote durable remissions to cancer patients.

The demand of T cell **expansion** to generate clinical infusion products is contradictory to the nature of T cell biology. The precedent to infuse high amounts of TILs or CAR-T cells stems from experiences in clinical trials whereby patients that received higher number of T cells exhibited enhanced clinical response rates (71, 72). However, the continuous expansion of T cells skews in favor of effector T cell development ( $T_{eff}$ ) and the onset of T cell exhaustion that limits the capacity to persist long-term *in vivo* (73). While the infusion of high numbers of T cells are associated with better clinical responses, there is mounting evidence that the infusion of T cells that are dominantly memory T cells ( $T_{mem}$ ) can also promote durable anti-tumor responses (58, 74-76). Notably,  $T_{mem}$  cells have a greater capacity to persist long term *in vivo*, but also give rise to  $T_{eff}$  cells which can conduct cytotoxic responses with haste. Thus, a balance between expanding high numbers of T cells and maintaining an abundance of  $T_{mem}$  appears to be ideal for most settings of ACT. One strategy to augment the expansion of  $T_{mem}$  has been the addition of IL-7 and/or IL-15 with IL-2 in T cell growth media (77). IL-2 selectively promotes the differentiation of  $T_{eff}$  cells at the expense of  $T_{mem}$ . In contrast, IL-7 and IL-15 are involved in

the maintenance of  $T_{\text{mem}}$ . Thus, an optimal stimulus may be achieved by utilizing a balance of cytokine signals that regulate  $T_{\text{mem}}$  and prevention excessive  $T_{\text{eff}}$  differentiation. Other strategies to enhance memory characteristics of T cells are highlighted in Figure 3.

A critical limiting factor for ACT is the presence of exhausted T cells ( $T_{\text{ex}}$ ) which have a finite ability to proliferate and are susceptible to apoptosis upon persistent TCR stimulation. Single-cell RNA sequencing studies have revealed a remarkable complexity and heterogeneity among  $T_{\text{ex}}$  cells in tumors, whereby subsets of  $T_{\text{ex}}$  cells maintain stem and resident memory characteristics that can differentiate to more proliferative T cells bearing an increased cytotoxic capacity (64, 65, 78). Despite that  $T_{\text{ex}}$  have an ability to persist within tumors, increasing evidence has suggested irreversible exhaustion can be the fate and potentially the demise of tumor-reactive T cells. Specifically, the transcription factor Thymocyte selection-associated high mobility group box protein (TOX) appears to be a master regulator of T cell exhaustion (79, 80). Hence, it is imperative that protocols to generate T cell infusion products take on approaches that minimize the onset of exhaustion during expansion.

The genetic **modification** of T cells has allowed researchers to exploit the deficiencies of ACT. The improvement of technology and protocols designed to genetically engineer T cells has led investigators to modify TILs for the purpose of ACT (81). In contrast to CAR T cells or TCR-transgenic T cells, the genetic modification designed to force antigen specificity is not required in TILs. Instead, investigators have focused on augmenting the cytotoxic potential of TILs via elimination of Programmed Death-1 (PD-1) (81) or inducible expression of IL-12 (82) by genetic engineering strategies. However, much like the single dose administration of recombinant IL-12 to patients (83), toxicity related to TIL IL-12 expression was deemed unsafe (82). Hence, the careful consideration of potential side effects is necessary when exploring

strategies involved with the modification of T cells. Other efforts to genetically modify TIL include the forced expression of CXCR2 to enhance TIL trafficking to tumor beds after infusion (84).

While the genetic modification of TILs is still within the immature stages of clinical development, several innovative approaches have been explored to enhance the activity of T cells for other modalities of ACT. Specifically, the “armoring” of T cells to produce cytokines or express co-stimulatory ligands engages adoptively transferred cells to enhance the anti-tumor response of local tumor-associated immune cells. For instance, the expression of IL-12 or CD40L by CAR-T cells can stimulate the maturation of DCs and potentiate the reprogramming of the tumor microenvironment resulting in the elimination and/or control of tumor growth (85-87). Other approaches have focused on specifically enhancing the *in vivo* expansion capacity of T cells. The engineering of synthetic mutant pairs of the IL-2R and its cognate ligand, IL-2, allows the selective expansion of the modified T cells with negligible toxicity (88). While CARs and transgenic TCRs have already demonstrated that genetically modified T cells engineered to target a specific-antigen is safe and efficacious, multiple clinical trials have been conducted that have further modified T cells including the knockout of PD-1 or the expression a dominant-negative form of TGF- $\beta$ RII to overcome tumor-mediated immunosuppression (53, 89). Together, the advanced technology involved in the genetic modification endows the potential to generate sophisticated T cells that can simultaneously overcome multiple barriers that limit the efficacy of ACT.

The coordination between adoptively transferred T cells and endogenous immune cells is vital to completely eradicate tumors, particularly in metastatic cancer patients. In the setting of ACT, the role of endogenous immune cells can be exploited by **host-conditioning**. As discussed



earlier in this chapter, the conditioning of hosts with lymphodepleting regimens is indispensable to observe durable clinical benefit in cancer patients. Previous efforts to mitigate immunosuppression in ACT regimens have included combinations with checkpoint blockade therapy (8, 71). However, these therapies inhibit T cell intrinsic suppressive mechanisms and the inhibition of immunosuppressive myeloid cells in combination with ACT has not been explored in clinical trials. The curtailment of myeloid-mediated immunosuppression after the adoptive transfer of T cells is a critical element in the promotion of tumor cytotoxicity that will be discussed later in Chapter 3.

Many other forms of host-conditioning have been explored in both pre-clinical models and in clinical trials. Most commonly, the administration of recombinant IL-2 immediately following the infusion of T cells has been consistently used in melanoma patients that receive autologous TILs (2, 6, 49). Similarly, the administration of IL-7, IL-15, and IL-1 $\beta$  have been shown to enhance the efficacy of ACT and promote the persistence of infused T cells in pre-clinical models (35, 37, 90). However, the administrations of these cytokines have been deemed unsafe due to toxicity or have yet to reach clinical trials. Other approaches to facilitate the expansion of adoptively transferred T cells *in vivo* include the electroporation of T cells with mRNA encoding IL-12 or 41BBL (91). In this study, tumor-specific T cells were electroporated with mRNA and infused intravenously or directly into tumor lesions. Remarkably, the direct injection of T cells into tumors led to the regression of distal untreated tumors indicating that the electroporated T cells could induce a systemic immune response. A similar approach implementing the intratumoral administration of IL-23, IL-36 $\gamma$ , and OX40L mRNA encapsulated within lipid nanoparticles has demonstrated potent systemic anti-tumor immune responses (92). The combination of tumor-immune reprogramming via mRNA therapy with ACT has not yet

been explored in clinical trials. However, this innovative approach effectively induces a systemic immune response against distal, untreated lesions. Thus, mRNA therapy is an attractive strategy that could condition the host during the course of ACT to enhance anti-tumor T cell responses. Collectively, a comprehensive approach addressing multiple components and deficiencies of ACT will most likely have the most success in boosting clinical response rates.

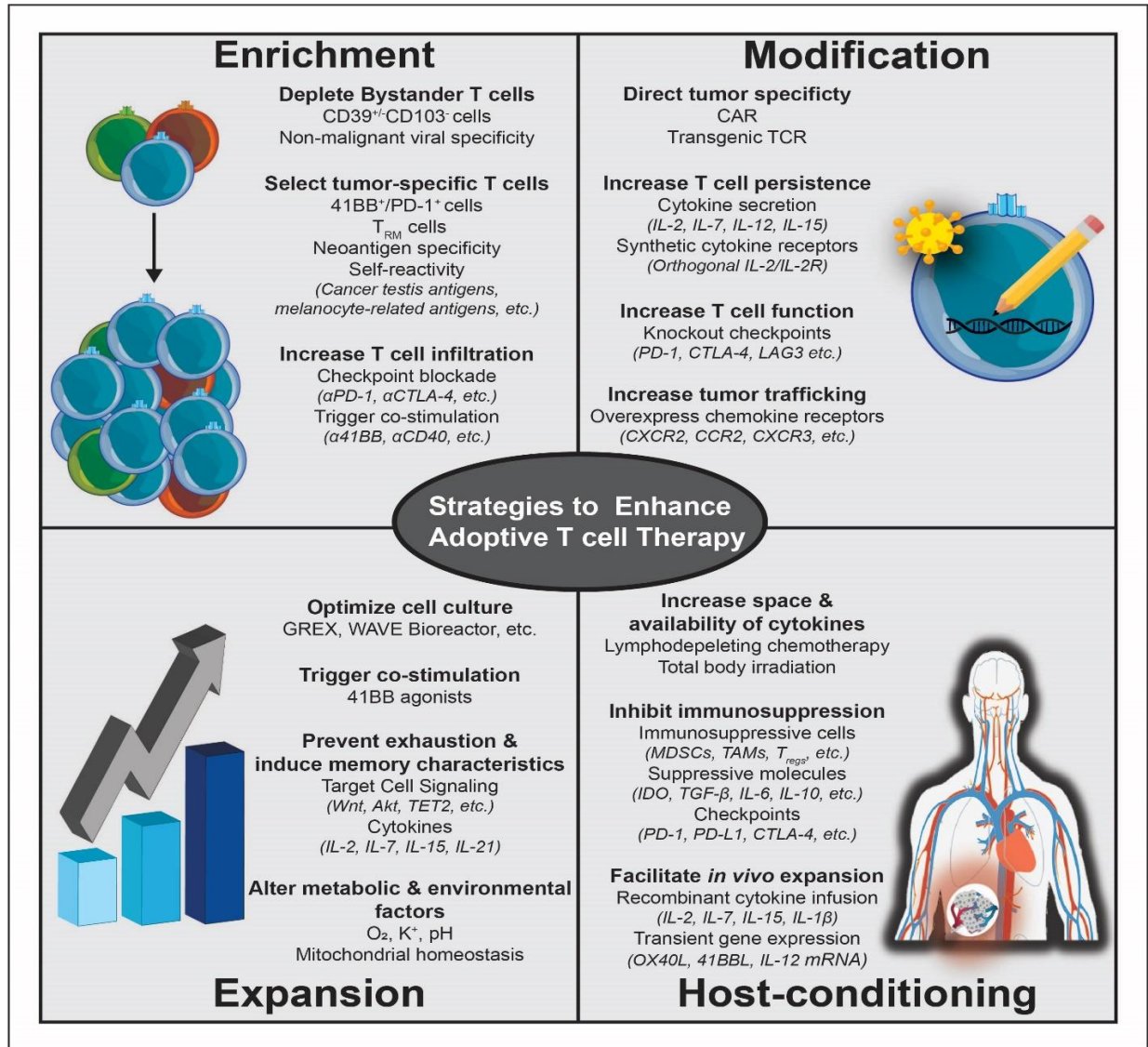


**Figure 3. Strategies to Enhance ACT.**

The “Enrichment” of tumor-specific T cell clones reduces the likelihood of a dilution effect by irrelevant T cell clones or competition for nutrients and cytokines that are necessary for the expansion of T cells. The “Modification” of T cells can be utilized to boost the anti-tumor functionality of T cells upon adoptive transfer. The “Expansion” of T cells is a critical aspect of ACT because high numbers of T cells are needed for infusion to elicit durable responses in cancer patients. “Host-conditioning” is a necessary aspect of ACT that facilitates the engraftment, long-term persistence of infused T cells, and regression of multiple tumor lesions.

**Table 2. List of references for Figure 3**

Category	Rationale for Strategies to Enhance ACT	Reference(s)
Enrichment	CD39 and CD103 identify bystander vs. tumor-specific T cells	(62, 65)
	41BB and PD-1 positivity identifies tumor-reactive T cells	(93)
	Tumor-specific T cells are enriched within a population of T <sub>RM</sub> cells	(62, 65, 66)
	Adoptive transfer of neoantigen-specific T cells elicits durable complete responses in multiple malignancies	(3, 4)
	Expansion of endogenous T cells specific for cancer testis antigens and melanocyte related antigens	(25, 94)
	Checkpoint blockade increases T cell infiltration within tumors	(95)
	41BB agonists expand tumor-specific T cells	(96)
	CD40 agonists expand tumor-specific T cells	(97)
Modification	T cells engineered to express IL-2, IL-7, IL-12, IL-15	(82, 87, 98)
	Engineering of orthogonal IL-2/IL-2R $\beta$ complexes allows for the selective potentiation of adoptively transferred T cells	(88)
	The knockout of checkpoints increases T cell function	(89)
	Tumors express an abundance of chemokines to attract various immune cells to tumor beds	(99, 100)
Expansion	GREX flasks and WAVE bioreactors enhance the <i>in vitro</i> expansion of T cells	(101, 102)
	41BB agonists enhance the <i>ex vivo</i> expansion of TILs from melanoma tumors	(96, 103)
	Activation of Wnt signaling enhances the generation of T <sub>SCM</sub> cells	(104)
	Inhibition of Akt enhances the expansion of memory T cells	(105)
	TET2 disruption by insertional mutagenesis potentiates the expansion of CD19-directed CAR-T cells <i>in vivo</i>	(75)
	<i>In vitro</i> expansion of T cells with cytokine cocktails containing IL-2/IL-7/IL-15/IL-21 promote the expansion of memory T cells	(106, 107)
	Hypoxia promotes the expansion of effector T cells	(108)
	High concentrations of potassium (K <sup>+</sup> ) within tumors promotes T cell stemness	(109)
	Acidic pH of the tumor microenvironment restricts T cell function	(110)
Host-conditioning	Lymphodepletion promotes the availability of homeostatic cytokines	(34)
	MDSCs, TAMs, and T <sub>regs</sub> suppress the activity of cytotoxic T cells	(111)
	The combination of checkpoint blockade with ACT elicits durable responses in patients with solid tumors	(8, 41)
	The infusion of IL-2, IL-7, IL-15, or IL-1 $\beta$ promotes the expansion and persistence of infused T cells	(35, 37, 90, 112)
	Electroporation of OX40L, 41BBL, or IL-12 mRNA into T cells promotes anti-tumor immunity upon adoptive transfer	(91, 92)

## CHAPTER TWO

### INTRATUMORAL ACTIVATION OF 41BB CO-STIMULATORY SIGNALS ENHANCES CD8 T CELL EXPANSION AND MODULATES TUMOR INFILTRATING MYELOID CELLS

**A note to the reader: the majority of this chapter has been accepted for publication in a research article in *The Journal of Immunology*, Innamarato et. al., 2020.**

#### **Introduction**

##### *The blockade of inhibitory signals enhances anti-tumor T cell functions*

It is well understood that despite the presence of T cells with tumor-cytotoxic potential in cancer patients, tumors progress and evade immune-mediated destruction. Despite that cancer promotes immune dysfunction, vaccine strategies have been utilized to promote the expansion of tumor-specific T cells, demonstrating that the immune system can be primed to recognize and eliminate tumors (113, 114). However, previous clinical trials have failed to during development due to the lack of clinical benefit (115, 116). Despite that the therapeutic efficacy of cancer vaccines could not be achieved on a sufficient scale to warrant its widespread use in the clinic, findings in these studies have catalyzed new strategies to leverage the immune system to combat cancer.

In recent years, immunotherapy in cancer has burgeoned due to the development and clinical implementation of therapeutics that alleviate tumor-mediated immunosuppression on T

cells. Tumors exploit immune checkpoints including Programmed Death 1 (PD-1) and Cytotoxic T-Lymphocyte Associated Protein 4 (CTLA-4) to deactivate T cells, leading to immune evasion. PD-1 and CTLA-4 are co-inhibitory cell surface receptors expressed by T cells that reduce T cell activation, induce anergy, and promote cell death when activated by their cognate ligands (117). In addition, the expression of Programmed Death Ligand 1 (PD-L1) is one of the primary mechanisms by which tumor cells evade and actively suppress cytotoxic T cells (118). Conversely, the blockade of PD-1 or its cognate ligand PD-L1 has been proven to reinvigorate cytotoxic T cells and promote immune clearance of tumors (119). Notably, antibodies that block PD-1 or CTLA-4 have had remarkable clinical success providing complete responses in variety of cancer patients (120). While complete responses in metastatic cancer patients has been widely observed upon treatment with antibodies that target immune checkpoints, the majority of patients fail to respond to these therapies which has led to the development strategies that combine anti-PD-1/PD-L1 or anti-CTLA-4 therapies with standard of care chemo-radiotherapy, small molecule inhibitors, and novel immune-based therapies (121, 122). In addition, the combination of immune checkpoint inhibitors with ACT with TIL has demonstrated clinical efficacy in metastatic melanoma patients, indicating that the relief of immune suppression of adoptively transferred T cells could improve clinical responses rates or enhance patient adherence throughout treatment on the clinical trial (8, 71).

### ***Triggering co-stimulation through 41BB revives tumor-cytotoxic T cells***

The state of exhaustion and dysfunction of T cells in tumors is due in part to the lack of co-stimulatory signals that can perpetuate the elimination of tumor cells. During naïve T cell priming, antigen-presenting cells (APCs) provide primary antigen-specific signals via membrane histocompatibility complex (MHC) proteins and secondary signals that stimulate co-stimulatory

receptors on T cells (123). Co-stimulatory molecules, CD80 and CD86, are expressed on APCs and engage the T cell co-stimulatory receptor, CD28, allowing efficient T cell priming and activation (124). The stimulation of activation signals in T cells can promote cytotoxic responses against tumor cells (125). In fact, the stratification of T cell subsets based on the expression of co-stimulatory molecules can indicate tumor-cytotoxic potential. In particular, the co-expression of the co-stimulatory receptor, 41BB, and PD-1 can identify a subset of cytotoxic TILs (93). In addition, upregulation of 41BB in TILs is consistent with the activation stimuli provided by autologous tumor (3). Hence, co-stimulatory molecules such as 41BB play a critical role in the identification and function of TILs.

The stimulation of 41BB has been widely explored in the purpose of potentiating T cell responses in tumors. Activating 4-1BB with monoclonal antibodies promotes IFN- $\gamma$  production, proliferation, and tumor regression in pre-clinical mouse models (126). Unfortunately, the robust anti-tumor immune responses exhibited in mice have not been replicated in clinical trials due to toxicity observed at efficacious doses of 41BB agonistic antibodies ( $\alpha$ 41BB) (127). Thus, newly developed therapeutics targeting 41BB have focused on selectively activating 41BB within tumor beds. This is in contrast to agonists that promote the systemic activation of 41BB and result in liver toxicity and other “on-target” co-morbidities (128). However, triggering co-stimulatory via 41BB is an effective strategy to promote T cell expansion *in vitro*. The use of  $\alpha$ 41BB is effective in enhancing the expansion of function of TILs *in vitro* for the purpose of treating melanoma patients with ACT (96). Intriguingly, the culture of tumors in media containing IL-2 alone may fail to result in the successful expansion of TILs. However, the stimulation of the same tumor with IL-2 and  $\alpha$ 41BB induces the expansion and enhances the cytotoxic potential of TILs. This suggests that co-stimulatory signals are often necessary to

expand TILs from tumors in culture (96, 129). Despite the hurdles of translating therapeutics that activate 41BB, it is clear that triggering 41BB can strongly potentiate anti-tumor immune responses.

### ***An overview 41BB-41BBL activity on myeloid cells***

41BB is widely known as a co-stimulatory molecule expressed by T cells, however nearly all subsets of immune cells express 41BB (130). Previous studies have identified that 41BB and 41BB ligand (41BBL) play critical, yet context-dependent roles in myeloid cell development and function (131, 132). In particular, the knockout of 41BB promotes the accumulation of myeloid cells under steady-state conditions, while triggering 41BB activation in dendritic cells (DCs) enhanced their capacity to stimulate T cell *in vitro* (131, 133). While accumulating evidence in mice has suggested that both 41BB and 41BBL are critical for directly regulating the function of myeloid cells, little is known about how this receptor-ligand axis potentiates myeloid-mediated anti-tumor immune responses in humans. Given that the importance of the inflammatory context in 41BB-41BBL signaling, a deeper understanding of 41BB-41BBL signaling in human myeloid cells, particularly in the context of tumor-mediated inflammation, is needed (131, 134).

In human biological systems, 41BBL acts as a maturation factor for monocytes, promoting the expression of co-stimulatory molecules and cytokines, including IL-12, IL-6, IL-8, TNF, and M-CSF (135). The stimulation of 41BBL with 41BB protein induces reverse signaling in monocytes, triggering their maturation to DCs (136). Although 41BB-41BBL bidirectional signaling between T cells and APCs has been shown to promote effector immune responses, it remains unclear how the context of inflammation within human tumors influence this process. At our institution, treatment of melanoma patients using ACT with TIL has resulted

in a 38% overall response rate (6, 8). Moreover, 41BB agonists are currently being explored for the ability to enhance TIL expansion for the use ACT (NCT02652455). The work outlined in this chapter highlights the importance of triggering co-stimulatory signals on T cells and how augmenting the interactions of 41BB-41BBL bidirectional signals provided by antigen presenting cells (APCs) ultimately provides support for the improvement of TIL expansion from primary tumor fragments and the promotion of anti-tumor immune responses *in vivo*.

## Results

### *Intratumoral 41BB activation leads to tumor regression in multiple models*

To determine the efficacy of 41BB agonists, we validated that systemic treatment via intraperitoneal (i.p.) administration led to tumor growth delay and complete regressions in mice with established MC38 tumors (Figure 4A, C). We observed that intratumoral (i.t.) administration with anti-41BB ( $\alpha$ 41BB) antibodies exhibited comparable efficacy to the i.p. route of administration by which the tumor growth kinetics and the frequency of complete regressions were similar (Figure 4B, D). We validated these results in two additional tumor models bearing the model ovalbumin antigen, Panc02-ZsGOVA (Figure 4E, G) and B16-OVA (Figure 4F, H). Intratumoral treatment of  $\alpha$ 41BB led to significant growth delay and tumor regression in mice with Panc02-ZsGOVA tumors (Figure 4E) and B16-OVA tumors (Figure 4F) compared to control mice that received i.t. isotype antibodies. Moreover, the survival of mice treated with i.t.  $\alpha$ 41BB was significantly enhanced in both models (Figure 4G-H). In mice with MC38 tumors, i.t.  $\alpha$ 41BB led to complete regressions in approximately 30% of treated mice (Figure 4D). Likewise, 70% of mice with Panc02-ZsGOVA tumors (Figure 4G) or B16-OVA tumors (Figure 4H) had no evidence of tumor growth after tumor inoculation (44 days and 70 days, respectively). This suggested that presence of a highly immunogenic antigen, such as



OVA, could potentially direct local anti-tumor immune responses after i.t. treatment with  $\alpha$ 41BB. Together, these data demonstrate that the intratumoral treatment with 41BB agonistic antibodies is a feasible approach to induce tumor regression in mice.

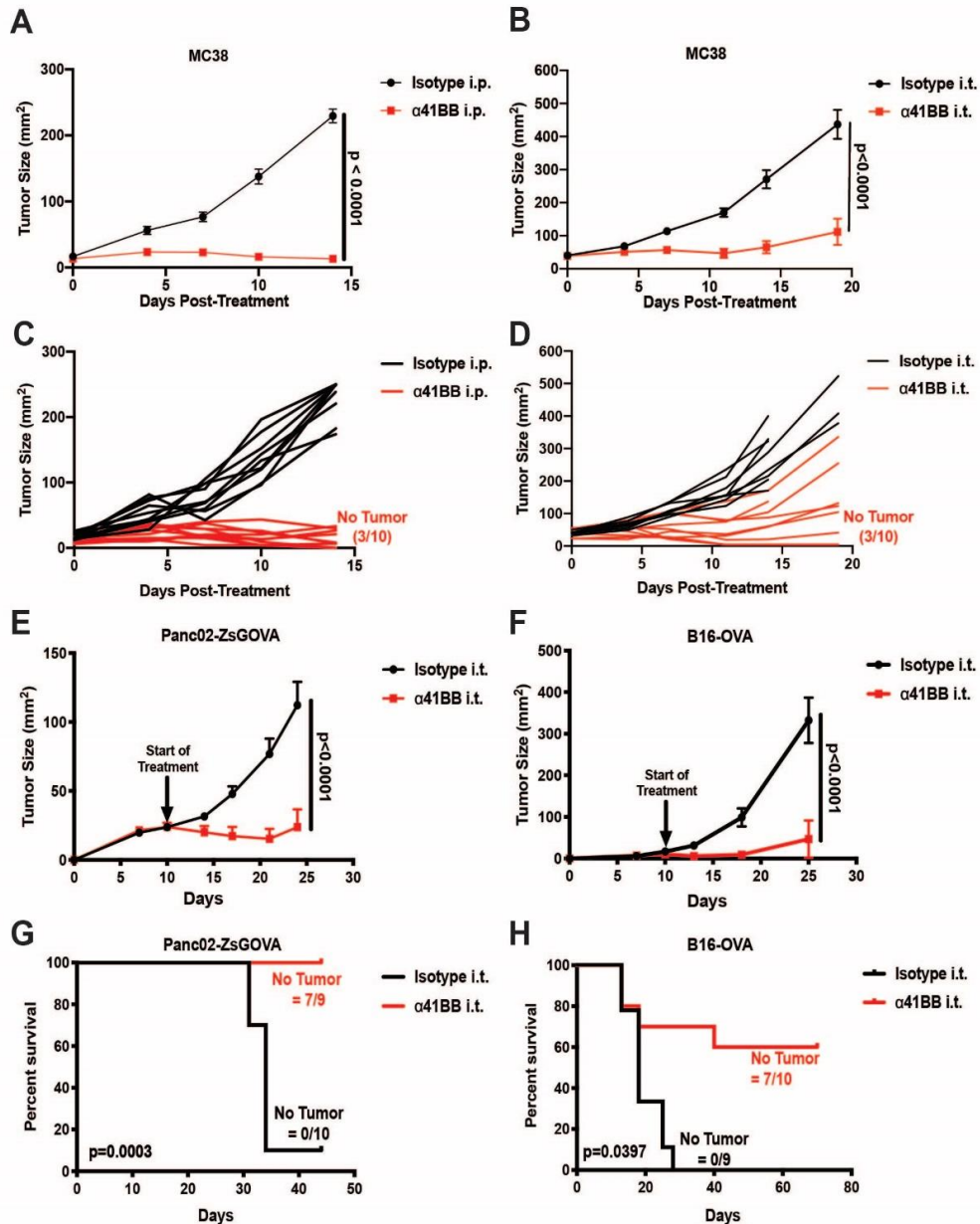


**Figure 4. Intratumoral treatment with agonistic 41BB antibodies promotes tumor regression in multiple mouse tumor models. (A and C)** Mice with MC38 tumors were treated with anti-41BB via intraperitoneal administration. (A) Tumor growth summary. (C) Tumor growth in individual mice. **(B and D)** Mice with MC38 tumors were treated with anti-41BB antibodies via intratumoral administration. (B) Tumor growth summary. (D) Tumor growth in individual mice. **(E)** Panc02-ZsGOVA tumor growth in mice that received intratumoral treatment with isotype or anti-41BB antibodies. **(F)** B16-OVA tumor growth in mice that received intratumoral treatment with isotype or anti-41BB antibodies. **(G-H)** Survival curves of mice from E and F. One of two representative experiments are shown.

### ***Intratumoral treatment with a 41BB agonist increases CD8 T cell infiltration***

We determined that within one week after the initial treatment with i.t.  $\alpha$ 41BB, the size of tumors was significantly reduced in mice with MC38 tumors (Figure 5A) and Panc02-ZsGOVA tumors (Figure 5B). The reduction in tumor size in response to i.t.  $\alpha$ 41BB treatment was associated with an increase of CD8 T cell infiltration in both tumor models compared to mice treated with isotype antibodies (Figure 5C-D). However, the frequency of CD4 TILs was unchanged between mice treated with isotype or  $\alpha$ 41BB (Figure 5C-D). We next determined that the increase of CD8 T cells in MC38 tumors was required for the anti-tumor efficacy because the depletion of CD8 T cells prior to the start of i.t.  $\alpha$ 41BB treatment abrogated the reduction of tumor growth (Figure 5E). In contrast, the depletion of CD8 T cells had no effect in mice that received i.t. treatment with isotype antibodies indicating that basal anti-tumor CD8 T cell responses are ineffective against MC38 tumors (Figure 5E). Not only was the presence of CD8 T cells necessary for the reduction of tumor growth, we found that TILs isolated from  $\alpha$ 41BB treated tumors exhibited higher IFN- $\gamma$  production in response to CD3 stimulation or co-culture with irradiated MC38 tumor cells (Figure 5F). Conversely, TILs from isotype treated tumors were successfully stimulated with CD3 antibodies but failed to produce IFN- $\gamma$  in cultures with MC38 tumor cells (Figure 5F). These results demonstrate that i.t. 41BB agonism can rejuvenate CD8 T cell responses leading to an improvement of anti-tumor immune responses.

### ***Intratumoral 41BB activation remodels the tumor immune microenvironment***

We demonstrated that the triggering of 41BB co-stimulation via i.t. treatment with  $\alpha$ 41BB converted tumors to a more T cell inflamed environment (Figure 5). Indeed, the ratio of

CD11b<sup>+</sup> myeloid cells relative to CD8<sup>+</sup> T cells was significantly reduced in tumors that received  $\alpha$ 41BB treatment compared to mice that received control isotype antibodies (Figure 6A). In contrast to control tumors whereby the majority of CD45<sup>+</sup> leukocytes were CD11b<sup>+</sup>MHCII<sup>+</sup>F480<sup>-</sup>CD11c<sup>-</sup> myeloid cells and CD11b<sup>+</sup>F480<sup>+</sup>Ly6C<sup>-</sup> tumor-associated macrophages (TAMs), we found that MC38 tumors treated with i.t.  $\alpha$ 41BB had a dramatic reduction in these myeloid cell populations (Figure 6B). Likewise,  $\alpha$ 41BB treatment decreased the frequency of CD11b<sup>+</sup>MHCII<sup>+</sup>F480<sup>-</sup>CD11c<sup>+</sup> cells (DCs). In isotype-treated tumors, CD11b<sup>+</sup>F480<sup>-</sup> Ly6C<sup>+</sup>Ly6G<sup>-</sup> monocytes and CD11b<sup>+</sup>F480<sup>-</sup>Ly6C<sup>+</sup>Ly6G<sup>+</sup> polymorphonuclear cells (PMNs), presumably monocytic- and PMN- myeloid derived suppressor cells (MDSCs), comprised <10% of CD45<sup>+</sup> cells. Conversely, the reduction of TAMs and other myeloid cell populations coincided with significant increases of monocytes and PMNs in tumors that received treatment with  $\alpha$ 41BB (Figure 6B). Nevertheless, the changes in myeloid cell frequency in response to  $\alpha$ 41BB treatment were associated with an increased abundance of CD80<sup>+</sup>CD86<sup>+</sup> DCs, TAMs, and monocytes (Figure 6C). Furthermore, DCs, TAMs, monocytes, and PMNs significantly upregulated CD80 and/or CD86 in tumors treated with  $\alpha$ 41BB compared to isotype controls (Figure 6D-G). Despite the loss of classical APCs within the tumor microenvironment, the increase in CD80 and CD86 among all tumor-associated myeloid cells may support anti-tumor T cell responses after intratumoral administration of 41BB agonists.

### ***Intratumoral $\alpha$ 41BB alters the immune stimulatory capacity of myeloid cells***

We further evaluated changes to intratumoral myeloid cells by examining the production of cytokines after i.t.  $\alpha$ 41BB. We harvested tumors from isotype and  $\alpha$ 41BB treated mice 7 days after treatment initiation and cultured the cells overnight. We found that myeloid cells from tumors produced IL-6 and TNF-alpha, but no difference was observed between cells from

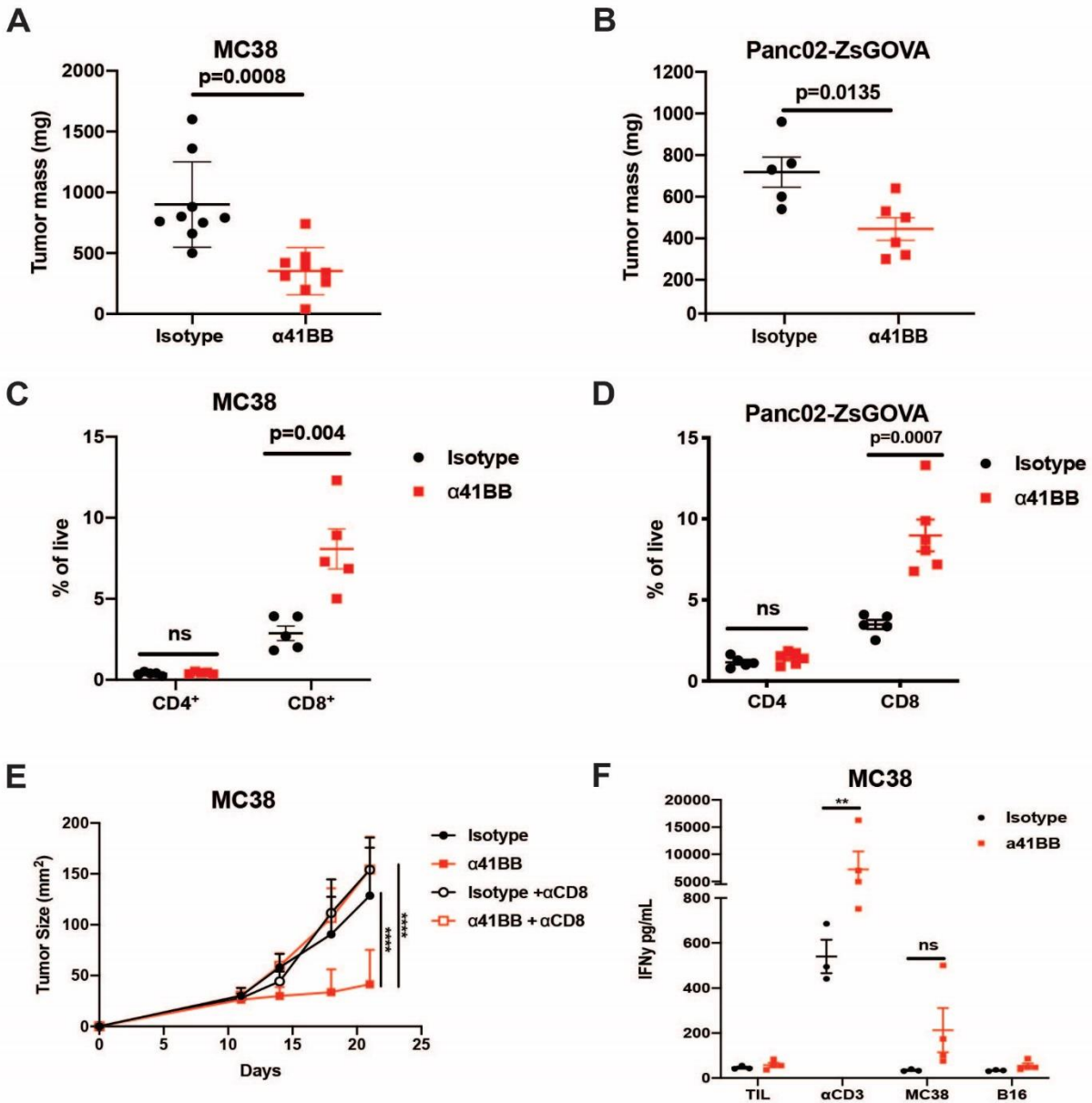


**Figure 5. Intratumoral treatment with agonistic 41BB antibodies increases CD8 T cell infiltration.** (A-B) Mass of MC38 and Panc02-ZsGOVA tumors harvested 7 days after initial anti-41BB treatment. (C-D) Frequency of CD4 and CD8 TILs in MC38 and Panc02-ZsGOVA tumors 7 days after initial anti-41BB treatment. (E) Mice with MC38 tumors were treated with isotype or anti-41BB antibodies in combination with CD8 depleting antibodies. Tumor growth is shown (n=5 mice per group). (F) TILs were isolated from MC38 tumors treated with intratumoral isotype or anti-41BB antibodies. TILs were cultured with immobilized anti-CD3 antibody or co-cultured with irradiated MC38 or B16 tumor lines for 48hrs. IFN- $\gamma$  was measured from supernatants. One of two representative experiments are shown. \* $p < 0.05$ , \*\* $p < 0.01$ , \*\*\* $p < 0.001$ , \*\*\*\* $p < 0.0001$ .

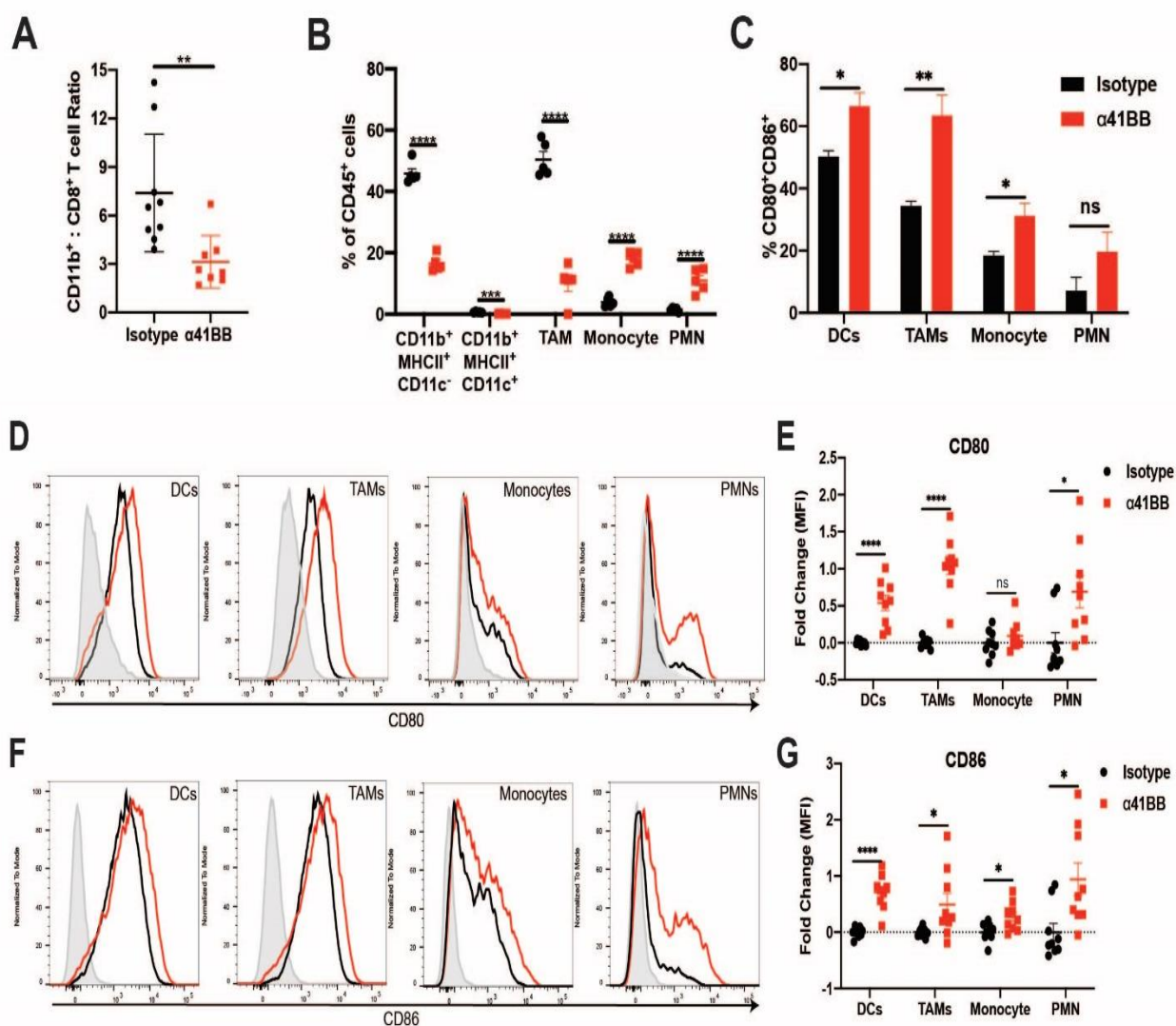


**Figure 6. Remodeling of the immune microenvironment after intratumoral administration of anti-41BB antibodies.** (A) Ratio of myeloid cells relative to CD8<sup>+</sup> TILs in MC38 tumors after antibody treatment. (B) Percentage of myeloid cell subsets in MC38 tumors. Tumors were harvested 7 days after initial antibody treatment. (n=5 mice/group). (C) Percentage of CD80 and CD86 double positive myeloid subsets is increased after anti-41BB treatment. (D and F) Representative histograms for CD80 (D) and CD86 (F) gated on indicated myeloid cell subset. Gray=FMO, Black=Isotype, Red= anti-41BB. (E and G) Fold change in CD80 (E) and CD86 (G) expression in myeloid cell subsets from MC38 tumors. (n= 9-10 mice/group). E, G, Data is a summation of two independent experiments. A-C, One of two independent experiments are shown. \*p<0.05, \*\*p<0.01, \*\*\*p<0.001, \*\*\*\*p<0.0001.

$\alpha$ 41BB or isotype tumors (Figure 7A, D). In contrast, DCs and TAMs had an elevated expression of IL-10, while CD11b<sup>+</sup>Gr-1<sup>+</sup> cells exhibited a reduced production of IL-10 (Figure 7B).

Similarly, DCs and TAMs exhibited an increased production of IL-12 (Figure 7C). While we

observed changes in cytokine expression among myeloid cell subsets, the frequency of DCs and

TAMs were significantly reduced by  $\alpha$ 41BB treatment (Figure 7B). Consistent with these data, the number of cytokine-producing DCs and TAMs were largely reduced in cultured tumor cell digests of  $\alpha$ 41BB treated tumors in comparison to isotype treated tumors (Figure 7E-H). Concordantly, the number of cytokine-producing monocytes and PMNs (CD11b<sup>+</sup>Gr-1<sup>+</sup> cells) were significantly elevated in  $\alpha$ 41BB treated tumors (Figure 7E-H). Because IL-10 and IL-12 are key regulators in T cell priming and activation by myeloid cells, we next evaluated the capacity of intratumoral myeloid cells to stimulate T cells after treatment. We found that OT-I T cells produced more IFN- $\gamma$  in co-cultures with myeloid cells from  $\alpha$ 41BB treated tumors both with and without *in vitro* IL-10 neutralization (Figure 7J). Upon examination of the phenotype of OT-I T cells after co-culture, we observed that T cells co-cultured with myeloid cells from  $\alpha$ 41BB-treated tumors had an elevated expression of cell surface 41BB compared to T cells cultured with myeloid cells from isotype-treated tumors (Figure 7K-M). Moreover, the *in vitro* neutralization of IL-10, but not IL-12, enhanced the expression of 41BB in OT-I T cells from co-cultures with tumor myeloid cells, suggesting that myeloid cell derived IL-10 restricted the expression of 41BB (Figure 7K-M). Similar to the increase of 41BB expression, IL-10 neutralization resulted in an increased expression of PD-1 in co-cultures with myeloid cells from isotype tumors (Figure 8A-C). Thus, i.t.  $\alpha$ 41BB treatment enhances the ability of tumor-myeloid cells to potentiate T cell responses.

#### ***41BB agonistic antibodies promote ex vivo human TIL expansion***

We have previously shown that the addition of 41BB agonistic antibodies enhances the expansion and function of melanoma TILs from primary tumor fragments *in vitro* (96). We obtained two melanoma specimens and attempted to expand TILs from tumor fragments placed in media containing IL-2 or IL-2 in combination with  $\alpha$ 41BB. In Patient 1, TILs expanded in

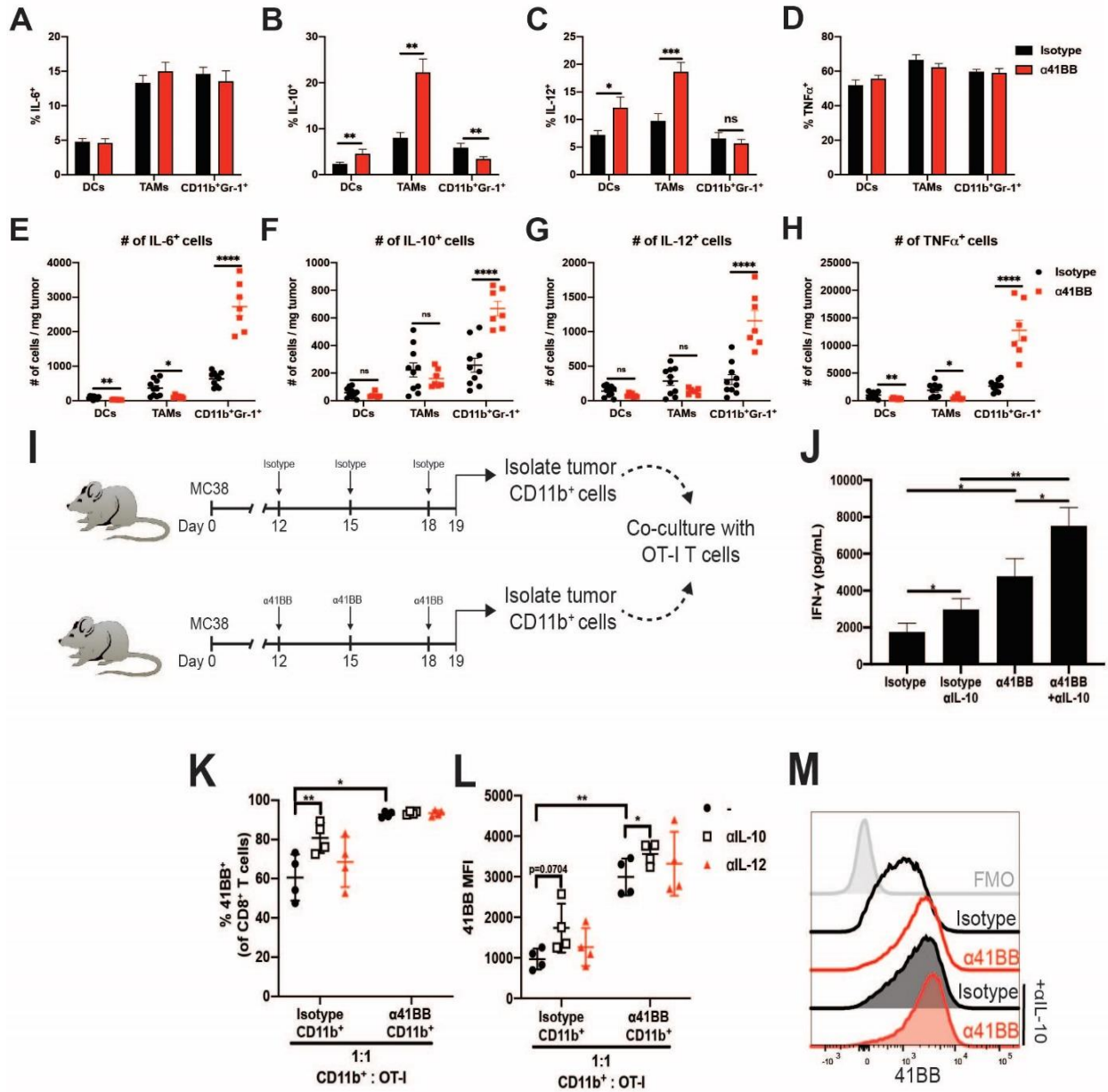


**Figure 7. Intratumoral anti-41BB treatment alters myeloid immunostimulatory capacity.** (A-D) Intracellular cytokine staining from myeloid cells from MC38 tumors treated with isotype or anti-41BB antibodies. (A) IL-6, (B) IL-10, (C) IL-12, (D) TNF-alpha. (n=7-10 mice/group). (E-H) The number of cytokine producing cells were determined by back-calculating the percentage of myeloid cell subsets relative to the total number of cells from each mouse tumor. (I) Experimental design for (J-M). (J-M) CD8<sup>+</sup>OT-I T cells after 72hrs with peptide stimulation with or without culture with myeloid cells from isotype or anti-41BB treated tumors. (J) IFN-γ was measured in supernatants from OT-I : myeloid cell co-cultures incubated with or without IL-10 neutralizing antibodies. (K-L) 41BB expression in OT-I T cells after 72hrs of co-culture with or without IL-10 or IL-12 neutralizing antibodies. Percentage of 41BB positive OT-I T cells (K) and expression level (L). (M) Representative histogram of 41BB expression. Each data point represents of pool of CD11b<sup>+</sup> cells collected from 3-4 individual mouse tumors. (n=13-16 individual mice/group). \*p<0.05, \*\*p<0.01, \*\*\*p<0.001, \*\*\*\*p<0.0001.

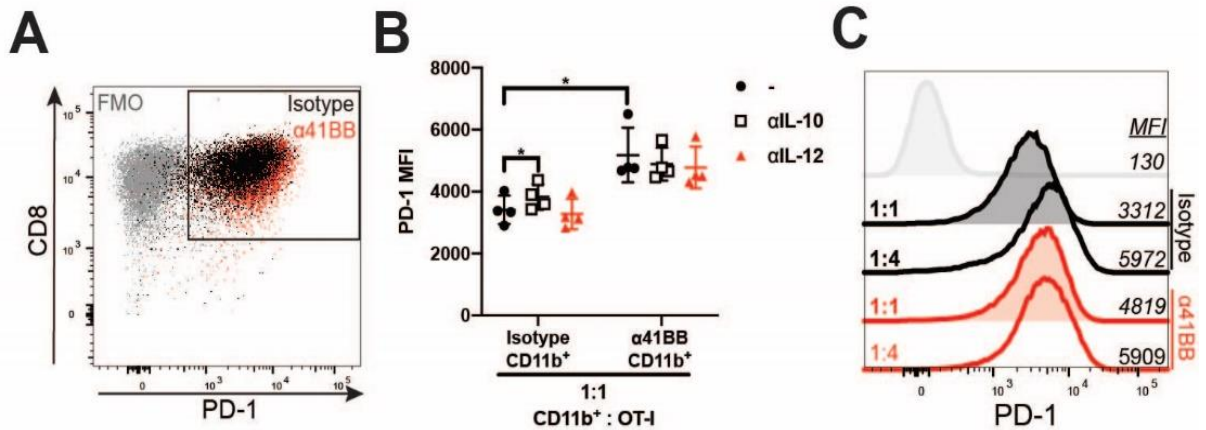


**Figure 8. Tumor-associated myeloid cells alter PD-1 expression on T cells.** (A) Representative dot plot for PD-1 expression. (B) PD-1 expression by OT-I T cells in myeloid cell co-cultures. (C) Representative histogram illustrating PD-1 expression after co-culture. Ratio of CD11b : OT-I indicated on the left. PD-1 MFI indicated on the right. OT-I T cells with Isotype myeloid cells in black; with anti-41BB myeloid cells in red.

cultures with IL-2+α41BB (5/6 fragments), while no expansion occurred in cultures with IL-2 only (0/6 fragments) (Figure 9A). Similarly, an enhancement of TIL expansion was observed in Patient 2 among fragments grown with IL-2 and α41BB (23/24 fragments) compared to TILs grown in IL-2 alone (12/24 fragments). Moreover, the number of TIL expanded per fragment was greater in cultures containing IL-2 and α41BB compared to IL-2 alone conditions (Figure 9B). Among fragments grown in IL-2 only, the distribution of CD4<sup>+</sup> TILs and CD8<sup>+</sup> TILs were approximately equal. In contrast, the combination of IL-2+α41BB almost exclusively promoted the expansion of CD8<sup>+</sup> TILs (Figure 9C). Because the yield of TILs from IL-2 alone cultures was relatively low, we pooled together TILs from fragments that exhibited the best expansion at the end of the culture. Similarly, we chose TILs expanded from 6 individual fragments grown in IL-2+α41BB that yielded the highest number of cells. We then co-cultured the selected TILs with autologous tumor digest and determined the magnitude of IFN-γ production. IFN-γ was detected and effectively blocked with MHC-I blocking antibodies in TILs grown in IL-2 alone and in 3/6 selected TILs grown in IL-2 and α41BB (Figure 9D). Notably,



the abundance of IFN- $\gamma$  was higher in co-cultures with TILs expanded with IL-2 and  $\alpha$ 41BB compared to TILs grown in IL-2 only (Figure 9D).

To better understand the contribution of myeloid cells in the process of *ex vivo* TIL expansion, we evaluated the frequency of leukocyte populations in a fresh tumor sample from melanoma Patient 1. We found that 17.1% of all live cells were CD45<sup>+</sup>, which 73% of CD45<sup>+</sup> cells consisted of CD11b<sup>+</sup>CD11c<sup>+</sup>CD14<sup>+</sup>HLA-DR<sup>+</sup> myeloid cells. Approximately 15% of CD45<sup>+</sup> cells were CD4<sup>+</sup> and CD8<sup>+</sup> T cells and the remainder consisted of a variety of myeloid cell subsets (Figure 9E). We next evaluated the production of cytokines in fresh tumor digests from Patient 1 and Patient 2. Fresh tumor cell digests were cultured overnight in IL-2 alone or in combination with  $\alpha$ 41BB. Tumors produced vast amounts of CCL2, IL-6, IL-8, IL-1 $\beta$ , IL-10, and TGF- $\beta$ . In response to IL-2 and IL-2 in combination with  $\alpha$ 41BB, we detected an increased production of CXCL10 and IFN- $\gamma$  in comparison to unstimulated tumor digests (Figure 9F-G). Moreover, a trend consistent with an increase of CXCL10 and IFN- $\gamma$  were observed when tumors were cultured with IL-2 and  $\alpha$ 41BB compared to IL-2 alone (Figure 9H). Collectively, these data demonstrate that the augmentation of *ex vivo* TIL expansion via IL-2 and 41BB stimulation is associated with increases in proinflammatory cytokine production.

### ***Stimulation of the 41BB-41BBL axis alters myeloid cell phenotype and function***

Next, we dissected how myeloid cells facilitate *ex vivo* TIL expansion via 41BB stimulation. First, we observed that CD11b<sup>+</sup> myeloid cells within a fresh melanoma tumor lacked the expression of 41BB (Figure 10A). Next, we phenotyped peripheral blood myeloid cells and found that CD11b<sup>+</sup> cells in PBMCs expressed HLA-DR/DP/DQ, CD14, CD86, CD11c, and low levels of PD-L1 and CD141 (Figure 10B). Moreover, these cells lacked expression of 41BB, but

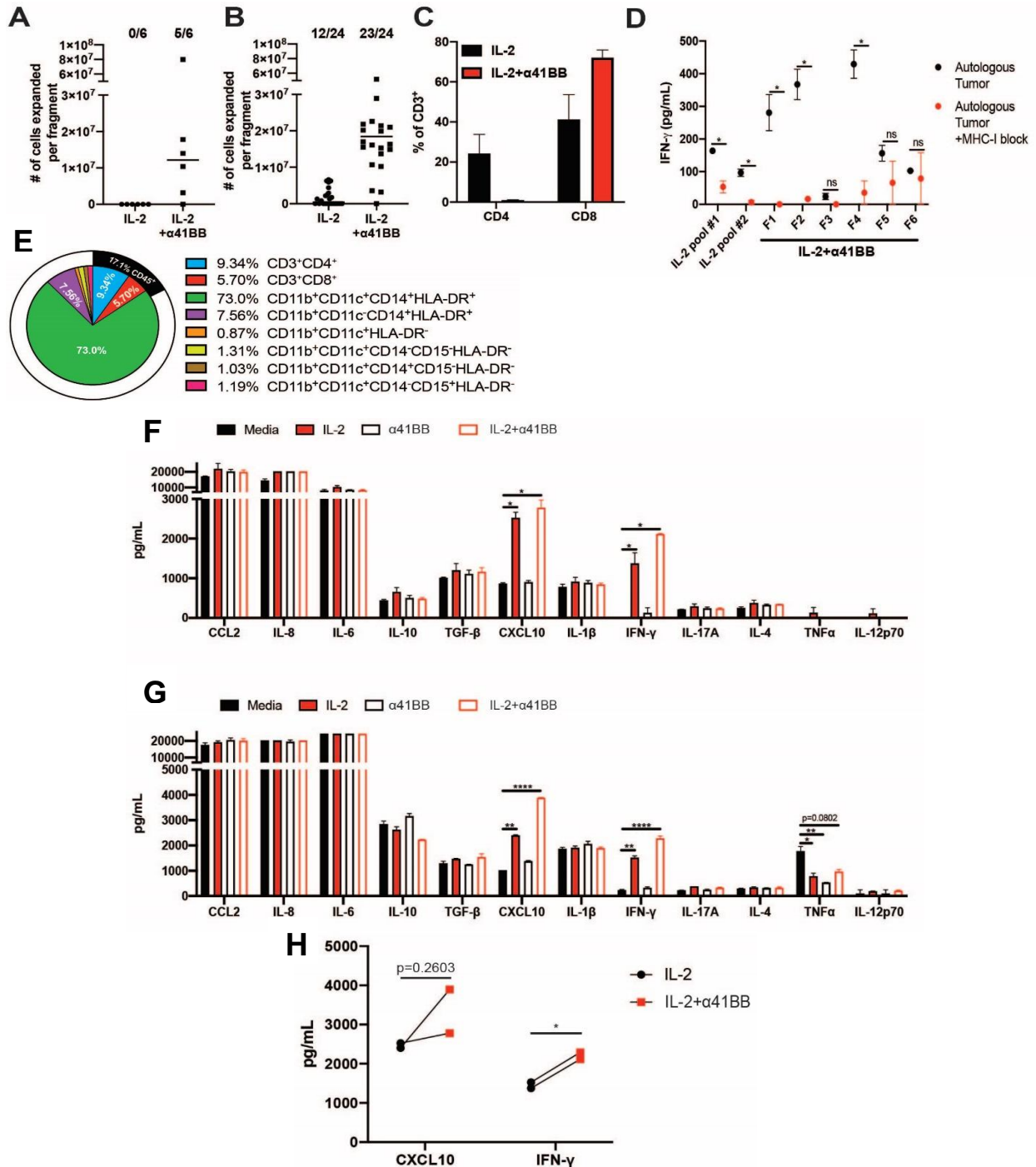


**Figure 9. 41BB agonism enhances the growth of TILs from primary human melanomas.** (A-B) Melanoma tumor fragments were grown in media containing IL-2 or IL-2 in combination with  $\alpha$ 41BB. Patient 1 (A) and Patient 2 (B). The number of fragments to successfully grow TILs are indicated above each plot. (C) Frequency of CD4 and CD8 TILs expanded from tumor fragments from Patient 2. (D) TILs from Patient 2 were co-cultured with autologous tumor digests with or with MHC-I blocking antibodies for 24hrs. IFN- $\gamma$  was measured in supernatants. (E) Tumor digest from Patient 1 was analyzed for immune infiltrates. Outer ring represents the frequency of CD45<sup>+</sup> cells among the total live cells. Inner pie chart represents the proportions of immune cell subsets. Cell subset frequency is indicated on pie chart and adjacent to the indicated cell subset on the right. (F-H) Cytokines in the supernatants of fresh tumor digests from Patient 1 (F) and Patient 2 (G) were cultured at  $1 \times 10^6$  cells/mL in indicated media overnight.

did express 41BBL (Figure 10B-C). Since the activation of 41BBL in monocytes is known to promote the maturation to DCs (138, 139), and 41BB expression was poorly expressed by myeloid cells, we examined how the stimulation of 41BBL could differ in activating myeloid cells in comparison to a 41BB agonistic antibody. We stimulated myeloid cells with immobilized  $\alpha$ 41BB to agonize 41BB or immobilized 41BB protein (41BB-Fc) to agonize 41BBL. The viability of donor myeloid cells was greatly reduced in unstimulated cultures or under stimulation with  $\alpha$ 41BB alone. In contrast, stimulation with 41BB-Fc alone maintained cell viability similar to that of cultures containing GMCSF (positive control) or GMCSF in combination with  $\alpha$ 41BB or 41BB-Fc (Figure 10D). This suggested that activation of 41BBL, but not 41BB, was sufficient to maintain the survival of myeloid cells and that 41BB(L) signals did not augment cell viability in the presence of GMCSF. Compared to pre-cultured cells, myeloid cells upregulated 41BBL expression, but not 41BB expression, when incubated with a GMCSF maturation stimuli (Figure 10E). In addition to maintaining myeloid cell viability, the stimulation with 41BB-Fc reduced the expression of CD14, while enhancing the expression of PD-L1, CD141, 41BBL, and CD86 compared to pre-culture myeloid cells (Figure 10F). Likewise, GMCSF-stimulated cells exhibited similar phenotypic changes to 41BB-Fc treated cells, however, GMCSF failed to upregulate CD86 (Figure 10G). The increase in CD86 expression was highly consistent between all donors (Figure 10H). In contrast to 41BB-Fc or GMCSF stimulation,  $\alpha$ 41BB alone failed to maintain myeloid viability (Figure 10D) and the phenotype was similar to myeloid cells cultured in media alone (Figure 10F-G). Likewise, the addition of  $\alpha$ 41BB or 41BB-Fc failed to augment cell surface marker expression when combined with GMCSF (Figure 10G). While increases in CD86 and 41BBL expression are indicative of an enhanced co-stimulatory capacity, we further interrogated the impact of 41BB-41BBL activation

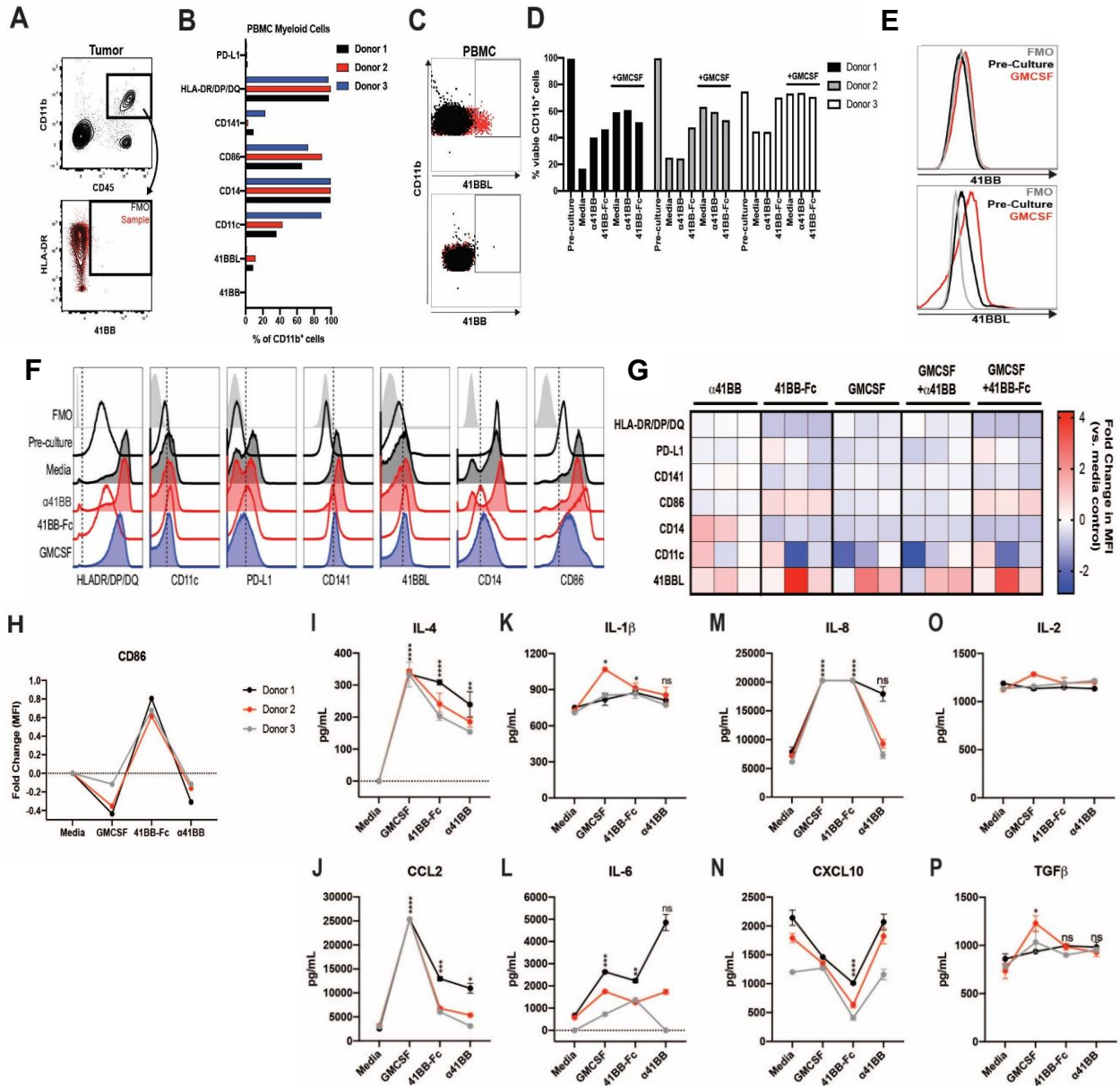


**Figure 10. Activation of 41BB and 41BBL alter myeloid cell phenotype and function.** (A) 41BB expression in myeloid cells from a fresh melanoma sample. (B) Phenotype of CD11b<sup>+</sup> cells from healthy donor PBMCs. (C) Representative dot plots for 41BBL and 41BB expression on CD11b<sup>+</sup> cells from PBMCs (left) or tumor myeloid cells (right). (D) Viability of sorted healthy donor myeloid cells were determined at pre-culture and after 3 days culture with immobilize urelumab, immobilized 41BB-Fc with or without GMCSF. (E) Representative histogram for 41BB and 41BBL expression on healthy donor myeloid cells. Gray=fluorescence minus one (FMO), Black=pre-culture, Red=3 days culture with GMCSF. (F) Histograms showing the expression of cell surface markers before and after culture with indicated conditions for one representative donor. Each condition is indicated on the far left. (G) Heatmap representing the fold change in MFI for respective cell surface markers comparing cell culture conditions to media alone control for 3 individual donor cells. (H) Fold change of CD86 expression normalized to media control. (I-P) Supernatants from donor myeloid cell cultures were collected after 3 days incubation with indicated conditions. Each line represents myeloid cells from an individual donor.

in myeloid cells by assessing cytokine production. We found that IL-4 and CCL2 expression was potently induced by GMCSF and to a lesser extent by  $\alpha$ 41BB and 41BB-Fc (Figure 10I-J). Similarly, IL-1 $\beta$ , IL-6, and IL-8 production was amplified by stimulation with GMCSF or 41BB-Fc, but not  $\alpha$ 41BB (Figure 10K-M). CXCL10 expression was reduced by 41BB-Fc stimulation but maintained with GMCSF or  $\alpha$ 41BB alone (Figure 10N). In addition, myeloid cells readily produced IL-2 and TGF- $\beta$ , but the culture conditions maintained or modestly increased the production of these cytokines (Figure 10O-P). In large part, 41BB activation alone via  $\alpha$ 41BB or its addition to GMCSF stimulus had little effect on cell viability, the expression of cell surface markers, or induction of cytokine expression (Figure 10D-P). Hence, it is possible that 41BB agonism on myeloid cells provides a weaker stimulus in comparison to reverse signaling through 41BBL.

#### ***The stimulation of TILs is potentiated by 41BBL on APCs***

The agonistic 41BB antibody urelumab does not compete with the binding of 41BBL to 41BB, thereby preserving native 41BBL-mediated co-stimulation (140). Consistent with our data in Figure 6, the maturation of monocytes via 41BBL reverse signaling leads to an increased potential to prime T cells characterized by increased CD86 expression and enhanced production of IL-6 and IL-8 (135). Hence, we hypothesized that the enhancement of *ex vivo* TIL expansion by 41BB agonists may be aided by additional co-stimulation mediated by myeloid 41BBL. To determine this, we generated APCs from CD11b<sup>+</sup> cells isolated from the pheresis product of a melanoma patient. The myeloid cells were incubated with immobilized 41BB-Fc for 3 days, collected, and then pulsed with autologous tumor lysate for 24hrs in the presence of GMCSF to generate 41BBL-conditioned APCs (41BBL APCs). First, we examined if  $\alpha$ 41BB could augment the production of cytokines in TIL co-cultures with autologous tumor or pulsed APCs.

A variety of cytokines were detected in cultures containing TILs stimulated with  $\alpha$ CD3 or co-cultures of TILs with autologous tumor cells. In particular, the combined stimulation of TILs with  $\alpha$ CD3 and  $\alpha$ 41BB increased the production CXCL10 and IFN- $\gamma$  (Figure 11A). As expected, IFN- $\gamma$  and TNF $\alpha$  were induced in TIL co-cultures with tumor cells, which were effectively reduced by MHC-I blockade (Figure 11B). Next, we determined the cytokine profile in TIL co-cultures with autologous APCs. When cultured alone, the 41BBL APCs produced high amounts of CCL2 and IL-8, and modest amounts of IL-2, TGF- $\beta$ , and IL-1 $\beta$ , which was not impacted by additional stimulation with soluble  $\alpha$ 41BB (Figure 11C). In comparison to unstimulated TILs and cultures with 41BBL APCs only, CXCL10, IL-2, IFN- $\gamma$ , IL-1 $\beta$ , TGF- $\beta$ , and IL-6 were elevated when TILs were cultured with APCs, which the production of some cytokines was augmented by the addition of agonistic  $\alpha$ 41BB and/or  $\alpha$ 41BBL blocking antibodies ( $\alpha$ 41BBL) (Figure 11D). Likewise, the addition of  $\alpha$ 41BB alone, 41BBL blockade alone, and/or the combination increased IFN- $\gamma$ , IL-1 $\beta$ , and TGF- $\beta$ . Moreover, IL-6 was absent in all conditions except in TIL-APC co-cultures with the addition of  $\alpha$ 41BB in combination with 41BBL blockade (Figure 11E). CXCL10 was only detected TIL-APC co-cultures, which suggested that cell-cell contact facilitated the production of CXCL10. Accordingly, we found that the production of CXCL10 and IL-2 was only augmented by 41BBL blockade, which was enhanced when 41BBL blocking was combined with  $\alpha$ 41BB. Similarly, we observed that CXCL10 was elevated in Panc02-ZsGOVA tumors taken from mice treated with i.t.  $\alpha$ 41BB (Figure 12). Next, we demonstrated that TILs from this patient readily proliferated in co-cultures with  $\alpha$ CD3 or irradiated autologous tumor cells compared to basal proliferation. The combination of  $\alpha$ 41BB with  $\alpha$ CD3 enhanced TIL proliferation but was reduced when 41BBL antibodies were present in culture. However, the addition of  $\alpha$ 41BB and/or  $\alpha$ 41BBL did not alter TIL proliferation in

cultures with tumor cells. In parallel, we co-cultured TILs with autologous 41BBL APCs pulsed with tumor lysate in combination with soluble  $\alpha$ 41BBL and/or  $\alpha$ 41BB. 41BBL APCs induced the proliferation of TILs, which was negatively impacted by 41BBL blockade alone or in combination with  $\alpha$ 41BB, indicating that the blockade of 41BBL dampened TIL proliferation and that additional co-stimulation with  $\alpha$ 41BB was not sufficient to reverse this effect (Figure 13). Together, these results demonstrate that myeloid 41BBL can contribute to the effect of 41BB agonists characterized by enhanced TIL proliferation and production of cytokines.

## Discussion

Overall, 41BB agonists are potent immune stimulators, but their translational potential has been heavily restricted by the onset of severe adverse events (*141*). Significant advancement in the development of tumor-selective 41BB agonists to limit or even eliminate any 41BB-related adverse events has revitalized the therapeutic feasibility of targeting 41BB in humans (*128, 142*). While we did not evaluate toxicity in mice that received intratumoral injections of  $\alpha$ 41BB, we did not observe any overt toxicity during the administered treatment regimen. Overall, our data support that stimulating 41BB in tumors is a feasible approach to promote anti-tumor immune responses. Consistent with other reports, the activity of 41BB agonists in our hands was not independent of changes to the myeloid-tumor immune milieu (*143, 144*). The anti-tumor activity of 41BB agonists is greatly reduced in the absence of BATF3-dependent DCs, suggesting that 41BB agonists may act directly on the myeloid compartment to promote the eradication of tumors in mice (*143*). Indeed, we observed that treatment with 41BB agonists in mice led to increases in monocytes and PMNs coincided by a depletion of macrophages and DCs within tumors. Furthermore, myeloid cells from  $\alpha$ 41BB-treated tumors induced the upregulation of 41BB on CD8<sup>+</sup> T cells and enhanced the production of IFN- $\gamma$  *in vitro* (Figure 7J-N). Hence, it

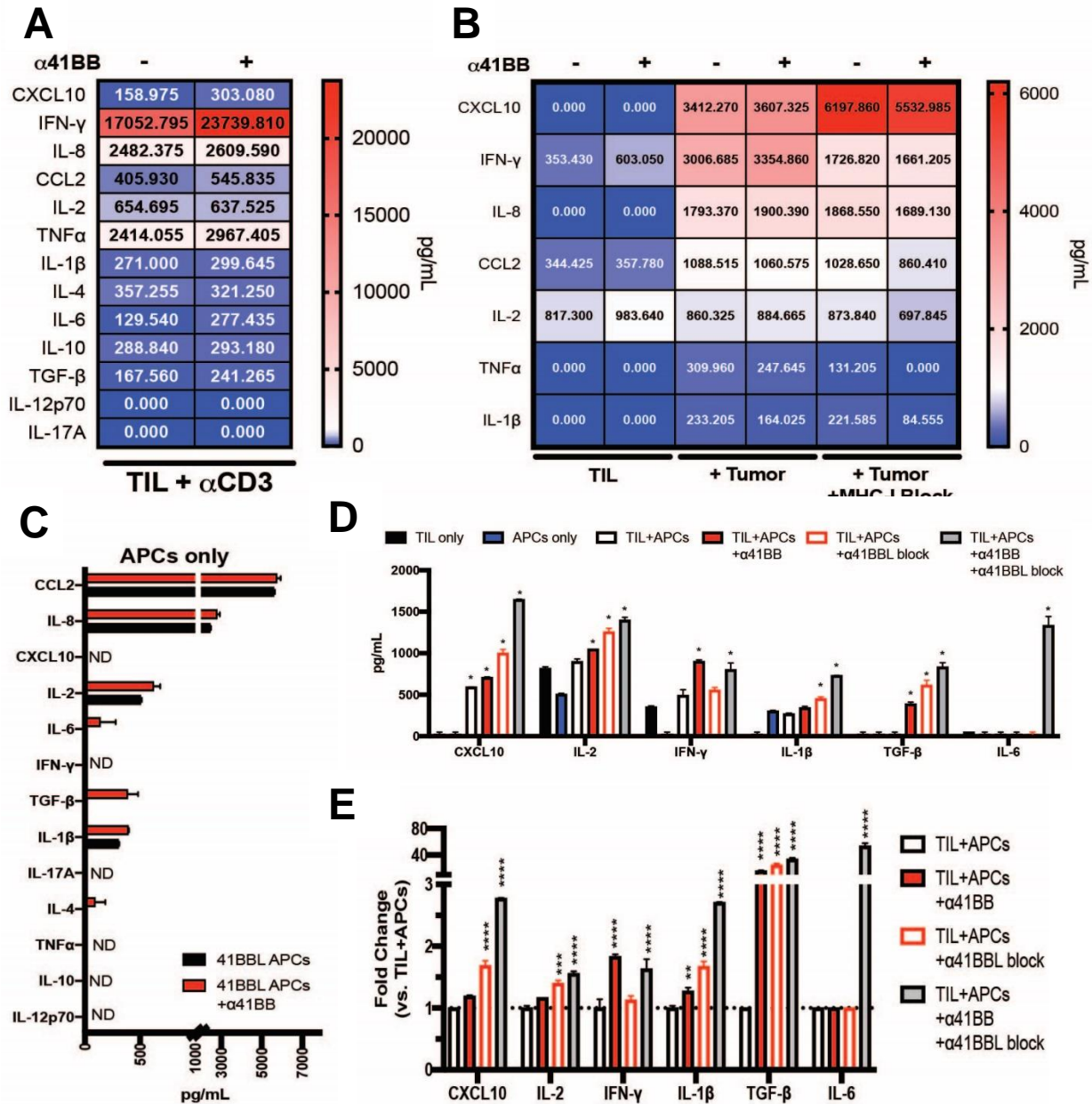


**Figure 11. Cytokine production in TIL-APC co-cultures.** TILs from a melanoma patient were cultured with  $\alpha\text{CD}3$ , autologous tumor cells at a 1:1 ratio, or tumor-lysate pulsed 41BBL-APCs at a 1:10 ratio for 72hrs. **(A-B)** Heatmap representing cytokine abundance in supernatants from cell cultures were collected at 72hrs. Numerical values are indicated for each parameter with its respective condition. Cytokine production by TIL stimulated with  $\alpha\text{CD}3$  +/- urelumab (A). Cytokines in TIL-tumor co-cultures +/-  $\alpha 41\text{BB}$  or MHC-I blocking antibodies (B). **(C)** 41BBL APCs were generated and then pulsed with autologous tumor lysate in the presence of GM-CSF. Pulsed APCs were then seeded in culture wells with or without  $\alpha 41\text{BB}$ . **(D)** Cytokines were measured in the supernatants of TIL-APC co-cultures incubated with  $\alpha 41\text{BB}$  and/or  $\alpha 41\text{BBL}$ . TIL only condition is the same data from (B); APCs only from (C). Statistics are indicated for cytokines that are higher than both TILs alone and APCs alone conditions. **(E)** Fold change in cytokine induction vs. TIL+APCs in co-cultures from (D). Dotted line represents the basal induction of cytokines in TIL-APC co-cultures. ND=not detected



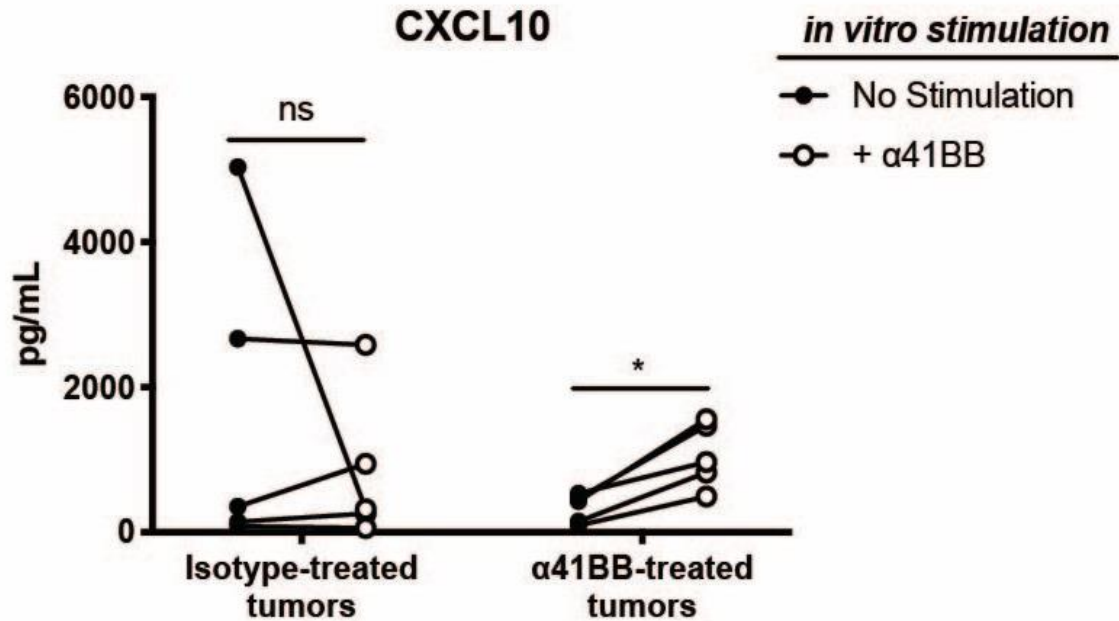


**Figure 12. Sustained 41BB agonism enhances CXCL10 expression in mouse tumors.** Tumors were collected from Panc02-ZsGOVA tumor bearing mice treated with i.t. isotype or  $\alpha$ 41BB antibodies. Tumors were cultured overnight in media +/-  $\alpha$ 41BB overnight. CXCL10 production was quantified in the supernatant (n=5 mice per group). Significance was determined by two-tailed student t test with Welch's correction.

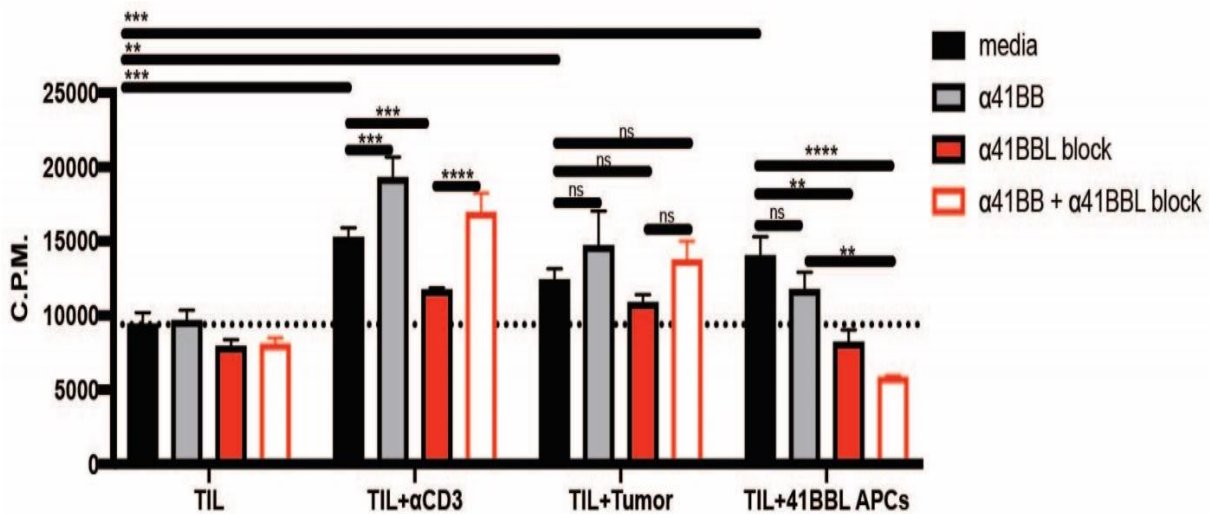


**Figure 13. 41BBL is necessary to induce TIL proliferation in co-cultures with APCs.** TIL proliferation in co-cultures was determined in the final 18hrs of the culture by 3H thymidine incorporation in the presence of soluble  $\alpha$ 41BB and/or soluble  $\alpha$ 41BBL. Dotted line represents basal TIL proliferation without additional stimulation. \* $p < 0.05$ , \*\* $p < 0.01$ , \*\*\* $p < 0.001$ , \*\*\*\* $p < 0.0001$ . Significance was determined by two-tailed t-test or 2-way ANOVA with Dunnett's multiple comparisons.

is possible that myeloid cells contribute to the efficacy of 41BB activation *in vivo* by inducing the upregulation of surface 41BB on T cells. We show that IL-10 was essential for restricting both the production of IFN- $\gamma$  and the expression 41BB on T cells (Figure 7J, L). While DCs and TAMs increased their production of IL-10 and IL-12 in response to 41BB agonism, the i.t. administration of  $\alpha$ 41BB simultaneously promoted the accumulation of monocytes and PMNs that produced IL-6, IL-12, IL-10, and TNF- $\alpha$  (Figure 7E-H). Thus, both the proportionality and function of distinct intratumoral myeloid cells are likely relevant factors in driving anti-tumor immune responses elicited by 41BB agonists.

It has been described that species differences exist between mouse and human myeloid cells in response to 41BBL signaling (145). While, we did not evaluate the role of 41BBL in murine models, the data we present in human cell culture systems provide relevance for the role of 41BBL in the ability of myeloid cells to potentiate T cell responses. Importantly, the upregulation of co-stimulatory markers, such as CD80 and/or CD86, in both mouse and human myeloid cells were consistent after exposure to 41BB or 41BBL stimulation suggesting that there are similar mechanisms dictating myeloid cell co-stimulatory responses in tumors after treatment (96). In this study, we found that 41BB agonism, contrary to 41BBL stimulation via 41BB-Fc, had little effect in augmenting human myeloid cell phenotypes and cytokine production (Figure 10). This, perhaps, was not surprising because CD11b<sup>+</sup> cells expressed little to no 41BB on their cell surface (Figure 10A-C). Concordantly, the stimulation of myeloid cells with a 41BB agonist alone failed to sustain myeloid cell viability, increase CD86 expression, or provide other maturation stimuli even when combined with GM-CSF. Moreover, the addition of  $\alpha$ 41BB to tumor-lysate pulsed APCs did not significantly alter basal cytokine production (Figure 11C). Hence, the 41BB agonist used in these experiments appears to be a weak stimulator of myeloid

cells at best. In mice, the engagement of 41BBL on myeloid cells by its cognate receptor, 41BB, restricts the accumulation of IL-12<sup>+</sup> cDCs and TAMs within tumors, leading to a diminished ability to control tumor growth (144). In a contradictory manner, 41BB knockout mice exhibit remarkably similar anti-tumor immune responses to mice treated with agonistic 41BB antibodies, which supports the hypothesis that the lack of interaction between 41BB with 41BBL on myeloid cells promotes anti-tumor immune responses. However, the evidence we provide in this study demonstrates that reverse 41BBL signaling can promote the immunostimulatory capacity of monocytes and APCs in humans. Consistent with previous reports in human cells (139, 146), we show that the induction of reverse 41BBL signaling in human monocytes via 41BB-Fc promoted the expression of co-stimulatory markers CD86 and 41BBL, while simultaneously increasing the production of IL-8, IL-6, IL-1 $\beta$ , CCL2, and IL-4 (Figure 10I-P). Thus, differences among species and experimental murine tumor models likely contribute to the contrasting findings in reports investigating the role 41BB-41BBL co-stimulatory axis in anti-tumor immunity. Together, these results demonstrate that the 41BB agonists may not act directly on human myeloid cells alone to promote the co-stimulatory capacity of APCs. Rather the activation of 41BBL, and potential bidirectional signaling between myeloid cells and T cells, were responsible for providing efficient maturation stimuli to enhance the capacity of APCs to prime T cells.

In contrast to other 41BB agonistic antibodies, urelumab facilitates the cross-linking of 41BBL to 41BB, suggesting that bidirectional signaling orchestrated by 41BBL<sup>+</sup> cells could augment the agonistic activity of  $\alpha$ 41BB (140, 147). We provide evidence here that the activation of 41BBL can contribute to the expansion of TILs stimulated with 41BB agonists because the proliferation of TILs cultured with 41BBL-conditioned APCs was reduced when 41BBL was blocked, even in the presence of urelumab ( $\alpha$ 41BB) (Figure 13). Intriguingly,

CXCL10 was elevated in TIL-APC co-cultures when 41BBL was blocked. Consistent with this data, the production of CXCL10 was reduced in donor myeloid cells conditioned with 41BB-Fc (Figure 9N), suggesting that the stimulation of 41BBL on myeloid cells represses CXCL10 expression which may have been relieved when blocking antibodies were present in TIL-APC co-cultures. Moreover, we acknowledge that IFN- $\gamma$  is a known inducer of CXCL10, a maturation factor for DCs (100), and can enhance the ability of 41BBL-APCs to prime cytotoxic T cell responses (148). Hence, it is possible that the induction of CXCL10 could have been indirectly promoted in the presence of  $\alpha$ 41BB through an increased abundance of IFN- $\gamma$ . While, the blockade of 41BBL can prevent the induction of T cell proliferation through interaction with its cognate receptor, we cannot rule out the possibility that the production of cytokines, such as IL-6, IL-1 $\beta$ , and TGF- $\beta$  by APCs may also have an impact on TIL proliferation. However, the cellular origin and the specific activity of these cytokines on TIL proliferation and function remains unclear. Hence, future studies need to determine the role of 41BB-41BBL induced cytokines, including CXCL10, IL-6, IL-1 $\beta$ , and TGF- $\beta$  and their impact on both, the expansion of TILs and the activity of 41BB agonists.

In our previous report, the addition of  $\alpha$ 41BB was associated with enhanced TIL expansion and the modulation of tumor-resident DC phenotypes characterized by the upregulation of CD80, CD86, and MHCII (96). We conclusively demonstrated that myeloid cells upregulated co-stimulatory markers CD86 and 41BBL and proinflammatory cytokines in response to 41BBL stimulation, but not in response to 41BB agonists. Moreover, tumor-lysate pulsed APCs that were matured via reverse 41BBL signaling effectively primed TILs. Together, our findings provide feasibility that 41BB-41BBL bidirectional signaling between immune cells can be exploited to enhance to the expansion and function of TILs (Figure 14).

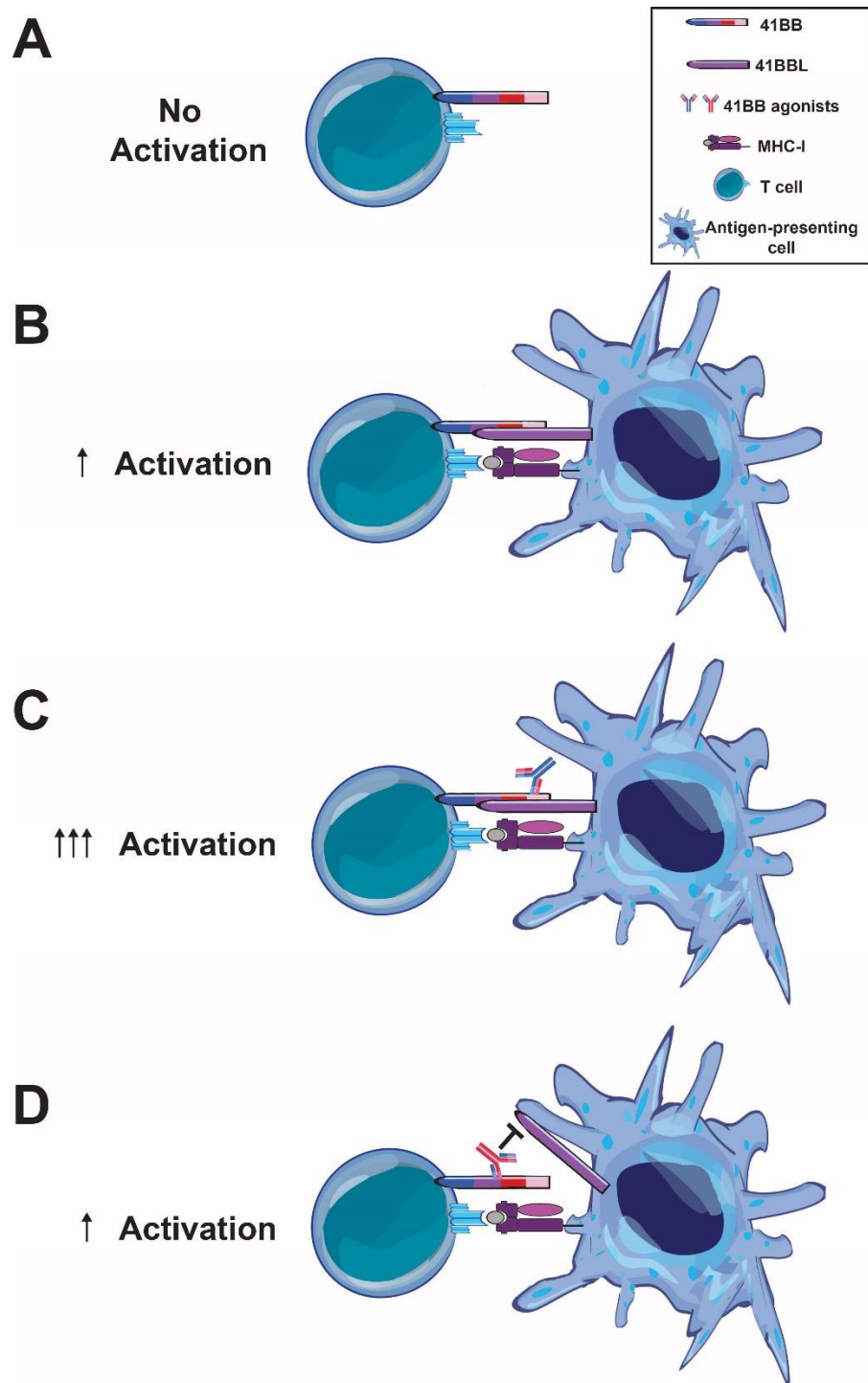


**Figure 14. Potential mechanisms of 41BB agonism in the context of APC-mediated stimulation**

(A) T cells that receive no TCR stimulation or 41BB co-stimulation are not activated. (B) Peptide presentation by APCs via MHC-I and co-stimulation provided by 41BBL stimulates T cell activation. (C) Certain 41BB agonistic antibodies can augment T cell activation by allowing 41BBL on APCs and 41BB agonists to provide a dual signal to T cells resulting in a strong activation stimulus. (D) Other 41BB agonistic antibodies bind to the native 41BBL binding domain on 41BB, preventing the simultaneous activation stimuli provided by agonistic antibodies and 41BBL.

## Methods

### *Human TIL specimens and tumor digest preparation*

Preparation of TIL was performed as previously described (8). Briefly, surgically resected tumors were minced to 1mm fragments and placed into individual wells of a 24 well plate containing 6000IU/mL IL-2 (aldesleukin, Prometheus Laboratories). TILs were expanded for up to 5 weeks and then tested for IFN-gamma production in co-cultures with autologous tumor cell lines or cryopreserved tumor digest cell suspensions. IFN-gamma<sup>+</sup> TILs underwent a rapid expansion protocol (REP) and were then cryopreserved in 90% human serum with 10% dimethyl sulfoxide (DMSO). A fully human IgG4 monoclonal agonistic anti-41BB antibody ( $\alpha$ 41BB mAb;BMS-663513, urelumab, Bristol-Myers Squibb) was added with media containing 6000IU/mL IL-2 to tumor fragments at the initiation of TIL expansion. Thereafter, TILs were fed every 3-4 days with media containing 6000IU/mL IL-2 only. Cryopreserved TILs were thawed and rested in media containing 3000IU/mL IL-2 for 3-4 days before being subjected to further stimulation and co-culture conditions. For the preparation of tumor digests, the remaining tumor tissue was suspended in digestion media containing collagenase type II and type IV, hyaluronidase, and DNase I (all from Fisher Scientific) and then subjected to GentleMACS dissociation (Miltenyi Biotec). Tumor digest cell suspensions were incubated at 37°C in a rocking water bath for 1hr and then filtered with 100 $\mu$ M cell strainers to remove large cellular debris.

### *Isolation and culture of human myeloid cells from peripheral blood mononuclear cells*

Peripheral blood mononuclear cells (PBMCs) were obtained from the whole blood of healthy donor volunteers or apheresis product from melanoma patients. For whole blood,

PBMCs were prepared by Ficoll-Pacque (GE Healthcare) and then cryopreserved. Thawed PBMCs were labeled with CD11b microbeads human and mouse (Miltenyi Biotec, 130-49-601) for magnetic activated cell sorting. Purity of CD11b<sup>+</sup> cells was >90%. For healthy donor myeloid cells, 2.5x10<sup>5</sup> cells were cultured in 6 well plates coated with 10µg/mL α41BB or 10µg/mL 41BB-Fc (R&D Systems) in media alone or media containing 100ng/mL human GMCSF (Peprotech) for 3 days. For the generation of APCs, CD11b<sup>+</sup> cells from the pheresis product of a melanoma patient were cultured with 10µg/mL immobilized 41BB-Fc for 3 days. Adherent cells were dissociated using Accutase (STEMCELL Technologies) and gentle pipetting. Cell lysate from an autologous melanoma cell line was prepared by suspending cells at 30x10<sup>6</sup>/mL in PBS and exposure to repeated and alternating temperatures (solid CO<sub>2</sub> ice and 37°C water). Five cycles of alternating temperature exposure at 5-minute intervals were performed. Three cell equivalents of tumor cell lysate were added to 1x10<sup>6</sup> 41BB-Fc conditioned APCs in media containing 100ng/mL GMCSF and incubated overnight. Tumor-lysate pulsed APCs were then dissociated using Accutase and gentle pipetting before co-culture with TILs as described below. Cytokines in supernatants were measured by LEGENDplex HU Essential Immune Response Panel (BioLegend) and acquired via BD FACSCelesta.

### ***Human TIL co-culture assays***

Thawed autologous tumor cell suspensions were added to 96-well round-bottom plates at a 1:1 ratio with TILs and cultured for 24hrs. Anti-human HLA-A,B,C (W6/32, BioLegend) was added to tumor cells at a concentration of 10µg/mL and incubated for 1hr at 37°C before adding TILs to respective wells. Anti-human CD3 (OKT3, Ortho Biotech Inc., Bridgewater, NJ) was immobilized on the bottom of wells at 5µg/mL. Supernatants were collected after 24hrs of TIL-tumor digest co-cultures and IFN-gamma was measured in supernatants via IFN-gamma ELISA

(BD Biosciences). For TIL co-cultures with autologous tumor cell lines or autologous tumor-lysate pulsed APCs, supernatants were collected after 72hrs of cultures. Prior to co-culture, autologous tumor cell lines were subjected to X-ray irradiation at a dose of  $2 \times 10^4$  rad. TILs were co-cultured at a 10:1 ratio with irradiated tumor cells or tumor-lysate pulsed APCs. Where indicated, soluble  $10 \mu\text{g/mL}$   $\alpha 41\text{BB}$  or anti-41BBL (5F4, BioLegend) was added to TIL co-cultures. Cytokines in supernatants were measured by LEGENDplex HU Essential Immune Response Panel (BioLegend) and acquired via BD FACSCelesta. Proliferation was measured by  $^3\text{H}$  thymidine uptake ( $1 \mu\text{Ci}$  added per well) during the final 18hrs of co-culture.

#### ***Detection of cytokines from primary melanomas***

Tumor digest cell suspensions were prepared as described above. One million cells were seeded in 48 well plates containing media with or without  $6000 \text{IU/mL}$  IL-2 in combination with soluble  $\alpha 41\text{BB}$  ( $10 \mu\text{g/mL}$ ). After 24hrs, cell-free supernatants were collected and stored at  $-80^\circ\text{C}$  until ready for analysis. Cytokines in supernatants were measured by LEGENDplex HU Essential Immune Response Panel (BioLegend) and acquired via BD FACSCelesta.

#### ***Flow cytometry***

Mouse spleens and tumors were harvested under sterile conditions. Spleens were homogenized by applying pressure to tissue on  $100 \mu\text{m}$  cell strainers. Single-cell suspensions were prepared, and red blood cells were removed using red blood cell lysis buffer (BioLegend). The resulting suspension was passed through a  $70 \mu\text{m}$  cell strainer and washed once with PBS. Mouse tumor cell suspensions were prepared by enzymatic digestion with media (Hank's Balanced Salt Solution, Life Technologies) containing  $1 \text{mg/mL}$  collagenase IV,  $0.1 \text{mg/mL}$  DNAaseI, and  $2.5 \text{U/mL}$  hyaluronidase (all from Sigma Aldrich) and then subjected to



GentleMACS dissociation (Miltenyi Biotec). Tumor digest cell suspensions were incubated at 37°C in a rocking water bath for 1hr. Red blood cells were removed using red blood cell lysis buffer (BioLegend) and then cell suspensions were filtered with 100µM cell strainers to remove large cellular debris. Cells were resuspended to a concentration of 0.5-1x10<sup>6</sup> cells/mL for flow cytometric analysis in FACS Buffer containing PBS, 5% fetal bovine serum, 1mM Ethylenediaminetetraacetic acid (EDTA) (Sigma Aldrich), and 0.1% sodium azide (Sigma Aldrich). Cell viability was measured by staining cell suspensions with ZombieNIR (BioLegend). Prior to surface staining, cells were incubated with Fc Shield (TonboBiosciences) for murine specimens and Fc Blocker (Miltenyi Biotec) for human specimens. For surface staining of murine specimens, cells were stained in FACS buffer with the following antibodies: CD3 (145-2C11), CD4 (GK1.5), CD8 (53-6.7), CD11b (M1/70), Ly6G (1A8), Ly6C (HK1.4), F4/80 (BM8), CD11c (N418), MHCII (M5/114.15.2), CD80 (16-10A1), CD86 (GL-1), PD-1 (29F.1A12) (all from BioLegend); 41BB (17B5-1H1, Miltenyi Biotec). For intracellular cytokine detection, cells were incubated for 18hrs with 1X Brefeldin A (BioLegend), stained with cell surface antibodies, subjected to fixation and permeabilization via Fixation and Permeabilization Solution Kit (BD Biosciences), and then stained anti-mouse antibodies against IL-12p40/p70 (BD Biosciences), IL-6 (MP5-20F3), IL-10 (JES5-16E3), TNFα (MP6-XT22) (all from BioLegend). For human specimens, cell surface staining was conducted with the following antibodies: CD3 (145-2C11), CD4 (RPA-T4), CD8 CD11c (Bly6), CD14 (MoP9), CD15 (HI98), CD11b (ICRF44), HLA-DR/DP/DQ (Tu39), CD86 (all from BD Biosciences); PD-L1 (29E-2A3), 41BBL (5F4), 41BB (4B4-1), CD45 (2D1) (from BioLegend); CD141 (AD5-14H12) (Miltenyi Biotec). Cells were acquired by FACS Celesta (BD Biosciences), and the data were analyzed with FlowJo (Tree Star).

### ***Mouse models***

Female C57BL/6 mice (6–8 weeks old) were purchased from Charles River Laboratories (Wilmington, MA). OT-I mice (originally obtained from Jackson Laboratories) were bred and housed at the Animal Research Facility of the H. Lee Moffitt Cancer Center and Research Institute. Mice were humanely euthanized by CO<sub>2</sub> inhalation and secondary cervical dislocation according to the American Veterinary Medical Association Guidelines. Mice were observed daily and were humanely euthanized if a solitary subcutaneous tumor exceeded 400 cm<sup>2</sup> in area or mice showed signs referable to metastatic cancer.

### ***Murine cell lines and in vivo treatment***

B16 melanoma, Panc02 pancreatic cancer, MC38 colorectal cancer cell lines (all obtained from ATCC), were cultured in complete media (CM): RPMI media supplemented with 10% heat-inactivated FBS, 0.1 mM nonessential amino acids, 1 mM sodium pyruvate, 2 mM fresh L-glutamine, 100 mg/ml streptomycin, 100 U/ml penicillin, 50 mg/ml gentamicin, 0.5 mg/ml fungizone (all from Life Technologies, Rockville, MD), and 0.05 mM 2-ME (Sigma-Aldrich, St. Louis, MO). B16 melanoma with pAc-neo-OVA plasmid (B16-OVA) was maintained in media with 0.8mg/mL G418 as previously described (137). To generate the ovalbumin (OVA) expressing fluorescent Panc02 cell line, cells were exposed to supernatants containing a lentiviral vector comprised of a fluorescent ZsGreen (ZsG) protein and OVA. Upon successful transfection, ZsGreen<sup>hi</sup> tumor cells were subjected to FACS using BD FACSAria. OVA-ZsGreen<sup>hi</sup> tumor cells were passaged *in vitro* 4 times whereby OVA expression was validated by staining for H2-K<sup>b</sup> bound to SIINFEKL peptide (25-D1.16, BioLegend). The cell lines tested negative for mycoplasma contamination. All cell lines were passaged less than 10 times after initial revival from frozen stocks. All cell lines were validated in core facilities prior to use.

Tumor cells ( $1 \times 10^5$ ) were implanted subcutaneously in the flank of mice. When tumors reached  $\sim 25 \text{mm}^2$ ,  $75 \mu\text{g}$  of InVivoPlus anti-mouse 41BB (clone LOB12.3) or rat IgG1 isotype control, anti-horseradish peroxidase (both from BioXCell), were injected in  $50 \mu\text{L}$  volume intratumorally. Injections were repeated twice weekly until experimental endpoint. In some experiments, anti-mouse 41BB (clone LOB12.3) or rat IgG1 isotype control, anti-horseradish peroxidase were injected with  $300 \mu\text{g}$  of antibody twice weekly until experimental endpoint. For CD8 T cell depletion,  $300 \mu\text{g}$  of InVivoPlus anti-mouse CD8 $\alpha$  (BioXCell) were injected intraperitoneally twice weekly for the duration of the experiment. CD8 T cell depletion was initiated prior to treatment with isotype or  $\alpha 41\text{BB}$  antibodies.

#### ***Tumor-myeloid cell co-culture with OT-I T cells***

Myeloid cells were isolated from MC38 tumors after treatment with isotype or  $\alpha 41\text{BB}$  antibodies using EasySep Mouse CD11b Positive Selection Kit II (STEMCELL Technologies). CD8 T cells were isolated from the spleens of OT-I mice using EasySep Mouse CD8 T cell Isolation Kit (STEMCELL Technologies). OT-I T cells were labeled with CellTrace Violet (Invitrogen) prior to co-culture. OT-I T cells were co-cultured with myeloid cells in media containing  $1 \mu\text{g}/\text{mL}$  OVA<sub>(257-264)</sub> peptide with or without neutralizing antibodies for IL-10 (JES5-2A5) or IL-12-p75 (R2-9A5) (both from BioXCell) at a concentration of  $10 \mu\text{g}/\text{mL}$  each. Cells and supernatants were harvested after 72hrs incubation. IFN-gamma in supernatants were measured by (Mouse IFN-gamma Quantikine ELISA Kit, R&D Systems).

### ***Isolation of murine TILs***

TILs from mice with MC38 tumors were isolated after treatment with isotype or  $\alpha$ 41BB antibodies using EasySep Mouse CD90.2 Positive Selection Kit II (STEMCELL Technologies). TILs were cultured in round-bottom 96 well plates with immobilized anti-CD3 antibodies (145-2C11 BD Biosciences) at a concentration of 5 $\mu$ g/mL or with irradiated tumor cell lines. MC38 or irrelevant target B16 tumor cells were exposed to X-ray irradiation at a dose of 2x10<sup>4</sup> rad and cultured with CD90.2<sup>+</sup> TILs at a 1:10 (target:TIL) ratio for 48hrs. Supernatants were collected and IFN-gamma was measured by (Mouse IFN-gamma Quantikine ELISA Kit, R&D Systems).

### ***Statistical analysis***

Graphs were generated using GraphPad Prism software. Graphs represent mean values with SEM. P values were calculated in each respective figure where statistical tests were indicated. For mouse-tumor growth studies, tumor growth curves are shown as mean with SEM and significance was determined by 2-way ANOVA and Sidak's multiple comparison's test. Mice were randomized after tumor cell implantation into respective treatment groups. Tumors were measured with Vernier calipers. Experimental groups were blinded to the operator throughout the duration of the experiment. For all other experiments, data were compared using either an unpaired 2-tailed Student's t-test corrected for multiple comparisons by a Bonferroni adjustment or Welch's correction. \* = P < 0.05; \*\* = P < 0.01; \*\*\* = P < 0.001; \*\*\*\* = P < 0.0001.

### ***Study Approval***

Studies were performed under approved Institutional Review Board (IRB) laboratory protocols at the H. Lee Moffitt Cancer Center (Tampa, FL). TIL, PBMC, and autologous tumors were collected from melanoma patients or PBMC from lung tumor patients as part of TIL ACT

clinical trials. All samples were de-identified prior to use in research studies. All patients signed approved consent forms. All animal experiments were approved by the University of South Florida Institutional Animal Care and Use Committee and performed in accordance with the U.S. Public Health Service policy and National Research Council guidelines.

**CHAPTER THREE**  
**REACTIVE MYELOPOIESIS TRIGGERED BY LYMPHODEPLETING**  
**CHEMOTHERAPY LIMITS THE EFFICACY OF ADOPTIVE T CELL THERAPY**

**A note to the reader: the majority of this chapter has been published in a research article in *Molecular Therapy*, Innamarato et. al., 2020 Jun 24;S1525-0016(20)30315-4.**

**doi:10.1016/j.ymthe.2020.06.025.**

**Introduction**

***Cancer co-opts myeloid cells to promote immunosuppression and tumor progression***

The tumor microenvironment consists of a heterogeneous population of tumor cells, endothelial cells, fibroblasts, and a variety of immune cells. Macrophages, dendritic cells, monocytes, granulocytes have been associated with poor survival and therapeutic relapses in cancer patients (149, 150). In addition, tumor cells produce factors that promote myeloid cells to facilitate angiogenesis, tissue remodeling, invasion, metastasis, and immunosuppression (151). Hence, the targeting of tumor-associated myeloid cells can provide therapeutic benefit by limiting tumor progression and reducing immune dysfunction. Currently, several approaches to targeting tumor-associated myeloid cells have been investigated in clinical trials including: facilitating macrophage phagocytosis of tumor cells by CD47 or SIRP $\alpha$  blockade (152), macrophage depletion via CSF-1/CSF-1R antibodies (153, 154), reprogramming of tumor associated-macrophages by BTK inhibition, PI3K-gamma inhibition (155, 156) or CD40 agonism (157), chemotaxis blockade via CCR2 (158), CXCR2 (159), and CXCR4 (160), and

depletion of myeloid-derived suppressor cells (MDSCs) by Death receptor 5 (DR5) agonistic antibodies (161). The diverse nature of myeloid cells in the tumor microenvironment underscores the importance of these cells in facilitating immune suppression and tumor progression. Thus, there are many opportunities to exploit myeloid cell biology to develop novel therapeutic strategies as anti-cancer treatments, which facilitate the immune system to eradicate tumor cells.

### ***Myeloid-derived suppressor cells are orchestrators of tumor-mediated immunosuppression***

Myeloid-derived suppressor cells (MDSCs) are a heterogeneous population of immature monocytes and granulocytes that possess potent immunosuppressive functions. In healthy individuals, MDSCs are exceedingly rare, but expand during pathological states.

Immunosuppression by MDSCs has been most widely described in the setting of cancer, but MDSCs also play an important role in preventing graft-versus-host disease (GvHD), organ graft rejection, maternal-fetal tolerance, autoimmune diseases, and bacterial infection (162). Two subsets of MDSCs have been widely described: Polymorphonuclear (PMN) MDSCs and monocytic (M-MDSCs). PMN-MDSCs resemble neutrophils while M-MDSCs share similar phenotypes to monocytes (163). A third subset of MDSCs, known as early MDSCs (e-MDSCs) was recently described, but these cells have not been robustly characterized (161).

A key distinction between MDSCs and normal physiologic neutrophils and monocytes is the ability of MDSCs to suppress T cell proliferation and effector functions (164, 165). MDSCs can inhibit T cell proliferation, cytokine production, lymph-node homing, and induce T cell apoptosis (166, 167). MDSCs possess an arsenal of functions that promote immunosuppression including: 1. The production of reactive oxygen species and peroxynitrite, which causes damage to lipid bilayers, induces DNA damage, and disrupts T cell receptor – MHC interactions

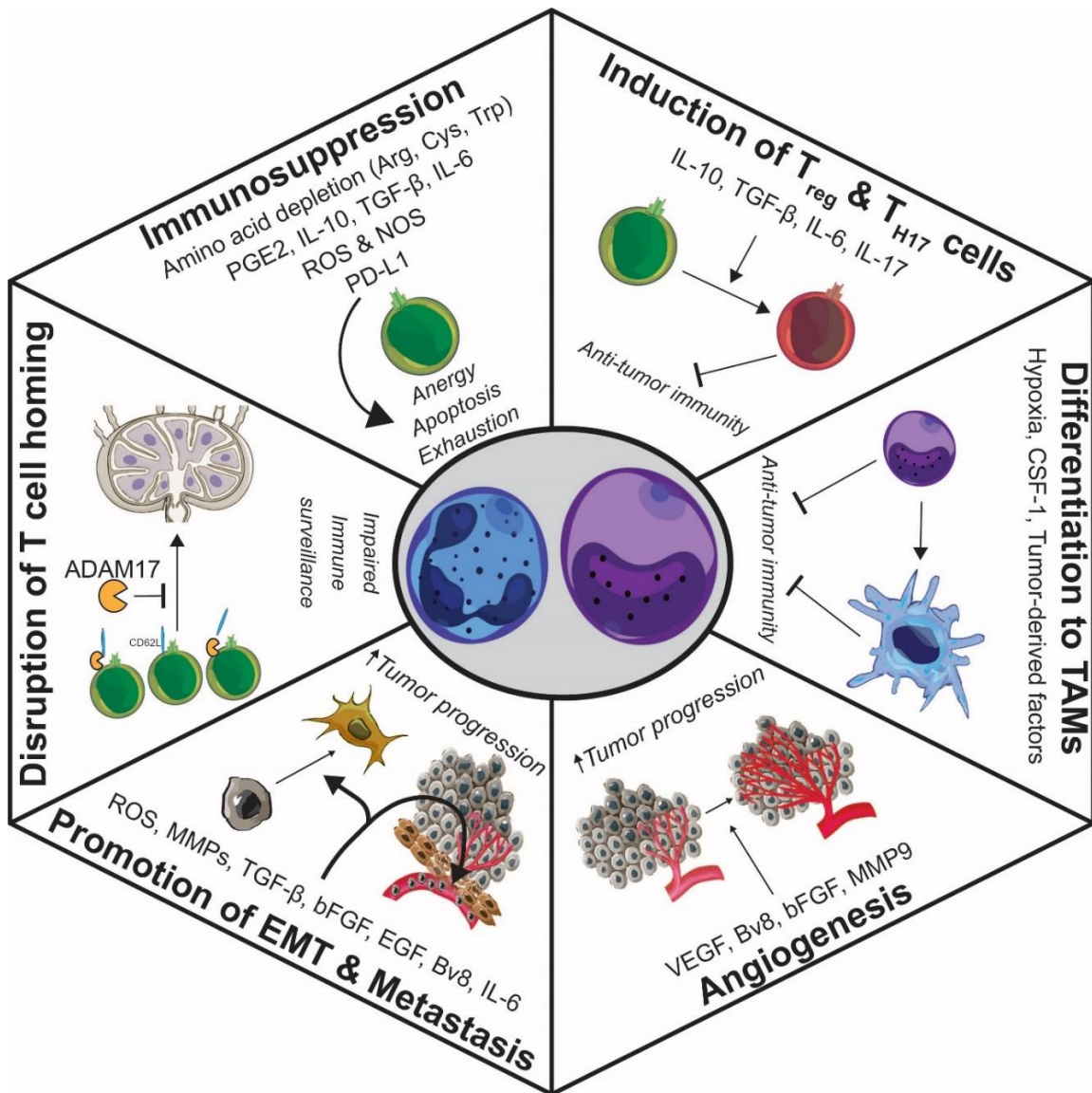


**Figure 15. MDSCs are dynamic immunosuppressive cells that promote tumor progression.**

MDSCs inhibit anti-tumor immunity via the production of cytokines and growth factors, depletion of amino acids, and promotion oxidative stress via ROS/NOS. T<sub>regs</sub> and T<sub>H17</sub> cells can be induced by MDSC-derived cytokines including IL-10, TGF-β, IL-6, and IL-17. In contrast to terminally differentiated PMN-MDSCs, M-MDSCs can differentiate into macrophages which promote tumor progression. Likewise, wound-healing functions of MDSCs promote tumor progression through augmenting angiogenesis and perpetuating the EMT/metastatic cascade through the production of growth factors, proteases, cytokines, and ROS. Systemically, the immune response can be disrupted through the production of ADAM17 by MDSCs which cleave CD62L and prevent lymph node homing of circulating T cells.

(168, 169), 2. The depletion of microenvironmental amino acids via arginase activity, indolamine 2-3 dioxygenase activity, and cysteine sequestration (170-172), 3. The production of cytokines and growth factors including, IL-6, IL-10, PGE2, and TGF-β that directly suppress T cells and promote immunosuppressive phenotypes of DCs, macrophages, and T regulatory cells (167,



173). Additional mechanisms of MDSC-mediated immunosuppression and the promotion of tumor progression have been described in recent review articles (166, 167, 174). Hence, MDSCs act as a suppressive regulator of anti-tumor immunity through the direct suppression of T cells and the promotion of suppressive immune cells.

### ***Reactive myelopoiesis – an immunological process that promotes MDSC accumulation***

The hematopoietic differentiation trajectory and the function of the immune system are hijacked by tumors to promote a growth advantage and evade immune clearance. While tumor cells can induce the polarization of mature myeloid cells such as macrophages and dendritic cells, the skewing of myeloid cell populations is profoundly impacted at the level of hematopoietic stem and progenitor cells (HSPCs). Under normal physiologic conditions, HSPCs differentiate to myeloid, lymphoid, and erythroid progenitors and maintain a balance between the frequency and turnover of individual immune cell subsets. However, during infection with pathogenic microbes, an immunological process known as “emergency myelopoiesis” bone marrow derived neutrophils and monocytes are rapidly mobilized into the peripheral blood and tissues to mediate an immune response to the pathogen. Simultaneously, HSPCs within the bone marrow proliferate and subsequently differentiate to neutrophils and monocytes, resulting in a massive increase in the number of circulating myeloid cells (175). This process can continue until the pathogen is cleared. Fascinatingly, this myelopoietic-driven stress response is tightly regulated and the unchecked proliferation and differentiation of HSPCs during emergency myelopoiesis can lead to bone marrow failure and lethality despite the clearance of a pathological stimulus (176). Hence, both the clearance of a pathogen and the resolution of inflammation are critical for a host’s immune system to return to homeostasis.

The term emergency myelopoiesis has been used to describe the enhanced production of neutrophils and monocytes in the presence of a microbial pathogen. However, in the absence of a microbe, the mechanisms driving an enhanced accumulation of myeloid cells are independent of stimulation via bacterial components, such as LPS. Therefore, the term “reactive myelopoiesis” has been adopted to describe the immunological response of HSPCs, granulocytes, and monocytes caused by tumor-induced inflammation or chemical compounds, including chemotherapy agents (175). Indeed, overlapping mechanisms can be observed in emergency and reactive myelopoiesis. However, the origin of the stimulus and ensuing immunological consequences differ between these immunological phenomena. In the instance of sepsis, the myelopoietic response is acute and resolves once the pathogen is cleared. However, a chronic inflammatory state also promotes an aberrant generation and abundance of myeloid cells that do not exhaust HSPCs or lead to bone marrow failure. Under chronic cancer-induced inflammation, the result of reactive myelopoiesis is an increase of MDSCs. A variety of tumor-derived cytokines and growth factors have been implicated in skewing the differentiation of HSPCs toward the development of MDSCs such as retinoic acid, G-CSF, GM-CSF, PGE2, and IL-6 (167, 177, 178). Together, tumor cells, constituent stromal cells, and infiltrating immune cells produce factors that can act distally on HSPCs within the bone marrow space to skew the differentiation of HSPCs to MDSCs and promote their chemoattraction to tumor beds (151, 174, 179). During tumor progression, an increased accumulation of MDSCs accumulation is observed within cancer patients presumably because the increased systemic inflammation further drives reactive myelopoiesis (180-182). This is evidenced by increases in MDSC-promoting cytokines such as IL-6 and IL-8 in association with an elevated frequency of MDSCs that correlates with

the stage of cancer and patient survival (180, 182, 183). Thus, the inhibition of MDSCs in cancer patients is crucial to promote anti-tumor immune responses and restrict immunosuppression.

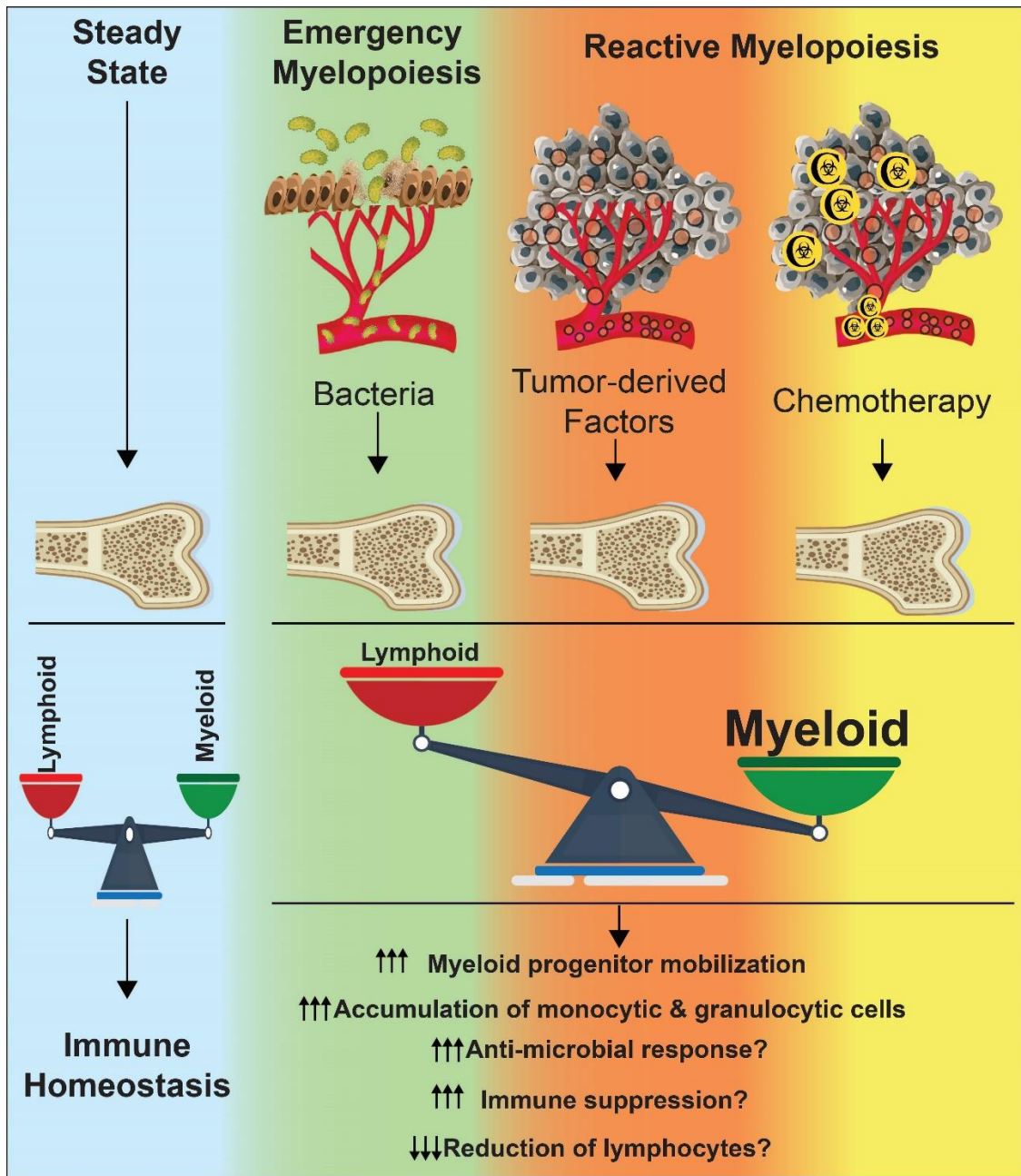


**Figure 16. Reactive myelopoiesis is a driver of tumor-induced immunosuppression.**

In the steady state, a balance between myeloid and lymphoid lineages are maintained. In the case of sepsis, the systemic bacterial infection drives emergency myelopoiesis resulting in the massive production of myeloid cells from the bone marrow. A similar process occurs when tumors are present and produce myelopoietic factors to enhance myeloid progenitor mobilization and the accumulation of monocytic and granulocytic cells (particularly MDSCs). Certain chemotherapeutic agents can exacerbate reactive myelopoiesis and simultaneously reduce the number of lymphocytes. It is not fully understood if the myeloid cells that expand during emergency myelopoiesis act primarily to eliminate microbes and hold immunosuppressive roles. In contrast, the anti-microbial role of highly immunosuppressive MDSCs during reactive myelopoiesis has not been rigorously evaluated.

### ***The role of reactive myelopoiesis in Adoptive T cell Therapy***

As outlined in the previous section of this chapter, the accumulation of MDSCs is resultant of chronic inflammation induced by tumors but can also be promoted by treatment with certain cytotoxic chemotherapy agents. In addition to its use for lymphodepleting regimens in patients receiving ACT and its use as a tumor-cytotoxic agent, cyclophosphamide has long been used to mobilize hematopoietic stem and progenitor cells (HSPCs) for autologous hematopoietic stem cell transplantation (HSCT). Subsequently, reactive myelopoiesis takes place after treatment with cyclophosphamide. However, the immunosuppressive capacity of myeloid cells that accumulate during this immunologic state has not been robustly evaluated (184-187). In adoptive T cell therapy settings, combinatorial approaches with HSCT have been successfully used to treat patients with hematologic malignancies (21, 48). In contrast, the benefit of combining ACT with HSCT in solid tumors settings, such as melanoma, remains unclear (27). Consequently, the specific mechanisms regulating the differentiation of immune cells from HSPCs and their ensuing impact on anti-tumor immune functions during the course of ACT for the treatment of cancer remains unknown. Thus, the work described in this chapter addresses these gaps of knowledge in the field of ACT in cancer and identifies mechanisms dictating myelopoiesis during immune recovery after lymphodepleting chemotherapy treatment that can be exploited to enhance the efficacy of ACT.

## Results

### *The accumulation of myeloid cells reduces the therapeutic efficacy of ACT with tumor infiltrating lymphocytes*

We examined myeloid cell recovery in melanoma patients after treatment with a lymphodepleting regimen and infusion of autologous TIL. As expected, patient peripheral blood mononuclear cell (PBMC) counts reached their nadir (Day 0) upon completion of a cyclophosphamide-fludarabine (Cy/Flu) lymphodepleting chemotherapy regimen, which rebounded after infusion with autologous TIL (Figure 17). Despite the rebound of total PBMC counts, the proportionality of myeloid cells significantly increased in comparison to their respective pre-treatment frequencies (Figure 18). We found that nearly all patients exhibited increases in CD11b<sup>+</sup> myeloid cells and subsets, CD11b<sup>+</sup>HLA-DR<sup>-low</sup>CD14<sup>-</sup> cells and CD11b<sup>+</sup>HLA-DR<sup>-low</sup>CD14<sup>+</sup> cells (M-MDSCs), 1-week post-TIL infusion (Figure 19). We confirmed that these myeloid cell populations suppressed T cell proliferation (Figure 20A). Additionally, M-MDSCs isolated from Week 1 Post-TIL infusion PBMCs suppressed autologous TIL proliferation in response to  $\alpha$ CD3/ $\alpha$ CD28 stimulation and autologous tumor stimulation (Figure 20B-C). We confirmed that PMN-MDSCs (CD11b<sup>+</sup>CD15<sup>+</sup>LOX-1<sup>+</sup> cells) were elevated in two melanoma patients at Week 1 Post-TIL infusion (Figure 20D-E, Figure 21) (165). PMN-MDSCs and M-MDSCs purified from Week 1 PBMCs suppressed autologous TIL production of IFN- $\gamma$  (Figure 20E). Furthermore, we confirmed that MDSCs collected at pre-treatment or at Week 2 post-TIL infusion potently suppressed donor T cell and TIL proliferation (Figure 22). We confirmed these findings by detecting increases of PMN-MDSCs after lymphodepletion and TIL infusion in 2 non-small cell lung cancer (NSCLC) patients (Figure 23).

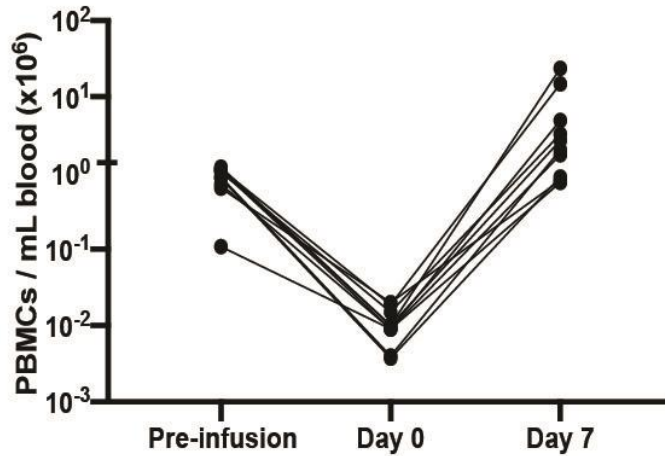


**Figure 17. The effect of lymphodepleting chemotherapy in melanoma patients receiving ACT with TILs.** The total number of PBMCs were quantified in patients prior to lymphodepletion and TIL infusion (Pre-infusion), on the final day of chemotherapy treatment (Day 0), and one week after TIL infusion (Day 7). (n=10)

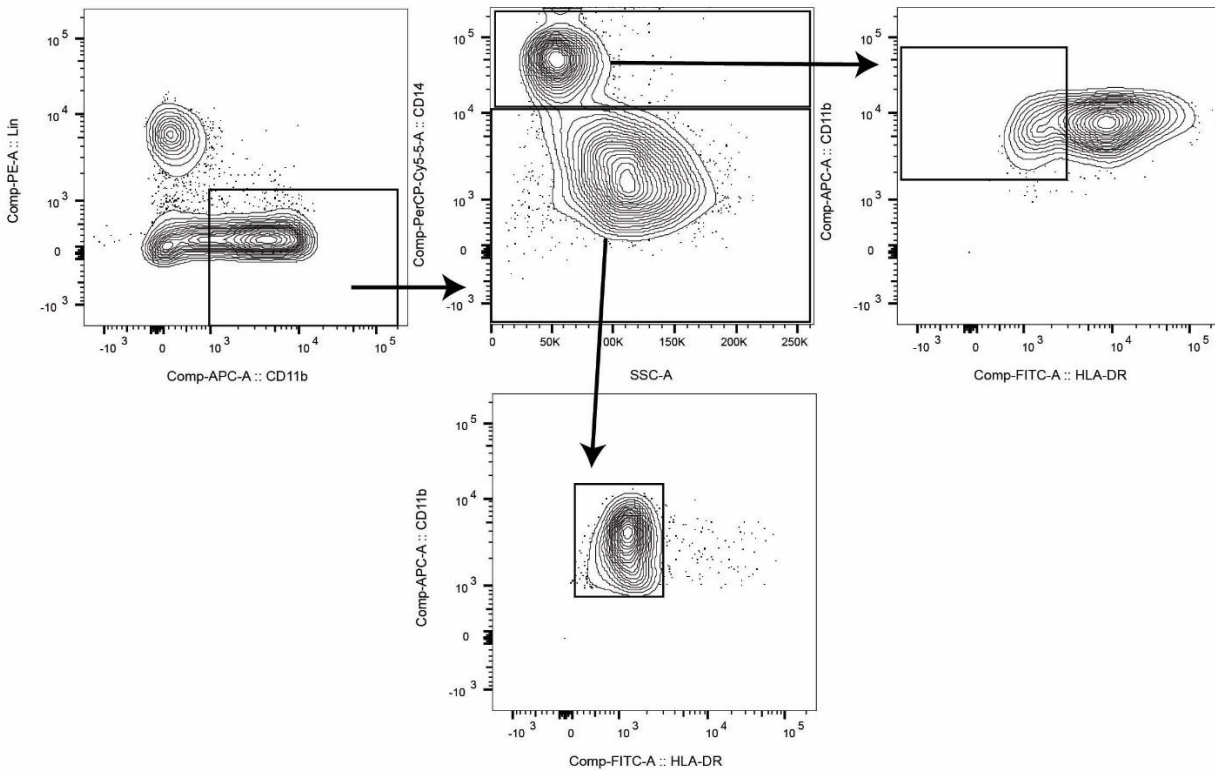


**Figure 18. Gating strategy for identification of myeloid cell subsets in patients.**

Starting from the left on Lin<sup>-</sup> (CD3<sup>-</sup>/CD19<sup>-</sup>/CD56<sup>-</sup>) CD11b<sup>+</sup> cells. Arrow indicate directionality of subgates.

Populations identified in Figure 1 were Lin<sup>-</sup>CD11b<sup>+</sup>CD14<sup>+</sup>HLA-DR<sup>-low</sup> (far right) and Lin<sup>-</sup>CD11b<sup>+</sup>CD14<sup>-</sup>HLA-DR<sup>-low</sup> (bottom).

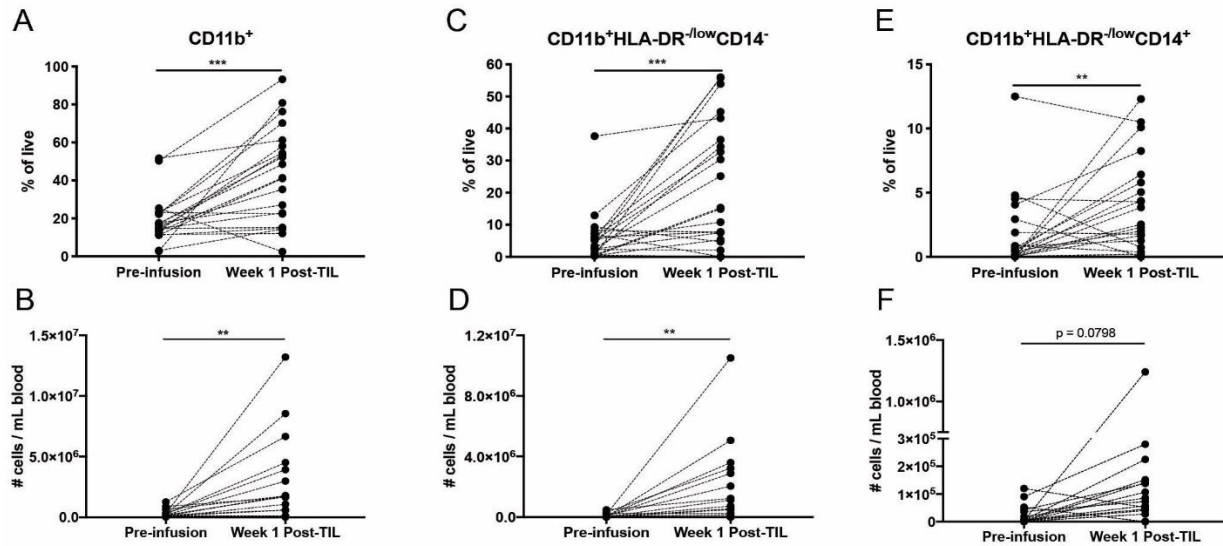


**Figure 19.** Myeloid cell frequency was determined by flow cytometry prior to and after treatment with lymphodepleting chemotherapy and TIL infusion in melanoma patients. The percentage and whole cell numbers of CD11b<sup>+</sup> cells (A-B), CD11b<sup>+</sup>HLA-DR<sup>-low</sup>CD14<sup>-</sup> cells (C-D), and CD11b<sup>+</sup>HLA-DR<sup>-low</sup>CD14<sup>+</sup> cells in PBMCs (E-F) (n=21).

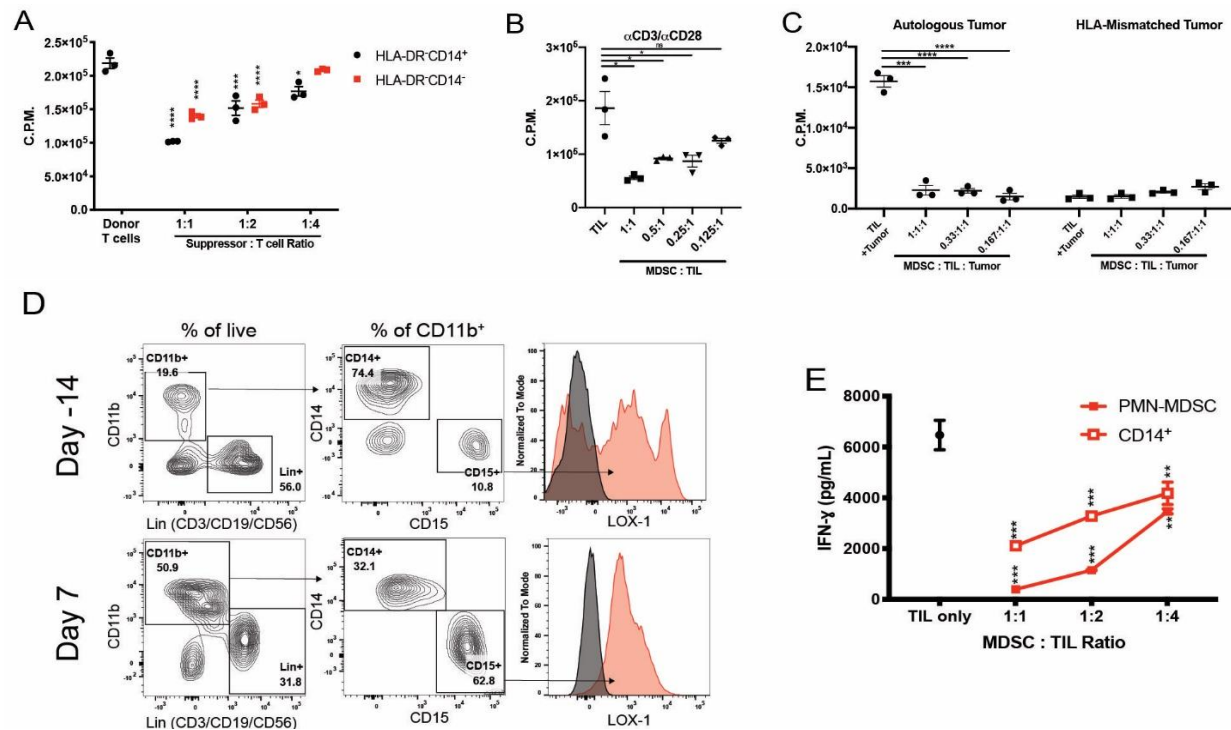


**Figure 20.** MDSCs suppress autologous TILs.

(A) Suppression of donor T cell proliferation in co-cultures with indicated cell subsets isolated from patient PBMCs. (B-C) Suppression of TIL proliferation in co-cultures with autologous M-MDSCs with CD3/CD28 stimulation (B), or cultures with autologous tumor cells (C). (D) Frequency of PMN-MDSCs determined at Day -14 and Day 7 Post-TIL. (E) Suppression of autologous TIL IFN- $\gamma$  production by the patient's CD14<sup>+</sup> cells and PMN-MDSCs collected from Week 1 Post-TIL PBMCs. Individual data points represent technical replicates.

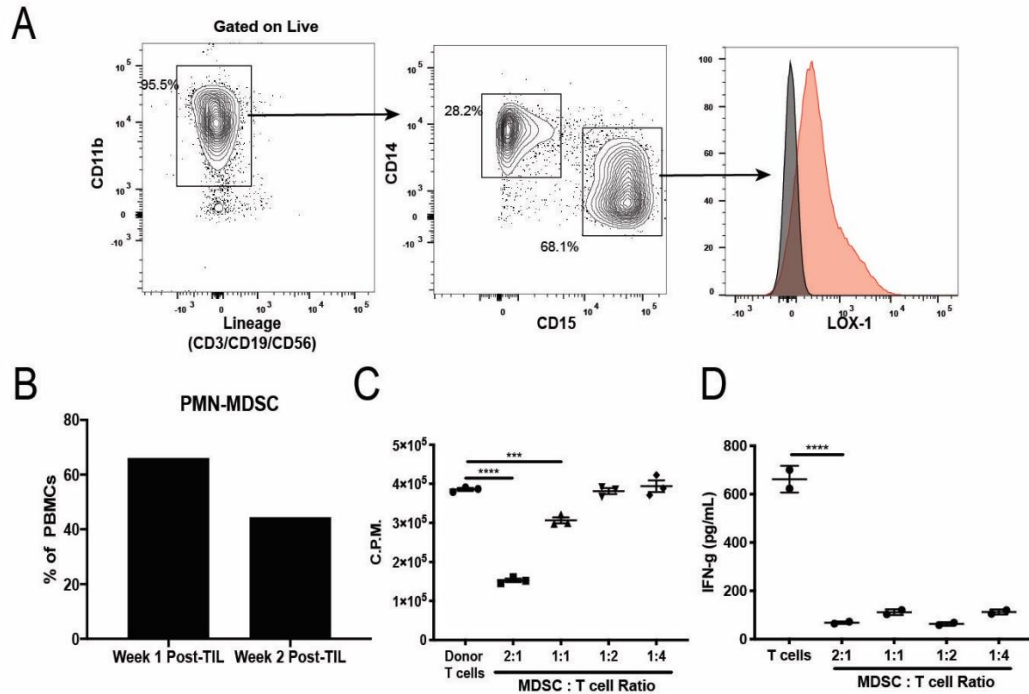


**Figure 21. PMN-MDSCs are abundant after lymphodepletion and TIL infusion.**

(A) Frequency of PMN-MDSCs at Week 1 Post-TIL. (B) Frequency of PMN-MDSCs at Week 1 and Week 2 Post-TIL. Suppression of donor T cell proliferation (C) and IFN- $\gamma$  production by PMN-MDSCs (D). Technical replicates are shown.

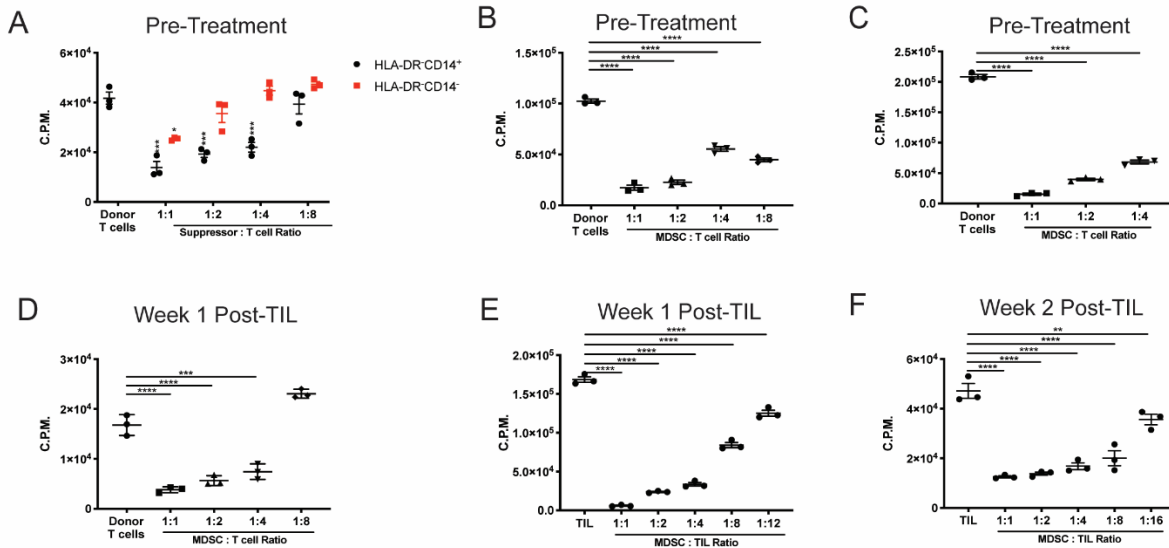


**Figure 22. MDSC suppressive capacity before and after TIL infusion.**

(A-D) MDSC subsets taken from Pre-treatment blood (A), CD11b<sup>+</sup>HLA-DR<sup>-</sup>CD14<sup>+</sup> cells from Pre-treatment blood or Week 1 Post-TIL blood were cultured with donor T cells (B-D). (E-F) CD11b<sup>+</sup>HLA-DR<sup>-</sup>CD14<sup>+</sup> cells from Week 1 Post-TIL (E) or Week 2 Post-TIL (F) blood were cultured with autologous TILs. T cell proliferation was determined by <sup>3</sup>H incorporation. Technical replicates are shown.



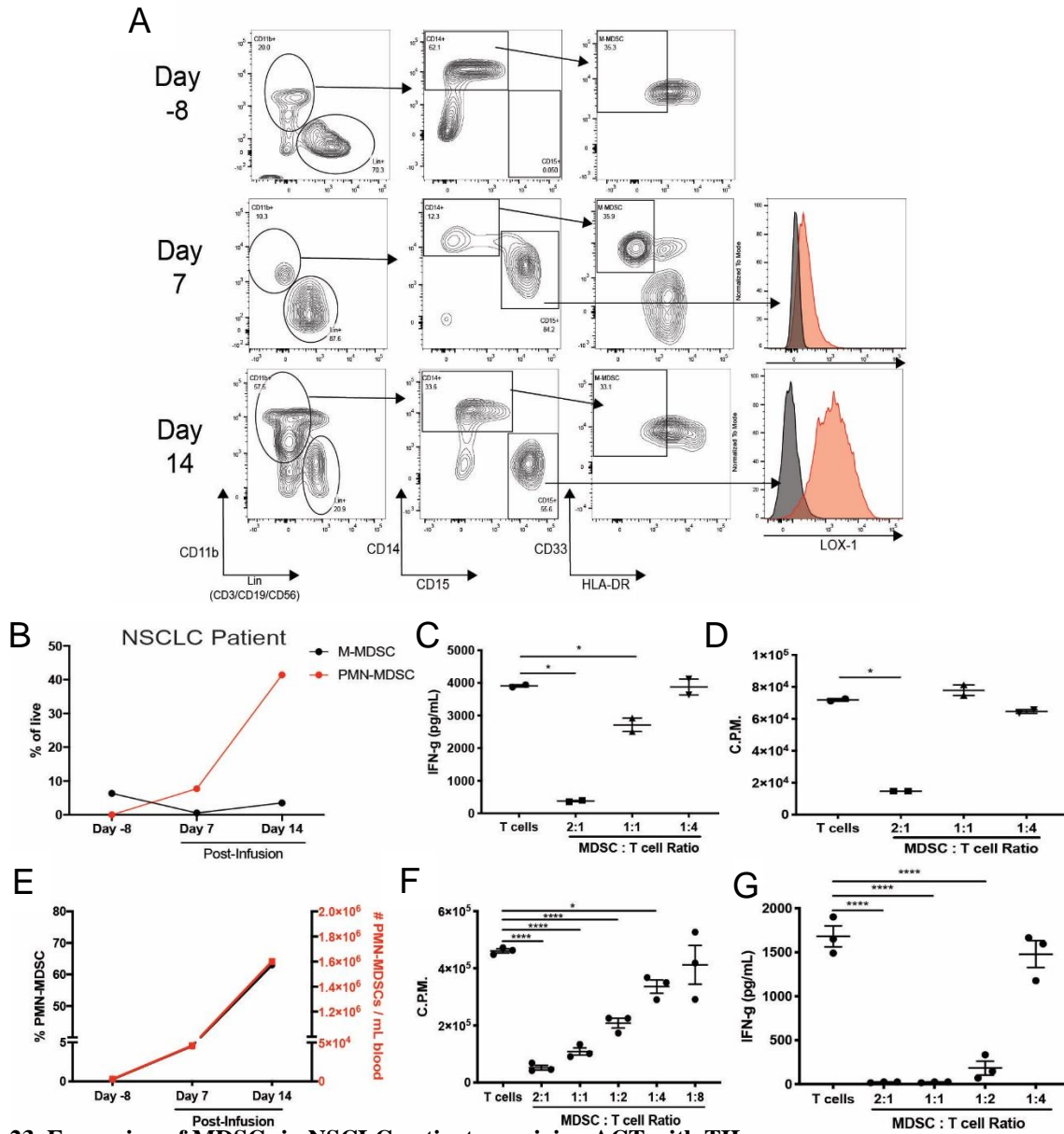


**Figure 23. Expansion of MDSCs in NSCLC patients receiving ACT with TIL.** (A) Gating strategy to identify PMN-MDSCs and M-MDSCs in NSCLC patient 1 at Day -8 before TIL infusion and Day 7 and Day 14 Post-TIL infusion and completion of a lymphodepleting chemotherapy regimen. Gates start from the percentage of live cells to subgates indicated by arrows with their respective frequency of parental gates. (B) Frequency of M-MDSCs and PMN-MDSCs of total live PBMCs at respective blood draws. (C-D) Suppression of IFN- $\gamma$  production (C) and T cell proliferation (D) by PMN-MDSCs after 72hrs of co-culture. (E) Frequency of PMN-MDSCs of total live cells in NSCLC patient 2. (F-G) Suppression of T cell proliferation (F) and IFN- $\gamma$  production (G) by PMN-MDSCs after 72hrs of co-culture. Technical replicates are shown.

Because MDSCs were significantly elevated immediately after TIL infusion, we hypothesized that the abundance of MDSCs would be associated with clinical responses.

Retrospective analysis revealed that higher frequencies of CD11b<sup>+</sup> myeloid cells (greater than

the median of 41%) detected at Week 1 post-TIL infusion were associated with worse progression-free survival (PFS) and overall survival (OS) (Figure 24A-B). We identified similar survival trends when we examined survival associations with myeloid cell subsets (CD11b<sup>+</sup>HLA-DR<sup>-low</sup>CD14<sup>-</sup> cells and M-MDSCs) (Figure 24C-F). Additionally, an increased ratio of the number of CD11b<sup>+</sup> cells relative to CD8<sup>+</sup> T cells detected at Week 1 post-infusion was associated with poor survival (Figure 25). We identified that the number of TIL infused in each melanoma patient did not correlate with the frequency of CD11b<sup>+</sup> cells, suggesting that the magnitude of myeloid cell accumulation after lymphodepletion is independent of TIL infusion (Figure 26A). Likewise, the frequency of CD11b<sup>+</sup> cells in patients prior to receiving lymphodepletion and ACT with TIL did not have an impact on PFS, suggesting that the pre-infusion myeloid cell abundance does not predispose patients to worse outcomes (Figure 26B). Because therapeutic responses to treatment with ACT with TIL are associated with the persistence of infused T cells (8, 72), we used TCR $\beta$  sequencing to identify persistent TIL clones after infusion. Strikingly, the frequency of infused TIL at Week 6 was inversely correlated with the frequency of CD11b<sup>+</sup> cells at Week 1 Post-TIL infusion (Figure 27A). Next, we examined the persistence of the Top 50 TIL clones from the time of infusion to 6 weeks post-infusion (Figure 27B-C). Overall, the proportion of the Top 50 TIL clones among the total T cell pool varied greatly amongst patients (15.6% to 96%). Moreover, the sum frequency of the Top 50 clones was reduced in all patients by Week 6 which was likely due to a dilution caused by the reconstitution of T cell clones that were not present within the infusion product (i.e. endogenous T cell clones) (Figure 28). Intriguingly, the persistence of the Top 50 TIL clones was negatively associated with the frequency of CD11b<sup>+</sup> cells at Week 1 Post-TIL infusion. Specifically, patients that had a frequency of myeloid cells above the median (>41% CD11b<sup>+</sup>) at Week 1 Post-

TIL infusion (CD11b<sup>high</sup>) exhibited a greater reduction in the frequency of the Top 50 TIL clones compared to patients that had <41% CD11b<sup>+</sup> myeloid cells at Week 1 Post-TIL infusion (CD11b<sup>low</sup>) (Figure 29). We next divided the patients from Figure 27A into two groups to interrogate survival analysis based on both the frequency of TILs at Week 6 post-infusion and the matched frequency of CD11b<sup>+</sup> cells at Week 1 post-infusion. The median Sum TIL frequency was 0.66 among patients (>0.66, TIL<sup>high</sup>; <0.66 TIL<sup>low</sup>). We determined that the combined metrics encompassing both TIL frequency and CD11b<sup>+</sup> cell frequency revealed that PFS and OS was poor in patients that exhibited low TIL persistence and a high frequency of CD11b<sup>+</sup> cells (TIL<sup>low</sup>CD11b<sup>high</sup>) in comparison to patients that exhibited high TIL persistence and a low frequency of CD11b<sup>+</sup> cells (TIL<sup>high</sup>CD11b<sup>low</sup>) (Figure 29). Collectively, these data demonstrate that the accumulation of immunosuppressive myeloid cells during treatment limits the efficacy of ACT with TIL, potentially by reducing the persistence of adoptively transferred tumor-specific T cells.

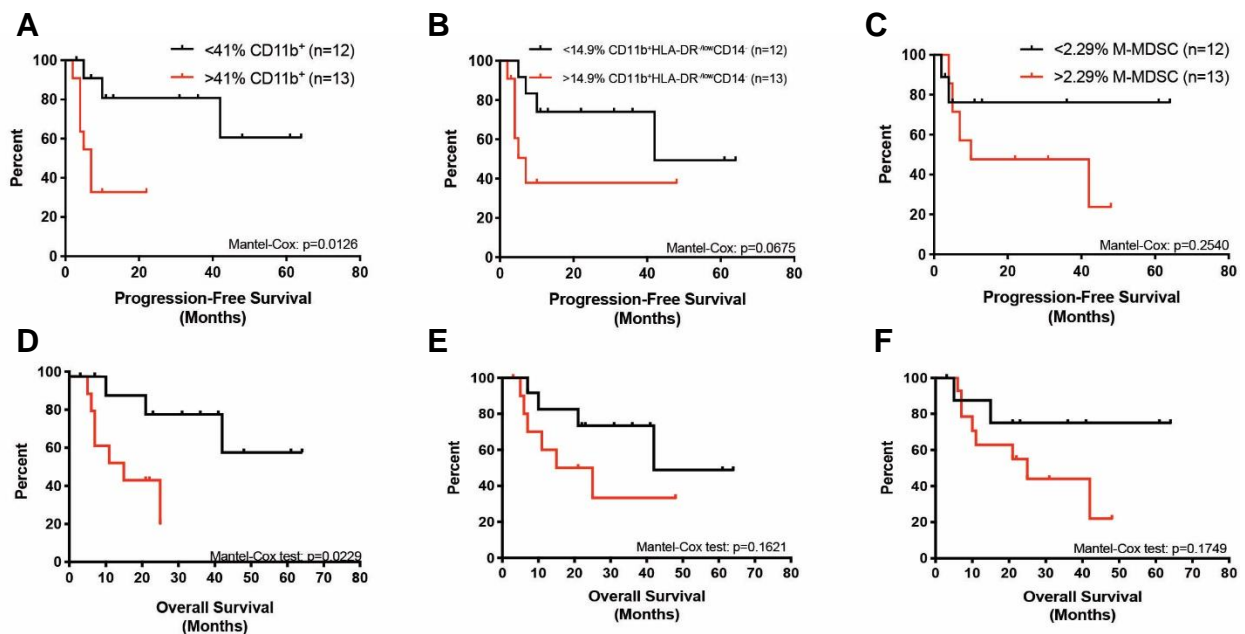


**Figure 24. The accumulation of MDSCs after lymphodepletion and TIL infusion is associated with patient outcomes.**

(A-F) Kaplan-Meier curves showing the PFS and OS in association with the frequency of CD11b<sup>+</sup> cells (A-B), CD11b<sup>+</sup>HLA-DR<sup>low</sup>CD14<sup>-</sup> cells (C-D), and M-MDSCs (E-F) at Week 1 Post-TIL.

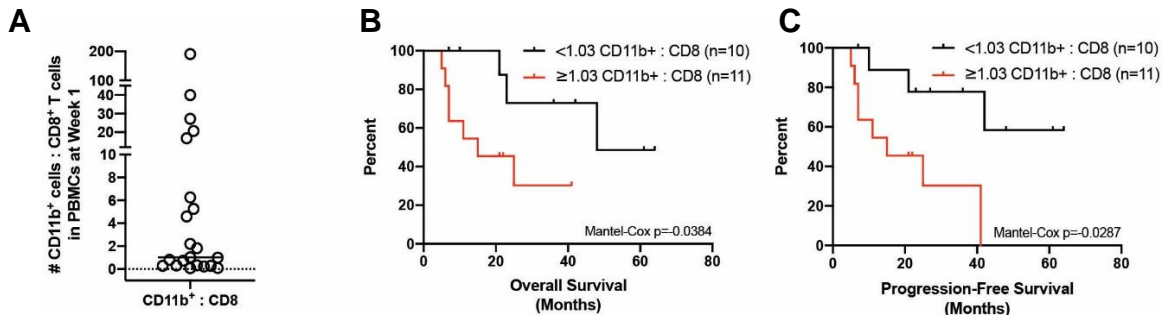


**Figure 25. The ratio of myeloid cells to CD8<sup>+</sup> T cells is associated with poor patient survival.** (A) The ratio of CD11b<sup>+</sup> cells to CD8<sup>+</sup> T cells was defined by the whole cell numbers of each immune cell subset within Week 1 Post-TIL PBMCs. Solid black bar = median (1.03). (B-C) A high CD11b:CD8 ratio is associated with worse OS (B) and PFS (C).

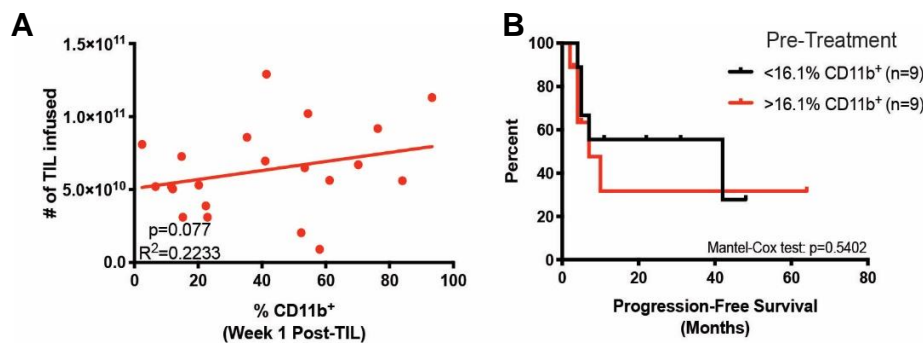


**Figure 26. Survival associations with the number of infused TILs and Pre-treatment myeloid cell frequency.** (A) Linear regression of the number of TILs infused and the frequency of CD11b<sup>+</sup> cells. (n=25) (B) The frequency of myeloid cells before lymphodepletion and TIL infusion is not associated with PFS.

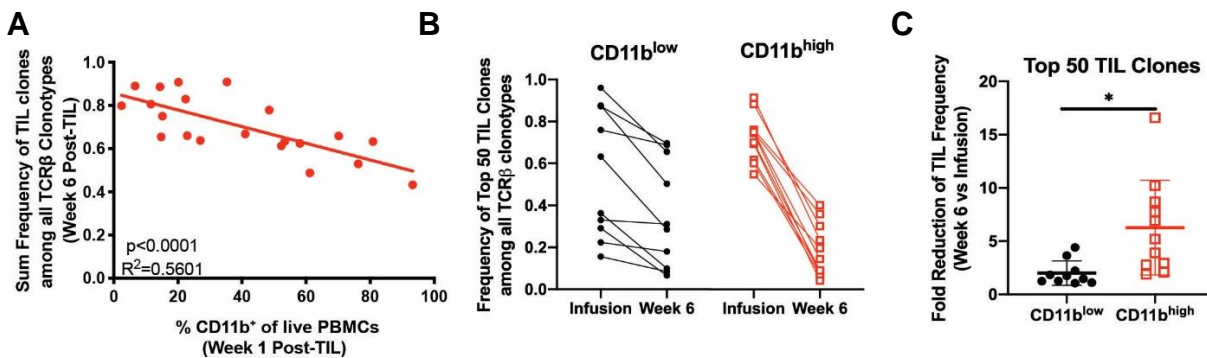


**Figure 27. The *in vivo* persistence of TILs is diminished by an abundance of myeloid cells.** (A) The sum frequency of TILs at Week 6 post-infusion is negatively correlated with the frequency of myeloid cells at Week 1 post-infusion (n=23). (B-C) The Top 50 clones within patients' TIL infusion product were quantified and tracked from infusion to Week 6. Two groups were split based on the median frequency of CD11b<sup>+</sup> cells. (C) The reduction of the Top 50 TIL clones was greater in the CD11b<sup>high</sup> group.

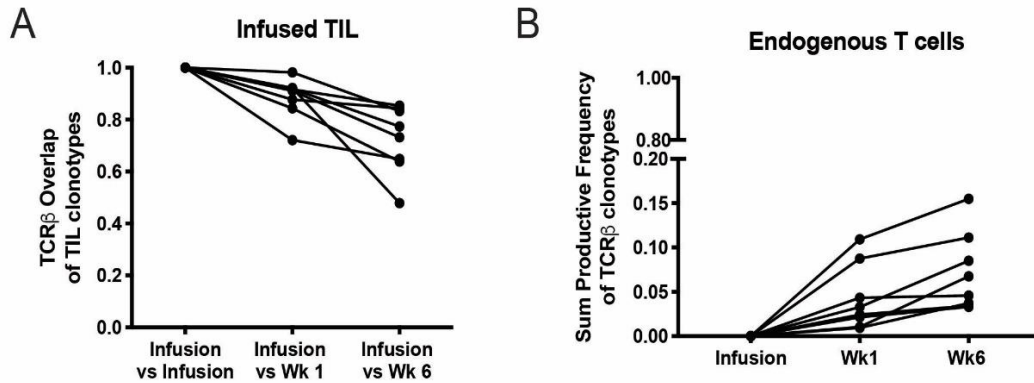


**Figure 28. Tracking TIL clonotypes and identification of endogenous T cells**

(A) TCR $\beta$  overlap of all TIL clonotypes in melanoma patients that received ACT with TIL. Overlap was compared to TILs detected from the time of infusion to Week (Wk) 1 and Wk 6 post-TIL infusion. (B) Sum frequency of all endogenous T cells that were not present within each respective patient's infusion product. The frequency of endogenous T cells increased over time as indicated at Wk1 and Wk6 post-TIL infusion.

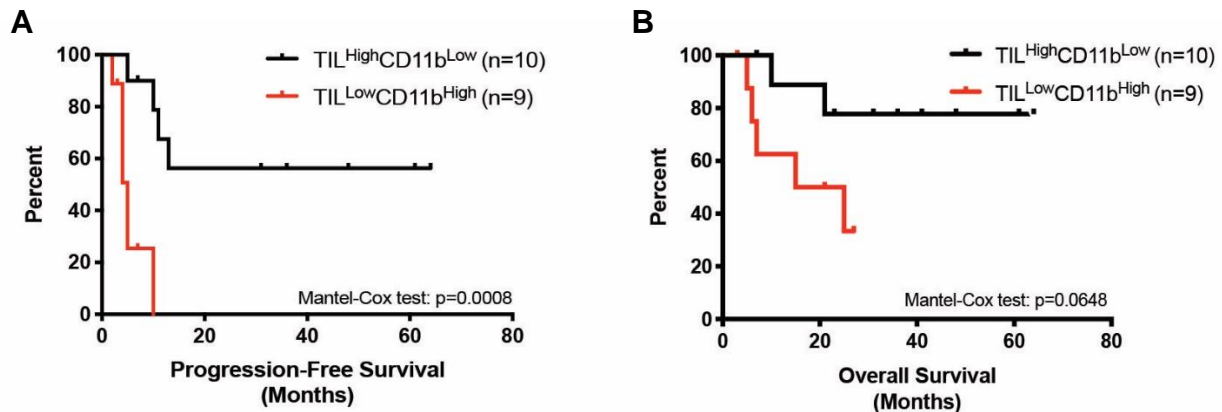


**Figure 29. The reduction of TIL persistence in relation to myeloid cell frequency is associated with poor survival in melanoma patients.**

(A-B) Kaplan-Meier curves of PFS (A) and OS (B) in patients determined by Week 6 TIL frequency in relation to Week 1 CD11b frequency calculated from Figure 27A.

### *Myeloid derived suppressor cells rapidly expand after treatment with lymphodepleting chemotherapy in mice*

The use of Cy/Flu-based regimens are widely applied clinically to induce lymphodepletion for ACT (6, 188). To examine endogenous immune cell reconstitution, we treated tumor-bearing mice with lymphodepleting doses of Cy/Flu and examined the frequency of immune cells in the spleen and bone marrow (BM) at multiple time points. At early time points, the cellularity of spleens and BM remained well below baseline, while at 7 days post-

lymphodepletion, total cell numbers were similar to non-treated (NT) mice (Figure 30A-C). However, the frequency of myeloid cells was dramatically increased in the spleens and BM of lymphodepleted (LD) mice (Figure 30D-F). As expected, the number of T cells remained significantly depleted at Day 7 post-lymphodepletion, while CD11b<sup>+</sup>Ly6C<sup>hi</sup>Ly6G<sup>-</sup> M-MDSCs and CD11b<sup>+</sup>Ly6C<sup>+</sup>Ly6G<sup>+</sup> PMN-MDSCs were present at 4-5 fold higher than untreated mice (Figure 30F-I). A similar trend was exhibited in the BM (Figure 30J-K). Furthermore, sorted Gr-1<sup>+</sup> cells from the spleens of NT and LD mice suppressed T cell proliferation and IFN- $\gamma$  production (Figure 31A-B). We validated these results in mice bearing Panc02 tumors and confirmed that T cells were effectively depleted, while MDSCs expanded upon lymphodepleting chemotherapy treatment (Figure 31C-D). Together, these data show that lymphodepleting chemotherapy induces the accumulation of immunosuppressive myeloid cells.

### ***MDSCs differentiate from mobilized hematopoietic progenitor cells in mice and humans***

We hypothesized that the elevated frequency of MDSCs post-lymphodepletion may arise from an increased number of circulating myeloid progenitor cells that mobilize from the BM because cyclophosphamide can mobilize HSPCs (189). We found that Lin<sup>-</sup>c-kit<sup>+</sup>Sca-1<sup>+</sup> and Lin<sup>-</sup>c-kit<sup>+</sup>Sca-1<sup>-</sup> HSPCs were dramatically increased in the spleens 7 days after lymphodepletion but were depleted 1 day after treatment compared to NT mice (Figure 32-33). In contrast, BM HSPCs remained depleted after treatment, suggesting that the progenitor cells egressed from the BM and remained in the periphery (Figure 33C). Likewise, Lin<sup>-</sup>c-kit<sup>+</sup>Sca-1<sup>-</sup>CD16/32<sup>-/low</sup>IL-7R<sup>-</sup> common myeloid progenitors (CMPs) and Lin<sup>-</sup>c-kit<sup>+</sup>Sca-1<sup>-</sup>CD16/32<sup>high</sup>IL-7R<sup>-</sup> granulocyte-macrophage progenitors (GMPs) were increased in the spleen at day 7 post-lymphodepletion when mice also exhibited peak MDSC expansion (Figure 33D).

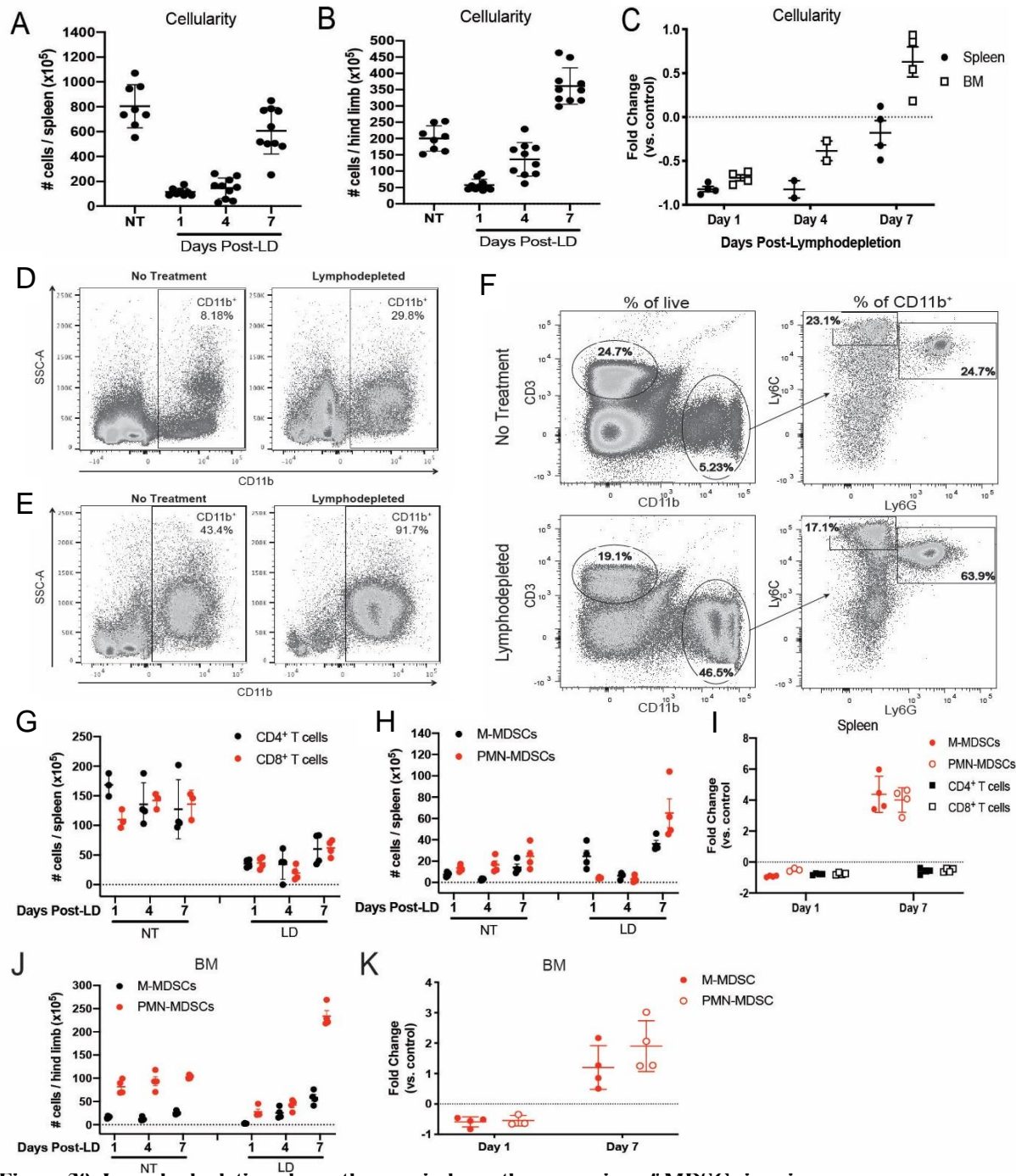


**Figure 30. Lymphodepleting chemotherapy induces the expansion of MDSCs in mice.**

(A-C) Whole cell numbers from spleens (A) and bone marrow extracted from the femurs and tibias (B) from NT or LD B16 tumor-bearing mice. (C) Fold change of whole cell numbers compared to control NT mice from 4 independent experiments. (D-E) Representative frequency of CD11b+ cells of total live cells in the spleen (D) and BM (E). (F) Representative gating strategy of MDSC subsets in mice. (G-I) Whole cell numbers of indicated immune cell populations in the spleens at respective time points. (G-H) Representative experiments showing the depletion of T cells (G) and expansion of MDSC subsets (H) ( $n=3-4$  mice per group). (I) Fold change of whole cell numbers compared to control NT mice from 4 independent experiments. (J) Representative experiment showing MDSC expansion in BM after lymphodepletion. (K) Fold change of whole cell numbers of MDSCs within BM compared to control NT mice from 4 independent experiments.

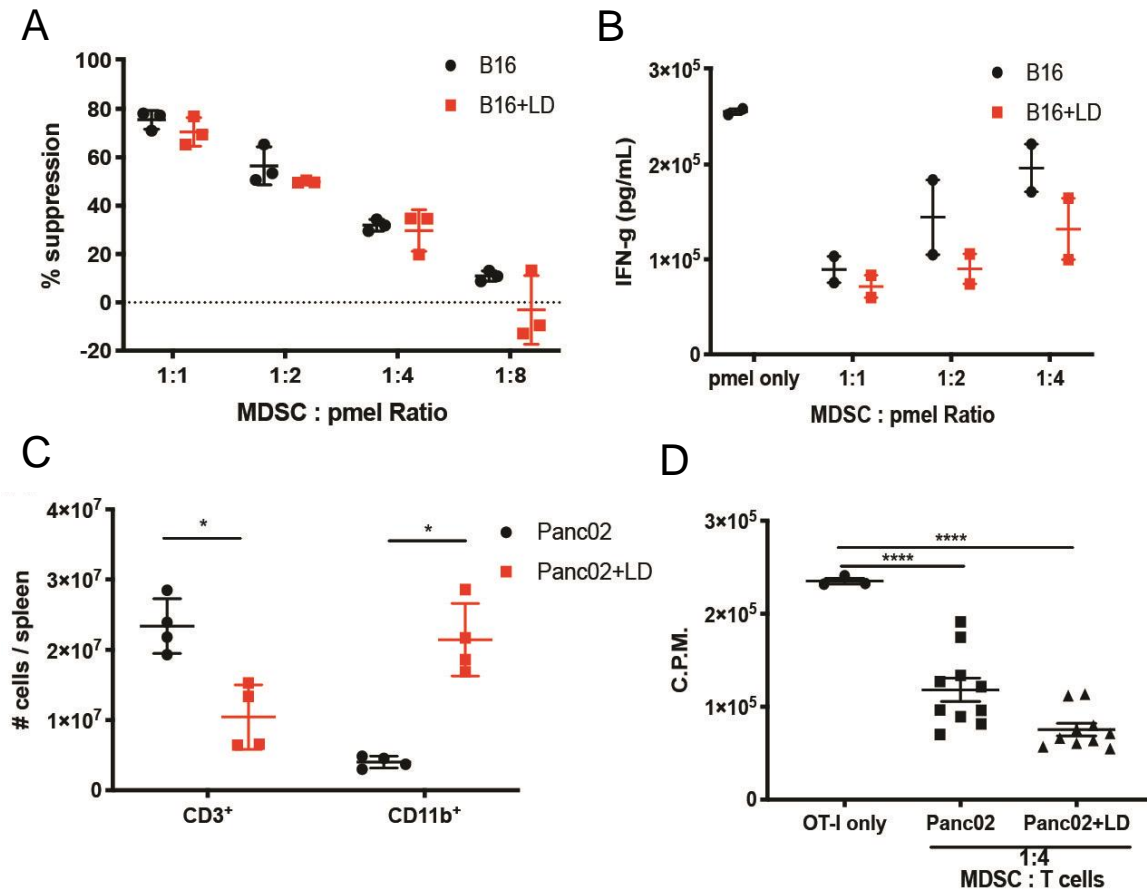


**Figure 31. Lymphodepletion-generated MDSCs are suppressive.**

(A-B) MDSCs were isolated from the spleens of untreated or LD mice with B16 tumors. Suppression of pmel T cell proliferation determined via <sup>3</sup>H incorporation (A) and IFN- $\gamma$  production (B) after co-culture with MDSCs from NT or LD mice. (C) The frequency of CD3<sup>+</sup> T cells and CD11b<sup>+</sup> myeloid cells were determined in NT mice and LD mice bearing Panc02 tumors 7 days post-LD. (D) OT-I T cell proliferation determined via <sup>3</sup>H incorporation in cultures with MDSCs from NT mice and LD mice bearing Panc02 tumors.

To examine the ability of mobilized progenitors to differentiate to MDSCs, we adoptively transferred HSPCs collected from lymphodepleted congenic CD45.1<sup>+</sup> tumor-bearing mice to CD45.2<sup>+</sup> recipient tumor-bearing mice that were left untreated or given lymphodepleting Cy/Flu before HSPC transfer (Figure 34A). As expected, LD recipient mice exhibited increases in endogenous CD45.1<sup>-</sup>CD11b<sup>+</sup> cells and CD45.1<sup>-</sup> HSPCs and reductions in CD45.1<sup>-</sup> lymphocytes in comparison to NT recipient mice (Figure 34B). The total frequency of donor CD45.1<sup>+</sup> cells were similar between non-treated and LD recipient mice 7 days after transfer (Figure 34C). However, the majority of donor CD45.1<sup>+</sup> HSPCs differentiated to CD11b<sup>+</sup> cells in LD recipient



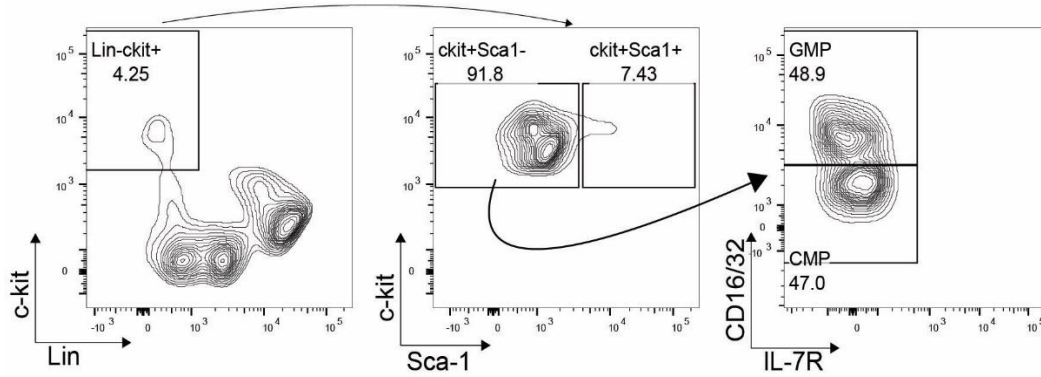


Figure 32. Gating strategy to identify mouse HSPCs

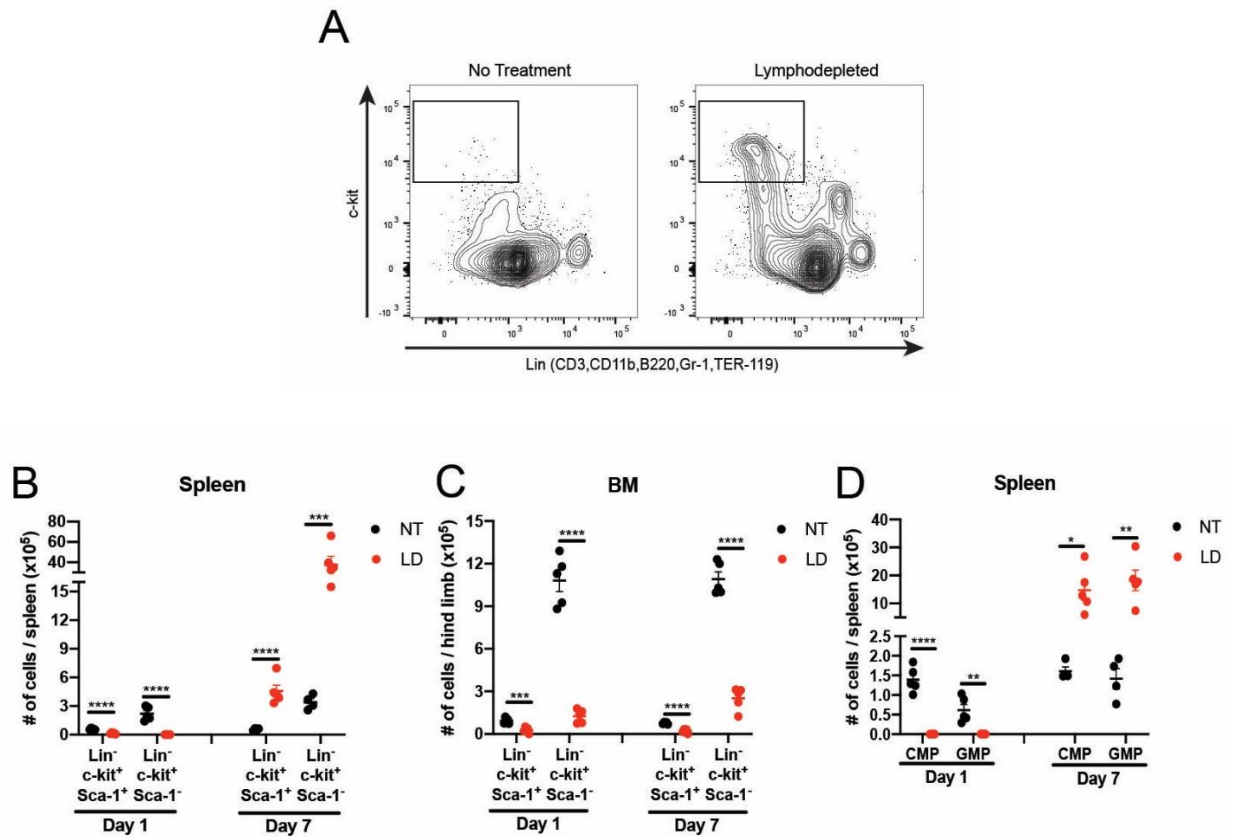
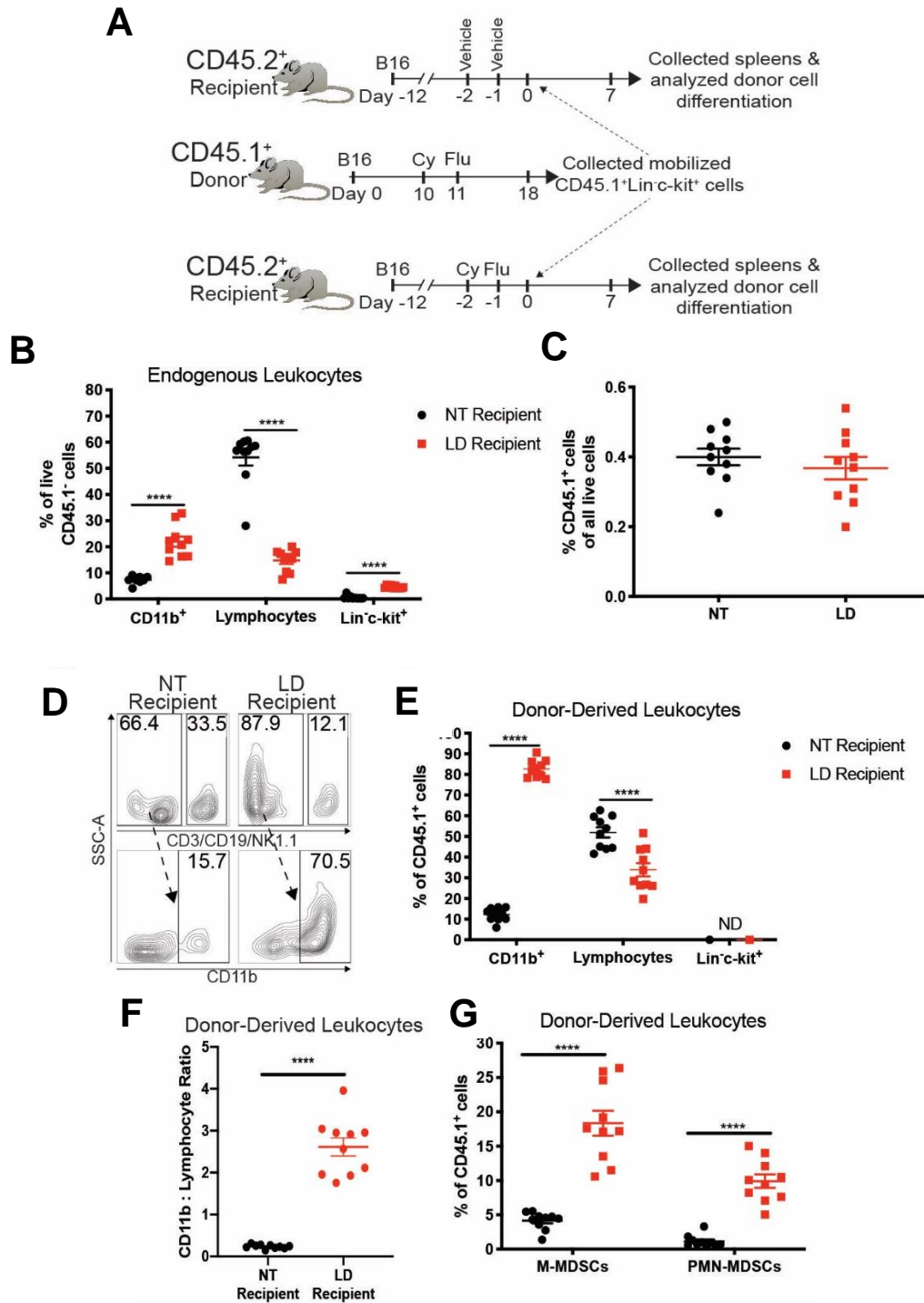


Figure 33. Lymphodepleting chemotherapy mobilizes HSPCs.

(A) Representative dot plots of Lin<sup>-</sup>c-kit<sup>+</sup> cells in spleens in untreated mice or day 7 post-LD treated mice. (B-D) The number of indicated HSPC populations were determined in NT mice and LD within spleens (B,D) or BM (C) at day 1 post-LD or day 7 post-LD.



**Figure 34. Mobilized HSPCs differentiate into MDSCs in lymphodepleted hosts**

(A) Experimental design for (B-G); (n=10 mice per group). (B) Frequency of CD45.1<sup>-</sup> endogenous leukocytes in recipient mice after adoptive transfer. (C) Frequency of total donor CD45.1<sup>+</sup> cells in the spleens of recipient mice. (D) Representative dot plots showing the percentage of myeloid cells and lymphocytes among donor-derived cells. Arrow indicates directionality of subgating with the frequency of parent gates indicated. (E) Frequency of donor-derived cells in recipient mice after adoptive transfer. (F) Ratio of the number myeloid cells in relation to lymphocytes that differentiated from donor CD45.1<sup>+</sup> cells. (G) Proportion of donor cells that differentiated to MDSCs in recipient mice.

mice (Figure 34D). Inversely, lymphocytes ( $CD3^+CD19^+NK1.1^+CD11b^-Ly6C^-Ly6G^-c-kit^-$ ) predominated the proportion of  $CD45.1^+$  donor-derived cells in NT recipient mice (Figure 34E). Furthermore, the ratio of  $CD11b^+$  cells relative to lymphocytes that differentiated from donor  $CD45.1^+$  HSPCs was significantly elevated in LD recipient mice, indicating that the mobilized progenitors preferentially differentiate to myeloid cells in a lymphodepleted environment (Figure 34F). Indeed, M-MDSCs and PMN-MDSCs derived from donor mice were more prevalent in LD recipient mice compared to NT recipient mice (Figure 34G).

In human samples, we confirmed that HSPCs ( $Lin^-CD34^+$  cells) were increased in melanoma patients at Week 1 Post-TIL infusion compared to pre-infusion levels (Figure 35). In addition to an increased abundance of  $Lin^-CD34^+$  cells at Week 1 post-infusion, we determined that the phenotype of HSPCs changed after TIL infusion. Nearly, all  $Lin^-CD34^+$  cells were also  $CD38^+$ , co-expressing  $CD45RA$  and/or  $CD90$ , which the abundance of  $CD34^+CD38^+CD90^+$  triple positive cells increased in patients at the Week 1 Post-TIL blood draw compared to the pre-treatment PBMCs (Figure 36). We confirmed that immunosuppressive myeloid cells could be generated from mobilized  $CD34^+$  cells collected from a melanoma patient that received ACT with TIL. In this melanoma patient, the frequency of  $CD34^+$  cells in PBMCs dramatically increased from 0.11% at pre-infusion to 10.8% at Week 1 post-TIL infusion (Figure 37).

We differentiated the  $CD34^+$  cells using tumor-conditioned media (TCM) in addition to CC110 (SCF, TPO, Flt3L) in combination with GCSF and successfully generated cells resembling  $CD15^+$  cells displaying elevated expression of  $CD11b$ ,  $LOX-1$ ,  $CD14$ , and  $PD-L1$  in response to treatment with tumor-conditioned media (TCM) (Figure 38). To determine the suppressive capacity of these cells, the tumor cells used to produce the TCM were co-cultured with autologous TILs and the *in vitro* generated suppressor cells at varying ratios.

As expected, TILs produced IFN- $\gamma$  when cultured with the tumor cells alone. However, the CD15<sup>+</sup> suppressor cells generated in the presence of TCM exhibited an enhanced capacity to inhibit IFN- $\gamma$  production in TIL:Tumor co-cultures in comparison to the suppressor cells generated without TCM (Figure 39). Together, these results confirm our findings in murine models demonstrating that lymphodepletion-mobilized HSPCs give rise to immunosuppressive myeloid cells.

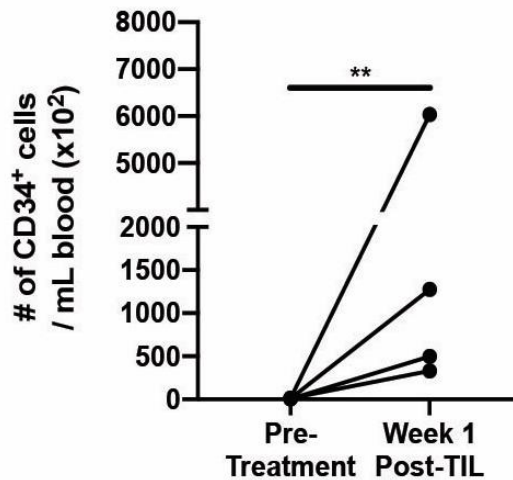


**Figure 35. HSPCs increase in melanoma patients after treatment with lymphodepleting chemotherapy and TIL infusion.**

The number of Lin<sup>-</sup>CD34<sup>+</sup> cells were quantified in the PBMCs of patients prior to and 1-week post-TIL infusion. Lin = CD3, CD14, CD15, CD19 CD11b, CD11c, CD56

### *The abrogation of CCR2 in recipient mice does not enhance the efficacy of ACT*

We previously observed that CCL-2, the ligand for CCR2, was elevated in the sera of lymphodepleted mice (data not shown). Moreover, the blockade of CCR2 has been reported to reduce the accumulation of M-MDSCs in tumor-bearing mice that received lymphodepleting doses of cyclophosphamide (190). We first measured the frequency of MDSCs in WT or CCR2<sup>KO</sup> mice bearing B16 tumors treated with or without lymphodepleting Cy/Flu.

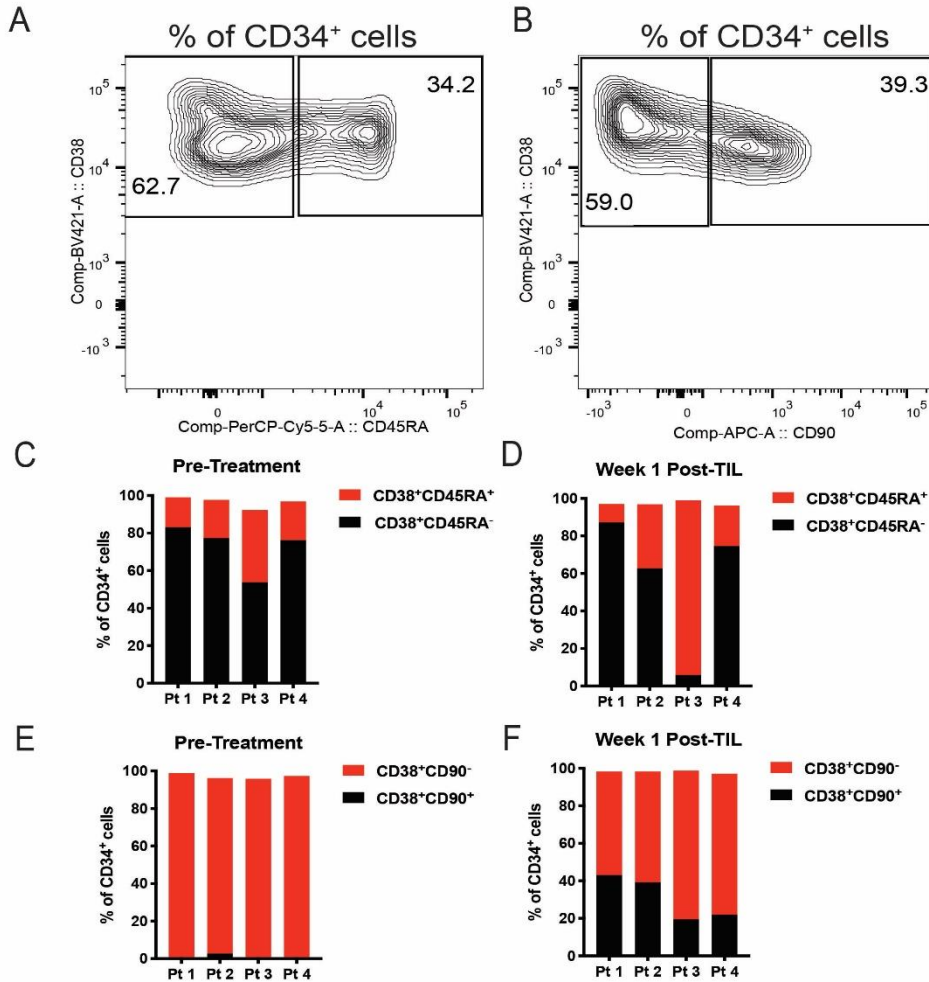


**Figure 36. Phenotype of CD34<sup>+</sup> cells in melanoma patients that received ACT with TIL.**

(A) CD38 and CD45RA expression in CD34<sup>+</sup> cells. (B) CD38 and CD90 expression in CD34<sup>+</sup> cells. (C-D) CD38 and CD45RA expression among CD34<sup>+</sup> cells from melanoma patients in PBMCs at Pre-treatment (C) and Week 1 post-TIL (D). (E-F) CD38 and CD90 expression among CD34<sup>+</sup> cells from melanoma patients at Pre-treatment with ACT (E) and Week 1 post-TIL (F).

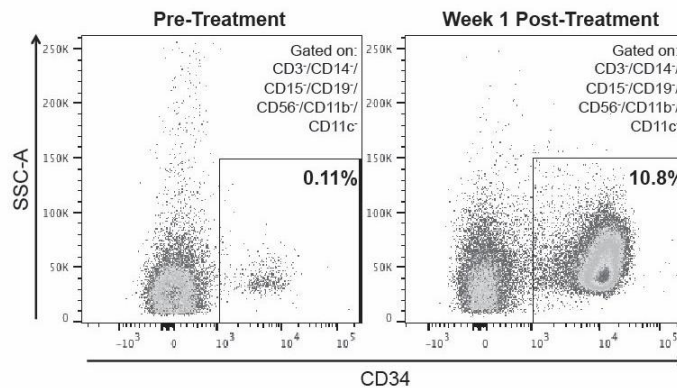


**Figure 37. Frequency of CD34<sup>+</sup> in a melanoma patient. Week 1 Post-Treatment CD34<sup>+</sup> cells were used to generate MDSCs as in Figure 38-39.**

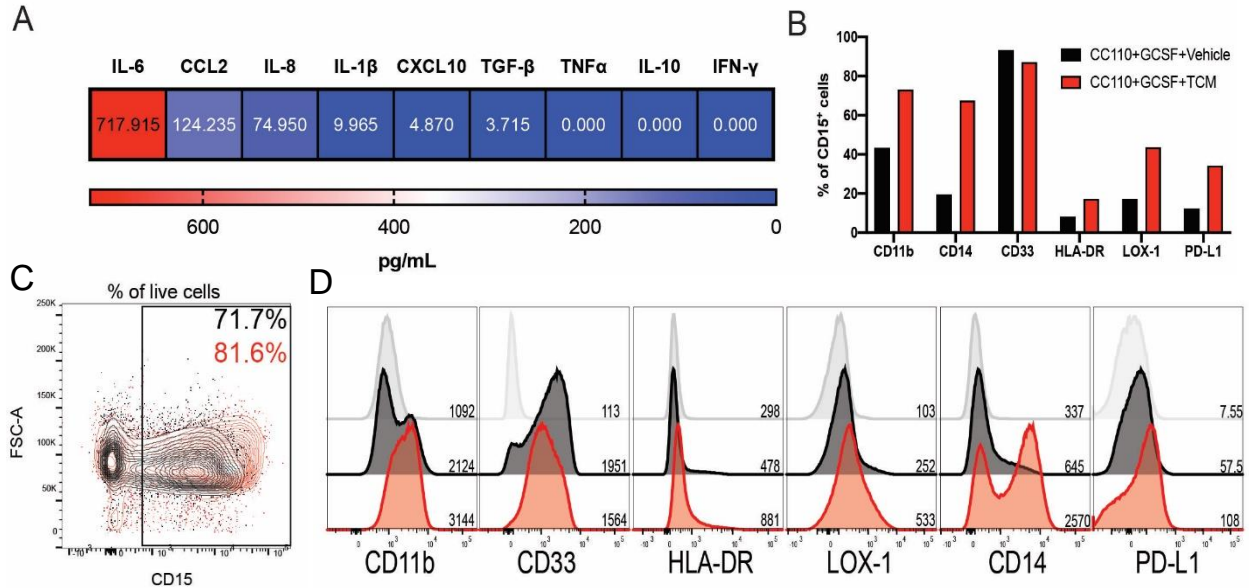


**Figure 38. Differentiation of immunosuppressive myeloid cells from lymphodepletion-mobilized CD34<sup>+</sup> cells.** (A) Detection of cytokines in the TCM collected from a primary melanoma tumor cell line. (B-D) PMN suppressor cells were differentiated from CD34<sup>+</sup> cells collected the Week 1 post-TIL PBMCs from a patient for 14 days in CC110+GCSF. On day 10, cells were refreshed with media containing CC110+GCSF in combination with vehicle (RPMI) or TCM from (A). (B) Phenotype of CD15<sup>+</sup> PMN suppressor cells differentiated from CD34<sup>+</sup> cells at day 14 of differentiation protocol. (C) Frequency of CD15<sup>+</sup> cells of all live cells at day 14. Black=CC110+GCSF+Vehicle, Red=CC110+GCSF+TCM. (D) Histograms of indicated myeloid cell markers. Parent gate is CD15<sup>+</sup> cells as in (C). Gray = FMO, Black=CC110+GCSF+Vehicle, Red=CC110+GCSF+TCM. MFI is indicated adjacent to each histogram.

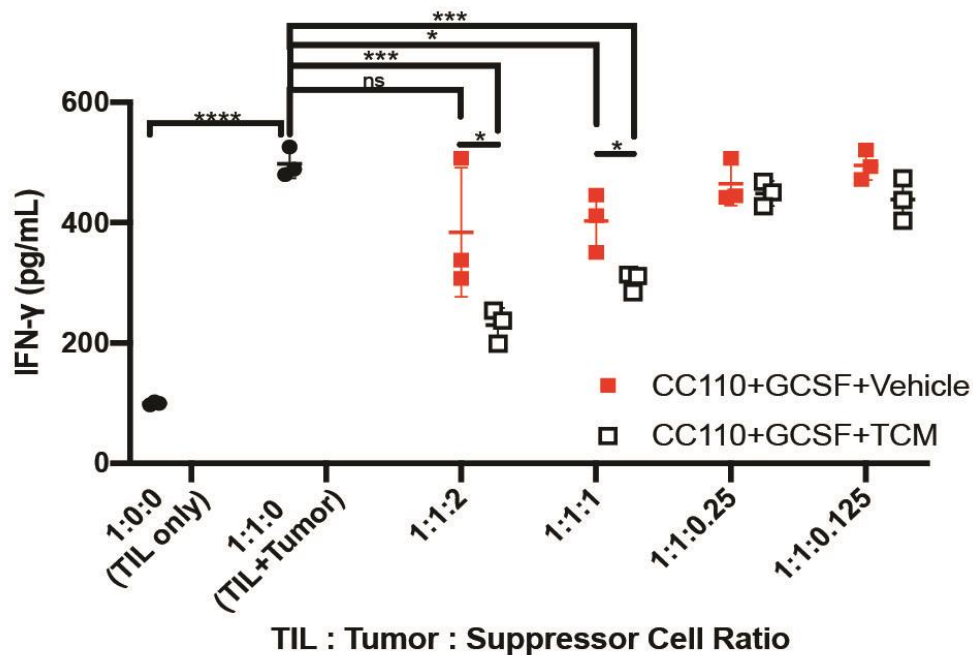


**Figure 39. MDSCs generated from mobilized CD34<sup>+</sup> cells suppress TIL effector function.** Allogeneic myeloid suppressor cells were differentiated from Lin<sup>-</sup>CD34<sup>+</sup> cells and co-cultured with TILs cultured and autologous tumor cells. Suppressor cells were conditioned with or without TCM. IFN- $\gamma$  production was determined by ELISA after 48hrs of culture.

In comparison to naïve mice, the frequency of CD11b<sup>+</sup>Gr-1<sup>+</sup> cells were elevated in both WT and CCR2<sup>KO</sup> mice. However, LD WT and CCR2<sup>KO</sup> mice exhibited increased levels of CD11b<sup>+</sup>Gr-1<sup>+</sup> cells (total MDSCs) compared to untreated counterparts (Figure 40A). As expected, CCR2<sup>KO</sup> mice lacked M-MDSCs, however a compensatory increase in PMN-MDSCs was observed in comparison to WT LD mice (Figure 40B). Next, we sorted CD11b<sup>+</sup>Gr-1<sup>+</sup> cells from the spleens of LD mice and assessed their ability to suppress OT-I T cell proliferation. Indeed, MDSCs from both WT and CCR2<sup>KO</sup> mice potently suppressed T cell proliferation (Figure 40C). Together, these data show that lymphodepleting chemotherapy increases MDSCs in CCR2<sup>KO</sup> mice despite the reduction of monocytic cells.

Because M-MDSCs were reduced in CCR2<sup>KO</sup> mice, we wanted to determine the effect of depleting both MDSC subsets on the infiltration of adoptively transferred T cells. To determine this, we used CCR2<sup>KO</sup> mice to deplete M-MDSCs and Ly6G depleting antibodies ( $\alpha$ Ly6G) to deplete PMN-MDSCs (Figure 41A). Indeed, CCR2<sup>KO</sup> mice exhibited a significant decrease of M-MDSCs within tumors in comparison to WT mice. Moreover,  $\alpha$ Ly6G effectively depleted PMN-MDSCs within tumors in WT and CCR2<sup>KO</sup> hosts. However, a strong compensatory effect was observed in CCR2<sup>KO</sup> mice characterized by a sharp increase in PMN-MDSCs in comparison to WT mice (Figure 41B). Despite, the lack of M-MDSCs and the depletion of PMN-MDSCs, we did not observe an increase in the number of adoptively transferred CD90.1<sup>+</sup> pmel T cells in tumor 48hrs after infusion. Next, we aimed to determine if the efficacy of ACT would be enhanced in CCR2<sup>KO</sup> hosts. First, we observed that the frequency of CD90.1<sup>+</sup> pmel T cells were similar between WT and CCR2<sup>KO</sup> recipient mice, suggesting that the lack of M-MDSCs did not promote T cell expansion *in vivo* (Figure 42A). Likewise, tumor growth and the survival of WT

and CCR2<sup>KO</sup> recipient mice were similar (Figure 42B-C). Together, these data demonstrate that the efficacy of ACT is not impacted in CCR2<sup>KO</sup> mice or the lack of M-MDSCs.

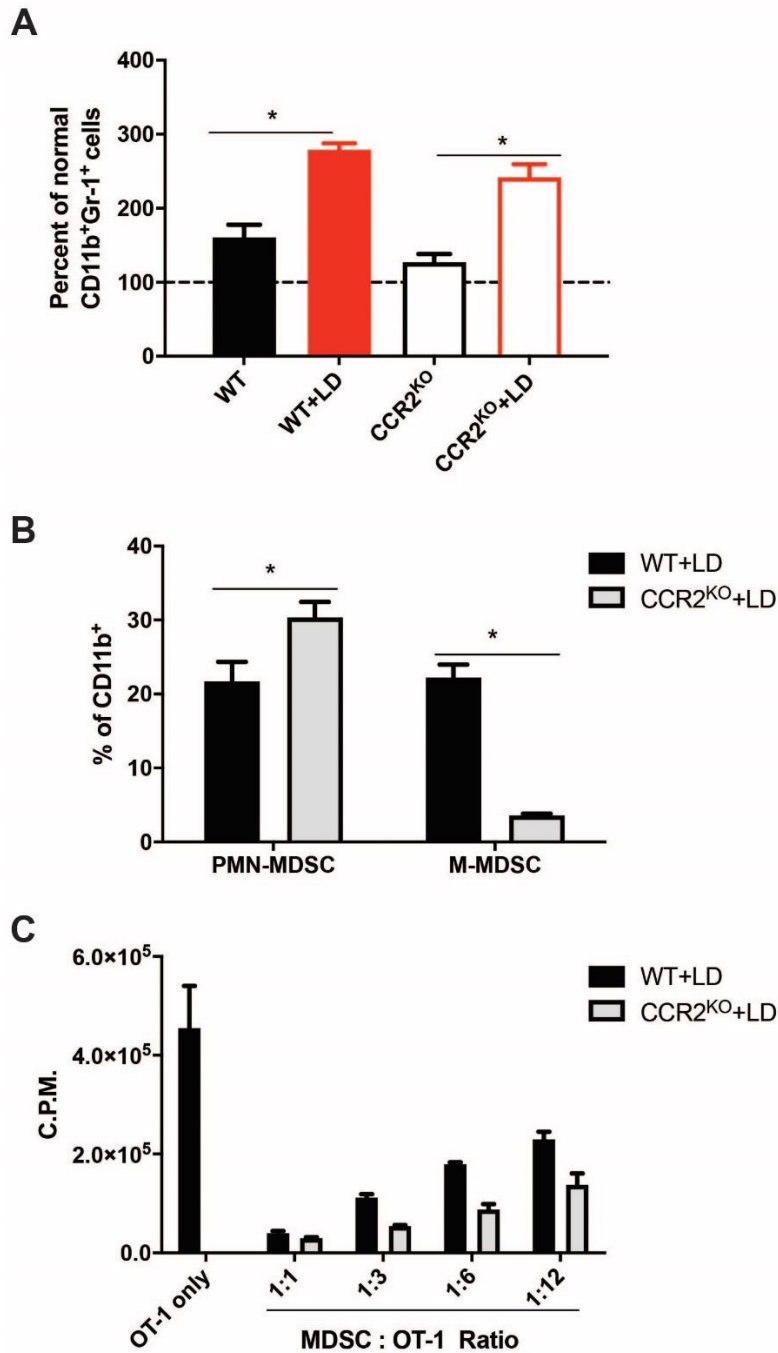


**Figure 40. MDSC reconstitution in CCR2<sup>KO</sup> mice.**

(A) CD11b<sup>+</sup>Gr-1<sup>+</sup> cells were measured in naïve mice, or B16 tumor-bearing mice treated with or without lymphodepletion. The number of CD11b<sup>+</sup>Gr-1<sup>+</sup> cells in spleens were measured at Day 7 post-LD and normalized to naïve mice. (B) Frequency of MDSC subsets in the spleens of WT and CCR2<sup>KO</sup> mice at Day 7 post-LD. (C) OT-I T cell proliferation in co-cultures with MDSCs from the spleens of WT and CCR2<sup>KO</sup> mice.



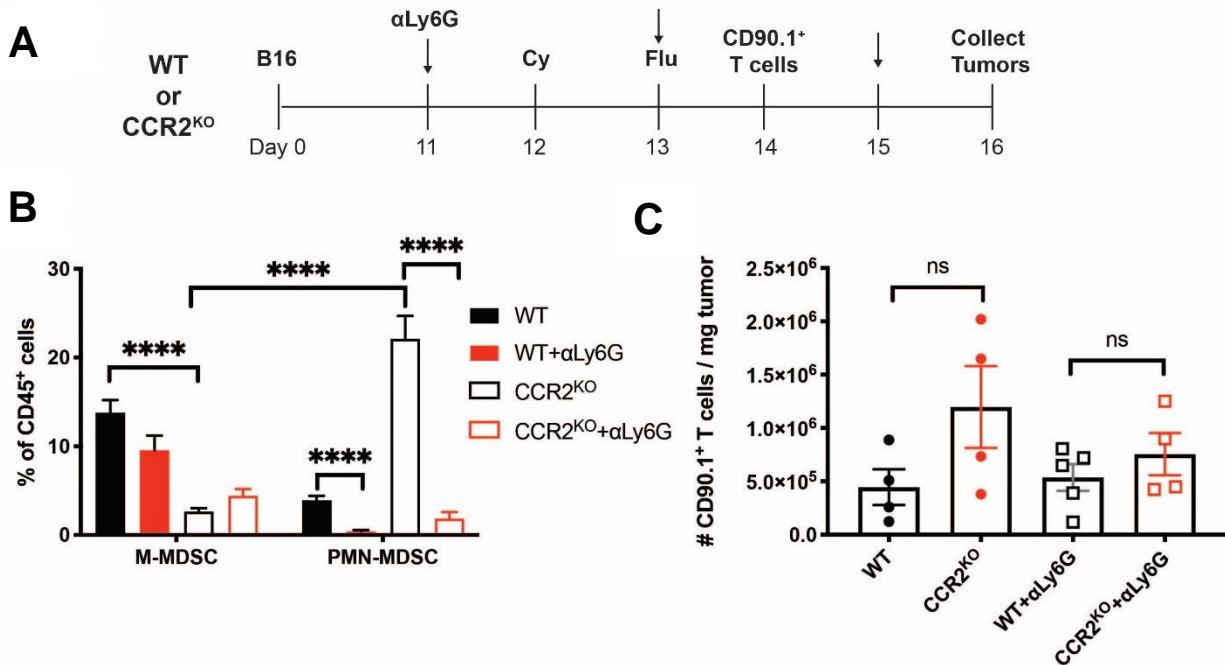


**Figure 41. Assessment of early T cell infiltration after ACT and depletion of MDSCs.**

(A) Experimental design for (B-C). Arrows indicated injection of αLy6G. (B) Frequency of tumor MDSCs after LD, ACT, and MDSC depletion. (C) Frequency of adoptively transferred CD90.1<sup>+</sup> pmel T cells in B16 tumors.

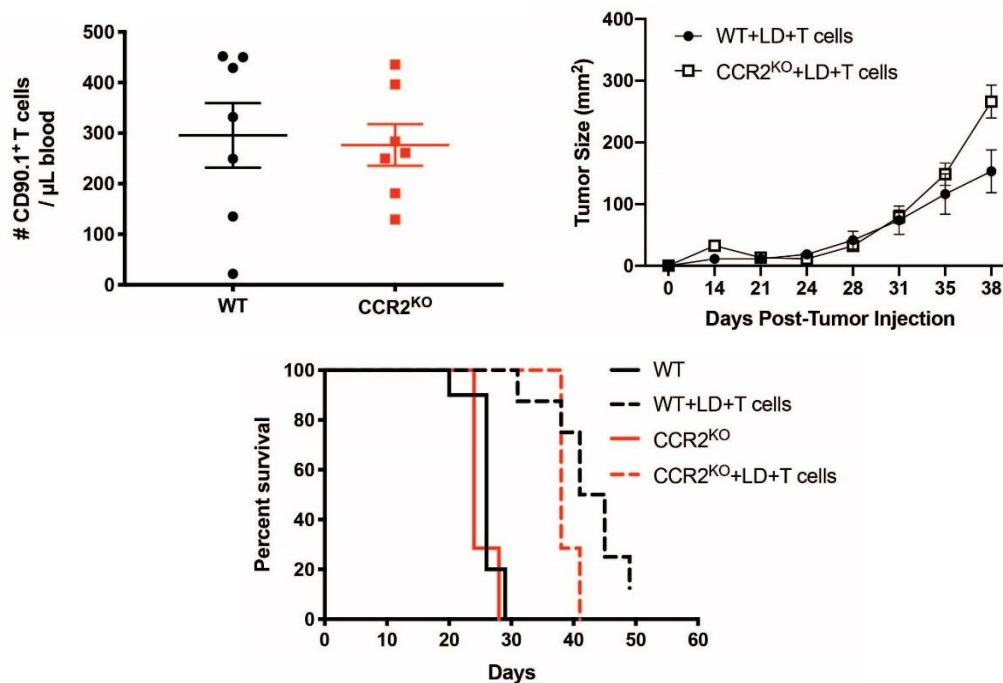


**Figure 42. ACT in CCR2<sup>KO</sup> mice does not enhance anti-tumor efficacy.**

(A) Frequency of CD90.1<sup>+</sup> T cells in the blood 7 days after ACT. (B-C) Tumor growth (B) and survival (C) in mice with B16 tumors.

### ***IL-6 promotes MDSC activity after lymphodepletion treatment***

To identify factors that contribute to MDSC accumulation after lymphodepletion, we performed RNA sequencing on PMN-MDSCs and M-MDSCs from NT and LD mice. Ingenuity Pathway Analysis (IPA) revealed that multiple functions were enriched due to changes induced by lymphodepletion, including cellular movement, hematological system development and function, cell cycle, cell death, and survival (Figure 43). We then enriched our dataset using IPA upstream regulator analyses and focused on cytokines as regulators (Figure 44). Because IL-6 enhances immunosuppressive functions and the differentiation in MDSCs (177, 191), we investigated the role of IL-6 on MDSCs during lymphodepletion recovery. Indeed, the transcriptional alterations induced by lymphodepletion were predicted to be regulated by multiple cytokines, including IL-6, in both PMN-MDSCs and M-MDSCs collected from LD mice compared to NT mice (Figure 44). Likewise, IL-6 was more abundant in the plasma of melanoma patients receiving ACT with TIL at Week 1 post-infusion (Figure 45A). To determine the role of IL-6 in ACT models, we lymphodepleted WT and IL-6<sup>KO</sup> mice bearing B16 tumors and measured the frequency of MDSCs. We observed significant increases of MDSCs in LD mice, but no difference was observed between WT and IL-6<sup>KO</sup> mice (Figure 45B). However, the ability of MDSCs from IL-6<sup>KO</sup> LD mice to suppress T cell proliferation was dampened (Figure 45C). We confirmed these results in mice with a conditional knockout of the IL-6R in myeloid cells (IL-6R<sup>M-KO</sup>) (Figure 46A). Intriguingly, the induction of IL-6R signaling failed to enhance the suppressive capacity of WT MDSCs. Likewise, the lack of immunosuppression by IL-6R<sup>M-KO</sup> MDSCs was not rescued upon stimulation with an IL-6/IL-6R chimeric protein (Figure 46B-D). Since MDSCs from LD knockout mice were less immunosuppressive, we hypothesized that ACT would be more efficacious in IL-6<sup>KO</sup> recipient mice. Indeed, IL-6<sup>KO</sup> recipient mice

exhibited reduced tumor growth and improved survival after ACT in comparison to WT recipient mice (Figure 47A-B). The improved efficacy was associated with an increased frequency of circulating donor CD90.1<sup>+</sup> pmel T cells (Figure 47C). Similarly, the treatment of ACT in combination with IL-6 receptor blocking antibodies ( $\alpha$ IL6R) significantly reduced tumor growth in comparison to mice that received ACT alone (Figure 48). To confirm MDSC-mediated suppression of ACT efficacy, MDSCs were purified from donor WT and IL-6<sup>KO</sup> lymphodepleted mice and co-transferred with pmel T cells (Figure 49A). Despite an initial reduction in tumor growth, recipient mice that received a co-transfer of pmel T cells with WT MDSCs exhibited a significant acceleration of tumor growth compared to mice that received T cells alone, whereas mice co-transferred with IL-6<sup>KO</sup> MDSCs and T cells exhibited a similar control of tumor growth compared to mice that received T cells alone (Figure 49B). Moreover, the percent change in tumor growth from the time of infusion was greatest in mice that received pmel T cells and WT MDSCs, while tumor growth was stabilized or reduced in most recipient mice that received T cells alone or T cells co-transferred with IL-6<sup>KO</sup> MDSCs (Figure 49C). Collectively, our results demonstrate that IL-6 regulates the suppressive capacity of MDSCs that accumulate post-lymphodepletion and that the efficacy of ACT is enhanced upon blockade of IL-6 signaling.

#### ***Lymphodepleting chemotherapy induces the production of IL-6 in bone marrow***

We established that IL-6 regulates the suppressive capacity of MDSCs in LD mice (Figure 45-46). To evaluate IL-6 signaling during recovery after lymphodepletion, we measured pSTAT3 in myeloid cells (Figure 50A). At peak expansion (Day 7 post-lymphodepletion), the abundance of pSTAT3<sup>+</sup> cells were reduced in myeloid cells from LD mice. In contrast, the

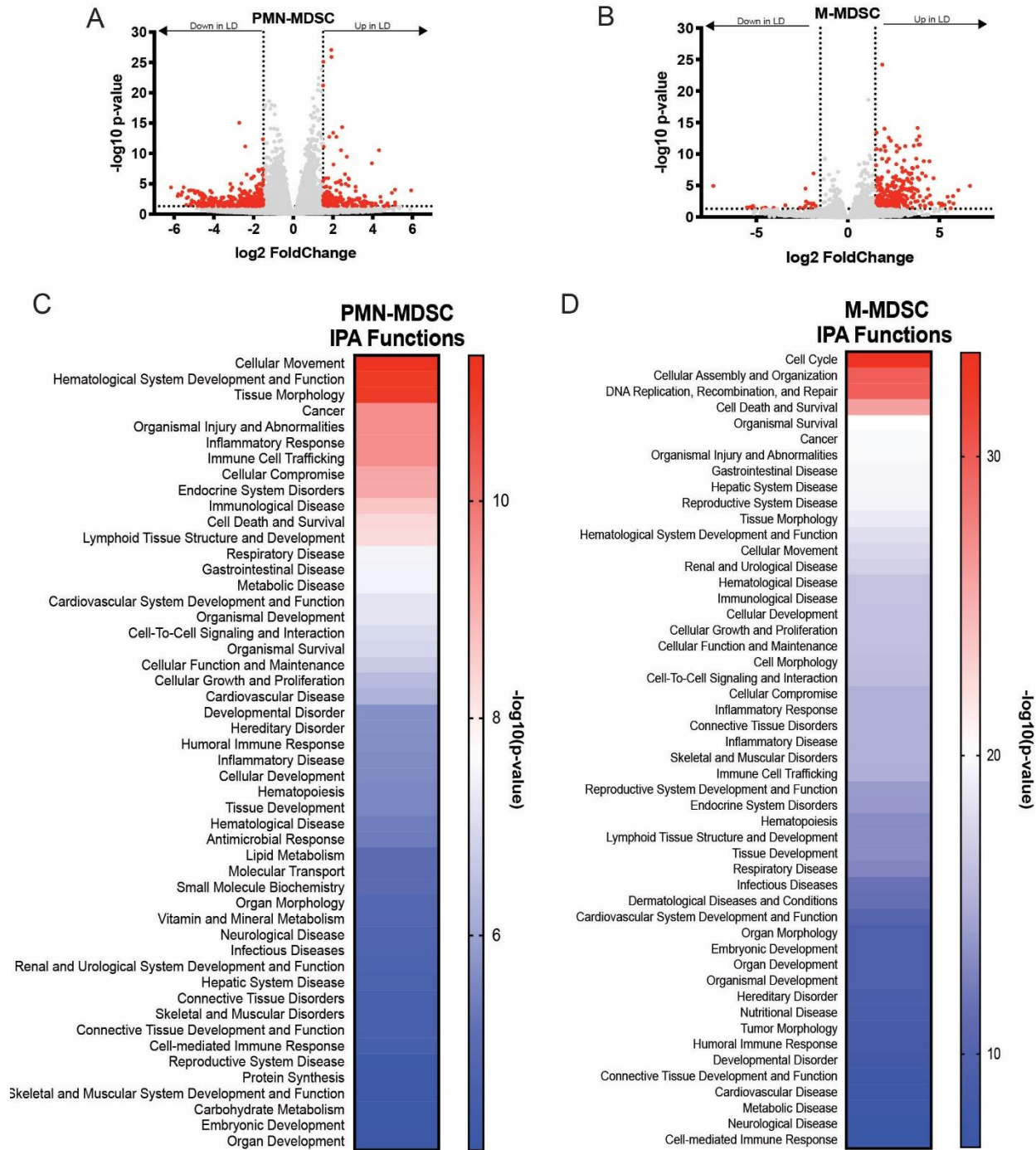


**Figure 43. RNA sequencing on MDSCs isolated from untreated and lymphodepleted tumor-bearing mice. (A-B)** Volcano plots representing significantly up- and down-regulated genes in MDSCs from LD mice. Dotted lines represent the Log2 fold change cutoff of 1.5 and  $-\log_{10} p\text{-value}$  of  $p=0.05$ . Significant genes are shown in red; non-significant in grey. **(C-D)** IPA analysis of functions enriched in MDSCs from lymphodepleted mice over MDSCs from untreated tumor-bearing mice.

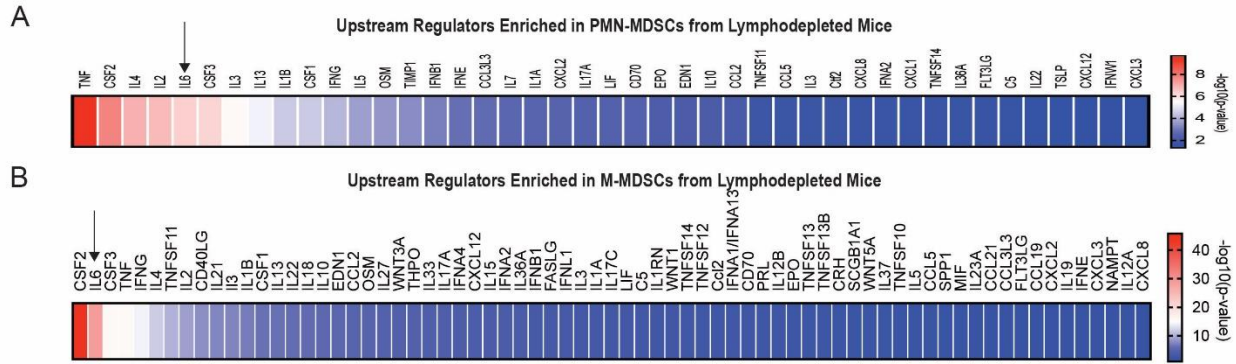


**Figure 44. Upstream cytokines regulators of MDSCs from lymphodepleted mice.** (A-B) IPA upstream regulator analysis enriched in MDSCs from lymphodepleted mice over MDSCs from untreated mice.

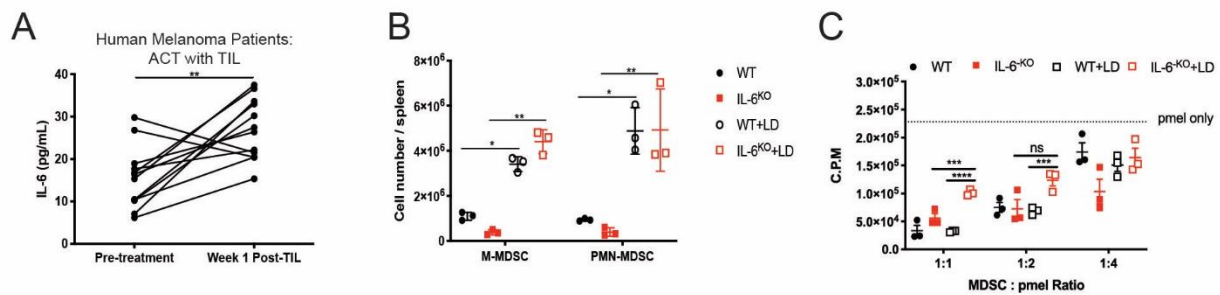


**Figure 45. IL-6 promotes the suppressive capacity of post-LD MDSCs** (A) IL-6 concentration in plasma samples obtained from melanoma patients receiving ACT with TIL (n=12). (B) MDSC frequency in the spleens of mice WT and IL-6<sup>KO</sup> mice (n=3-4 per group). (C) Pmel T cell proliferation determined by <sup>3</sup>H thymidine incorporation in cultures with MDSCs were purified from NT or LD, WT and IL-6<sup>KO</sup> mice.

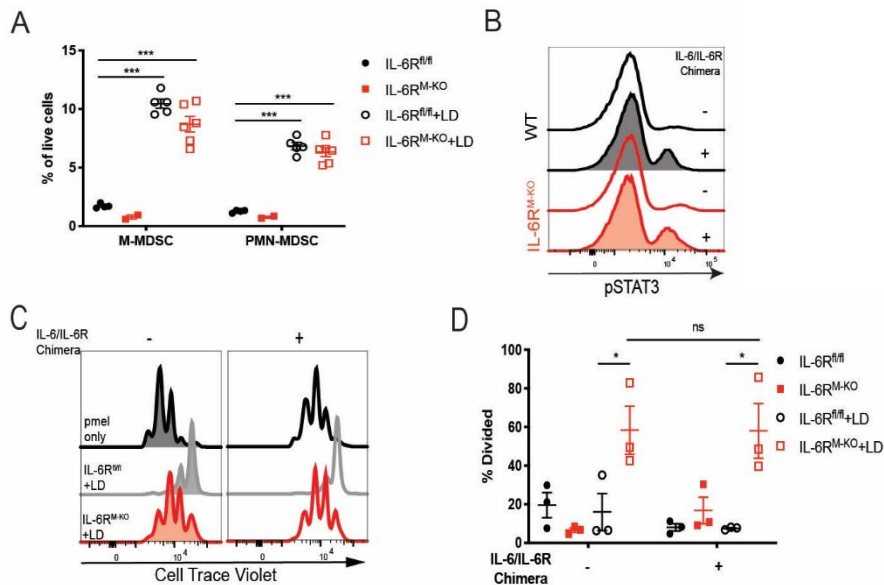


**Figure 46. The induction of IL-6R signaling fails to rescue MDSC suppressive capacity.** (A) Frequency of MDSC subsets IL-6R<sup>fl/fl</sup> and IL-6R<sup>M-KO</sup> bearing B16 tumors 7 days post-LD. (B) Induction of pSTAT3 with IL-6/IL-6R Chimeric protein. (C-D) Pmel T cell proliferation in culture with MDSCs and IL-6/IL-6R chimera. (C) Representative histogram. (D) Data summary (n=3/group)

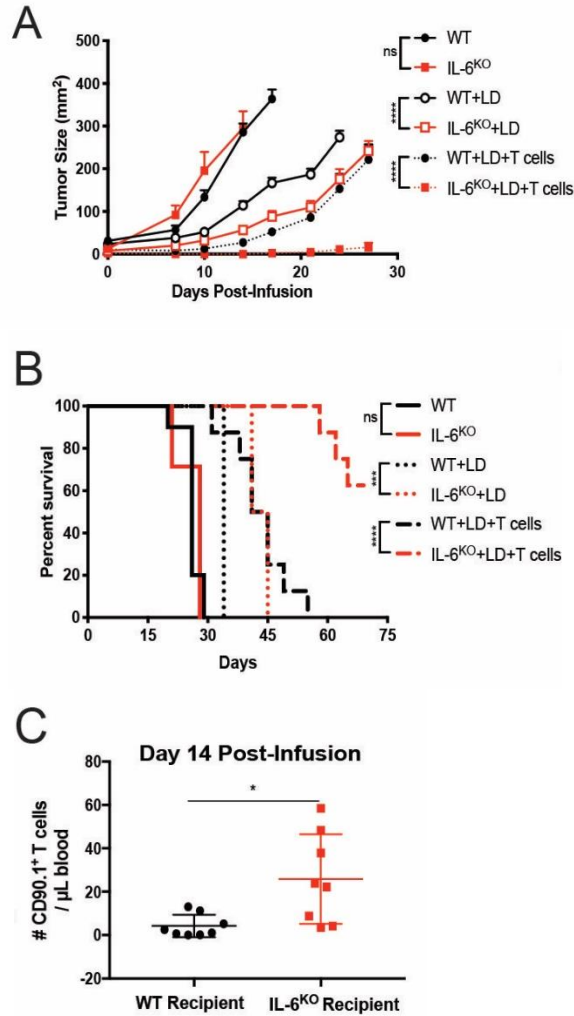


**Figure 47. The efficacy of ACT is enhanced in IL-6<sup>KO</sup> recipients.**

(A-B) Tumor growth (A) and survival (B) after LD +/- ACT with pmel T cells in mice with B16 tumors among WT or IL-6<sup>KO</sup> recipient mice (n=8-10 mice per group). (C) Donor pmel T cell frequency in blood of mice from (A-B).

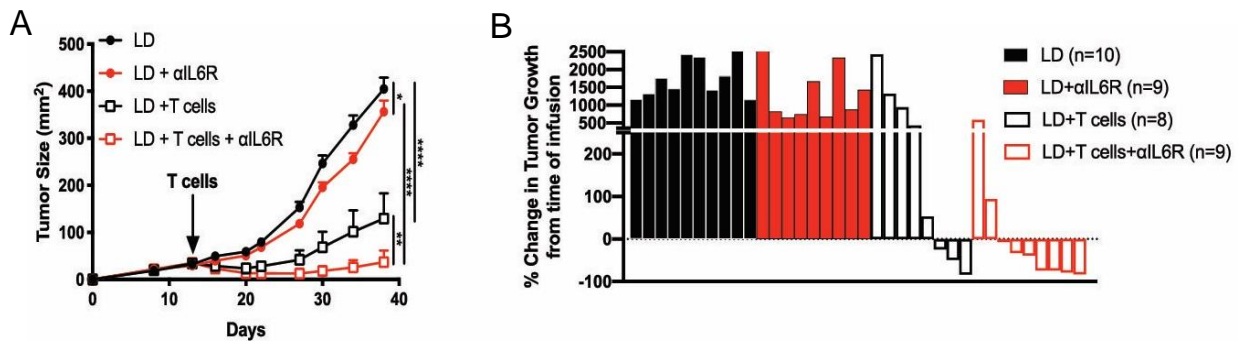


**Figure 48. IL-6R blockade enhances the efficacy of ACT.**

(A) Tumor growth in B16 tumor-bearing LD mice treated with ACT with or without αIL6R blocking antibodies (n=8-10 mice per group). (B) Waterfall plot showing percent change in tumor growth in mice from (A) at the termination of the experiment.

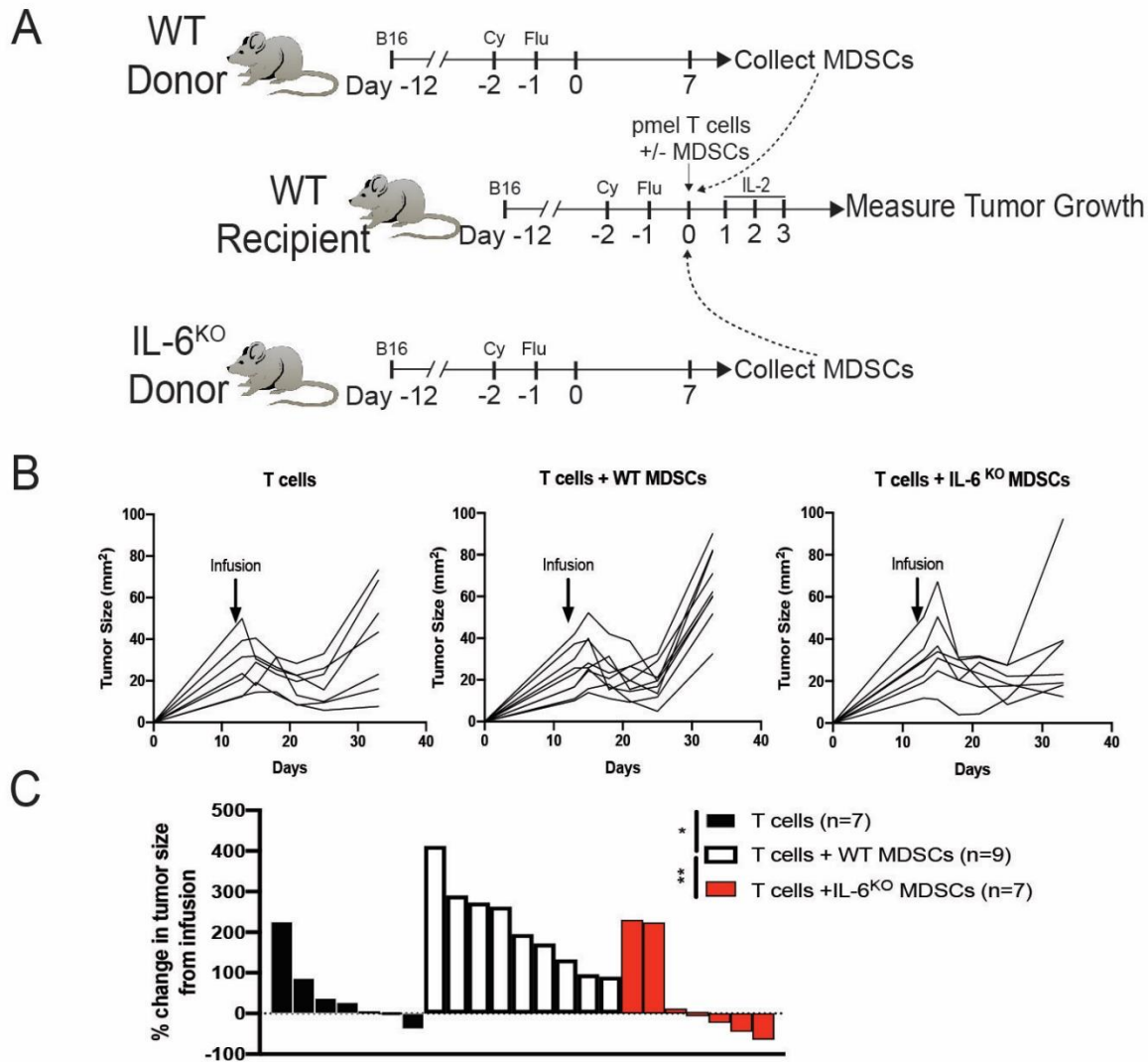


**Figure 49. Co-transfer of MDSCs with T cells**

(A) Experimental design for (B-C). Recipient mice received  $2.5 \times 10^6$  pmel T cells alone or in combination with  $2.5 \times 10^6$  MDSCs from lymphodepleted WT or IL-6<sup>KO</sup> donor mice. (B) Tumor growth for individual mice are shown. (C) Waterfall plot showing percent change in tumor growth in mice from at the termination of the experiment.

percentage of pSTAT3<sup>+</sup> cells were elevated in myeloid cells at Day 1 post-lymphodepletion (Figure 50B). In response to *ex vivo* IL-6 stimulation, pSTAT3 was elevated at day 1 and day 3 post-LD compared to cells from NT mice, suggesting that IL-6 may be acting on myeloid cells soon after chemotherapy treatment rather than at peak expansion (Figure 50B). We defined that CMPs, GMPs, M-MDSCs, and PMN-MDSCs expressed IL-6R (Figure 50C-G). However, the expression of the IL-6R was elevated in CMPs and GMPs in the BM of LD mice at Day 1 post-

lymphodepletion (Figure 50D), while MDSCs in the spleens or BM did not exhibit any change the IL-6R expression compared to NT mice (Figure 50E-G). We then identified that BM CD11b<sup>+</sup> cells were the primary producers of IL-6 in NT or LD mice with B16 tumors, and the proportion of IL-6<sup>+</sup> cell subsets were similar between both groups (Figure 51A-B). However, all BM-derived cells produced more IL-6 within 24hrs after lymphodepletion both with and without the presence of *ex vivo* lipopolysaccharide (LPS) stimulation (Figure 51C-D). Although, the expression values for lymphocytes and CD45<sup>-</sup>Lin<sup>-</sup> cells were lower compared to CD11b<sup>+</sup> and HSPCs cells. Nevertheless, both CD11b<sup>+</sup> cells and Lin<sup>-</sup>c-kit<sup>+</sup> cells had an enhanced production of IL-6 post-lymphodepletion. Together, our data shows that lymphodepleting chemotherapy induces the expression of IL-6 in BM-derived cells, which may drive the function of MDSCs.

### ***IL-6 regulates the survival and resistance to Fas-induced apoptosis in lymphodepletion-induced MDSCs***

To elucidate the effect of IL-6 signaling on the suppressive capacity of MDSCs in LD mice, we performed RNA sequencing on MDSC subsets sorted from WT and IL-6<sup>KO</sup>, NT and LD mice (Figure 52). In both MDSC subsets, there were little transcriptional differences between MDSCs from WT NT mice in comparison to MDSCs from IL-6<sup>KO</sup> NT mice. In M-MDSCs, 600 gene transcripts calculated to be statistically significant were up- or down-regulated among M-MDSCs from LD mice in comparison to M-MDSCs from WT NT mice. However, there was little difference in M-MDSCs when we compared cells from WT LD mice to IL-6<sup>KO</sup> LD mice. In contrast, 146 gene transcripts calculated to be statistically significant were up- or down-regulated among PMN-MDSCs from WT LD mice in comparison to PMN-MDSCs from IL-6<sup>KO</sup> LD mice, suggesting that IL-6 may have a broader impact in the development of PMN-MDSCs (Figure 52A-F). We next performed gene set enrichment analysis on PMN-MDSCs and identified that



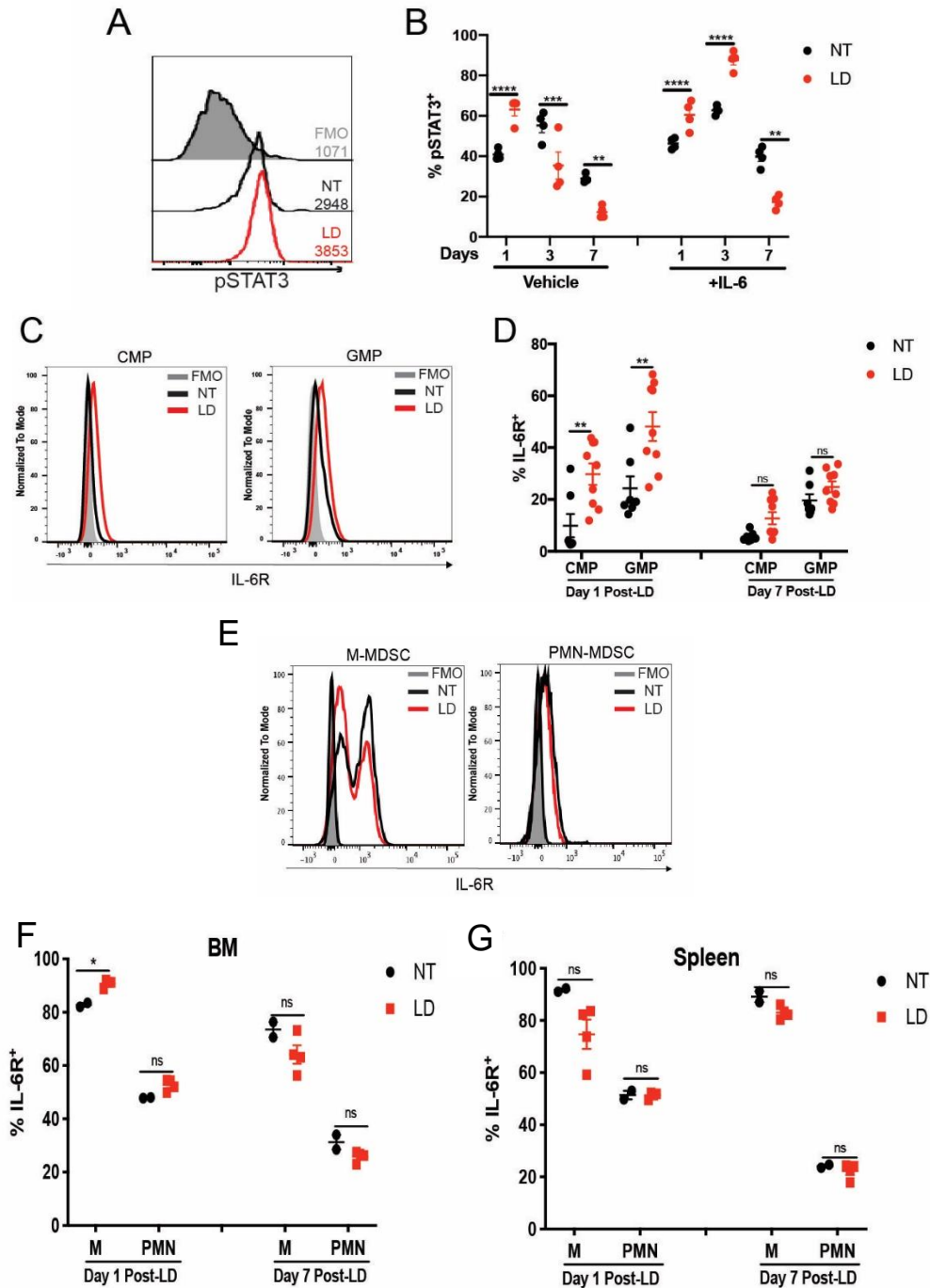


**Figure 50. IL-6R expression in MDSCs and myeloid progenitors**

(A-B) pSTAT3 expression was determined by flow cytometry among splenic myeloid cells collected from NT or LD mice treated with or without ex vivo IL-6 stimulation. (A) Representative histogram with MFI values indicated adjacent to each histogram. (B) Summarized data from a representative experiment. (C) Representative histogram showing IL-6R expression among BM CMPs and GMPs from NT or LD mice at Day 1 Post-LD. (D) Percent of IL-6R<sup>+</sup> CMPs and GMPs at Day 1 and Day 7 Post-LD. (E) Representative histogram of IL-6R expression from Day 7 post-LD splenic MDSC subsets. (F-G) IL-6R expression was determined on M-MDSCs and PMN-MDSCs from NT or LD mice at indicated time points as in the BM (B) and spleen (B). Data is representative of 3 independent experiments.

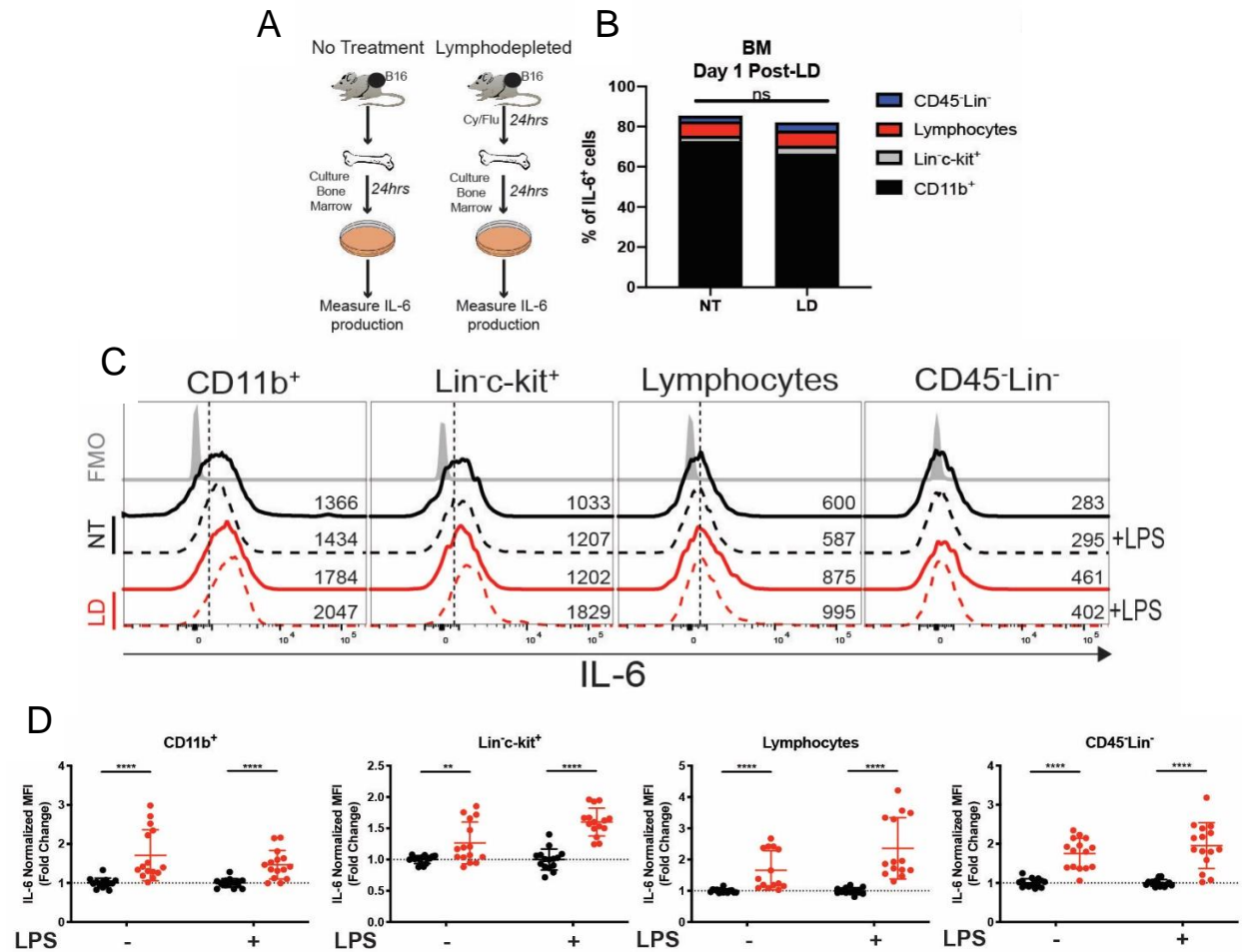


**Figure 51. IL-6 production is induced in the bone marrow by lymphodepleting chemotherapy.**

(A) Experimental design for (B-D). Bone marrow was collected from NT or LD B16-bearing mice and cultured for 24hrs. (B) Stacked bar chart of intracellular IL-6 expression by CD11b<sup>+</sup> myeloid cells, Lin<sup>-</sup>c-kit<sup>+</sup> HSPCs, Lymphocytes (CD3<sup>+</sup>/CD19<sup>+</sup>/NK1.1<sup>+</sup>) and CD45<sup>-</sup>Lin<sup>-</sup> cells as determined by flow cytometry. (C) Representative histograms showing IL-6 expression among individual BM cell subsets with or without ex vivo LPS stimulation. MFI is indicated on the right of each histogram. (D) Fold change in IL-6 expression among individual BM cell subsets. Data is representative of 2-3 independent experiments. (D) Normalized data is a compilation of 3 independent experiments with biological replicates shown. Data was normalized to NT or NT+LPS.

pathways and functions associated with apoptosis were significantly enriched in PMN-MDSCs from WT LD mice in comparison to PMN-MDSCs from IL-6<sup>KO</sup> LD mice (Figure 52G-H). Indeed, LD mice exhibited an increased frequency of viable MDSCs compared to mice with no treatment (Figure 53A). Moreover, MDSCs from LD mice were sensitive to apoptosis mediated by T cells, which was blocked by the addition of a FasL blocking antibody ( $\alpha$ FasL) (Figure

53B). Because MDSCs can undergo Fas-induced apoptosis (192), we next compared the survival of MDSCs from WT and IL-6<sup>KO</sup> mice. First, we observed that Fas expression was reduced in MDSCs from WT LD mice compared to WT NT mice. Conversely, IL-6<sup>KO</sup> MDSCs from LD mice exhibited an increase in Fas expression compared to WT MDSCs from LD mice (Figure 53C-D). Next, we cultured MDSCs from WT and IL-6<sup>KO</sup> mice with Fas agonistic antibodies ( $\alpha$ Fas). As expected, MDSCs from WT LD mice exhibited an increased percentage of live cells compared to MDSCs from NT mice after culture, even in the presence of  $\alpha$ Fas. In contrast, the percentage of live cells from IL-6<sup>KO</sup> LD mice was reduced compared to MDSCs from WT LD mice both with and without treatment with  $\alpha$ Fas (Figure 53E). We then determined that the frequency of myeloid cells was reduced after treatment with lymphodepleting chemotherapy followed by infusion with CD90.1<sup>+</sup> pmel T cells (Figure 53F). Specifically, M-MDSCs and PMN-MDSCs were reduced in the blood and spleens of lymphodepleted IL-6<sup>KO</sup> recipient mice compared to WT recipient mice (Figure 53G-I). Furthermore, the ratio of PMN-MDSCs to T cells was reduced in the spleens of IL-6<sup>KO</sup> recipient mice in comparison to WT recipient mice (Figure 53J). In addition, similar results were observed in LD mice treated *in vivo* with a JAK/STAT3 inhibitor, JSI-124, compared to mice treated with a vehicle control (Figure 54). Together, these data indicated that IL-6 regulates MDSC survival and Fas expression after lymphodepletion treatment.

***IL-6 signaling during progenitor differentiation to MDSCs is essential for the regulation of Fas expression and resistance to apoptosis***

In cells from IL-6R conditional knockout mice, we observed that the rescue of IL-6R signaling did not promote the immunosuppressive capacity of MDSCs (Figure 46). Moreover, exogenous IL-6 did not enhance the ability human PMN-MDSCs to suppress autologous TILs

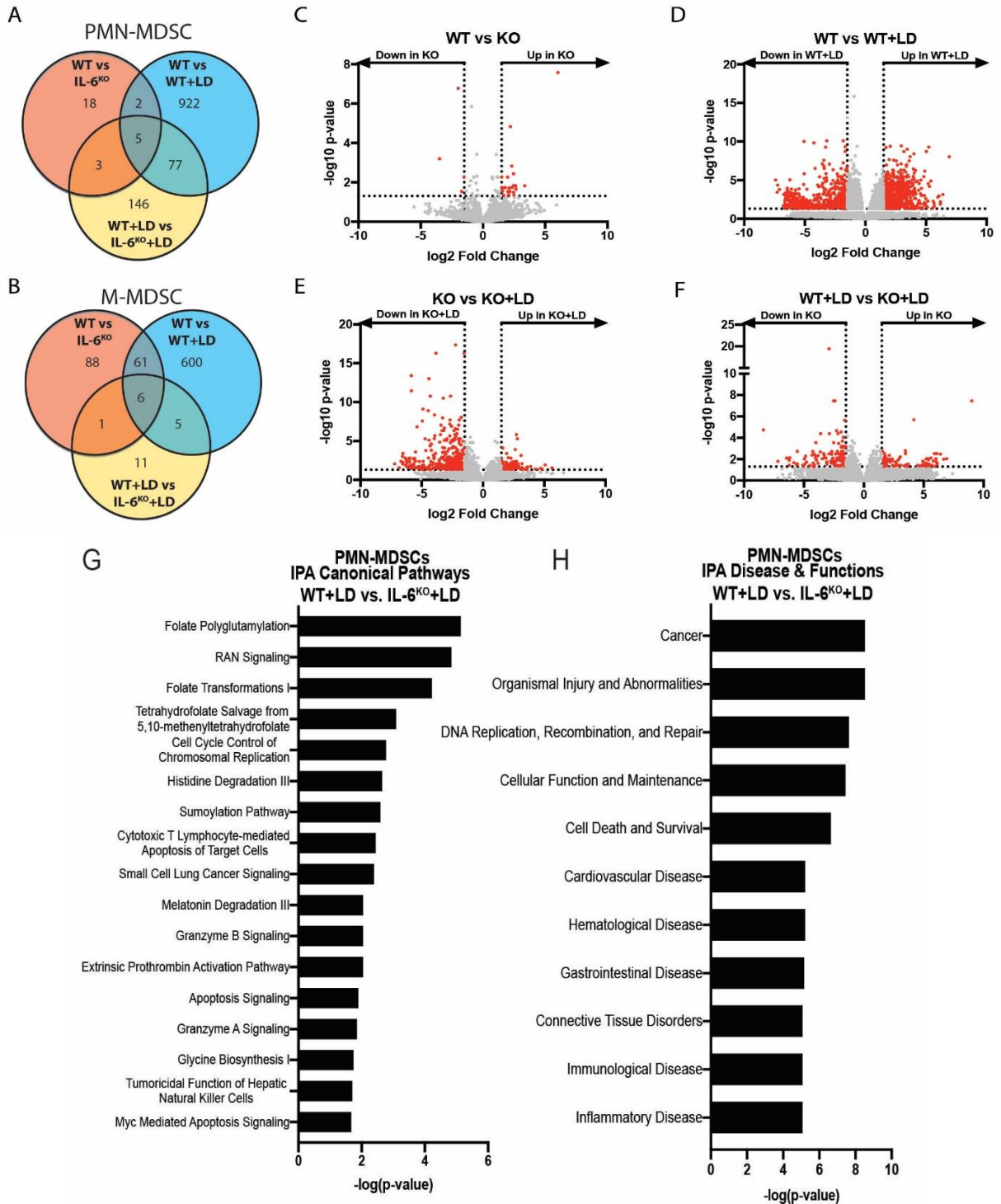


**Figure 52. RNA sequencing of WT and IL-6<sup>KO</sup> MDSCs from non-treated and lymphodepleted mice.** (A-B) Venn diagrams demonstrating the number of up- and down-regulated genes among each comparison and the overlap between comparisons. (C-F) Volcano plots of significantly altered genes in PMN-MDSCs comparing WT vs IL-6<sup>KO</sup> (C), WT vs WT+LD (D), IL-6<sup>KO</sup> vs IL-6<sup>KO</sup>+LD (E), WT+LD vs IL-6<sup>KO</sup>+LD (F). Dotted lines represent cutoffs of 1.5 fold change and log-transformed values of p<0.05. Significant genes are colored in red. (G-H) Ingenuity Pathway Analysis on genes enriched in WT+LD PMN-MDSCs over PMN-MDSCs from IL-6<sup>KO</sup> mice treated with lymphodepleting chemotherapy.

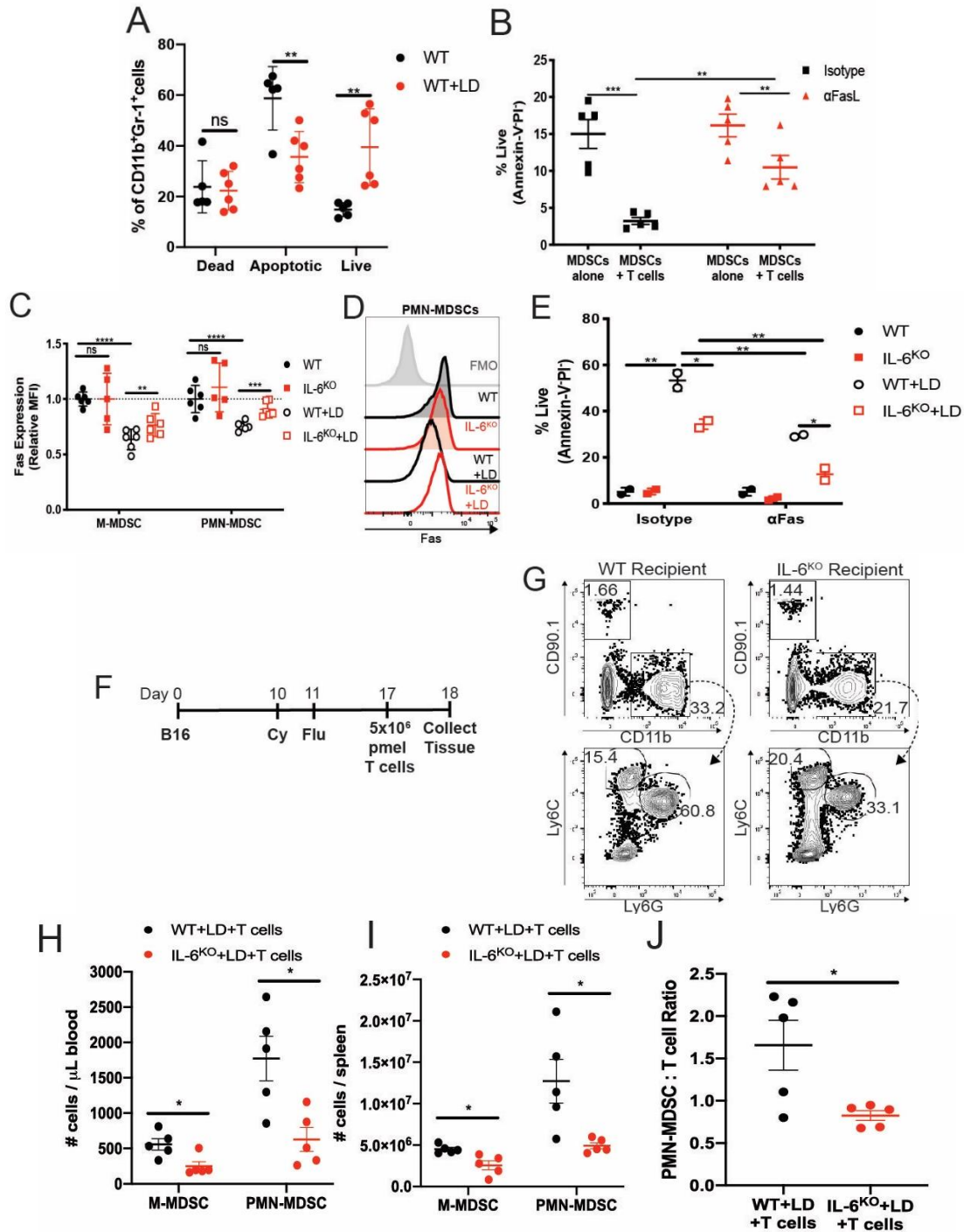


**Figure 53. IL-6 reduces Fas expression in MDSCs that expand post-lymphodepletion.**

(A) Annexin-V and PI staining among MDSCs cultured for 48hrs. (B) Frequency of live MDSCs from lymphodepleted mice after 24hrs co-culture with T cells +/- FasL blockade. (C-D) Expression of Fas in PMN-MDSCs. Compiled data from 3 independent experiments with biological replicates (C) with representative histogram (D) are shown. (E) Frequency of live PMN-MDSCs cultured for 24hrs with isotype antibodies or αFas. (F) Experiment design for (G-J). (G) Representative dot plots showing donor CD90.1<sup>+</sup> pmel T cells and reduced CD11b<sup>+</sup> cells in IL-6KO recipients 24hrs after infusion. (H-J) Frequency of MDSCs in blood (H) and spleen (I) 24hrs after ACT. (J) PMN-MDSC : T cell ratio in the spleens of mice 24hrs after ACT. Data is reflective of 2-3 independent experiments.

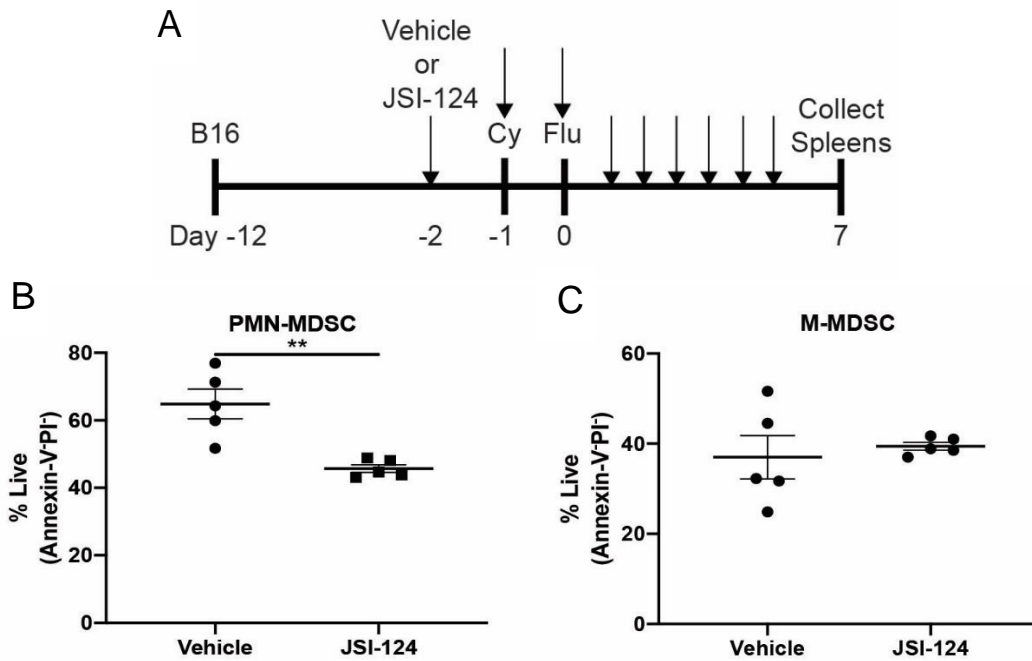


**Figure 54. In vivo JAK/STAT3 inhibition reduces PMN-MDSC survival.** (A) Experimental design for (B-C). Mice were treated with vehicle or 1mg/kg JSI-124 (indicated with arrows), once daily starting 1 day prior to lymphodepleting treatment. Day 7 post-LD, MDSCs from vehicle-treated or JSI-124-treated mice were cultured for 24hrs. Live cells were determined by Annexin-V and PI negativity. (B) PMN-MDSCs; (C) M-MDSCs. P values were determined by two-tailed t-test. Data is representative of two independent experiments (n=5 mice per group).

(Figure 55-56). Hence, we postulated that IL-6 may be most relevant during the differentiation of MDSCs from mobilized progenitors. To test our hypothesis, we collected mobilized HSPCs from LD mice and differentiated these cells to MDSCs *in vitro*. MDSCs were generated in the presence of GM-CSF alone or GM-CSF in combination with IL-6 for 4 days (Figure 57A). MDSCs that were differentiated from HSPCs in the presence of GM-CSF and IL-6 exhibited reduced Fas expression compared to MDSCs differentiated with GM-CSF alone (Figure 57B-C). Next, we cultured the MDSCs collected on Day 4 for an additional 24hrs in media containing IL-6. Intriguingly, the addition of IL-6 failed to reduce Fas expression in MDSCs generated from HSPCs in the presence of GM-CSF alone or GM-CSF and IL-6, suggesting that the expression of

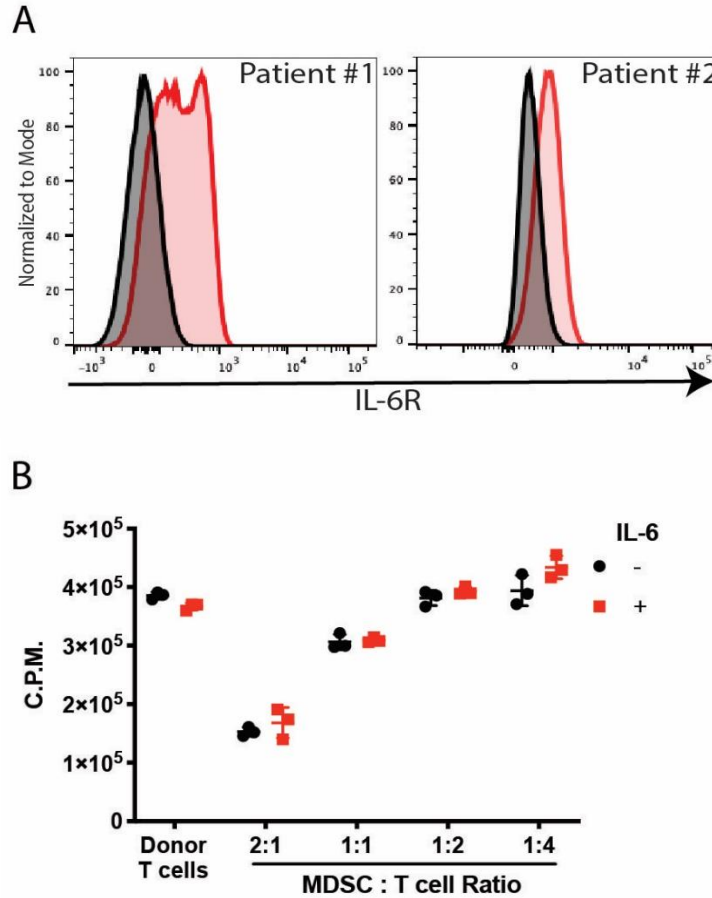


**Figure 55. Exogenous IL-6 does not alter MDSC suppressive capacity.**

(A) IL-6R surface expression on PMN-MDSCs in Week 1 Post-TIL PBMCs from melanoma patient 1 (left) and melanoma patient 2 (right). (B) PMN-MDSCs purified from Week 1 Post-TIL PBMCs and co-cultured with donor T cells in media with or without 40ng/mL IL-6. T cell proliferation was determined after 72hrs of culture. P values were determined by two-tailed t-test. Technical replicates are shown.

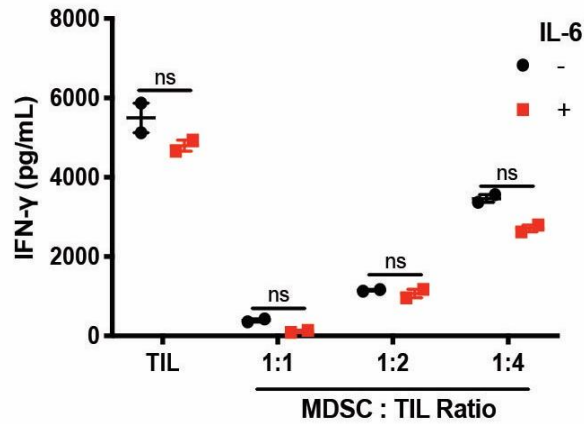


**Figure 56. IL-6 does not promote MDSC suppression of TILs**

IL-6 was added to co-cultures of TILs and PMN-MDSCs collected from a melanoma patient. TIL proliferation was measured by <sup>3</sup>H thymidine incorporation after 72hrs of culture.

Fas in MDSCs may be inherited from parental cells (Figure 57D). In parallel, we cultured the MDSCs collected on Day 4 and exposed them to Fas agonistic antibodies with or without IL-6. Consistent with the reduction of Fas expression in MDSCs generated with GMCSF and IL-6, survival was superior in response to Fas agonism compared to MDSCs generated with GMCSF alone (Figure 57E). Notably, the addition of IL-6 to MDSCs in this post-differentiation culture only had a modest effect on the viability of cells or promoting any resistance to Fas agonism in cells differentiated in either GMCSF alone or the combination of GMCSF with IL-6 (Figure 57E). We validated these results by differentiating mobilized HSPCs from WT and IL-6<sup>KO</sup> mice that were treated with lymphodepleting chemotherapy with the same protocol as in Figure 57A. GMCSF-generated MDSCs from mobilized IL-6<sup>KO</sup> HSPCs exhibited a reduced viability in T cell co-cultures in the presence of an isotype antibody and  $\alpha$ FasL compared to MDSCs derived from WT mice (Figure 58A). In contrast, MDSC viability was similar between cells differentiated from WT and IL-6<sup>KO</sup> HSPCs with the addition of GMCSF and IL-6. This suggests that the IL-6 signal received during differentiation conferred resistance to apoptosis even in IL-6 naïve cells that were collected from IL-6<sup>KO</sup> mice (Figure 58B). Additionally, Fas expression was reduced in GMCSF+IL-6-generated MDSCs compared to MDSCs generated with GMCSF alone from both WT and IL-6<sup>KO</sup> progenitors (Figure 58C). Importantly, the suppressive capacity of MDSCs generated from mobilized IL-6<sup>KO</sup> HSPCs was impaired compared to MDSCs differentiated from WT HSPCs. When T cells were cultured alone, the blockade of FasL enhanced T cell proliferation. Despite this enhancement of T cell proliferation, MDSCs potently suppressed T cells, which was enhanced upon FasL blockade. Specifically, weakly suppressive MDSCs generated from IL-6<sup>KO</sup> HSPCs became highly suppressive upon FasL blockade, indicating that the ability of MDSCs to survive during contact with T cells was critical to mediate



immunosuppressive functions (Figure 58D). Together, these data demonstrate that IL-6 differentiation signals regulate the survival and Fas expression patterns of post-lymphodepletion MDSCs that are necessary to resist apoptotic signals from T cells and mount immunosuppressive functions.

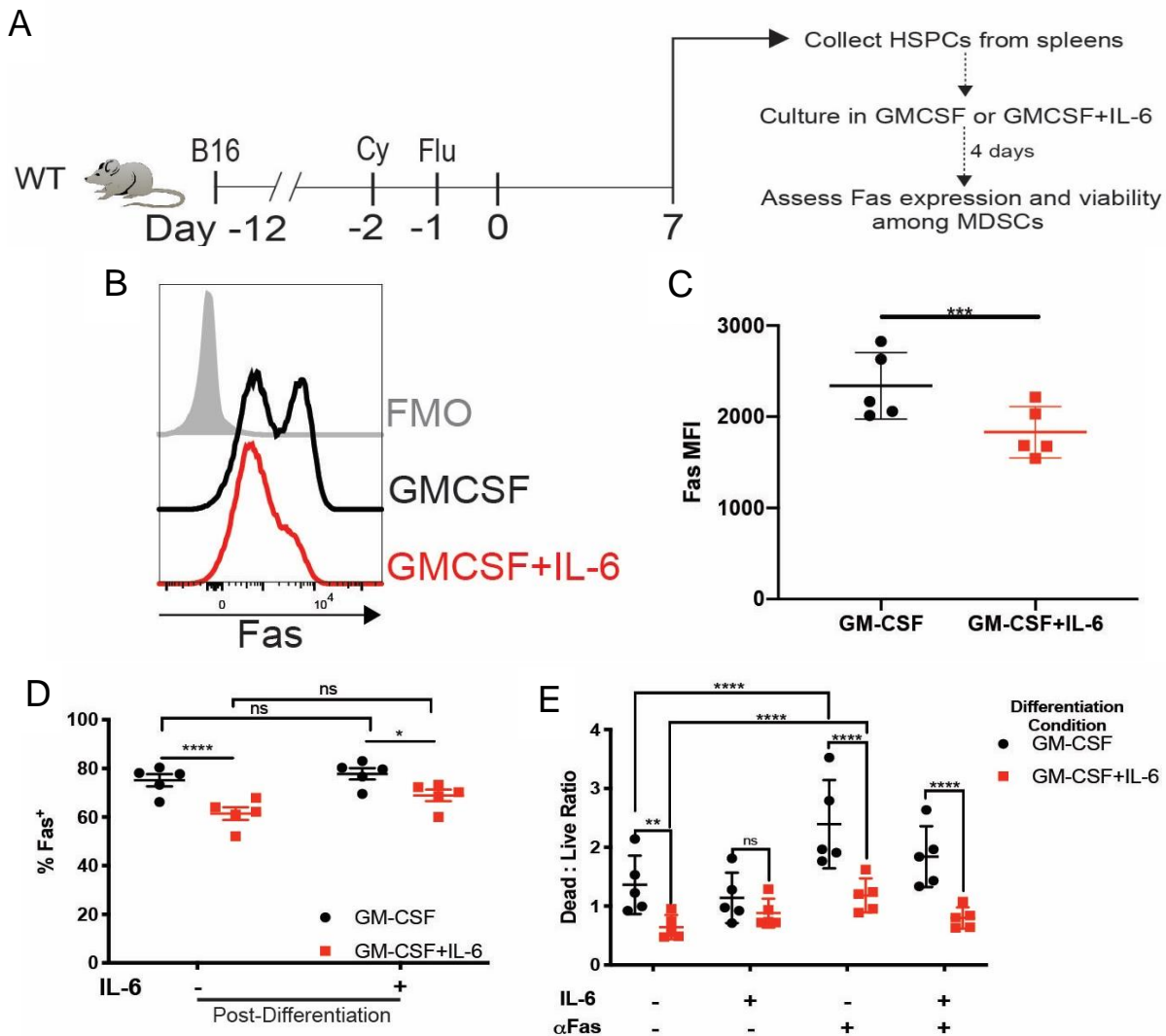


**Figure 57. IL-6 differentiation signals reduces Fas expression and increases MDSC survival.**

(A) Experimental design for (B-E). (B-C) Fas expression in MDSCs measured on day 4 of differentiation protocol. (B) Representative histogram showing Fas expression, (C) summarized data. (D) Differentiated MDSCs were collected on day 4 and then cultured for an additional 24hrs with or without IL-6. Fas expression is shown. (E) The ratio of dead:live cells after differentiated MDSCs were cultured for 24hrs in the indicated conditions. Data is reflective of 2-3 independent experiments. Each data point is representative of cells pooled from 5 mice; 20 mice total.

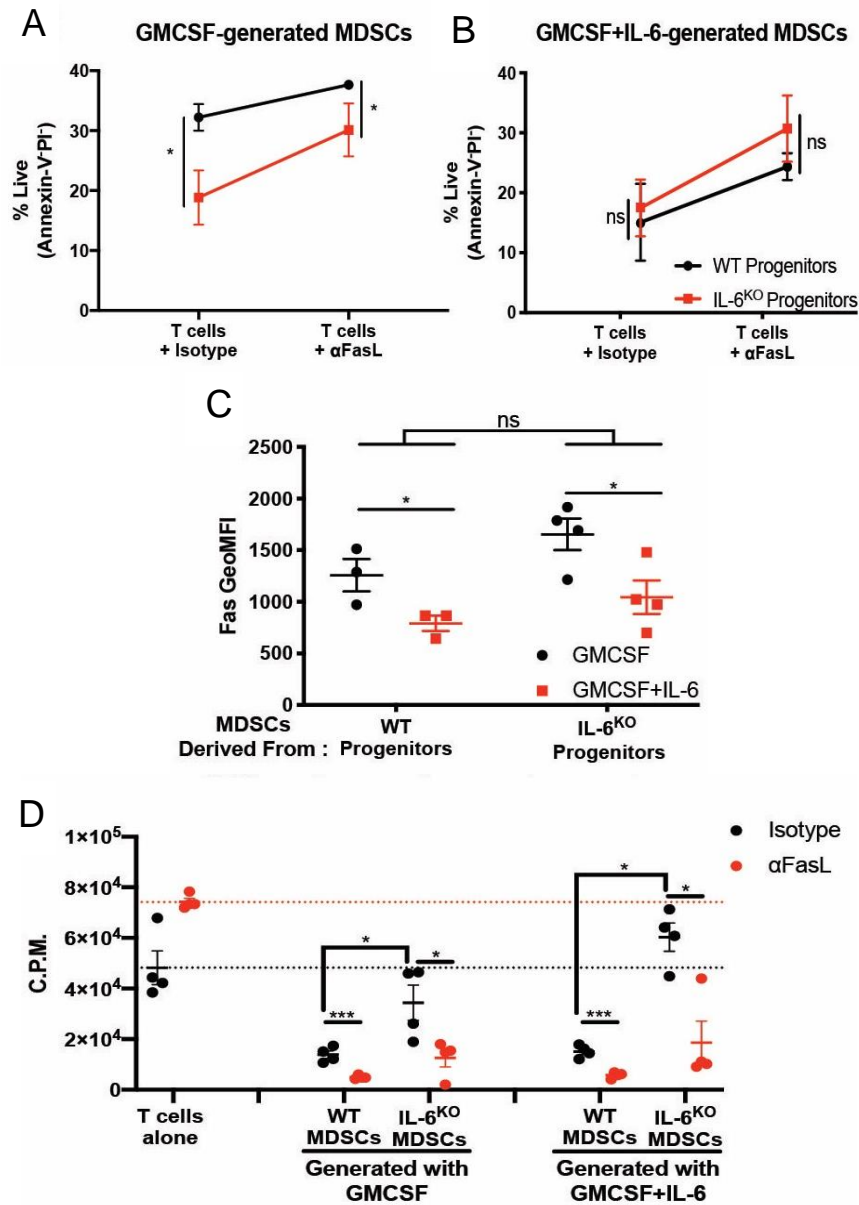


**Figure 58. IL-6 differentiation signals promote resistance to Fas-induced cell death**

(A-B) MDSCs were differentiated from Lin<sup>-</sup>c-kit<sup>+</sup> cells as in Figure 57. (A-B) Percent viability in MDSCs after 24hr co-culture with T cells and isotype antibodies or αFasL. (C) Fas expression measured in MDSCs differentiated from WT or IL-6<sup>KO</sup> HSPCs. (D) T cell proliferation in co-cultures with in vitro-generated MDSCs at a 1:8 ratio as in +/- FasL blockade. dotted lines represent the mean of pmel T cell proliferation upon culture with cognate peptide with isotype antibodies (black) or FasL blocking antibodies (red). Data is reflective of 2-3 independent experiments.

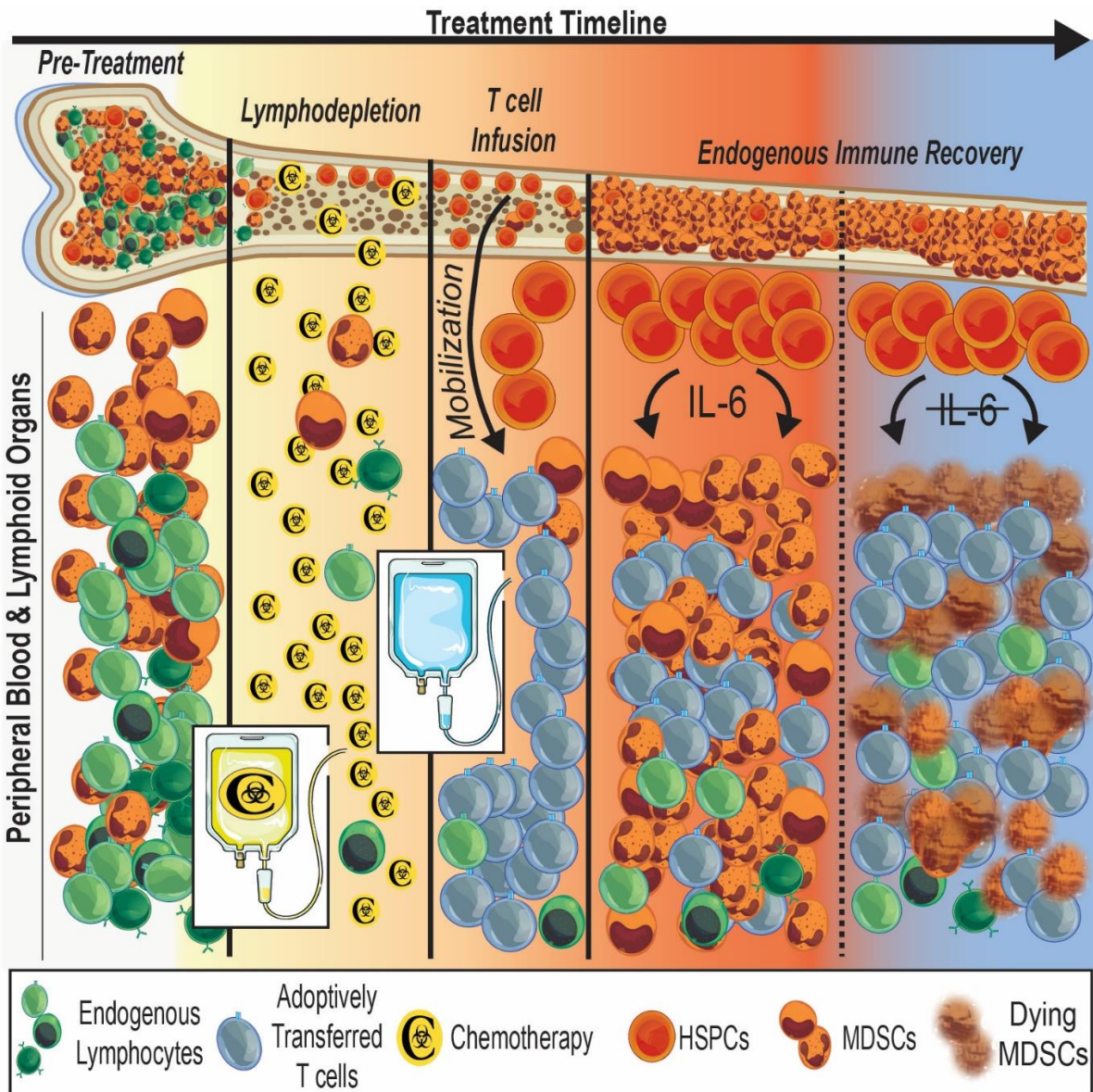


**Figure 59. Graphical Abstract**

Under homeostatic conditions, a balance of lymphocytes and myeloid cells, including MDSCs, is maintained. The administration of lymphodepleting chemotherapy acutely eliminates the majority of circulating and BM leukocytes. Early after chemotherapy treatment, HSPCs are mobilized from the bone marrow. Simultaneously, T cells are adoptively transferred following lymphodepletion. As the endogenous immune system recovers, myeloid-biased HSPCs expand in the periphery and BM and rapidly differentiate into MDSCs. This massive and concurrent accumulation of MDSCs diminishes the efficacy of ACT. However, the blockade of IL-6 differentiation signals disrupts the survival capacity of MDSCs that is inherited from parental HSPCs. As a result, the lack of IL-6 limits the survival of MDSCs, particularly when in contact with T cells. Ultimately, this leads to an enhancement of T cell persistence and anti-tumor efficacy of ACT.

## Discussion

Melanoma patient responses to ACT with TILs have been associated with T cell-intrinsic differences amongst patients including the number of TIL infused, expression of B and T-lymphocyte attenuator (BTLA), *in vivo* T cell persistence, and the magnitude of IFN- $\gamma$  production by TIL (8, 71, 193). Our data suggest that lymphodepleting chemotherapy induces the rapid expansion of MDSCs that ultimately impact the function of adoptively transferred T cells leading to diminished therapeutic efficacy and reduced TIL persistence. Importantly, the overlap of lymphodepleting regimens in patients treated with ACT with TILs, CAR-T cells, and T cells with transgenic-TCRs is highly suggestive that similar mechanisms of MDSC-mediated suppression may take place in most ACT settings (6, 46, 194). We show that the repertoire of T cell clonotypes were diminished in patients that had high frequencies of CD11b<sup>+</sup> myeloid cells, which was ultimately associated with poor long-term survival (Figure 27). It is feasible that the most abundant adoptively transferred TIL clones have a higher probability of interacting with and being suppressed by MDSCs. However, we cannot rule out that characteristic differences among individual TIL clones, such as the prevalence of tumor-reactive clones or phenotypic memory characteristics, could make certain T cells more susceptible to MDSC suppression (62, 195). Hence, a deeper understanding of the interactions between MDSCs and adoptively transferred T cells is necessary to guide strategies to render T cells more resistant to myeloid-mediated immune suppression and promote *in vivo* T cell persistence.

Cyclophosphamide, a common chemotherapeutic drug used in lymphodepleting regimens, has been described to have immunomodulatory effects that promote immunosuppressive myeloid cell accumulation (190, 196). In breast cancer patients, the frequency of Lin<sup>-</sup>HLA-DR<sup>+</sup>CD11b<sup>+</sup>CD33<sup>+</sup> MDSCs increased after treatment with a doxorubicin-

cyclophosphamide chemotherapy regimen (180). In mouse models, lymphodepleting doses of total body irradiation (197) and cessation of treatment with Gr-1 depleting antibodies (198) promoted the subsequent accumulation of myeloid cells. Hence, it is likely that non-myeloablative immunodepleting methods can lead to “reactive myelopoiesis” (175). While previous studies have shown that cyclophosphamide leads to the accumulation of MDSCs, little is known about the mechanisms that drive the expansion of MDSCs during the recovery phase after lymphodepletion treatment, particularly in human patients. Moreover, the immunosuppressive capacity of granulocytes and monocytes that accumulate in non-malignant pathological settings of emergency myelopoiesis have not been examined (184, 185). Nearly all patients in our study exhibited a significant elevation of myeloid cells after lymphodepletion and ACT which potently suppressed donor T cells and autologous TILs (Figure 19). It is known that during tumor progression, myeloid cells acquire immunosuppressive characteristics in part by a skewing that occurs during myeloid progenitor commitment (179, 181). Intriguingly, we observed a strong myelopoietic bias when HSPCs were transferred to lymphodepleted recipients (Figure 34), which suggests that host-derived factors potentiate myeloid differentiation in response to lymphodepleting chemotherapy. Tumor-derived factors such as retinoic acid can skew the differentiation of M-MDSCs to macrophages at the expense of generating dendritic cells, and the administration of all-trans retinoic acid (ATRA) can reverse this effect (178, 199). However, early precursors such as GMPs and CMPs need to be targeted to skew the development of terminally differentiated PMN-MDSCs (179, 200). CMPs and GMPs are rare populations of cells often restricted to the BM space, which may make it a challenge to manipulate differentiation signals specific to these cell populations (201). Interestingly, the rapid increase of myeloid progenitors that we observed shortly after lymphodepleting chemotherapy

treatment may provide a therapeutic window to target the differentiation of myeloid cells when myelopoietic signals are most relevant. Hence, the manipulation of differentiation signals and the exploitation of progenitor cell plasticity to modulate the immunosuppressive capacity of daughter cells, including MDSCs, during ACT regimens is an attractive therapeutic strategy and warrants further investigation.

We aimed to determine what factors could drive the massive accumulation of MDSCs after lymphodepleting chemotherapy. A previous screen of sera taken from mice treated with a lymphodepleting dose of total body irradiation revealed that CCL2 was elevated post-LD (data not shown). We investigated whether targeting the CCL2-CCR2 axis could attenuate the accumulation of MDSCs post-LD and enhance the efficacy of ACT. A previous study identified that the blockade of CCR2 after the administration of a lymphodepleting dose of cyclophosphamide effectively reduced the accumulation of M-MDSCs and enhanced the efficacy of ACT with CD4<sup>+</sup> T cells (190). Moreover, PMN cells that expanded after cyclophosphamide treatment lacked immunosuppressive capabilities on CD4<sup>+</sup> T cells suggesting that cyclophosphamide treatment promoted the accumulation of neutrophils rather than PMN-MDSCs. However, our findings contrasted these results in the following manner: 1. CCR2<sup>KO</sup> mice lack M-MDSCs, but undergo a compensatory accumulation of PMN-MDSCs, 2. Splenic MDSCs from CCR2<sup>KO</sup> mice which are predominately PMN-MDSCs potentially suppress CD8<sup>+</sup> T cell proliferation. Importantly, we show that both M-MDSCs and PMN-MDSCs from melanoma and NSCLC patients suppressed donor T cell and autologous TIL proliferation and IFN- $\gamma$  production. We acknowledge that differences in experimental tumor models, including the strain of mice and lymphodepleting regimen, and the ability of MDSCs to suppress CD4<sup>+</sup> T cells could contribute to the conflicting findings between our study and the results of Ding et. al. (190, 202).

In support of our study, the inhibition of c-MET effectively reduces the accumulation of PMN-MDSCs that accumulate after treatment with cyclophosphamide and ACT with CD8<sup>+</sup> pmel T cells leading to tumor regression in mice (203). Thus, the accumulation of PMN-MDSCs after lymphodepleting chemotherapy limits the efficacy of ACT with CD8<sup>+</sup> T cells.

We directed our attention to explore other strategies to target MDSCs in the setting of ACT because the compensatory increase of MDSCs after myeloid depletion regimens and the mechanisms associated with anti-CCL2 treatment cessation strongly contribute to tumor progression and therapy resistance in multiple settings (158, 198, 204-206). Instead, we aimed to investigate factors that could dictate the immunosuppressive capacity of MDSCs. IL-6 and STAT3 are known to promote the function, differentiation, and survival of MDSCs (177, 207). In this study, we show that lymphodepletion prompted bone marrow progenitor mobilization and that IL-6 was required for promoting survival signals during differentiation. Likewise, IL-6 has been reported to simultaneously drive the expansion of HSPCs, enhance myelopoiesis, and block lymphopoiesis (208, 209). Notably, we describe that the role of IL-6 goes beyond providing an enhancement of immunosuppressive capabilities during the differentiation from progenitor cells (177). Our functional studies in murine models and RNA sequencing indicated that post-lymphodepletion MDSCs exhibited distinct biological and transcriptional characteristics compared to MDSCs from non-treated mice. The inhibition of IL-6 signals in murine models improved the efficacy of ACT by causing the dysregulation of survival signals and the sensitization of MDSCs to Fas-induced apoptosis. In the setting of an acute induction of lymphopenia, we show that a cytokine signal, like IL-6, is critical during progenitor differentiation. IL-6 imparted an improved survival capacity and reduced Fas expression in daughter cells during the differentiation from progenitors (Figure 58). We show that the addition

of IL-6 to already differentiated MDSCs failed to improve the viability of cells or reduce Fas expression. Together, these data indicated that survival patterns can be inherited from parental hematopoietic cells which impact downstream immunosuppressive capabilities of MDSCs. Hence, MDSCs have the potential to be targeted uniquely in the setting of ACT by targeting factors specifically induced by lymphodepleting regimens which can impact the differentiation trajectory of mobilized HSPCs.

We showed that lymphodepleting chemotherapy enhances IL-6 production in BM-derived myeloid cells and HSPCs early after treatment. Subsequently, the IL-6 differentiation signal was critical for promoting MDSC resistance to T cell-mediated apoptosis. We found that a single infusion of MDSCs along with T cells was sufficient to accelerate tumor growth in comparison to mice that received T cells alone. Importantly, the transfer of IL-6 naïve MDSCs taken from IL-6<sup>KO</sup> donor mice failed to negatively impact the efficacy of ACT in IL-6 competent recipients (Figure 49). This provides further support that IL-6 impacts MDSC function indirectly during their differentiation from progenitors, rather than on cells in a post-differentiation state. In addition to IL-6, our RNA sequencing experiments revealed that several upstream regulators, including tumor necrosis factor alpha (TNF $\alpha$ ) and GM-CSF (CSF2) may drive the expansion and function of MDSCs that expand after treatment with lymphodepleting chemotherapy. TNF $\alpha$  can promote the survival of HSPCs and promote the accumulation of myeloid cells in response to stimulation with polyinosinic:polycytidylic acid (poly I:C), LPS, or treatment with 5-fluorouracil (5-FU) (210). Meanwhile, GM-CSF has been shown to promote extramedullary myelopoiesis within inflamed joints of mice with experimental spondyloarthritis (186). Interestingly, TNF $\alpha$  and GM-CSF promoted a myelopoietic bias in these experimental settings, which aligns with the differentiation bias of HSPCs that we observed in lymphodepleted mice (Figure 34).



Furthermore, the overexpression of IL-1 $\beta$  in murine breast cancer cells can generate MDSCs that are more resistant to Fas-induced cell death (211). While we did not examine other factors in this current study, we are actively investigating the role of other cytokines and growth factors in the regulation of lymphodepletion-driven myelopoiesis. Collectively, the determination of key host-factor signals and the characterization of myelopoietic niches during lymphodepletion-driven myelopoiesis could identify new therapeutic targets with the potential to enhance patient responses to ACT.

In patients receiving CAR-T cells, the onset of cytokine release syndrome (CRS) was attributed to the production of IL-6 and IL-1 $\beta$  by monocytes after CAR-T cell infusion and that the symptoms of CRS could be ameliorated by the administration of IL-6R blocking antibodies and/or IL-1 receptor antagonists (212). However, it is unclear which host factors induced by lymphodepleting chemotherapy, including IL-6 and IL-1 $\beta$ , are responsible for the induction of myeloid-mediated immunosuppression during ACT regimens. Notably, patients that receive ACT with TIL do not exhibit symptoms of CRS, but rather endure toxicities related to lymphodepleting chemotherapy and/or bolus high dose IL-2 administration (49). Thus, the role of IL-6 beyond its role in the induction of CRS remains unclear in a variety of ACT settings. However, the ongoing clinical use of IL-6R blocking antibodies in patients receiving CD19-directed CAR-T cells provides feasibility for this treatment to be used prophylactically to reduce myeloid-mediated immunosuppression in patients receiving any modality of ACT in combination with lymphodepleting chemotherapy (213). We acknowledge that immunological abnormalities associated with pre-existing cytopenias, late-onset neutropenia, and a history of HSCT which are frequently observed in patients with hematological malignancies could have an impact on myelopoiesis in patients receiving CD19-directed CAR-T cells (214, 215). Thus,

differences associated with lymphodepletion-driven myelopoiesis between patients with solid tumors and hematological malignancies remain unclear. Moreover, the impact of MDSCs on patient outcomes after CAR-T cell infusion has not been thoroughly evaluated and is an active point of investigation for our group.

This study is characterized by important limitations. For example, the small patient sample size limits the statistical power of our study. Hence, future prospective studies that analyze MDSC accumulation and its impact on the survival of patients receiving ACT are necessary. Importantly, we focused on peripheral immune suppression during lymphodepletion recovery in this study. It is well established that tumor-derived factors can enhance the suppressive capacity of MDSCs (216). We also demonstrated this by generating immunosuppressive myeloid cells from a patient's CD34<sup>+</sup> cells in tumor-condition medium (Figure 37-39). However, the lack of patient tumor biopsies post-TIL infusion limited our ability to evaluate therapy-related changes in the tumor microenvironment. Hence, future studies in murine models and patient specimens will evaluate the differentiation and infiltration of HSPCs and myeloid cells in the tumor microenvironment after treatment with lymphodepleting chemotherapy and its ensuing impact on the efficacy of ACT.

While the therapeutic efficacy of ACT and the persistence of infused T cells are associated with lymphodepletion-induced increases of T cell homeostatic cytokines (26, 36, 44), we highlight an opposing mechanism in that lymphodepleting chemotherapy regimens prompt the mobilization of HSPCs followed by dramatic expansion of immunosuppressive myeloid cells. With the evidence provided in our study, we propose that the full benefits of pre-conditioning lymphodepletion regimens may be achieved by inhibiting counter immunosuppressive reactions, potentially through skewing the differentiation of progenitor cells.

Accordingly, we report that the modulation of MDSCs by blocking IL-6 differentiation signals is a feasible approach to enhance therapeutic outcomes in patients receiving ACT with TIL and provides support for future clinical trials.

## **Methods**

### ***Study Design***

The primary research objective was to evaluate mechanisms that drive the expansion and function of immunosuppressive myeloid cells in patients receiving ACT and relevant murine models. For human specimen analysis, the data shown includes all acquired data for the patient cohorts for this study. For murine experiments, animals were randomized after tumor inoculation and experiments were repeated between two and four times as noted.

### ***Patient Samples***

Patient lymphodepletion was carried out via administration of cyclophosphamide (60 mg/kg/day) and mesna (20 mg/kg) were given intravenously on day -7 and day -6 relative to the anticipated TIL infusion date. Fludarabine (25 mg/m<sup>2</sup>) was given daily intravenously from day -5 to day -1. The TIL infusion was administered on day 0 and a 720,000-IU/kg IV bolus of IL-2 (aldesleukin, Prometheus Laboratories Inc., San Diego, CA, USA) was given every 8–16 h for up to 15 doses, beginning 12–16 h after TIL infusion. Preparation of TIL was performed as previously described (8). Briefly, surgically resected tumors were minced to 1mm pieces and placed into individual wells of a 24 well plate containing 6000IU/mL IL-2. TILs were expanded for up to 5 weeks and then tested for IFN- $\gamma$  production in co-cultures with autologous tumor cell lines or cryopreserved tumor digest cell suspensions. IFN- $\gamma$ <sup>+</sup> TILs underwent a rapid expansion protocol (REP) (8). For TIL-MDSC co-cultures, cryopreserved Post-REP TIL were thawed and

rested for 48-72hrs in AIM-V (ThermoFisher) containing 3000 IU/mL IL-2 prior to co-culture. Myeloid cells were sorted from fresh PBMCs collected from melanoma or non-small cell lung cancer (NSCLC) patients. Sorted MDSCs were cultured with autologous TIL or donor T cells as indicated below.

### ***Myeloid cell isolation for functional assays***

For human specimens, PMN-MDSCs were purified from fresh PBMCs using CD15 Microbeads (Miltenyi Biotec). M-MDSCs were purified by the negative selection PBMCs by labeling with biotinylated antibodies for CD3, CD19, CD56, and HLA-DR. The negative fraction was then labeled with CD14 Microbeads (Miltenyi Biotec). MDSCs isolated from human specimens were cultured with donor T cells or autologous TIL. T cells were stimulated using Dynabeads™ Human T-Activator CD3/CD28 for T Cell Expansion and Activation (ThermoFisher Scientific, 11132D). When available, TILs were co-cultured with autologous tumor cell lines and varying concentrations of MDSCs. For murine specimens, MDSCs were purified from spleens using anti-Gr-1 biotinylated antibodies, anti-biotin microbeads, or streptavidin microbeads (Miltenyi Biotec) with a purity >90% after elution through magnetic columns. CD8<sup>+</sup> T cells were purified from the spleens of pmel or OT-I mice using EasySep™ Mouse CD8<sup>+</sup> T Cell Isolation Kit (StemCell Technologies). Gr-1<sup>+</sup> cells were co-cultured with pmel or OT-I T cells for 72 hours in round-bottom 96 well plates. Co-cultures were incubated in media containing 1µg/mL of cognate peptide, gp100<sub>25-33</sub> or OVA<sub>SIINFEKL</sub> (both from AnaSpec). T cell proliferation was assessed by CellTrace Violet dilution (ThermoFisher Scientific) or <sup>3</sup>H thymidine incorporation. For <sup>3</sup>H thymidine incorporation, <sup>3</sup>H thymidine was added at the final 18 hours of culture and cells were harvested at 72hrs. For detection of IFN-γ, supernatants were

collected after 72hrs of culture and concentrations were measured by ELISA (BD or R&D Systems).

### ***Generation of human melanoma cell line and tumor conditioned medium***

A surgically resected melanoma tumor was subjected to a TIL expansion protocol as described above. The remaining tumor was digested in media containing collagenase (type II and type IV), hyaluronidase, and DNAase (Fisher Scientific Co., Pittsburgh, PA, USA) for 1 hour at 37°C and mechanical dissociation by GentleMACS (Miltenyi Biotec). After digestion, the cell suspension was filtered to remove undigested tumor and connective tissue to generate a single-cell suspension. Cells were suspended in complete media (CM) containing RPMI media supplemented with 10% heat-inactivated FBS, 0.1 mM nonessential amino acids, 1 mM sodium pyruvate, 2 mM fresh L-glutamine, 100 mg/ml streptomycin, 100 U/ml penicillin, 50 mg/ml gentamicin, 0.5 mg/ml fungizone (all from Life Technologies, Rockville, MD), and 0.05 mM 2-ME (Sigma-Aldrich, St. Louis, MO) and grown to confluency. Adherent cells were passaged multiple times. To generate tumor conditioned medium (TCM), tumor cells were grown to confluency in CM and dissociated using Cell Dissociation Buffer, Enzyme-Free, PBS (ThermoFisher). Cells were pelleted and washed twice with PBS before suspending in serum-free RPMI at  $1 \times 10^6$  cells/mL and cultured in a 24 well plate for 24hrs. Cell-free supernatant was harvested and stored at -80°C until ready for use. Cytokine concentrations were determined by LEGENDplex™ HU Essential Immune Response Panel (13-plex) (BioLegend).

### ***MDSC differentiation***

For murine specimens, Lin<sup>-</sup>c-kit<sup>+</sup> cells were collected from the spleens of lymphodepleted mice.  $1 \times 10^6$  cells were cultured in 6 well plates for 4 days in 4mL of media containing 40ng/mL

recombinant murine GMCSF (PeproTech) or GMCSF in combination with 40ng/mL recombinant murine IL-6 (PeproTech). At the end of culture, Gr-1<sup>+</sup> cells were isolated and used for functional analysis. For human specimens, CD34<sup>+</sup> cells were purified from cryopreserved patient PBMCs using CD34 MicroBead kit, human (Miltenyi Biotec) with a purity >95%. 5x10<sup>4</sup> CD34<sup>+</sup> cells were cultured in 6 well plates in StemSpan<sup>TM</sup> SFEMII supplemented with StemSpan<sup>TM</sup> CC110 (StemCell Technologies), 100 mg/ml streptomycin, and 100 U/ml penicillin. SFEMII+CC110 media was supplemented with 40ng/mL recombinant human GCSF (PeproTech). CD34<sup>+</sup> cells were cultured for the first 7 days in media containing cytokines and CC110 diluted 1:100 per the manufacturer recommendation. For the final 7 days of culture, CC110 was diluted 1:1000 from the manufacturer stock concentration. Media was refreshed every 4 days by addition of fresh media and cytokines to each well. For the final 4 days of culture, media was refreshed containing cytokines plus 30% RPMI (Vehicle) or TCM. At the end of the culture (14 days total), cells were harvested and co-cultured with TILs for functional analysis.

### ***Mouse models and treatment***

Female C57BL/6 mice (6–8 weeks old) were purchased from Charles River Laboratories (Wilmington, MA). B6.129S2-*Il6*<sup>tm1Kopf</sup>/J (IL-6<sup>KO</sup>) and B6.129S4-*Ccr2*<sup>tm1Ifc</sup>/J (CCR2<sup>KO</sup>) mice were purchased from Jackson Laboratories (Bar Harbor, ME). To generate a conditional IL-6R knockout, B6;SJL-*Il6ra*<sup>tm1.1Drew</sup>/J mice (Jackson Laboratories) were bred with B6.129P2-*Lyz2*<sup>tm1(cre)lfo</sup>/J mice (Jackson Laboratories). *Il6ra*<sup>+fl</sup> heterozygotes, hemizygous for *Lyz2*-cre were bred with homozygous *Il6ra*<sup>fl/fl</sup> mice to generate mice that were *Il6ra*<sup>fl/fl</sup>*Lyz2*<sup>cre</sup> (denoted as IL-6R<sup>M-KO</sup>; M=myeloid). Cre<sup>-</sup> littermates (*Il6ra*<sup>fl/fl</sup>) were used as control mice. Female B6.SJL-*Ptprc*<sup>a</sup> *Pepc*<sup>b</sup>/BoyJ CD45.1<sup>+</sup> (6-8 weeks old) were purchased from Jackson Laboratories. Pmel and OT-I were bred and housed at the Animal Research Facility of the H. Lee Moffitt Cancer

Center and Research Institute. Mice were humanely euthanized by CO<sub>2</sub> inhalation according to the American Veterinary Medical Association Guidelines. Mice were observed daily and were humanely euthanized if a solitary subcutaneous tumor exceeded 400 cm<sup>2</sup> in area or mice showed signs referable to metastatic cancer.

### ***Murine Cell Lines***

B16 melanoma (obtained from ATCC) and Panc02 pancreatic cancer (obtained from ATCC) cell lines, were cultured in complete media (CM): RPMI media supplemented with 10% heat-inactivated FBS, 0.1 mM nonessential amino acids, 1 mM sodium pyruvate, 2 mM fresh L-glutamine, 100 mg/ml streptomycin, 100 U/ml penicillin, 50 mg/ml gentamicin, 0.5 mg/ml fungizone (all from Life Technologies, Rockville, MD), and 0.05 mM 2-ME (Sigma-Aldrich, St. Louis, MO). The cell lines tested negative for mycoplasma contamination. All cell lines were passaged less than 10 times after initial revival from frozen stocks. All cell lines were validated in core facilities prior to use.

### ***In vitro T cell culture, lymphodepletion, adoptive transfer, and in vivo treatment***

T cells were isolated from the spleens of pmel EasySep™ Mouse CD8+ T Cell Isolation Kit (StemCell Technologies). Pmel T cells were cultured for 3 days in CM containing 10 IU/ml IL-2 and 5 ug/ml gp100<sub>25-33</sub> peptide. Recipient mice with established tumors were lymphodepleted by intraperitoneal injection of 200mg/kg cyclophosphamide (Baxter) followed by 100mg/kg fludarabine (Sagent Pharmaceuticals) 24hrs after cyclophosphamide injection. Adoptive transfer of 2.5x10<sup>6</sup> activated pmel T cells were infused intravenously via tail vein injection 24hrs after fludarabine administration. For the adoptive transfer of MDSCs, B16 tumor-bearing mice with established tumors were given lymphodepleting chemotherapy. Seven days after treatment, recipient mice were lymphodepleted and MDSCs were isolated from the spleens

of mice and co-transferred at a 1:1 ratio with activated pmel T cells 24hrs after fludarabine administration. IL-2 (2.5e5 IU) was given i.p. following T cell injection, continuing every 12 hours for three days, for a total of six injections. Following this treatment, tumor size was measured and recorded every 3-4 days.

For the adoptive transfer of HSPCs, CD45.1<sup>+</sup> mice with established B16 tumors were given lymphodepleting treatment. Seven days after treatment, HSPCs were purified from spleens by depleting Lin<sup>+</sup> cells using Direct Lineage Depletion Kit (Miltenyi Biotec) followed by positive selection using CD117 microbeads (Miltenyi Biotec). Purity of Lin<sup>-</sup>c-kit<sup>+</sup> cells was >90%. 5x10<sup>6</sup> CD45.1<sup>+</sup>Lin<sup>-</sup>c-kit<sup>+</sup> cells were infused intravenously via tail vein injection to CD45.2<sup>+</sup> C57BL/6 mice.

For IL-6R blockade, mice were administered via intraperitoneal injection of 1.0mg of anti-IL-6R antibody (15A7, BioXCell) one day prior to cyclophosphamide injection, followed by 0.5mg anti-IL-6R antibody every 5 days for the duration of the experiment. For JAK2/STAT3 inhibition, lymphodepleted tumor-bearing mice were administered 1mg/kg JSI-124 (Cayman Chemical) by intraperitoneal injection once daily starting one day prior to cyclophosphamide injection. DMSO was the carrier and used as a vehicle control.

### ***Flow Cytometry***

Spleens and bone marrow were harvested under sterile conditions. Spleens were homogenized by applying pressure to tissue on 100µm cell strainers. BM was harvested by flushing media with a needle and syringe through femurs and tibias. Bones were then crushed and the resulting BM was collected. Single-cell suspensions were prepared, and red blood cells were removed using red blood cell lysis buffer (BioLegend). The resulting suspension was passed through a 70µm cell strainer and washed once with PBS. Cells were resuspended in to a



concentration of  $0.5-1 \times 10^6$  cells/mL for flow cytometric analysis in FACS Buffer containing PBS, 5% fetal bovine serum, 1mM Ethylenediaminetetraacetic acid (EDTA) (Sigma Aldrich), and 0.1% sodium azide (Sigma Aldrich). Cell viability was measured by staining cell suspensions with ZombieNIR (BioLegend). Prior to surface staining, cells were incubated with Fc Shield (TonboBiosciences) for murine specimens and Fc Blocker (Miltenyi Biotec) for human specimens. For surface staining of murine specimens, cells were stained in FACS buffer with the following antibodies: CD3 (145-2C11), CD4 (GK1.5), CD8 (53-6.7), CD19 (1D3), NK1.1 (PK136), CD11b (M1/70), Ly6G (1A8), Ly6C (HK1.4), F4/80 (BM8), c-kit (2B8), Sca-1 (D7), CD16/32 (93), IL-7R (A7R34), IL-6R (D7715A7) (all from BioLegend), Fas (Jo2) (BD Biosciences), and Lineage Cocktail (TonboBiosciences). For human specimens, cell surface staining was conducted with the following antibodies: CD3 (145-2C11), CD4 (RPA-T4), CD8 (RPA-T8), CD19 (HIB19), CD56 (B159), CD11c (Bly6), CD14 (MoP9), CD15 (HI98), CD11b (ICRF44), CD33 (P67-6), HLA-DR (G46-6), IL-6R (M5), CD34 (581), CD38 (HIT2), CD45RA (HI100), CD90 (5E10) (all from BD Biosciences), and LOX-1 (15C4), PD-L1 (29E-2A3) (from BioLegend). Cells were acquired by LSR II or FACS Celesta (BD Biosciences), and the data were analyzed with FlowJo (Tree Star).

### ***IL-6 detection and in vitro stimulation of IL-6 signaling***

IL-6 was measured in plasma samples collected from melanoma patients that received ACT with TIL at the Moffitt Cancer Center using Human IL-6 Quantikine ELISA Kit (R&D Systems). For human specimens, 40ng/mL recombinant human IL-6 (Peprotech) was added to T cell / TIL co-cultures with patient-derived MDSCs. For murine specimens, 40ng/mL recombinant murine IL-6 (Peprotech) was added to MDSC : T cell co-cultures. Where indicated, 200ng/mL recombinant mouse IL-6/IL-6R alpha protein chimera (R&D Systems) was added to

co-cultures containing MDSCs collected from IL-6R<sup>M-KO</sup> mice. For intracellular IL-6 staining, BM cells were incubated in CM with and without 1mg/mL lipopolysaccharide (LPS) for 18hrs in 24 well plates at a concentration of  $5 \times 10^5$  cells per well. During the final 6hrs of culture, 500ng/mL brefeldin A solution (BioLegend) was added to each well. After 6hrs of incubation with brefeldin A, non-adherent cells were collected. Adherent cells were collected after incubation with 1mM EDTA solution and gentle scraping. Adherent cells were pooled with non-adherent cells. Cells were stained with ZombieNIR, Fc Shield, and cell surface markers followed by fixation and permeabilization via Cytofix/Cytoperm kit (BD Biosciences). Cells were stained with anti-IL-6 antibodies, washed twice, and then data were acquired immediately by FACS Celesta (BD Biosciences). For pSTAT3 (pY705) staining, cells were incubated in serum-free RPMI for 30 minutes at 37°C. To induce STAT3 phosphorylation, cells were incubated with 100ng/mL IL-6 (Peprotech) or 200ng/ml recombinant mouse IL-6/IL-6R alpha protein chimera (R&D Systems). Cells were washed and stained for cells surface markers. BD Phosflow Lyse/Fix Buffer was added to each sample for fixation followed by permeabilization with BD Phosflow Perm Buffer III. Permeabilized cells were incubated with antibodies specific for pSTAT3 for 30 minutes at room temperature. Cells were washed three times and then data were acquired immediately for flow cytometric analysis.

### ***MDSC apoptosis***

Purified MDSCs were cultured for 24-48hrs in 24 well plates at  $5 \times 10^5$ - $1 \times 10^6$  cells per well in media containing 1 $\mu$ g/mL purified hamster anti-mouse Fas (CD95), (Jo2, BD Biosciences) or isotype Armenian Hamster IgG<sub>2</sub> (BD Biosciences). In MDSC co-cultures with activated T cells, cells were incubated with 10 $\mu$ g/mL purified anti-mouse CD178 (FasL),

(MFL3, BioLegend) or isotype mouse IgG1 (BioLegend). Apoptosis was measured by Annexin-V and PI staining (ThermoFisher Scientific) and assessed by flow cytometric analysis.

### ***TCR-beta sequencing and analysis***

DNA extraction was performed using the DNeasy Blood & Tissue Kit (Qiagen) on Post-REP TIL, apheresis samples collected 6 weeks post-TIL infusion, and patient PBMCs. Samples were subjected to T cell receptor (TCR) clonotyping and TCR-*beta* CDR3 regions were analyzed using the ImmunoSEQ™ Analyzer (Adaptive Biotechnologies). TIL frequency was determined by identifying unique V-beta and J-beta genes identified within each sample and calculating the sum frequency of productive rearrangements among the total detected in both Post-REP TIL and post-TIL infusion PBMCs. A persistent TIL clone in post-TIL infusion PBMCs or apheresis products were determined by the detection of the same rearrangements initially identified in Post-REP TIL. The fold change of TIL frequency was determined by identifying overlapping unique rearrangements detected in Post-REP TIL and post-TIL infusion PBMCs and calculating their respective proportion of the total detected rearrangements. Fold change was calculated between the sum productive frequency of overlapping rearrangements detected at week-6 post-TIL infusion by the frequency of the same rearrangements detected in Post-REP TIL and correlated with CD11b<sup>+</sup> cell frequency.

### ***RNA-Sequencing***

M-MDSCs (CD11b<sup>+</sup>Ly6C<sup>+</sup>Ly6G<sup>-</sup>) and PMN-MDSCs (CD11b<sup>+</sup>Ly6C<sup>+</sup>Ly6G<sup>+</sup>) were sorted by FACS Aria SORP (BD Biosciences) with a purity >99%. Sorted cells were washed and stored as dry pellets. RNA was extracted by RNeasy Mini Kit (Qiagen). Paired-end RNA sequencing reads were subjected to adaptor trimming and quality assessment before being aligned to mouse reference genome mm10 using STAR v2.5.3a [PMID: [23104886](https://pubmed.ncbi.nlm.nih.gov/23104886/)]. Quantification of read counts

aligned to the region associated with each gene was performed using HTSeq v0.6.1 [PMID:[25260700](#)] based on RefSeq gene model. Read counts of all samples were normalized based on library size estimation using the R/Bioconductor package DESeq2 v1.6.3 [PMID: [25516281](#)]. Differential gene expression between different conditions was performed by serial dispersion estimation and statistical model fitting procedures implemented in DESeq2. Genes with Benjamini-Hochberg corrected p-value of less than 0.05 were considered to be significantly differentially expressed. Significant genes affected by at least two-fold were analyzed for enrichment of upstream regulators using QIAGEN's Ingenuity Pathway Analysis software (IPA, QIAGEN, [www.qiagen.com/ingenuity](http://www.qiagen.com/ingenuity), “canonical pathways”; “diseases and functions”; “upstream regulators” options). For upstream regulator analysis, cytokine upstream regulators were filtered and sorted by p-value for the dataset overlap between molecules known to be regulated by that given cytokine.

### ***Statistical analysis***

Graphs were generated using GraphPad Prism software. Graphs represent mean values with SEM. P values were calculated in each respective Figure where statistical tests were indicated. Retrospective analysis for patient survival was performed. Mantel-Cox p-values are shown on each respective Kaplan-Meier plot. Patient groups for Kaplan-Meier survival plots were established by determining the median cutoff by frequency distribution analysis. The median follow-up for survival analysis was determined by reverse Kaplan-Meier analysis (Median follow-up = 22 months). P values and  $R^2$  values were determined by two-tailed Pearson r correlation test. For mouse-tumor growth studies, tumor growth curves are shown as mean with SEM and significance was determined by 2-way ANOVA and Sidak's multiple comparison's test. Mice were randomized after tumor cell implantation into respective treatment groups. For

all other experiments, data were compared using either an unpaired 2-tailed Student's t-test corrected for multiple comparisons by a Bonferroni adjustment or Welch's correction. \*=P<0.05; \*\*=P<0.01; \*\*\*=P<0.001; \*\*\*\*=P<0.0001.

### ***Study Approval***

All animal experiments were approved by the University of South Florida Institutional Animal Care and Use Committee and performed in accordance with the U.S. Public Health Service policy and National Research Council guidelines. Studies were performed under approved Institutional Review Board (IRB) laboratory protocols at the H. Lee Moffitt Cancer Center (Tampa, FL). TILs, PBMCs, and autologous tumors were collected from melanoma patients or PBMCs from NSCLC tumor patients as part of TIL ACT clinical trials. All samples were de-identified prior to use in research studies. All patients signed approved consent forms. Specimens were obtained from patients that were enrolled in the following clinical trials: Vemurafenib With Lymphodepletion Plus Adoptive Cell Transfer & High Dose IL-2 Metastatic Melanoma, 16992, NCT01659151, Ipilimumab With Lymphodepletion Plus Adoptive Cell Transfer and High Dose IL-2 in Melanoma Mets Pts, 17057, NCT01701674, Combining PD-1 Blockade, CD137 Agonism and Adoptive Cell Therapy for Metastatic Melanoma, 18377, NCT02652455, Nivolumab and Tumor Infiltrating Lymphocytes (TIL) in Advanced Non-Small Cell Lung Cancer, 19122, NCT03215810.

## CHAPTER FOUR

### CONCLUSIONS AND FUTURE PERSPECTIVES

In recent years, many studies have shown the importance of the coordination between the innate and adaptive immune system in the eradication of tumors, particularly in the application of immunotherapeutics. In these studies, we have demonstrated that 41BB agonists do not act solely on T cells to promote TIL expansion and the elimination of tumor cells (Chapter 2). Rather, 41BB agonists may act indirectly on APCs by enhancing the interaction of myeloid 41BBL with 41BB<sup>+</sup> T cells and/or polarizing myeloid cells towards an immunostimulatory phenotype. In mouse models, the intratumoral administration of 41BB agonistic antibodies remodeled the myeloid-tumor milieu and increased the capacity of tumor-associated myeloid cells to potentiate T cell responses. In human tumor explants, 41BB agonists promoted TIL expansion and tumor reactivity. However, our mechanistic studies on human myeloid cells revealed an emphasis on 41BBL playing a larger role in promoting APC maturation, even in the presence of 41BB agonists. Specifically, the stimulation of 41BBL, but not 41BB, enhanced the maturation of myeloid cells and their ability to stimulate TIL proliferation. This is in partial contrast to our previous study that demonstrated that 41BB agonistic antibodies enhance DC maturation, including the expression of 41BB (96). However, the functional relevance of 41BB was not evaluated in that study. In the current study, we did not observe 41BB expression in myeloid cells from a primary melanoma tumor or in conditioned monocytes taken from PBMCs. Thus, we acknowledge the possibility that 41BB expression on subsets of APCs could have a functional impact in the presence of 41BB agonists that we did not capture in this study.

However, the maturation stimuli provided by 41BBL activation, but not 41BB agonists, in myeloid cells is suggestive that 41BBL may play a larger role in generating immunostimulatory APCs. We believe that both the 41BB-41BBL axis and the activity of tumor-associated APCs likely play critical roles in the “Enrichment” of tumor-reactive TILs. Together, the work outlined in Chapter 2 poses many interesting questions such as: (1) Does 41BB activate human myeloid cells? And do 41BB agonists truly activate myeloid cells directly? Or indirectly by enhancing the signal transduction through 41BBL and bidirectional signaling with 41BB? and (2) How do constituent tumor infiltrating immune cells contribute to the expansion of TILs? Do APCs or B cells provide the co-stimulation necessary to promote the expansion of TILs? APCs appear to be important for the early emigration and expansion of TILs from a tumor fragment *in vitro*. Our group has observed that the single addition of 41BB agonists at the initiation of a TIL expansion culture yields remarkably similar results to cultures where 41BB agonists are added at the same concentration throughout the 4 week culture. This is highly suggestive that the tumor microenvironment may play a role in the initiation of TIL expansion from tumor fragments. We reason that the co-stimulatory signal provided by 41BB agonists is null once TILs have emigrated from tumor fragments and are no longer in proximity to other tumor associated immune cell populations. Recent studies have demonstrated that the presence of tertiary lymphoid structures and the prevalence of B cells within tumors are advantageous to patients receiving immune checkpoint blockade therapy (217-219). Collectively, it is feasible that a supportive and organized immune network within tumors is essential for the expansion and activity of tumor-reactive TILs *in vivo* and *ex vivo*. Future studies will need to address these questions to better understand the complexity of the tumor microenvironment during the *ex vivo* expansion of TILs and the mechanistic activity of 41BB agonists.

Despite the extensive evidence that demonstrates the benefit of lymphodepleting chemotherapy in promoting clinical responses and/or the *in vivo* persistence of T cells after infusion, the work described in Chapter 3 highlights a concomitant immunosuppressive mechanism that restricts the efficacy of ACT. It is likely that the expansion of MDSCs within the first two weeks after T cell infusion negates the full advantageous effect of lymphodepleting chemotherapy provided by the availability of homeostatic cytokines, such as IL-7 and IL-15. Thus, this work emphasizes the importance of “host-conditioning” in forging a niche to achieve durable responses to ACT in patients with cancer. Specifically, a high abundance of MDSCs correlated with the reduced persistence of TILs in melanoma patients and was associated with poor survival. This profound effect on dampening the efficacy of ACT warrants further investigation into how the immune microenvironment in tumors is reshaped during recovery after lymphodepleting chemotherapy. How does this change to the tumor microenvironment dictate anti-tumor immune responses after ACT? And do MDSCs rapidly accumulate in tumors post-lymphodepletion? Interestingly, residual immune cells within tumors may resist death upon chemotherapy treatment. For instance,  $T_{RM}$  cells within tumors can survive clinically relevant doses of irradiation and mediate tumor control thereafter (220). It is unclear if endogenous chemo-resistant T cells act in conjunction with infused T cells upon adoptive transfer. Nevertheless, this introduces the possibility that reconstituting immune cells, pre-existent chemo-resistant immune populations that reside in tumors, and adoptively transferred T cells can mount a coordinated attack against tumors. Our group has preliminary data that MDSCs rapidly accumulate in tumors after treatment with lymphodepleting chemotherapy and we are currently investigating the impact of an increased MDSC abundance within tumors after lymphodepletion and ACT to address these questions.



HSPCs appear to be a critical source of MDSCs after treatment with lymphodepleting chemotherapy. We demonstrate that the lack of IL-6 shunts the differentiation of progenitors to MDSCs that exhibit a diminished survival capacity. These results imply that lymphodepletion-mobilized HSPCs can be reprogrammed and raises an intriguing question: Can the differentiation trajectory of these HSPCs be altered to generate more immunostimulatory myeloid cells at the expense of generating MDSCs? Previous reports have demonstrated the importance of DCs during recovery after lymphodepleting treatment (221, 222), and the potentiation of anti-tumor T cell responses is severely abrogated in models that lack conventional DCs (223-225). Moreover, the administration of Flt3L can increase the differentiation of DC precursors towards CD103<sup>+</sup> cDCs, while G-CSF antagonizes this developmental pathway of myelopoiesis and favors the accumulation of MDSCs (226). Thus, it is feasible to skew the fate of HSPCs with the goal of promoting immune cell populations that potentiate anti-tumor immunity. However, it is unclear how the lymphodepleted host environment dictates the differentiation of HSPCs and dendritic cell precursors towards generating immunostimulatory DCs. The administration of cytokines after ACT with the goal of promoting favorable myeloid cell populations during immune recovery after lymphodepletion has not been rigorously explored. Thus, we propose that treatment with DC promoting regimens (e.g. Flt3L,  $\alpha$ CD40) and/or the neutralization of MDSC-inducing cytokines (e.g. IL-6, G-CSF), are valid strategies to skew the differentiation of HSPCs in lymphodepleted hosts with the goal of promoting anti-tumor immunity evoked during ACT treatment strategies.

Future clinical trials will need to prospectively examine the role of HSPCs and MDSCs in patients receiving ACT. Interestingly, ACT with human TILs is feasible to model in immunocompromised mice engineered to stably express human IL-2 (227). However, modeling

MDSCs in these mice is not easily achieved. Humanizing mice with human CD34<sup>+</sup> hematopoietic cells can recapitulate lymphocyte populations *in vivo*, but these mice lack a fully functional myeloid compartment, particularly granulocytes (212, 228). Thus, it is challenging to model human reactive myelopoiesis and the impact of MDSCs within humanized mice. However, murine MDSCs can suppress human T cells *in vivo* (19). Hence, it is possible to model the immunosuppressive role of murine MDSCs on adoptively transferred human TILs. Furthermore, we developed a protocol to generate PMN-MDSC-like cells from mobilized CD34<sup>+</sup> cells that effectively suppressed TIL IFN- $\gamma$  production (Figure 37-39). Thus, serial infusions of *in vitro* generated human MDSCs after the transfer of human TILs into autologous tumor-bearing mice is a strategy that could effectively model human reactive myelopoiesis and is an undertaking currently in development by our group.

In conclusion, our work advances the knowledge associated with immunological responses that relate to ACT regimens and highlights novel treatment combinations that can enhance the efficacy of ACT. Specifically, the activity of 41BB agonists resulting in the enrichment and expansion of tumor-reactive T cells both *in vitro* and *in vivo* are aided by constituent myeloid cells. Moreover, we describe that the full benefits of host-conditioning via lymphodepletion and the efficacy of ACT are dampened by a concomitant accumulation of MDSCs, which define this as a key resistance mechanism. Collectively, an increased understanding of the mechanisms and specific functions of myeloid cells in all stages of ACT will profoundly impact the therapeutic success and translation of T cell-based immunotherapies.

## REFERENCES

1. S. A. Rosenberg, IL-2: the first effective immunotherapy for human cancer. *Journal of immunology* **192**, 5451-5458 (2014).
2. M. E. Dudley *et al.*, Cancer regression and autoimmunity in patients after clonal repopulation with antitumor lymphocytes. *Science* **298**, 850-854 (2002).
3. E. Tran *et al.*, T-Cell Transfer Therapy Targeting Mutant KRAS in Cancer. *The New England journal of medicine* **375**, 2255-2262 (2016).
4. N. Zacharakis *et al.*, Immune recognition of somatic mutations leading to complete durable regression in metastatic breast cancer. *Nature medicine* **24**, 724-730 (2018).
5. S. Stevanovic *et al.*, A Phase II Study of Tumor-infiltrating Lymphocyte Therapy for Human Papillomavirus-associated Epithelial Cancers. *Clinical cancer research : an official journal of the American Association for Cancer Research* **25**, 1486-1493 (2019).
6. S. Pilon-Thomas *et al.*, Efficacy of adoptive cell transfer of tumor-infiltrating lymphocytes after lymphopenia induction for metastatic melanoma. *Journal of immunotherapy* **35**, 615-620 (2012).
7. L. Gattinoni, D. J. Powell, Jr., S. A. Rosenberg, N. P. Restifo, Adoptive immunotherapy for cancer: building on success. *Nature reviews. Immunology* **6**, 383-393 (2006).
8. J. E. Mullinax *et al.*, Combination of Ipilimumab and Adoptive Cell Therapy with Tumor-Infiltrating Lymphocytes for Patients with Metastatic Melanoma. *Frontiers in oncology* **8**, 44 (2018).
9. C. H. June, R. S. O'Connor, O. U. Kawalekar, S. Ghassemi, M. C. Milone, CAR T cell immunotherapy for human cancer. *Science* **359**, 1361-1365 (2018).
10. S. L. Maude *et al.*, Chimeric antigen receptor T cells for sustained remissions in leukemia. *The New England journal of medicine* **371**, 1507-1517 (2014).
11. M. M. D'Aloia, I. G. Zizzari, B. Sacchetti, L. Pierelli, M. Alimandi, CAR-T cells: the long and winding road to solid tumors. *Cell death & disease* **9**, 282 (2018).
12. C. E. Brown *et al.*, Regression of Glioblastoma after Chimeric Antigen Receptor T-Cell Therapy. *The New England journal of medicine* **375**, 2561-2569 (2016).
13. G. L. Beatty *et al.*, Mesothelin-specific chimeric antigen receptor mRNA-engineered T cells induce anti-tumor activity in solid malignancies. *Cancer immunology research* **2**, 112-120 (2014).
14. C. U. Louis *et al.*, Antitumor activity and long-term fate of chimeric antigen receptor-positive T cells in patients with neuroblastoma. *Blood* **118**, 6050-6056 (2011).
15. M. Martinez, E. K. Moon, CAR T Cells for Solid Tumors: New Strategies for Finding, Infiltrating, and Surviving in the Tumor Microenvironment. *Frontiers in immunology* **10**, 128 (2019).
16. R. G. Majzner, C. L. Mackall, Tumor Antigen Escape from CAR T-cell Therapy. *Cancer discovery* **8**, 1219-1226 (2018).
17. L. Jin *et al.*, CXCR1- or CXCR2-modified CAR T cells co-opt IL-8 for maximal antitumor efficacy in solid tumors. *Nature communications* **10**, 4016 (2019).

18. S. Mohammed *et al.*, Improving Chimeric Antigen Receptor-Modified T Cell Function by Reversing the Immunosuppressive Tumor Microenvironment of Pancreatic Cancer. *Molecular therapy : the journal of the American Society of Gene Therapy* **25**, 249-258 (2017).
19. A. H. Long *et al.*, Reduction of MDSCs with All-trans Retinoic Acid Improves CAR Therapy Efficacy for Sarcomas. *Cancer immunology research* **4**, 869-880 (2016).
20. T. M. Schmitt, I. M. Stromnes, A. G. Chapuis, P. D. Greenberg, New Strategies in Engineering T-cell Receptor Gene-Modified T cells to More Effectively Target Malignancies. *Clinical cancer research : an official journal of the American Association for Cancer Research* **21**, 5191-5197 (2015).
21. A. G. Chapuis *et al.*, T cell receptor gene therapy targeting WT1 prevents acute myeloid leukemia relapse post-transplant. *Nature medicine* **25**, 1064-1072 (2019).
22. R. Thomas *et al.*, NY-ESO-1 Based Immunotherapy of Cancer: Current Perspectives. *Frontiers in immunology* **9**, 947 (2018).
23. P. F. Robbins *et al.*, A pilot trial using lymphocytes genetically engineered with an NY-ESO-1-reactive T-cell receptor: long-term follow-up and correlates with response. *Clinical cancer research : an official journal of the American Association for Cancer Research* **21**, 1019-1027 (2015).
24. E. A. Stadtmauer *et al.*, Long-term safety and activity of NY-ESO-1 SPEAR T cells after autologous stem cell transplant for myeloma. *Blood Adv* **3**, 2022-2034 (2019).
25. C. Yee *et al.*, Melanocyte destruction after antigen-specific immunotherapy of melanoma: direct evidence of t cell-mediated vitiligo. *The Journal of experimental medicine* **192**, 1637-1644 (2000).
26. M. E. Dudley *et al.*, Adoptive cell therapy for patients with metastatic melanoma: evaluation of intensive myeloablative chemoradiation preparative regimens. *Journal of clinical oncology : official journal of the American Society of Clinical Oncology* **26**, 5233-5239 (2008).
27. S. L. Goff *et al.*, Randomized, Prospective Evaluation Comparing Intensity of Lymphodepletion Before Adoptive Transfer of Tumor-Infiltrating Lymphocytes for Patients With Metastatic Melanoma. *Journal of clinical oncology : official journal of the American Society of Clinical Oncology* **34**, 2389-2397 (2016).
28. M. T. Little, R. Storb, History of haematopoietic stem-cell transplantation. *Nature reviews. Cancer* **2**, 231-238 (2002).
29. A. Ribas *et al.*, Pembrolizumab versus investigator-choice chemotherapy for ipilimumab-refractory melanoma (KEYNOTE-002): a randomised, controlled, phase 2 trial. *The Lancet Oncology* **16**, 908-918 (2015).
30. J. S. Weber *et al.*, Nivolumab versus chemotherapy in patients with advanced melanoma who progressed after anti-CTLA-4 treatment (CheckMate 037): a randomised, controlled, open-label, phase 3 trial. *The Lancet Oncology* **16**, 375-384 (2015).
31. S. Santarone *et al.*, Fludarabine and pharmacokinetic-targeted busulfan before allografting for adults with acute lymphoid leukemia. *Biology of blood and marrow transplantation : journal of the American Society for Blood and Marrow Transplantation* **17**, 1505-1511 (2011).
32. R. Kobos *et al.*, High-dose cyclophosphamide for the treatment of refractory T-cell acute lymphoblastic leukemia in children. *J Pediatr Hematol Oncol* **36**, e265-270 (2014).

33. C. M. Suryadevara *et al.*, Temozolomide lymphodepletion enhances CAR abundance and correlates with antitumor efficacy against established glioblastoma. *Oncoimmunology* **7**, e1434464 (2018).
34. L. Gattinoni *et al.*, Removal of homeostatic cytokine sinks by lymphodepletion enhances the efficacy of adoptively transferred tumor-specific CD8<sup>+</sup> T cells. *The Journal of experimental medicine* **202**, 907-912 (2005).
35. Z. C. Ding *et al.*, Adjuvant IL-7 potentiates adoptive T cell therapy by amplifying and sustaining polyfunctional antitumor CD4<sup>+</sup> T cells. *Scientific reports* **7**, 12168 (2017).
36. C. B. Johnson *et al.*, Effector CD8<sup>+</sup> T-cell Engraftment and Antitumor Immunity in Lymphodepleted Hosts Is IL7Ralpha Dependent. *Cancer immunology research* **3**, 1364-1374 (2015).
37. C. B. Johnson *et al.*, Enhanced lymphodepletion is insufficient to replace exogenous IL-2 or IL-15 therapy in augmenting the efficacy of adoptively transferred effector CD8<sup>+</sup> T cells. *Cancer research*, (2018).
38. E. W. Su *et al.*, IL-2Ralpha mediates temporal regulation of IL-2 signaling and enhances immunotherapy. *Science translational medicine* **7**, 311ra170 (2015).
39. D. J. Neitzke *et al.*, Murine Th17 cells utilize IL-2 receptor gamma chain cytokines but are resistant to cytokine withdrawal-induced apoptosis. *Cancer immunology, immunotherapy : CII* **66**, 737-751 (2017).
40. A. V. Hirayama *et al.*, The response to lymphodepletion impacts PFS in patients with aggressive non-Hodgkin lymphoma treated with CD19 CAR T cells. *Blood* **133**, 1876-1887 (2019).
41. A. Heczey *et al.*, CAR T Cells Administered in Combination with Lymphodepletion and PD-1 Inhibition to Patients with Neuroblastoma. *Molecular therapy : the journal of the American Society of Gene Therapy* **25**, 2214-2224 (2017).
42. C. U. Louis *et al.*, Enhancing the in vivo expansion of adoptively transferred EBV-specific CTL with lymphodepleting CD45 monoclonal antibodies in NPC patients. *Blood* **113**, 2442-2450 (2009).
43. I. Ramachandran *et al.*, Systemic and local immunity following adoptive transfer of NY-ESO-1 SPEAR T cells in synovial sarcoma. *Journal for immunotherapy of cancer* **7**, 276 (2019).
44. J. N. Kochenderfer *et al.*, Lymphoma Remissions Caused by Anti-CD19 Chimeric Antigen Receptor T Cells Are Associated With High Serum Interleukin-15 Levels. *Journal of clinical oncology : official journal of the American Society of Clinical Oncology* **35**, 1803-1813 (2017).
45. C. Wrzesinski *et al.*, Hematopoietic stem cells promote the expansion and function of adoptively transferred antitumor CD8 T cells. *The Journal of clinical investigation* **117**, 492-501 (2007).
46. C. J. Turtle *et al.*, Immunotherapy of non-Hodgkin's lymphoma with a defined ratio of CD8<sup>+</sup> and CD4<sup>+</sup> CD19-specific chimeric antigen receptor-modified T cells. *Science translational medicine* **8**, 355ra116 (2016).
47. D. W. Lee *et al.*, Long-Term Outcomes Following CD19 CAR T Cell Therapy for B-ALL Are Superior in Patients Receiving a Fludarabine/Cyclophosphamide Preparative Regimen and Post-CAR Hematopoietic Stem Cell Transplantation. *Blood* **128**, 218 (2016).

48. D. W. Lee *et al.*, T cells expressing CD19 chimeric antigen receptors for acute lymphoblastic leukaemia in children and young adults: a phase 1 dose-escalation trial. *The Lancet* **385**, 517-528 (2015).
49. M. J. Besser *et al.*, Comprehensive single institute experience with melanoma TIL: Long term clinical results, toxicity profile, and prognostic factors of response. *Mol Carcinog*, (2020).
50. M. Faurschou *et al.*, Prolonged risk of specific malignancies following cyclophosphamide therapy among patients with granulomatosis with polyangiitis. *Rheumatology (Oxford)* **54**, 1345-1350 (2015).
51. M. A. Khan *et al.*, p53 mutations in cyclophosphamide-associated bladder cancer. *Cancer Epidemiology Biomarkers & Prevention* **7**, 397 (1998).
52. L. M. Morton *et al.*, Association of Chemotherapy for Solid Tumors With Development of Therapy-Related Myelodysplastic Syndrome or Acute Myeloid Leukemia in the Modern Era. *JAMA Oncol* **5**, 318-325 (2019).
53. C. M. Bollard *et al.*, Tumor-Specific T-Cells Engineered to Overcome Tumor Immune Evasion Induce Clinical Responses in Patients With Relapsed Hodgkin Lymphoma. *Journal of clinical oncology : official journal of the American Society of Clinical Oncology* **36**, 1128-1139 (2018).
54. M. A. Pule *et al.*, Virus-specific T cells engineered to coexpress tumor-specific receptors: persistence and antitumor activity in individuals with neuroblastoma. *Nature medicine* **14**, 1264-1270 (2008).
55. C. R. Cruz *et al.*, Infusion of donor-derived CD19-redirected virus-specific T cells for B-cell malignancies relapsed after allogeneic stem cell transplant: a phase 1 study. *Blood* **122**, 2965-2973 (2013).
56. A. R. Haas *et al.*, Phase I Study of Lentiviral-Transduced Chimeric Antigen Receptor-Modified T Cells Recognizing Mesothelin in Advanced Solid Cancers. *Molecular therapy : the journal of the American Society of Gene Therapy* **27**, 1919-1929 (2019).
57. A. P. Rapoport *et al.*, NY-ESO-1-specific TCR-engineered T cells mediate sustained antigen-specific antitumor effects in myeloma. *Nature medicine* **21**, 914-921 (2015).
58. C. J. Turtle *et al.*, CD19 CAR-T cells of defined CD4+:CD8+ composition in adult B cell ALL patients. *The Journal of clinical investigation* **126**, 2123-2138 (2016).
59. S. J. Schuster *et al.*, Tisagenlecleucel in Adult Relapsed or Refractory Diffuse Large B-Cell Lymphoma. *The New England journal of medicine* **380**, 45-56 (2019).
60. E. W. Weber, M. V. Maus, C. L. Mackall, The Emerging Landscape of Immune Cell Therapies. *Cell* **181**, 46-62 (2020).
61. A. D. Fesnak, C. H. June, B. L. Levine, Engineered T cells: the promise and challenges of cancer immunotherapy. *Nature Reviews Cancer* **16**, 566-581 (2016).
62. Y. Simoni *et al.*, Bystander CD8(+) T cells are abundant and phenotypically distinct in human tumour infiltrates. *Nature*, (2018).
63. A. Magen *et al.*, Single-Cell Profiling Defines Transcriptomic Signatures Specific to Tumor-Reactive versus Virus-Responsive CD4+ T Cells. *Cell reports* **29**, 3019-3032.e3016 (2019).
64. H. Li *et al.*, Dysfunctional CD8 T Cells Form a Proliferative, Dynamically Regulated Compartment within Human Melanoma. *Cell* **176**, 775-789 e718 (2019).
65. T. Duhon *et al.*, Co-expression of CD39 and CD103 identifies tumor-reactive CD8 T cells in human solid tumors. *Nature communications* **9**, 2724 (2018).

66. P. Savas *et al.*, Single-cell profiling of breast cancer T cells reveals a tissue-resident memory subset associated with improved prognosis. *Nature medicine* **24**, 986-993 (2018).
67. R. Yossef *et al.*, Enhanced detection of neoantigen-reactive T cells targeting unique and shared oncogenes for personalized cancer immunotherapy. *JCI Insight* **3**, (2018).
68. A. D. Williams *et al.*, Immunotherapy for Breast Cancer: Current and Future Strategies. *Curr Surg Rep* **5**, (2017).
69. P. Malekzadeh *et al.*, Neoantigen screening identifies broad TP53 mutant immunogenicity in patients with epithelial cancers. *The Journal of clinical investigation* **129**, 1109-1114 (2019).
70. D. C. Deniger *et al.*, T-cell responses to TP53 "hotspot" mutations and unique neoantigens expressed by human ovarian cancers. *Clinical cancer research : an official journal of the American Association for Cancer Research*, (2018).
71. M. A. Forget *et al.*, Prospective Analysis of Adoptive TIL Therapy in Patients with Metastatic Melanoma: Response, Impact of Anti-CTLA4, and Biomarkers to Predict Clinical Outcome. *Clinical cancer research : an official journal of the American Association for Cancer Research* **24**, 4416-4428 (2018).
72. S. A. Rosenberg *et al.*, Durable complete responses in heavily pretreated patients with metastatic melanoma using T-cell transfer immunotherapy. *Clinical cancer research : an official journal of the American Association for Cancer Research* **17**, 4550-4557 (2011).
73. C. U. Blank *et al.*, Defining 'T cell exhaustion'. *Nature reviews. Immunology*, (2019).
74. S. Gautam *et al.*, The transcription factor c-Myb regulates CD8(+) T cell stemness and antitumor immunity. *Nature immunology* **20**, 337-349 (2019).
75. J. A. Fraietta *et al.*, Disruption of TET2 promotes the therapeutic efficacy of CD19-targeted T cells. *Nature* **558**, 307-312 (2018).
76. S. Terakura *et al.*, Generation of CD19-chimeric antigen receptor modified CD8+ T cells derived from virus-specific central memory T cells. *Blood* **119**, 72-82 (2012).
77. C. J. Dwyer *et al.*, Fueling Cancer Immunotherapy With Common Gamma Chain Cytokines. *Frontiers in immunology* **10**, 263 (2019).
78. J. C. Beltra *et al.*, Developmental Relationships of Four Exhausted CD8(+) T Cell Subsets Reveals Underlying Transcriptional and Epigenetic Landscape Control Mechanisms. *Immunity* **52**, 825-841 e828 (2020).
79. A. C. Scott *et al.*, TOX is a critical regulator of tumour-specific T cell differentiation. *Nature*, (2019).
80. M. Philip *et al.*, Chromatin states define tumour-specific T cell dysfunction and reprogramming. *Nature* **545**, 452-456 (2017).
81. J. D. Beane *et al.*, Clinical Scale Zinc Finger Nuclease-mediated Gene Editing of PD-1 in Tumor Infiltrating Lymphocytes for the Treatment of Metastatic Melanoma. *Molecular therapy : the journal of the American Society of Gene Therapy*, (2015).
82. L. Zhang *et al.*, Tumor-infiltrating lymphocytes genetically engineered with an inducible gene encoding interleukin-12 for the immunotherapy of metastatic melanoma. *Clinical cancer research : an official journal of the American Association for Cancer Research* **21**, 2278-2288 (2015).
83. J. P. Leonard *et al.*, Effects of Single-Dose Interleukin-12 Exposure on Interleukin-12-Associated Toxicity and Interferon- $\gamma$  Production. *Blood* **90**, 2541-2548 (1997).

84. M. A. Forget *et al.*, A Novel Method to Generate and Expand Clinical-Grade, Genetically Modified, Tumor-Infiltrating Lymphocytes. *Frontiers in immunology* **8**, 908 (2017).
85. H. J. Pegram *et al.*, Tumor-targeted T cells modified to secrete IL-12 eradicate systemic tumors without need for prior conditioning. *Blood* **119**, 4133-4141 (2012).
86. N. F. Kuhn *et al.*, CD40 Ligand-Modified Chimeric Antigen Receptor T Cells Enhance Antitumor Function by Eliciting an Endogenous Antitumor Response. *Cancer cell* **35**, 473-488 e476 (2019).
87. A. Alsaieedi, A. Holler, P. Velica, G. Bendle, H. J. Stauss, Safety and efficacy of Tet-regulated IL-12 expression in cancer-specific T cells. *Oncoimmunology* **8**, 1542917 (2019).
88. J. T. Sockolosky *et al.*, Selective targeting of engineered T cells using orthogonal IL-2 cytokine-receptor complexes. *Science* **359**, 1037-1042 (2018).
89. E. A. Stadtmauer *et al.*, CRISPR-engineered T cells in patients with refractory cancer. *Science* **367**, eaba7365 (2020).
90. P. H. Lee *et al.*, Host conditioning with IL-1beta improves the antitumor function of adoptively transferred T cells. *The Journal of experimental medicine* **216**, 2619-2634 (2019).
91. I. Etxeberria *et al.*, Intratumor Adoptive Transfer of IL-12 mRNA Transiently Engineered Antitumor CD8+ T Cells. *Cancer cell*, (2019).
92. S. L. Hewitt *et al.*, Durable anticancer immunity from intratumoral administration of IL-23, IL-36gamma, and OX40L mRNAs. *Science translational medicine* **11**, (2019).
93. A. Gros *et al.*, PD-1 identifies the patient-specific CD8(+) tumor-reactive repertoire infiltrating human tumors. *The Journal of clinical investigation* **124**, 2246-2259 (2014).
94. D. K. Krishnadas, Y. Wang, K. Sundaram, F. Bai, K. G. Lucas, Expansion of cancer germline antigen-specific cytotoxic T lymphocytes for immunotherapy. *Tumour Biol* **39**, 1010428317701309 (2017).
95. T. D. Wu *et al.*, Peripheral T cell expansion predicts tumour infiltration and clinical response. *Nature*, (2020).
96. J. A. Chacon *et al.*, Manipulating the tumor microenvironment ex vivo for enhanced expansion of tumor-infiltrating lymphocytes for adoptive cell therapy. *Clinical cancer research : an official journal of the American Association for Cancer Research* **21**, 611-621 (2015).
97. G. L. Beatty *et al.*, CD40 agonists alter tumor stroma and show efficacy against pancreatic carcinoma in mice and humans. *Science* **331**, 1612-1616 (2011).
98. T. Shum, R. L. Kruse, C. M. Rooney, Strategies for enhancing adoptive T-cell immunotherapy against solid tumors using engineered cytokine signaling and other modalities. *Expert Opin Biol Ther* **18**, 653-664 (2018).
99. S. Spranger, D. Dai, B. Horton, T. F. Gajewski, Tumor-Residing Batf3 Dendritic Cells Are Required for Effector T Cell Trafficking and Adoptive T Cell Therapy. *Cancer cell* **31**, 711-723 e714 (2017).
100. D. Dangaj *et al.*, Cooperation between Constitutive and Inducible Chemokines Enables T Cell Engraftment and Immune Attack in Solid Tumors. *Cancer cell* **35**, 885-900 e810 (2019).
101. M.-A. Forget *et al.*, The beneficial effects of a gas-permeable flask for expansion of Tumor-Infiltrating lymphocytes as reflected in their mitochondrial function and respiration capacity. *Oncoimmunology* **5**, e1057386-e1057386 (2015).



102. X. Wang, I. Rivière, Clinical manufacturing of CAR T cells: foundation of a promising therapy. *Mol Ther Oncolytics* **3**, 16015-16015 (2016).
103. J. A. Hernandez-Chacon *et al.*, Costimulation through the CD137/4-1BB pathway protects human melanoma tumor-infiltrating lymphocytes from activation-induced cell death and enhances antitumor effector function. *Journal of immunotherapy* **34**, 236-250 (2011).
104. L. Gattinoni *et al.*, Wnt signaling arrests effector T cell differentiation and generates CD8+ memory stem cells. *Nature medicine* **15**, 808-813 (2009).
105. J. G. Crompton *et al.*, Akt Inhibition Enhances Expansion of Potent Tumor-Specific Lymphocytes with Memory Cell Characteristics. *Cancer research* **75**, 296 (2015).
106. S. J. Santegoets *et al.*, IL-21 promotes the expansion of CD27+ CD28+ tumor infiltrating lymphocytes with high cytotoxic potential and low collateral expansion of regulatory T cells. *Journal of translational medicine* **11**, 37 (2013).
107. D. Alizadeh *et al.*, IL-15-mediated reduction of mTORC1 activity preserves the stem cell memory phenotype of CAR-T cells and confers superior antitumor activity. *Cancer immunology research*, (2019).
108. A. Palazon *et al.*, An HIF-1 $\alpha$ /VEGF-A Axis in Cytotoxic T Cells Regulates Tumor Progression. *Cancer cell* **32**, 669-683 e665 (2017).
109. S. K. Vodnala *et al.*, T cell stemness and dysfunction in tumors are triggered by a common mechanism. *Science* **363**, (2019).
110. S. Pilon-Thomas *et al.*, Neutralization of Tumor Acidity Improves Antitumor Responses to Immunotherapy. *Cancer research*, (2015).
111. D. Hanahan, L. M. Coussens, Accessories to the crime: functions of cells recruited to the tumor microenvironment. *Cancer cell* **21**, 309-322 (2012).
112. S. A. Rosenberg *et al.*, Use of Tumor-Infiltrating Lymphocytes and Interleukin-2 in the Immunotherapy of Patients with Metastatic Melanoma. *New England Journal of Medicine* **319**, 1676-1680 (1988).
113. J. J. Mule, Dendritic cell-based vaccines for pancreatic cancer and melanoma. *Annals of the New York Academy of Sciences* **1174**, 33-40 (2009).
114. L. Lowenfeld *et al.*, Dendritic Cell Vaccination Enhances Immune Responses and Induces Regression of HER2(pos) DCIS Independent of Route: Results of Randomized Selection Design Trial. *Clinical cancer research : an official journal of the American Association for Cancer Research* **23**, 2961-2971 (2017).
115. S. Antonia, J. J. Mule, J. S. Weber, Current developments of immunotherapy in the clinic. *Current opinion in immunology* **16**, 130-136 (2004).
116. R. E. Hollingsworth, K. Jansen, Turning the corner on therapeutic cancer vaccines. *NPJ Vaccines* **4**, 7 (2019).
117. K. Baksh, J. Weber, Immune Checkpoint Protein Inhibition for Cancer: Preclinical Justification for CTLA-4 and PD-1 Blockade and New Combinations. *Seminars in oncology* **42**, 363-377 (2015).
118. D. S. Shin, A. Ribas, The evolution of checkpoint blockade as a cancer therapy: what's here, what's next? *Current opinion in immunology* **33**, 23-35 (2015).
119. R. S. Herbst *et al.*, Predictive correlates of response to the anti-PD-L1 antibody MPDL3280A in cancer patients. *Nature* **515**, 563-567 (2014).
120. S. C. Wei, C. R. Duffy, J. P. Allison, Fundamental Mechanisms of Immune Checkpoint Blockade Therapy. *Cancer discovery* **8**, 1069-1086 (2018).

121. M. J. Smyth, S. F. Ngiew, A. Ribas, M. W. Teng, Combination cancer immunotherapies tailored to the tumour microenvironment. *Nature reviews. Clinical oncology*, (2015).
122. J. Weber *et al.*, Phase I/II Study of Metastatic Melanoma Patients Treated with Nivolumab Who Had Progressed after Ipilimumab. *Cancer immunology research* **4**, 345-353 (2016).
123. D. S. Chen, I. Mellman, Oncology meets immunology: the cancer-immunity cycle. *Immunity* **39**, 1-10 (2013).
124. D. M. Sansom, C. N. Manzotti, Y. Zheng, What's the difference between CD80 and CD86? *Trends in immunology* **24**, 313-318 (2003).
125. K. S. Peggs, S. A. Quezada, J. P. Allison, Cell intrinsic mechanisms of T-cell inhibition and application to cancer therapy. *Immunological reviews* **224**, 141-165 (2008).
126. S. L. Buchan *et al.*, Antibodies to Costimulatory Receptor 4-1BB Enhance Anti-tumor Immunity via T Regulatory Cell Depletion and Promotion of CD8 T Cell Effector Function. *Immunity* **49**, 958-970 e957 (2018).
127. M. F. Sanmamed, I. Etxeberria, I. Otano, I. Melero, Twists and turns to translating 4-1BB cancer immunotherapy. *Science translational medicine* **11**, (2019).
128. C. Claus *et al.*, Tumor-targeted 4-1BB agonists for combination with T cell bispecific antibodies as off-the-shelf therapy. *Science translational medicine* **11**, (2019).
129. J. A. Chacon *et al.*, Co-stimulation through 4-1BB/CD137 improves the expansion and function of CD8(+) melanoma tumor-infiltrating lymphocytes for adoptive T-cell therapy. *PloS one* **8**, e60031 (2013).
130. D. S. Vinay, B. S. Kwon, 4-1BB signaling beyond T cells. *Cellular & molecular immunology* **8**, 281-284 (2011).
131. S. W. Lee *et al.*, Identification of regulatory functions for 4-1BB and 4-1BBL in myelopoiesis and the development of dendritic cells. *Nature immunology* **9**, 917-926 (2008).
132. Y. J. Kang *et al.*, Cell surface 4-1BBL mediates sequential signaling pathways 'downstream' of TLR and is required for sustained TNF production in macrophages. *Nature immunology* **8**, 601-609 (2007).
133. R. A. Wilcox *et al.*, Cutting edge: Expression of functional CD137 receptor by dendritic cells. *Journal of immunology* **168**, 4262-4267 (2002).
134. Q. Tang *et al.*, CD137 ligand signaling enhances myelopoiesis during infections. *European journal of immunology* **43**, 1555-1567 (2013).
135. Z. Shao, H. Schwarz, CD137 ligand, a member of the tumor necrosis factor family, regulates immune responses via reverse signal transduction. *Journal of leukocyte biology* **89**, 21-29 (2011).
136. Z. Harfuddin *et al.*, Transcriptional and functional characterization of CD137L-dendritic cells identifies a novel dendritic cell phenotype. *Scientific reports* **6**, 29712 (2016).
137. H. Liu *et al.*, Intralesional rose bengal in melanoma elicits tumor immunity via activation of dendritic cells by the release of high mobility group box 1. *Oncotarget*, (2016).
138. Q. Zeng, Y. Zhou, H. Schwarz, CD137L-DCs, Potent Immune-Stimulators-History, Characteristics, and Perspectives. *Frontiers in immunology* **10**, 2216 (2019).
139. J. Langstein *et al.*, CD137 (ILA/4-1BB), a Member of the TNF Receptor Family, Induces Monocyte Activation via Bidirectional Signaling. *The Journal of Immunology* **160**, 2488 (1998).

140. S. M. Chin *et al.*, Structure of the 4-1BB/4-1BBL complex and distinct binding and functional properties of utomilumab and urelumab. *Nature communications* **9**, (2018).
141. N. H. Segal *et al.*, Results from an Integrated Safety Analysis of Urelumab, an Agonist Anti-CD137 Monoclonal Antibody. *Clinical cancer research : an official journal of the American Association for Cancer Research* **23**, 1929-1936 (2017).
142. M. Compte *et al.*, A tumor-targeted trimeric 4-1BB-agonistic antibody induces potent anti-tumor immunity without systemic toxicity. *Nature communications* **9**, 4809 (2018).
143. A. R. Sanchez-Paulete *et al.*, Cancer Immunotherapy with Immunomodulatory Anti-CD137 and Anti-PD-1 Monoclonal Antibodies Requires BATF3-Dependent Dendritic Cells. *Cancer discovery* **6**, 71-79 (2016).
144. S. W. Kang *et al.*, Anti-CD137 Suppresses Tumor Growth by Blocking Reverse Signaling by CD137 Ligand. *Cancer research* **77**, 5989-6000 (2017).
145. Q. Tang, D. Jiang, Z. Shao, J. M. Martinez Gomez, H. Schwarz, Species difference of CD137 ligand signaling in human and murine monocytes. *PloS one* **6**, e16129 (2011).
146. M. M. S. Kwajah, H. Schwarz, CD137 ligand signaling induces human monocyte to dendritic cell differentiation. *European journal of immunology* **40**, 1938-1949 (2010).
147. Y. Li *et al.*, Limited Cross-Linking of 4-1BB by 4-1BB Ligand and the Agonist Monoclonal Antibody Utomilumab. *Cell reports* **25**, 909-920 e904 (2018).
148. Z. Harfuddin, S. Kwajah, A. Chong Nyi Sim, P. A. Macary, H. Schwarz, CD137L-stimulated dendritic cells are more potent than conventional dendritic cells at eliciting cytotoxic T-cell responses. *Oncoimmunology* **2**, e26859 (2013).
149. A. J. Gentles *et al.*, The prognostic landscape of genes and infiltrating immune cells across human cancers. *Nature medicine* **21**, 938-945 (2015).
150. D. G. DeNardo *et al.*, Leukocyte complexity predicts breast cancer survival and functionally regulates response to chemotherapy. *Cancer discovery* **1**, 54-67 (2011).
151. D. I. Gabrilovich, S. Ostrand-Rosenberg, V. Bronte, Coordinated regulation of myeloid cells by tumours. *Nature reviews. Immunology* **12**, 253-268 (2012).
152. R. Advani *et al.*, CD47 Blockade by Hu5F9-G4 and Rituximab in Non-Hodgkin's Lymphoma. *The New England journal of medicine* **379**, 1711-1721 (2018).
153. S. Mok *et al.*, Inhibition of CSF-1 receptor improves the antitumor efficacy of adoptive cell transfer immunotherapy. *Cancer research* **74**, 153-161 (2014).
154. S. Hoves *et al.*, Rapid activation of tumor-associated macrophages boosts preexisting tumor immunity. *The Journal of experimental medicine* **215**, 859-876 (2018).
155. A. J. Gunderson *et al.*, Bruton Tyrosine Kinase-Dependent Immune Cell Cross-talk Drives Pancreas Cancer. *Cancer discovery* **6**, 270-285 (2016).
156. P. Foubert, M. M. Kaneda, J. A. Varner, PI3Kgamma Activates Integrin alpha4 and Promotes Immune Suppressive Myeloid Cell Polarization during Tumor Progression. *Cancer immunology research* **5**, 957-968 (2017).
157. R. H. Vonderheide, CD40 Agonist Antibodies in Cancer Immunotherapy. *Annual review of medicine*, (2019).
158. T. M. Nywening *et al.*, Targeting tumour-associated macrophages with CCR2 inhibition in combination with FOLFIRINOX in patients with borderline resectable and locally advanced pancreatic cancer: a single-centre, open-label, dose-finding, non-randomised, phase 1b trial. *The Lancet Oncology* **17**, 651-662 (2016).
159. S. L. Highfill *et al.*, Disruption of CXCR2-mediated MDSC tumor trafficking enhances anti-PD1 efficacy. *Science translational medicine* **6**, 237ra267 (2014).

160. M. C. Schmid *et al.*, Combined blockade of integrin- $\alpha 4\beta 1$  plus cytokines SDF-1 $\alpha$  or IL-1 $\beta$  potently inhibits tumor inflammation and growth. *Cancer research* **71**, 6965-6975 (2011).
161. G. A. Dominguez *et al.*, Selective Targeting of Myeloid-Derived Suppressor Cells in Cancer Patients Using DS-8273a, an Agonistic TRAIL-R2 Antibody. *Clinical cancer research : an official journal of the American Association for Cancer Research*, (2016).
162. F. Veglia, M. Perego, D. Gabrilovich, Myeloid-derived suppressor cells coming of age. *Nature immunology*, (2018).
163. V. Bronte *et al.*, Recommendations for myeloid-derived suppressor cell nomenclature and characterization standards. *Nature communications* **7**, 12150 (2016).
164. J. I. Youn, S. Nagaraj, M. Collazo, D. I. Gabrilovich, Subsets of Myeloid-Derived Suppressor Cells in Tumor-Bearing Mice. *The Journal of Immunology* **181**, 5791-5802 (2008).
165. T. Condamine *et al.*, Lectin-type oxidized LDL receptor-1 distinguishes population of human polymorphonuclear myeloid-derived suppressor cells in cancer patients. *Science Immunology* **1**, aaf8943-aaf8943 (2016).
166. D. Marvel, D. I. Gabrilovich, Myeloid-derived suppressor cells in the tumor microenvironment: expect the unexpected. *The Journal of clinical investigation* **125**, 3356-3364 (2015).
167. K. H. Parker, D. W. Beury, S. Ostrand-Rosenberg, Myeloid-Derived Suppressor Cells: Critical Cells Driving Immune Suppression in the Tumor Microenvironment. *Advances in cancer research* **128**, 95-139 (2015).
168. S. Nagaraj *et al.*, Altered recognition of antigen is a mechanism of CD8+ T cell tolerance in cancer. *Nature medicine* **13**, 828-835 (2007).
169. O. Canli *et al.*, Myeloid Cell-Derived Reactive Oxygen Species Induce Epithelial Mutagenesis. *Cancer cell* **32**, 869-883 e865 (2017).
170. P. C. Rodriguez *et al.*, Arginase I in myeloid suppressor cells is induced by COX-2 in lung carcinoma. *The Journal of experimental medicine* **202**, 931-939 (2005).
171. M. K. Srivastava, P. Sinha, V. K. Clements, P. Rodriguez, S. Ostrand-Rosenberg, Myeloid-derived suppressor cells inhibit T-cell activation by depleting cystine and cysteine. *Cancer research* **70**, 68-77 (2010).
172. R. B. Holmgaard *et al.*, Tumor-Expressed IDO Recruits and Activates MDSCs in a Treg-Dependent Manner. *Cell reports* **13**, 412-424 (2015).
173. D. W. Beury *et al.*, Cross-talk among myeloid-derived suppressor cells, macrophages, and tumor cells impacts the inflammatory milieu of solid tumors. *Journal of leukocyte biology* **96**, 1109-1118 (2014).
174. V. Kumar, S. Patel, E. Tcyganov, D. I. Gabrilovich, The Nature of Myeloid-Derived Suppressor Cells in the Tumor Microenvironment. *Trends in immunology* **37**, 208-220 (2016).
175. M. G. Manz, S. Boettcher, Emergency granulopoiesis. *Nature reviews. Immunology* **14**, 302-314 (2014).
176. M. Guillamot *et al.*, The E3 ubiquitin ligase SPOP controls resolution of systemic inflammation by triggering MYD88 degradation. *Nature immunology* **20**, 1196-1207 (2019).
177. I. Marigo *et al.*, Tumor-induced tolerance and immune suppression depend on the C/EBP $\beta$  transcription factor. *Immunity* **32**, 790-802 (2010).

178. S. Devalaraja *et al.*, Tumor-Derived Retinoic Acid Regulates Intratumoral Monocyte Differentiation to Promote Immune Suppression. *Cell*, (2020).
179. L. Strauss *et al.*, RORC1 Regulates Tumor-Promoting "Emergency" Granulo-Monocytopoiesis. *Cancer cell* **28**, 253-269 (2015).
180. C. M. Diaz-Montero *et al.*, Increased circulating myeloid-derived suppressor cells correlate with clinical cancer stage, metastatic tumor burden, and doxorubicin-cyclophosphamide chemotherapy. *Cancer immunology, immunotherapy : CII* **58**, 49-59 (2009).
181. S. Patel *et al.*, Unique pattern of neutrophil migration and function during tumor progression. *Nature immunology* **19**, 1236-1247 (2018).
182. R. P. Tobin *et al.*, IL-6 and IL-8 Are Linked With Myeloid-Derived Suppressor Cell Accumulation and Correlate With Poor Clinical Outcomes in Melanoma Patients. *Frontiers in oncology* **9**, 1223 (2019).
183. T. X. Cui *et al.*, Myeloid-derived suppressor cells enhance stemness of cancer cells by inducing microRNA101 and suppressing the corepressor CtBP2. *Immunity* **39**, 611-621 (2013).
184. H. Zhang *et al.*, STAT3 controls myeloid progenitor growth during emergency granulopoiesis. *Blood* **116**, 2462-2471 (2010).
185. H. J. Kwak *et al.*, Myeloid cell-derived reactive oxygen species externally regulate the proliferation of myeloid progenitors in emergency granulopoiesis. *Immunity* **42**, 159-171 (2015).
186. D. Regan-Komito *et al.*, GM-CSF drives dysregulated hematopoietic stem cell activity and pathogenic extramedullary myelopoiesis in experimental spondyloarthritis. *Nature communications* **11**, 155 (2020).
187. M. Guillamot *et al.*, The E3 ubiquitin ligase SPOP controls resolution of systemic inflammation by triggering MYD88 degradation. *Nature immunology* **20**, 1196-1207 (2019).
188. C. Wrzesinski *et al.*, Increased intensity lymphodepletion enhances tumor treatment efficacy of adoptively transferred tumor-specific T cells. *Journal of immunotherapy* **33**, 1-7 (2010).
189. D. E. Wright *et al.*, Cyclophosphamide/granulocyte colony-stimulating factor causes selective mobilization of bone marrow hematopoietic stem cells into the blood after M phase of the cell cycle. *Blood* **97**, 2278 (2001).
190. Z. C. Ding *et al.*, Immunosuppressive myeloid cells induced by chemotherapy attenuate antitumor CD4+ T-cell responses through the PD-1-PD-L1 axis. *Cancer research* **74**, 3441-3453 (2014).
191. T. Condamine, D. I. Gabrilovich, Molecular mechanisms regulating myeloid-derived suppressor cell differentiation and function. *Trends in immunology* **32**, 19-25 (2011).
192. P. Sinha *et al.*, Myeloid-derived suppressor cells express the death receptor Fas and apoptose in response to T cell-expressed FasL. *Blood* **117**, 5381-5390 (2011).
193. S. S. Chandran *et al.*, Treatment of metastatic uveal melanoma with adoptive transfer of tumour-infiltrating lymphocytes: a single-centre, two-stage, single-arm, phase 2 study. *The Lancet Oncology* **18**, 792-802 (2017).
194. A. G. Chapuis *et al.*, Tracking the Fate and Origin of Clinically Relevant Adoptively Transferred CD8+ T Cells In Vivo. *Sci Immunol* **2**, (2017).

195. P. L. Raber *et al.*, T cells conditioned with MDSC show an increased anti-tumor activity after adoptive T cell based immunotherapy. *Oncotarget*, (2016).
196. I. Angulo *et al.*, Nitric oxide-producing CD11b<sup>+</sup>Ly-6G(Gr-1)<sup>+</sup>CD31(ER-MP12)<sup>+</sup> in the spleen of cyclophosphamide-treated mice: implications for T-cell responses in immunosuppressed mice. *Blood* **95**, 212 (2000).
197. K. N. Kodumudi, A. Weber, A. A. Sarnaik, S. Pilon-Thomas, Blockade of myeloid-derived suppressor cells after induction of lymphopenia improves adoptive T cell therapy in a murine model of melanoma. *Journal of immunology* **189**, 5147-5154 (2012).
198. T. Condamine *et al.*, ER stress regulates myeloid-derived suppressor cell fate through TRAIL-R-mediated apoptosis. *The Journal of clinical investigation* **124**, 2626-2639 (2014).
199. R. P. Tobin *et al.*, Targeting myeloid-derived suppressor cells using all-trans retinoic acid in melanoma patients treated with Ipilimumab. *Int Immunopharmacol* **63**, 282-291 (2018).
200. J. I. Youn *et al.*, Epigenetic silencing of retinoblastoma gene regulates pathologic differentiation of myeloid cells in cancer. *Nature immunology* **14**, 211-220 (2013).
201. W. W. Pang *et al.*, Human bone marrow hematopoietic stem cells are increased in frequency and myeloid-biased with age. *Proceedings of the National Academy of Sciences of the United States of America* **108**, 20012-20017 (2011).
202. S. Nagaraj *et al.*, Antigen-specific CD4(+) T cells regulate function of myeloid-derived suppressor cells in cancer via retrograde MHC class II signaling. *Cancer research* **72**, 928-938 (2012).
203. N. Glodde *et al.*, Reactive Neutrophil Responses Dependent on the Receptor Tyrosine Kinase c-MET Limit Cancer Immunotherapy. *Immunity* **47**, 789-802.e789 (2017).
204. V. Kumar *et al.*, Cancer-Associated Fibroblasts Neutralize the Anti-tumor Effect of CSF1 Receptor Blockade by Inducing PMN-MDSC Infiltration of Tumors. *Cancer cell* **32**, 654-668 e655 (2017).
205. L. Bonapace *et al.*, Cessation of CCL2 inhibition accelerates breast cancer metastasis by promoting angiogenesis. *Nature* **515**, 130-133 (2014).
206. T. M. Nywening *et al.*, Targeting both tumour-associated CXCR2(+) neutrophils and CCR2(+) macrophages disrupts myeloid recruitment and improves chemotherapeutic responses in pancreatic ductal adenocarcinoma. *Gut* **67**, 1112-1123 (2018).
207. D. I. Gabrilovich, S. Nagaraj, Myeloid-derived suppressor cells as regulators of the immune system. *Nature reviews. Immunology* **9**, 162-174 (2009).
208. K. Maeda *et al.*, IL-6 blocks a discrete early step in lymphopoiesis. *Blood* **106**, 879-885 (2005).
209. K. Maeda *et al.*, Interleukin-6 aborts lymphopoiesis and elevates production of myeloid cells in systemic lupus erythematosus-prone B6.Sle1.Yaa animals. *Blood* **113**, 4534-4540 (2009).
210. M. Yamashita, E. Passegue, TNF-alpha Coordinates Hematopoietic Stem Cell Survival and Myeloid Regeneration. *Cell stem cell*, (2019).
211. O. Chornoguz *et al.*, Proteomic pathway analysis reveals inflammation increases myeloid-derived suppressor cell resistance to apoptosis. *Molecular & cellular proteomics : MCP* **10**, M110 002980 (2011).

212. M. Norelli *et al.*, Monocyte-derived IL-1 and IL-6 are differentially required for cytokine-release syndrome and neurotoxicity due to CAR T cells. *Nature medicine* **24**, 739-748 (2018).
213. R. Q. Le *et al.*, FDA Approval Summary: Tocilizumab for Treatment of Chimeric Antigen Receptor T Cell-Induced Severe or Life-Threatening Cytokine Release Syndrome. *Oncologist* **23**, 943-947 (2018).
214. S. Fried *et al.*, Early and late hematologic toxicity following CD19 CAR-T cells. *Bone Marrow Transplant* **54**, 1643-1650 (2019).
215. K. R. Juluri *et al.*, Severe Cytokine Release Syndrome Is Associated with Impaired Hematopoietic Recovery after CD19-Targeted CAR-T Cell Therapy. *Blood* **134**, 3229-3229 (2019).
216. P. T. Thevenot *et al.*, The stress-response sensor chop regulates the function and accumulation of myeloid-derived suppressor cells in tumors. *Immunity* **41**, 389-401 (2014).
217. R. Cabrita *et al.*, Tertiary lymphoid structures improve immunotherapy and survival in melanoma. *Nature* **577**, 561-565 (2020).
218. B. A. Helmink *et al.*, B cells and tertiary lymphoid structures promote immunotherapy response. *Nature* **577**, 549-555 (2020).
219. F. Petitprez *et al.*, B cells are associated with survival and immunotherapy response in sarcoma. *Nature* **577**, 556-560 (2020).
220. A. Arina *et al.*, Tumor-reprogrammed resident T cells resist radiation to control tumors. *Nature communications* **10**, 3959 (2019).
221. M. L. Salem *et al.*, Cyclophosphamide induces dynamic alterations in the host microenvironments resulting in a Flt3 ligand-dependent expansion of dendritic cells. *Journal of immunology* **184**, 1737-1747 (2010).
222. C. M. Paulos *et al.*, Microbial translocation augments the function of adoptively transferred self/tumor-specific CD8+ T cells via TLR4 signaling. *The Journal of clinical investigation* **117**, 2197-2204 (2007).
223. M. L. Broz *et al.*, Dissecting the tumor myeloid compartment reveals rare activating antigen-presenting cells critical for T cell immunity. *Cancer cell* **26**, 638-652 (2014).
224. A. de Mingo Pulido *et al.*, TIM-3 Regulates CD103(+) Dendritic Cell Function and Response to Chemotherapy in Breast Cancer. *Cancer cell* **33**, 60-74 e66 (2018).
225. S. Hegde *et al.*, Dendritic Cell Paucity Leads to Dysfunctional Immune Surveillance in Pancreatic Cancer. *Cancer cell* **37**, 289-307.e289 (2020).
226. M. A. Meyer *et al.*, Breast and pancreatic cancer interrupt IRF8-dependent dendritic cell development to overcome immune surveillance. *Nature communications* **9**, 1250 (2018).
227. H. Jespersen *et al.*, Clinical responses to adoptive T-cell transfer can be modeled in an autologous immune-humanized mouse model. *Nature communications* **8**, 707 (2017).
228. A. M. Coughlan *et al.*, Myeloid Engraftment in Humanized Mice: Impact of Granulocyte-Colony Stimulating Factor Treatment and Transgenic Mouse Strain. *Stem Cells Dev* **25**, 530-541 (2016).

## APPENDIX A

### Funding

This work was funded by a by the American Cancer Society - Leo and Anne Albert Charitable Foundation Research Scholar Grant - RSG-16-117-01-LIB, Bankhead Coley Cancer Research Grant for the Florida Department of Health, a Miles for Moffitt award, and Swim Across America. Dr. Amod A. Sarnaik was supported by NCI-5K23CA178083.



## APPENDIX B


### INSTITUTIONAL ANIMAL CARE AND USE COMMITTEE APPROVAL



RESEARCH INTEGRITY & COMPLIANCE  
INSTITUTIONAL ANIMAL CARE & USE COMMITTEE

#### MEMORANDUM

TO: Shari Pilon-Thomas, Ph.D.

FROM:   
Farah Moulvi, MSPH, IACUC Coordinator  
Institutional Animal Care & Use Committee  
Research Integrity & Compliance

DATE: 1/27/2020

PROJECT TITLE: Lymphodepletion-generated myeloid derived suppressor cells decrease the efficacy of adoptive T cell therapy for melanoma

FUNDING SOURCE: Federal government or major agency that awards grants based on peer-reviewed proposals (NIH, NSF, DOD, AHA, ACS, etc.)  
Bankhead Coley

IACUC PROTOCOL #: R IS00007684

PROTOCOL STATUS: **APPROVED**

The Institutional Animal Care and Use Committee (IACUC) reviewed your application requesting the use of animals in research for the above-entitled study. The IACUC **APPROVED** your request to use the following animals in your protocol for a one-year period beginning 1/27/2020:

Mouse: C57BL/6 (6-8 week, F/M)	720
Mouse: C57BL/LysMcre-IL6rafl (IL-6R knockout) (6-12 week, F/M)	240
Mouse: C57BL/6 - OT-I (6-20 week, M/F)	144
Mouse: C57BL/6 - pmel (6-20 week, M/F)	144
Mouse: C57BL/6 IL-6 k/o (6-8 week, F/M)	240
Mouse: C57BL/6 - HPV-E7 (6-8 week, F/M)	144

Please take note of the following:

• IACUC approval is granted for a one-year period at the end of which, an annual renewal form must be submitted for years two (2) and three (3) of the protocol through the eIACUC system. After three years all continuing studies must be completely re-described in a new electronic application and submitted to IACUC for review.

• All modifications to the IACUC-Approved Protocol must be approved by the IACUC prior to initiating the modification. Modifications can be submitted to the IACUC for review and approval as an Amendment or Procedural Change through the eIACUC system. These changes must be within the scope of the original research hypothesis, involve the original species and justified in writing. Any change in the IACUC-approved protocol that does not meet the latter definition is considered a major protocol change and requires the submission of a new application.


• **All costs invoiced to a grant account must be allocable to the purpose of the grant.** Costs allocable to one protocol may not be shifted to another in order to meet deficiencies caused by overruns, or for other reasons convenience. Rotation of charges among protocols by month without establishing that the rotation schedule credibly reflects the relative benefit to each protocol is unacceptable.

---

INSTITUTIONAL ANIMAL CARE AND USE COMMITTEE  
PHS No. A4100-01, AAALAC No. 000434, USDA No. 58-R-0015  
University of South Florida • 12901 Bruce B. Downs Blvd., MDC35 • Tampa, FL 33612-4799  
(813) 974-7106 • FAX (813) 974-7091

MEMORANDUM

TO: Shari Pilon-Thomas, Ph.D.

FROM:   
Farah Moulvi, MSPH, IACUC Coordinator  
Institutional Animal Care & Use Committee  
Research Integrity & Compliance

DATE: 5/17/2019

PROJECT TITLE: Enhancement of T cell activity to improve adoptive cell therapy  
Modulating the tumor microenvironment to improve immunotherapy in melanoma  
Metabolic Reprogramming to Improve Immunotherapy in Melanoma

FUNDING SOURCE: American Cancer Society  
Moffitt Cancer Center

IACUC PROTOCOL #: R IS00006642

PROTOCOL STATUS: APPROVED

The Institutional Animal Care and Use Committee (IACUC) reviewed your application requesting the use of animals in research for the above-entitled study. The IACUC APPROVED your request to use the following animals in your protocol for a one-year period beginning 5/17/2019:

Mouse: C57BL/6 - Pmel/OT-II/OT-II (6-12 week, f/m)	520
Mouse: NSG or NSG IL-2 (6-8 week, f/m)	300
Mouse: C57BL/6 (6-8 week / female)	1280
Mouse: C57BL/6SjL congenic (6-8 week, female)	400
Mouse: B6.Cg-Xcr1(tm2(HBEGF)/Venus)Ksho (6-8 week, M/F)	320
Mouse: C57BL/6, B6(Cg)-Zbtb46tm1(HBEGF)Mn/J (6-8 weeks, MF)	320

Please take note of the following:

- IACUC approval is granted for a one-year period at the end of which, an annual renewal form must be submitted for years two (2) and three (3) of the protocol through the eIACUC system. After three years all continuing studies must be completely re-described in a new electronic application and submitted to IACUC for review.
- All modifications to the IACUC-Approved Protocol must be approved by the IACUC prior to initiating the modification. Modifications can be submitted to the IACUC for review and approval as an Amendment or Procedural Change through the eIACUC system. These changes must be within the scope of the original research hypothesis, involve the original species and justified in writing. Any change in the IACUC-approved protocol that does not meet the latter definition is considered a major protocol change and requires the submission of a new application.

• All costs invoiced to a grant account must be allocable to the purpose of the grant. Costs allocable to one protocol may not be shifted to another in order to meet deficiencies caused by overruns, or for other reasons convenience. Rotation of charges among protocols by month without establishing that the rotation schedule credibly reflects the relative benefit to each protocol is unacceptable.

---

RESEARCH & INNOVATION • RESEARCH INTEGRITY AND COMPLIANCE  
INSTITUTIONAL ANIMAL CARE AND USE COMMITTEE  
PHS No. A4100-01, AAALAC No. 000434, USDA No. 58-R-0015  
University of South Florida • 12901 Bruce B. Downs Blvd., MDC35 • Tampa, FL 33612-4799  
(813) 974-7106 • FAX (813) 974-7091

## APPENDIX C

### COPYRIGHT USE AND PERMISSION FORM

8/31/2020

Rightslink® by Copyright Clearance Center



RightsLink®



Home



Help



Email Support



Sign in



Create Account



#### Reactive Myeloiposis Triggered by Lymphodepleting Chemotherapy Limits the Efficacy of Adoptive T Cell Therapy

**Author:**

Patrick Innamarato, Krithika Kodumudi, Sarah Asby, Benjamin Schachner, MacLean Hall, Amy Mackay, Doris Wiener, Matthew Beatty, Luz Nagle, Ben C. Creelan, Amod A. Sarnaik, Shari Pilon-Thomas

**Publication:** Molecular Therapy

**Publisher:** Elsevier

**Date:** Available online 24 June 2020

© 2020 The American Society of Gene and Cell Therapy.

Please note that, as the author of this Elsevier article, you retain the right to include it in a thesis or dissertation, provided it is not published commercially. Permission is not required, but please ensure that you reference the journal as the original source. For more information on this and on your other retained rights, please visit: <https://www.elsevier.com/about/our-business/policies/copyright#Author-rights>

BACK

CLOSE WINDOW

© 2020 Copyright - All Rights Reserved | Copyright Clearance Center, Inc. | [Privacy statement](#) | [Terms and Conditions](#)  
Comments? We would like to hear from you. E-mail us at [customer-care@copyright.com](mailto:customer-care@copyright.com)